Biological activity of anthocyanins and their phenolic degradation products and metabolites in human vascular endothelial cells

Michael Edwards BSc (Hons)

A thesis submitted to the University of East Anglia in accordance with the requirements of the Degree of Doctor of Philosophy

Department of Nutrition, Norwich Medical School

University of East Anglia

October 2013

Abstract

Human, animal, and *in vitro* data indicate significant vasoprotective activity of anthocyanins. However, few studies have investigated the activity of anthocyanin degradation products and metabolites which are likely to mediate bioactivity *in vivo*. The present thesis therefore examined the vascular bioactivity *in vitro* of anthocyanins, their phenolic degradants, and the potential for interactions between dietary bioactive compounds. Seven treatment compounds (cyanidin-, peonidin-, petunidin- & malvidin-3-glucoside, and protocatechuic, vanillic, and syringic acid) and two treatment combinations (cyanidin-3-glucoside or protocatechuic acid with epicatechin, quercetin, and ascorbic acid) were screened in a human endothelial cell model for effects on endothelial nitric oxide synthase (eNOS) activity (via ELISA & colourimetric assay), and NADPH oxidase (NOX)-mediated superoxide production (by cytochrome c reduction assay, optimised in-house). A bioactive treatment was then chosen to explore possible mechanisms of NOX inhibition, namely gene expression of NOX2, NOX4, $p47^{phox}$, $p67^{phox}$, $p22^{phox}$, & haem oxygenase-1 (HO-1), and activation/expression of $p47^{phox}$ and HO-1 protein; using RT-qPCR and immunoblotting (optimised for cell stimulation conditions and qPCR reference genes). Differential bioactivity of parent anthocyanins and their phenolic degradants was observed at physiologically relevant concentrations, as only anthocyanins upregulated eNOS expression (by 4- to 7-fold; $p < 0.01$), whereas both anthocyanins and degradants appeared to reduce endothelial superoxide levels (by 1- to 8-fold; $p < 0.05$). The phenolic degradant vanillic acid significantly reduced ($p < 0.05$) superoxide by 2-fold at 1µM, and has been reported at low micromolar levels in human serum; therefore vanillic acid was selected to elucidate pathways potentially underlying observed bioactivity. Vanillic acid did not significantly modulate expression of NOX isoforms/subunits, but an apparent induction of the cytoprotective enzyme HO-1 by vanillic acid (2-fold increase) was observed in human umbilical vein and coronary artery endothelial cells, although changes were non-significant ($p \geq 0.3$). In conclusion, anthocyanin phenolic degradants could enhance vascular function *in vivo* by decreasing superoxide production, and thus scavenging of the key mediator nitric oxide (NO). Vanillic acid might inhibit endothelial superoxide production through modulation of HO-1, thereby preserving NO bioavailability and vascular homoeostasis, and this pathway should be the focus of future research.

Table of Contents

List of Tables

List of Figures

List of Abbreviations

ABC	ATP-binding cassette
ADMA	Asymmetric dimethylarginine
AGE	Advanced glycation end products
Akt	Protein kinase B
AL	Auto-inhibitory loop
AMP	Adenosine monophosphate
AMPK	AMP-activated protein kinase
Ang II	Angiotensin II
ANOVA	Analysis of variance
ApoE	Apolipoprotein E
ARE	Antioxidant response element
Arg	L-arginine
AT	Angiotensin
BAEC	Bovine artery endothelial cell
BCA	Bicinchoninic acid
BH_4	Tetrahydrobiopterin
BSA	Bovine serum albumin
C3G	Cyanidin-3-glucoside
CaM	Calmodulin
CBG	Cytosolic B-glucosidase
CBD	Calmodulin binding domain
CGD	Chronic granulomatous disease
cGMP	Cyclic guanosine monophosphate
CHD	Coronary heart disease
CO	Carbon monoxide
COMT	Catechol-O-methyltransferase
COX	Cyclo-oxygenase

CV	Coefficient of variation
CVD	Cardiovascular disease
Cy	Cyanidin
CYBA/B	Cytochrome b-245 alpha ($p22^{phox}$) or beta (NOX2) polypeptide
DDAH	Dimethylarginine dimethylaminohydrolase
DMEM	Dulbecco's Modified Eagle Medium
DMSO	Dimethyl sulphoxide
(c)DNA	(complementary) deoxyribonucleic acid
DNase	Deoxyribonuclease
dNTP	Deoxyribonucleotide triphosphate
Dp	Delphinidin
DTT	Dithiothreitol
DUOX	Dual oxidases
EC	Endothelial cell
EDRF	Endothelium-derived relaxing factor
EDTA	Ethylene diamine tetra acetate
EGTA	Ethylene glycol tetra acetic acid
ELISA	Enzyme-linked immunosorbent assay
EPIC	European Prospective Investigation into Cancer and Nutrition
EpRE	Electrophile response element
ERK	Extracellular signal regulated protein kinase
ET-1	Endothelin-1
FAD	Flavin adenine dinucleotide
FBS	Foetal bovine serum
FCS	Foetal calf serum
FCDB	Food composition database
FMN	Flavin mononucleotide
GAPDH	Glyceraldehyde-3-phosphate dehydrogenase

GDP	Guanosine diphosphate
GLUT2	Glucose transporter 2
GTP	Guanosine triphosphate
h	Hour(s)
HCAEC	Human coronary artery endothelial cell
HIAEC	Human iliac artery endothelial cell
HMEC	Human microvascular endothelial cell
HO	Haem oxygenase
HPFS	Health Professionals Follow-Up Study
HUVEC	Human umbilical vein endothelial cell
ICAM-1	Intracellular adhesion molecule 1
IFN-γ	Interferon-γ
IgG	Immunoglobulin G
IL-1α/β	Interleukin-1α/β
IR	Infra-red
JNK	c-Jun-N-terminal kinase
LDL	Low-density lipoprotein
LPC	Lysophosphatidylcholine
LPH	Lactase phloridzin hydrolase
LPS	Lipopolysaccharide
M3G	Malvidin-3-glucoside
MAEC	Mouse aortic endothelial cell
MAPK	Mitogen-activated protein kinase
MPO	Myeloperoxidase
mRNA	Messenger ribonucleic acid
MRP	Multidrug resistance protein
Mv	Malvidin
NADH	Nicotinamide adenine dinucleotide (reduced form)

NADPH	Nicotinamide adenine dinucleotide phosphate (reduced form)
NCF1/2	Neutrophil cytosolic factor 1 ($p47^{phox}$) or 2 ($p67^{phox}$)
NF-κB	Nuclear factor kappa B
NHANES	National Centre for Health Statistics
NHS	Nurse's Health Study
NO	Nitric oxide
(e/i/n) NOS	(endothelial/inducible/neuronal) Nitric oxide synthase
NOX	NADPH oxidase
NOXA1	NOX activator 1
NOXO1	NOX organiser 1
Nrf2	Nuclear factor-erythroid 2-related factor 2
OD	Optical density
oxLDL	Oxidised low density lipoprotein
PBMC	Peripheral blood mononuclear cell
PBS(T)	Phosphate-buffered saline (with Tween® 20)
PCA	Protocatechuic acid
PCR	Polymerase chain reaction
Pe	Peonidin
Peo3G	Peonidin-3-glucoside
Pet3G	Petunidin-3-glucoside
Pg	Pelargonidin
PGA	Phloroglucinol aldehyde
P-gp	P-glycoprotein
PK A/B/C	Protein kinase A/B/C
PMA	Phorbol myristate acetate
PMSF	Phenylmethylsulfonylfluoride
POLDIP2	Polymerase δ-interacting protein 2
PP1	Protein phosphatase-1

Pt	Petunidin
PVDF	Polyvinylidene fluoride
RNase	Ribonuclease
RNS	Reactive nitrogen species
ROS	Reactive oxygen species
RT-qPCR	Quantitative reverse transcription polymerase chain reaction
SA	Syringic acid
SD	Standard deviation
SDS-PAGE	Sodium dodecyl sulphate polyacrylamide gel electrophoresis
Ser	Serine
SGLT1	Sodium-dependent glucose transporter 1
SMC	Smooth muscle cell
SOD	Superoxide dismutase
SULT	Sulphotransferase
TGF-β1	Transforming growth factor-beta 1
Thr	Threonine
TMD	Transmembrane domain
TNF-α	Tumour necrosis factor-α
U	Unit(s)
UGT	Uridine-5’-diphosphate glucuronosyltransferase
UK	United Kingdom
USA	United States of America
USDA	United States Department of Agriculture
UV	Ultraviolet light
VA	Vanillic acid
VCAM-1	Vascular cell adhesion molecule-1
VSMC	Vascular smooth muscle cell
XO	Xanthine oxidase

Acknowledgements

I gratefully acknowledge the unstinting help and support of my primary and secondary supervisors, Dr Colin Kay, Professor Aedín Cassidy and Dr Yongping Bao, throughout the duration of my research project and the preparation of this thesis. Equally, I would like to thank both past and present members of the analytical laboratory group, especially Hiren Amin, Dr Charles Czank, Rachel de Ferrars, Jess di Gesso and Dr Jason Kerr; and other members of the Department of Nutrition in general, for their assistance and encouragement over the past three years. I am particularly indebted to Wouter Hendrickx and Sandra Bednar for assistance with immunoblotting methodology. Finally, I am most grateful to the Biotechnology and Biological Sciences Research Council, and GlaxoSmithKline, for providing the financial support which made this research project possible.

1 Flavonoids: review of the scientific literature

1.1 Introduction

Fruits and vegetables consumed as part of the human diet contain a variety of phytochemicals, some of which may be beneficial to human health (Geleijnse and Hollman, 2008, Crozier et al., 2009). Phytochemicals can be classified into several groups, one of which is the class of phenolic compounds; covering over 8,000 aromatic structures occurring throughout the plant kingdom (Erdman et al., 2007, Crozier et al., 2009). This compound class can be further subdivided, with the family of polyphenolic compounds termed flavonoids forming a large sub-group – over 5,000 distinct flavonoids have been identified (Erdman et al., 2007). Flavonoids are water-soluble compounds found in many plants, and thus in commonly consumed plant-derived foodstuffs (Erdman et al., 2007, Geleijnse and Hollman, 2008, Crozier et al., 2009). They share a common structure of two aromatic rings linked through three carbons (Crozier et al., 2009), generally forming an oxygenated heterocycle nucleus (Grassi et al., 2009) (Figure 1.1).

Figure 1.1 **Basic structure of flavonoids showing two aromatic rings (labelled A &B) linked by heterocyclic (C) ring.**

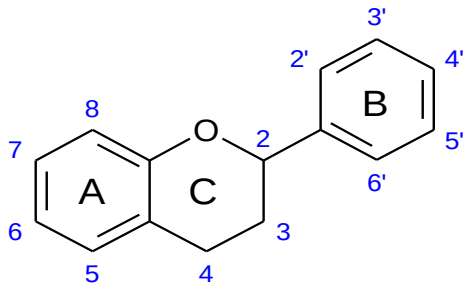

Adapted from (Erdman et al., 2007).

Flavonoids can be subdivided into several classes based on ring substituents and C-ring structure (Erdman et al., 2007). A number of epidemiological studies have suggested a protective association between dietary components rich in flavonoids and cardiovascular mortality (Hertog et al., 1993, Geleijnse et al., 2002, Mink et al., 2007, McCullough et al., 2012, Cassidy et al., 2013), although not all studies concur (Huxley and Neil, 2003, Arts and Hollman, 2005, Curtis et al., 2009). Moreover, predominantly *in vitro* data indicate flavonoids may have anti-inflammatory and immunomodulatory activity (González-Gallego et al., 2010), whilst dietary intervention studies point to positive effects of flavonoid-rich foods on memory and cognition (Spencer, 2010).

This review aims to provide an overview of the dietary occurrence, bioavailability and bioactivity of flavonoids, focusing primarily on the flavonoid sub-group anthocyanidins; which in plants are usually found as sugar conjugates termed anthocyanins (Crozier et al., 2009). Epidemiological

data and *in vitro* studies indicate anthocyanins may act to reduce the risk of cardiovascular disease by modulating key vascular signalling pathways (Lazze et al., 2006, Bell and Gochenaur, 2006, Cassidy et al., 2010); thus the pathophysiology of the chronic inflammatory disease atherosclerosis (Ross, 1999, Libby et al., 2002, Bonomini et al., 2008) and underlying endothelial dysfunction (Landmesser et al., 2004, Higashi et al., 2009) will also be considered. Finally deficiencies in current knowledge of anthocyanin bioavailability and bioactivity are discussed, which it is hoped will be addressed in part by this thesis.

1.2 Flavonoids

1.2.1 Dietary occurrence and relevance to human health

Flavonoids are phenolic phytochemicals, the latter defined as plant secondary metabolites which may accumulate in high concentrations in plants, but which are not essential nutritional components of the human diet (Crozier et al., 2009). Flavonoids have important roles in plant physiology including modulation of transport of the plant hormone auxin, defence, and providing colour to flowers (Buer et al., 2010). Over 5,000 flavonoids have been identified, of which some hundreds are present in common foodstuffs such as fruits, vegetables and beverages including tea and red wine (Aherne and O'Brien, 2002, Erdman et al., 2007); in fact flavonoids represent the most common plant polyphenolics derived from a typical plant-based diet (Chun et al., 2007). Dietary flavonoids can be grouped by structure into flavonols, flavones, flavanones, flavan-3-ols (and proanthocyanidin oligomers), isoflavones and anthocyanins (glycosylated anthocyanidins) (Erdman et al., 2007) (Figure 1.2). Flavonoids, with the exception of flavan-3-ols, are usually found in plants and most foods as glycosides; conjugated to one or more sugar molecules (Erdman et al., 2007, Crozier et al., 2009).

Flavonols, for example quercetin and kaempferol, represent the most widespread flavonoids in foods, with rich sources including onions, curly kale, broccoli and apples (Erdman et al., 2007); however, the dietary content of flavonols is comparatively low (Manach et al., 2005). Flavones, such as luteolin and apigenin, are less common and occur in parsley and celery (Erdman et al., 2007); whilst flavanones, for example glycosides of hesperetin and naringenin, are a small compound group found in citrus fruits, (Manach et al., 2005). Flavan-3-ols, or flavanols, represent the subclass with most structural complexity; from simple monomers such as (+)-catechin and the isomer (-)-epicatechin to oligomeric and polymeric proanthocyanidins, including procyanidins [proanthocyanidins consisting of (epi)catechin units only] (Crozier et al., 2009). Major dietary sources of flavanols are apples, grapes, red wine, chocolate, and tea (Manach et al., 2005); whereas isoflavones such as daidzein and genistein occur almost exclusively in leguminous plants (Crozier et al., 2009) and are derived from only soy bean based products in the diet (Manach et

al., 2005). Finally anthocyanins, including glycosides of cyanidin and pelargonidin, are found in aubergines, berries, cherries and black grapes; and thus in derived products such as juices and red wine (Wu et al., 2006b, Zamora-Ros et al., 2011).

Figure 1.2 Example chemical structures for flavonoid subclasses.

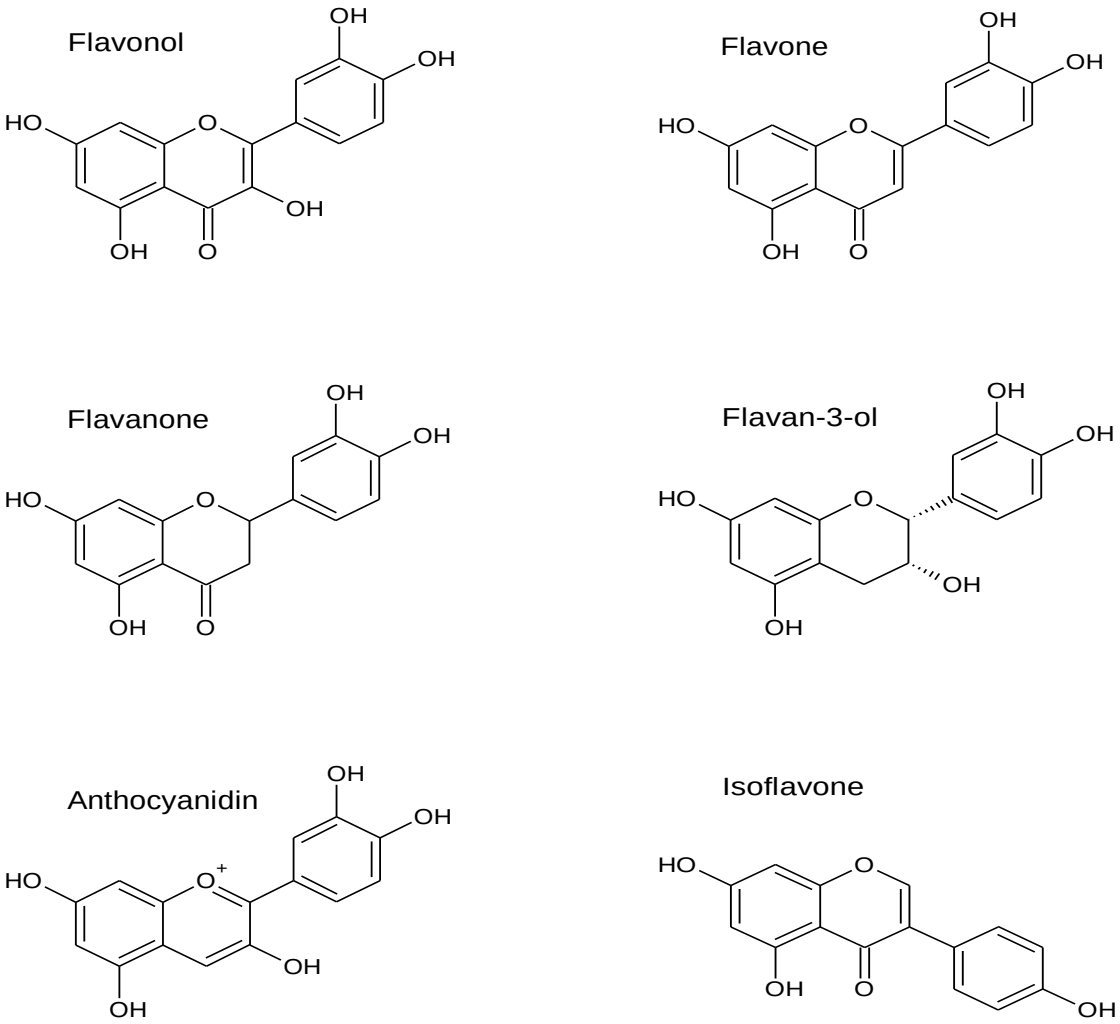

Adapted from (Hooper et al., 2008).

Regarding human dietary intake of flavonoids, it is apparent that a diet with substantial consumption of fruits and vegetables, and plant-derived beverages such as wines, tea and fruit juices, should contain significant flavonoid content. However, estimation of human flavonoid intake has proved difficult, owing to a lack of information on food content of flavonoids and variations in methods of estimation and national dietary habits (Chun et al., 2007, Zamora-Ros et al., 2010). Flavonoid content can also be influenced by factors such as plant species, cultivation, ripeness, and food preparation and processing (Aherne and O'Brien, 2002). Zamora-Ros *et al* (2010) and Chun *et al* (2007) have estimated daily flavonoid intakes of 313.26 ± 213.75mg and 189.7 ± 11.6mg for adult populations in Spain (Zamora-Ros et al., 2010) and the United States of America (USA) (Chun et al., 2007) respectively (Table 1.1). Although anthocyanins apparently

formed a small part of daily flavonoid intake, consideration must be given to the high concentrations of anthocyanins which may be achieved in some diets through consumption of berries and grapes and derived beverages (Manach et al., 2005, Wu et al., 2006b). Equally, the paucity of nutrient databases with comprehensive quantitation of anthocyanin content (Curtis et al., 2009), and anthocyanin molecular stability and concomitant issues with detection methodology (section 1.3.2), could result in under-estimation of anthocyanin consumption.

Table 1.1 Estimated daily flavonoid intake for Spanish and American adult populations.

Flavonoid class	**Estimated intake in mg/day (mean ± SD)[1]**	
	(1) Spain	*(2) United States of America*
Flavonols	18.7 ± 11.06	12.9 ± 0.4
Flavones	3.4 ± 2.92	1.6 ± 0.2
Flavanones	50.55 ± 47.15	14.4 ± 0.6
Flavan-3-ols	32.47 ± 51.8	156.5 ± 11.3
Proanthocyanidin multimers	189.17 ± 164.07	-
Anthocyanidins	18.88 ± 21.5	3.1 ± 0.5
Isoflavones	0.08 ± 0.33	1.2 ± 0.2
Total	*313.26 ± 213.75*	*189.7 ± 11.6*

[1]Estimated daily individual and total flavonoid intakes of (1) 40,683 Spanish adults (aged 35 - 64 years) included in the European Prospective Investigation into Cancer and Nutrition (EPIC) study Spanish cohort (recruited between 1992 - 1996) (Zamora-Ros et al., 2010); and (2) 8,809 adults (aged 19 years or over) in the United States of America (USA) derived from The National Centre for Health Statistics (NHANES) 24-hour dietary recall survey 1999-2002 (Chun et al., 2007).

Whilst estimation of dietary flavonoid intake within and between populations may be problematic, there is considerable interest in the relevance of these non-essential nutrients to maintenance of human health. An epidemiological study reported during the 1990s, the Zutphen Elderly Study, indicated a significant protective effect of several flavonols against mortality owing to coronary heart disease (Hertog et al., 1993). Data from subsequent epidemiological studies, for example the Rotterdam study (Geleijnse et al., 2002) and Iowa Women's Health Study (Mink et al., 2007), have indicated a protective effect of flavonoids for risk of cardiovascular mortality, though not all studies confirm this association (Huxley and Neil, 2003, Arts and Hollman, 2005). A recent review covering 20 prospective studies (derived from 12 cohorts) of dietary flavonoid consumption and cardiovascular disease (CVD) occurrence/outcomes concluded that an association between flavonoid intake and reduced CVD incidence or mortality was observed in eight studies (Peterson et al., 2012). Moreover, a systematic review and meta-analysis by Hooper *et al* (2008) examined 133 randomised controlled trials of flavonoid/flavonoid-rich food interventions and risk factors for CVD (Hooper et al., 2008). Certain flavonoid-rich foods were

associated with beneficial effects on risk factors, such as a reduction in systolic and diastolic blood pressure (BP) with chocolate or cocoa consumption (Hooper et al., 2008). However, it is worth noting that associations with foodstuffs, rather than discrete chemicals, could wholly or partly reflect bioactivity of other components of food/beverages (Halliwell, 2007, Hooper et al., 2008, Sies, 2010).

1.2.2 Metabolism and bioactivity of flavonoids

In order for flavonoids to elicit biological effects *in vivo*, bioactive forms must be present in the systemic circulation at sufficiently high concentrations, and for an adequate length of time, to elicit effects on putative molecular targets. As with all ingested xenobiotics, to reach the systemic circulation flavonoids must pass through and be absorbed from the gastro-intestinal tract, during which molecules are subject to metabolism by intestinal and hepatic enzymes (Grassi et al., 2009, Wang and Ho, 2009). Colonic microbes also play a key metabolic role, catabolising unabsorbed flavonoids into smaller molecules such as phenolic and aromatic acids, which can be absorbed (Williamson and Clifford, 2010).

Following gastric digestion, absorption of flavonoids occurs in the small and large intestine, with a few reports suggesting anthocyanins can be absorbed in the stomach (Erdman et al., 2007, Wang and Ho, 2009, Grassi et al., 2009). Absorption of flavonoid glycosides in the small intestine is usually associated with hydrolysis, to yield the more lipophilic aglycone form (Crozier et al., 2009). The enzyme lactase phloridzin hydrolase (LPH), located in the brush border of intestinal epithelial cells/enterocytes, demonstrates broad specificity for flavonoid-*O*-B-D-glucosides; with the resulting aglycone penetrating epithelial cells by passive diffusion (Walle, 2004, Crozier et al., 2009). Alternatively, flavonoid glycosides could be hydrolysed within enterocytes by cytosolic B-glucosidase (CBG), although in this case the polar glycoside form must be transported into cells (Crozier et al., 2009). The sodium-dependent glucose transporter 1 (SGLT1) protein may act as a mechanism for such uptake (Walle, 2004), though it has been questioned as to whether SGLT1 actually transports flavonoid glycosides (Crozier et al., 2009).

Absorbed aglycones are metabolised within enterocytes to generate predominantly sulphated, glucuronidated and/or methylated forms; catalysed by sulphotransferases (SULT), uridine-5'-diphosphate glucuronosyltransferases (UGT) and catechol-*O*-methyltransferases (COMT) respectively (Walle, 2004, Crozier et al., 2009, Del Rio et al., 2010). Other metabolites, such as flavonoid thiol conjugates (with glutathione or cysteine), have been less extensively studied (Wang and Ho, 2009). Efflux of flavonoid glycosides and/or metabolites from enterocytes, either into the intestinal lumen or basolateral blood supply, may be mediated by transporter proteins such as multidrug resistance proteins (MRP) and P-glycoprotein (P-gp), which are members of the

ATP-binding cassette (ABC) family of transporters (Walle, 2004, Brand et al., 2006, Crozier et al., 2009). Compounds entering the bloodstream may be subject to further hepatic metabolism before reaching the systemic circulation (Del Rio et al., 2010).

Thus, for flavonoids consumed as part of the diet, the parent compound(s) may not be responsible for perceived bioactivity post-absorption; instead this may be mediated by metabolites present in the systemic circulation (Wang and Ho, 2009). Possible mechanisms of flavonoid bioactivity have been the subject of many *in vitro* studies; but the physiological relevance of doses used in such studies is of great significance, as is the duration of exposure to compounds tested. Low levels of dietary flavonoids and derived molecules are present in the systemic circulation (generally the maximum concentration is < 10µmol/L in total), yet it is argued that for any such molecule to exert a biologically significant effect *in vivo* it must have sufficient potency to do so at 50% of its transient plasma C_{max} (Crozier et al., 2009). Crozier *et al* (2009) have summarised several possible molecular mechanisms of actions for phenolic compounds and metabolites, including flavonoids (Crozier et al., 2009, Del Rio et al., 2010).

One signalling pathway which has been the subject of extensive study is that of NF-κB (nuclear factor kappa B); an ubiquitous redox sensitive transcription factor which regulates expression of pro-inflammatory cytokines, and other mediators of inflammation such as inducible nitric oxide synthase (iNOS) and cyclo-oxygenase 2 (COX-2) (Bremner and Heinrich, 2002, Crozier et al., 2009, González-Gallego et al., 2010, Wallace, 2011). The flavonol quercetin has demonstrated inhibition of NF-κB activation in several cell types, including stimulated human umbilical vein endothelial cells (HUVECs) (González-Gallego et al., 2010), and similar activity has been reported for anthocyanins in both human monocytic cells (Karlsen et al., 2007) and human articular chondrocytes (Haseeb et al., 2013). Flavonoids may also interact with the mitogen-activated protein kinase (MAPK) or extracellular signal regulated protein kinase (ERK) signalling pathways; which are highly conserved eukaryotic kinase signalling cascades involved in intracellular signal transduction (Robinson and Cobb, 1997, Crozier et al., 2009). Moreover, methylated metabolites of (-)-epicatechin have been shown to inhibit the reactive-oxygen species generating NADPH oxidase (NOX) enzyme (Cai et al., 2003, Bedard and Krause, 2007) in HUVECs, leading to improved steady-state level of nitric oxide (NO) in endothelial cells (Steffen et al., 2007b, Steffen et al., 2008). NO exhibits vasodilatory, anti-coagulant and anti-inflammatory properties, and thereby serves a key role in protection of the vascular endothelium (Michel and Vanhoutte, 2010).

1.2.3 Flavonoids and in vitro antioxidant activity

Flavonoids, and other phenolic compounds in foodstuffs, have been the subject of increasing interest owing to epidemiological data suggesting an inverse correlation between consumption of

these compounds and incidence of diseases such as CVD (Geleijnse and Hollman, 2008, Crozier et al., 2009). Initially, the putative beneficial effects of flavonoids were often attributed to antioxidant activity *in vivo* (Halliwell et al., 2005), owing to the ability of almost every group of flavonoids to function in this capacity *in vitro* (Rice-Evans et al., 1996, Nijveldt et al., 2001); and substantial evidence that oxidative stress is associated with, and contributes to development of, major age-related diseases such as CVD (Halliwell et al., 2005).

Direct antioxidant activity arises from inactivation, or 'scavenging' of reactive radical species (Rice-Evans et al., 1996), which are molecules with an unpaired electron such as hydroxyl ($^{\cdot}OH$), superoxide ($O_2^{\cdot-}$), nitric oxide ($NO^{\cdot}$), and peroxynitrite ($^{-}ONOO$; formed by the reaction of nitric oxide and superoxide) (Forman et al., 2002, Naseem, 2005). Such species can be extremely reactive, to the extent that free hydroxyl radical essentially does not exist (Forman et al., 2002), and reactions initiated by free radicals can have damaging consequences; for example lipid oxidation of cell membranes with potential membrane damage or alteration of function (Galleano et al., 2010). Reactive oxygen species (ROS) are generated within the cell from sources such as the mitochondrial electron transport chain, and enzymes including NOX, myeloperoxidase (MPO) and xanthine oxidase (XO) which generate superoxide (Leopold and Loscalzo, 2009). Superoxide reacts rapidly with protons to yield the non-radical hydrogen peroxide (H_2O_2) (dismutation), and this reaction is accelerated by the superoxide dismutase (SOD) family of enzymes (Forman et al., 2002). Reactive nitrogen species (RNS) include nitric oxide, synthesised by the nitric oxide synthase (NOS) family of enzymes (Forman et al., 2002), and derived species such as peroxynitrite, nitrite (NO_2^-; terminal oxidation product of $NO^{\cdot}$) and nitrogen dioxide ($^{\cdot}NO_2$; formed by reaction of $NO^{\cdot}$ with oxygen) (Forman et al., 2002, Leopold and Loscalzo, 2009).

More recently, the limited bioavailability of flavonoids *in vivo,* and extent of metabolism during absorption, have led to the recognition that direct antioxidant activity *in vivo* is very unlikely to form part of flavonoid bioactivity (Halliwell, 2007, Crozier et al., 2009, Sies, 2010, Galleano et al., 2010, Hollman et al., 2011). Flavonoids undergo extensive metabolism post-absorption, such as glucuronidation, sulphation and methylation reactions; which may block phenolic hydroxyl groups required for direct radical scavenging activity (Halliwell et al., 2005, Halliwell, 2007). Moreover, endogenous enzymatic and molecular mechanisms exist to counter oxidative challenges to cells and tissues (Sies, 2007). Key enzymes include SOD, which occurs in three different forms (mitochondrial, cytosolic and extracellular) and rapidly converts superoxide to hydrogen peroxide; and glutathione peroxidase, which utilises glutathione to reduce hydrogen peroxide and possibly peroxynitrite (Forman et al., 2002). Hydrogen peroxide is also reduced to water by the activity of the catalase enzyme (Leopold and Loscalzo, 2009). Small molecules, including vitamins and trace elements, form part of antioxidant defences by inclusion in larger molecules (for example cysteine

in glutathione, or selenium as part of the active site in glutathione peroxidase); or acting as antioxidants directly (such as ascorbate and urate circulating in plasma) (Sies, 2007). Indeed, plasma total antioxidant capacity has been estimated as > 10^3µmol/L, therefore detection of a statistically significant increase in such assays would require a minimum of 20-50µmol/L additional antioxidant to be present – yet flavonoid/metabolite plasma concentrations are transient and unlikely to exceed very low micromolar levels (Halliwell et al., 2005, Crozier et al., 2009, Galleano et al., 2010).

1.3 Anthocyanins

1.3.1 Dietary occurrence and consumption of anthocyanins

Anthocyanins, from the Greek *anthos* (flower) and *kyanos* (blue), are plant pigments (Kong et al., 2003). Over 600 naturally-occurring anthocyanins have been reported (Wu et al., 2006b, Wallace, 2011), and are present throughout the plant kingdom, particularly in fruits and vegetables where they provide red, blue and purple colouration (Crozier et al., 2009). Anthocyanins are glycoside or acylglycoside conjugates of anthocyanidin aglycones (Wu et al., 2006b), and glycosides represent the form invariably present *in planta* (Crozier et al., 2009). Approximately 17 anthocyanidins occur in plants, of which cyanidin (Cy), delphinidin (Dp), malvidin (Mv), pelargonidin (Pg), peonidin (Pe), and petunidin (Pt) are distributed ubiquitously (Wu et al., 2006b, Crozier et al., 2009).

With regard to human dietary occurrence of anthocyanins, these compounds are found mainly in fresh berries, fruits, and certain vegetables (Manach et al., 2005, Wu et al., 2006b, Zamora-Ros et al., 2011). Zamora-Ros *et al* (2011) have recently published estimates of dietary anthocyanin intake, and food sources, based upon 24 hour dietary recall data for 36,037 subjects (between 35 - 74 years of age) participating in the European Prospective Investigation into Cancer and Nutrition (EPIC) study (covering 27 centres in ten European countries) (Zamora-Ros et al., 2011). A food composition database was developed from scientific literature and internet-based sources, detailing anthocyanidin content for 1877 food items (Zamora-Ros et al., 2011) (Table 1.2). Cyanidin displays the widest distribution in foods examined, although with considerable variation in concentrations. Raw elderberries contained the highest concentration of cyanidin, as opposed to blackcurrants for delphinidin, and blueberries for malvidin and petunidin (Zamora-Ros et al., 2011). The optimum sources of pelargonidin and peonidin were strawberries and bilberries respectively (Zamora-Ros et al., 2011).

Table 1.2 Anthocyanin composition of selected food sources estimated from food composition databases derived from scientific literature and internet-based sources (Zamora-Ros et al., 2011).

Food	Anthocyanidin aglycones (milligrammes) per 100 grammes fresh weight*						
	Cy	***Dp***	***Mv***	***Pg***	***Pe***	***Pt***	***Total***
Bilberry, raw	112.59	161.93	54.37	-	51.01	51.01	430.91
Blackberries, raw	90.31	-	-	0.15	-	-	90.46
Blueberries, wild raw	42.47	92.71	103.8	-	23.49	58.23	320.70
Cranberries, raw	41.81	7.66	0.31	-	42.10	-	91.88
Currants, European black, raw	85.63	181.11	-	1.17	0.66	3.87	272.44
Eggplant (aubergine), raw	0.02	13.76	-	0.02	-	-	13.80
Elderberries, raw	758.48	-	61.35	1.13	-	-	820.96
Grapes, red, raw	1.46	3.67	34.71	0.02	2.89	2.11	44.86
Pistachio nuts, raw	6.06	-	-	-	-	-	6.06
Radishes, raw	-	-	-	25.66	-	-	25.66
Raspberries, black	323.47	-	-	0.15	0.55	-	324.17
Raspberries, red, raw	35.84	0.29	0.70	1.85	-	-	38.68
Strawberries, raw	1.96	0.32	-	31.27	-	0.08	33.63

Anthocyanin composition of selected items from food composition database (FCDB) developed using dietary recall data for 36,037 subjects participating in the European Prospective Investigation into Cancer and Nutrition (EPIC) study (covering 27 centres in ten European countries) (Zamora-Ros et al., 2011). The FCDB database was based on the United States Department of Agriculture database (USDA, 2007) and expanded with values from Phenol Explorer (Neveu et al., 2010). *Anthocyanidin aglycones per 100 g fresh weight, calculated as sum of available forms (glycosides and aglycones). Abbreviations used are Cy, cyanidin; Dp, delphinidin; Mv, malvidin; Pg, pelargonidin; Pe, peonidin; Pt, petunidin.

Anthocyanin intake in the United States of America has been estimated as 12.5mg/day/person (Wu et al., 2006b) (Table 1.3), although dietary intake estimates can vary within and between regions. For example, average daily intake of anthocyanins in Germany was reported as 2.7mg/person in 2002 (Wu et al., 2006b), whilst mean dietary intake in Finland has been estimated as 82mg/day (Manach et al., 2005). Zamora-Ros *et al* (2011) described total anthocyanidin intake for males ranging from 19.8mg/day in The Netherlands (study centre at Bilthoven) to 64.9mg/day in Italy (Turin) (mean 29.4mg/day), and for females from 18.7mg/day in Spain (Granada) to 44.1mg/day in Italy (Turin) (mean 33.5mg/day) (Zamora-Ros et al., 2011). The high content of anthocyanins found in grapes and berries indicates that a substantial daily intake of anthocyanins may be achieved with regular consumption of these foods and derived beverages (Manach et al., 2005, Wu et al., 2006b), such that doses of 400 - 500mg anthocyanins could be consumed in a single serving (Kay et al., 2009). This is of particular relevance for grape and berry juices, which could therefore serve as accessible dietary sources of anthocyanins.

Table 1.3 Summary of estimates of daily anthocyanin consumption from beverages, fruits and vegetables in the United States of America.

Food group	Daily anthocyanin consumption (mg)*
Beverages (grape juice & wine)	1.68
Fruits (raw, 11 foods)	8.75
Nuts (pistachio nut)	0.004
Vegetables (raw, 6 foods)	2.19
Total	12.53

*Food intake data from the National Health and Nutrition Examination Survey (NHANES 2001-2002) [derived from (Wu et al., 2006b)].

A substantial body of epidemiological evidence suggests that consumption of flavonoid-rich food and beverages is inversely associated with the risk of CVD (Erdman et al., 2007, Mazza, 2007, Geleijnse and Hollman, 2008, Wallace, 2011), though it should be noted that not all such studies have supported this association (Geleijnse and Hollman, 2008, Curtis et al., 2009, Wallace, 2011). Moderate red wine consumption has been associated with decreased coronary heart disease (CHD) mortality in several epidemiological studies (Rimm et al., 1991, Gaziano et al., 1993), and may be partly ascribed to anthocyanin content of this beverage (Dell'Agli et al., 2004, Erdman et al., 2007). Furthermore, data from over 30,000 post-menopausal women enrolled in the Iowa Women's Health Study suggested a significant inverse relationship between dietary anthocyanin consumption (median intake 0.2mg/day versus no intake) and mortality owing to CHD and CVD over a 16 year follow-up period (Mink et al., 2007). Anthocyanin intake (highest versus lowest grouping) has also been associated with a reduced relative risk of hypertension in a prospective study (14 year follow-up) of participants enrolled from the Nurse's Health Study (NHS) I and II (46,672 and 87,242 women, respectively) and Health Professionals Follow-Up Study (HPFS; 23,043 men) (Cassidy et al., 2010).

More recently, anthocyanidin intake (top versus bottom quintile of intake) was associated with a lower risk of fatal CVD for subjects enrolled in the Cancer Prevention Study II Nutrition Cohort (38,180 men and 60,289 women) during seven years of follow-up (McCullough et al., 2012); and anthocyanin intake was inversely correlated with risk of myocardial infarction in a population of 93,600 young- and middle-aged women from the NHS II over 18 years of follow-up (32% decrease in risk for highest versus lowest quintile of intake) (Cassidy et al., 2013). Moreover, an inverse relationship between anthocyanin intake and measures of central blood pressure (specifically peripheral systolic blood pressure, central systolic blood pressure, & mean arterial pressure) and arterial stiffness (as assessed by pulse wave velocity) has been reported from a cross-sectional study of 1898 women drawn from the TwinsUK registry (Jennings et al., 2012). Of particular interest, the observed decrease in pulse wave velocity between lowest and highest quintiles of anthocyanin intake corresponded to a mean difference in intake of 44mg, which the authors noted to be equivalent to one or two portions of certain berries (Jennings et al., 2012).

Data from animal and *in vitro* studies have demonstrated a variety of potential cardiovascular activities of anthocyanins (Domitrovic, 2011), including vasodilatory and vasoprotective effects (Bell and Gochenaur, 2006, Ziberna et al., 2013), anti-thrombotic activity (Rechner and Kroner, 2005, de Pascual-Teresa et al., 2010, Yang et al., 2011, Yang et al., 2012), activation and/or upregulation of endothelial nitric oxide synthase (eNOS) (Xu et al., 2004b, Xu et al., 2004a, Lazze et al., 2006, Chalopin et al., 2010, Simoncini et al., 2011, Edirisinghe et al., 2011, Paixão et al., 2012), decreased production of the vasoconstrictor endothelin-1/ET-1 (Lazze et al., 2006), and inhibition of angiotensin-converting enzyme (Persson et al., 2009, Hidalgo et al., 2012). Thus, dietary anthocyanin intake may elicit beneficial effects on cardiovascular health (Basu et al., 2010, Wallace, 2011, Tsuda, 2011, Landberg et al., 2012), and to that end anthocyanin chemistry, bioavailability and bioactivity are considered in more detail within the following sections.

1.3.2 Chemistry and stability of anthocyanin compounds

Anthocyanins are glycosides of polyhydroxy, and polymethoxy, derivatives of flavylium (2-phenylbenzopyrylium) salts (Kong et al., 2003). In common with other flavonoids, the anthocyanin molecule contains two benzoyl rings (A and B), linked by a heterocyclic oxygen ring (C); giving the characteristic C_6-C_3-C_6 structure (Kong et al., 2003, McGhie and Walton, 2007, Wallace, 2011). Anthocyanins are differentiated according to the number of hydroxyl groups attached to the molecule, and extent of methylation of these groups; together with the type, number and position of linked sugar moieties (Kong et al., 2003, McGhie and Walton, 2007) (Figure 1.3). Commonly occurring glycosides are 3-monosides, 3-biosides (disaccharides), 3-triosides and 3,5-diglycosides; associated with the sugars glucose, galactose, rhamnose, arabinose and xylose (Kong et al., 2003, McGhie and Walton, 2007).

Figure 1.3 Chemical structure of an anthocyanin molecule.

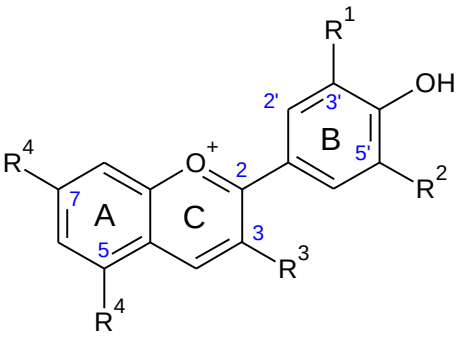

Anthocyanidin	Substituent	
	R^1	R^2
Pelargonidin	-H	-H
Cyanidin	-OH	-H
Peonidin	$-OCH_3$	-H
Delphinidin	-OH	-OH
Petunidin	$-OCH_3$	-OH
Malvidin	$-OCH_3$	$-OCH_3$

Flavylium cation form of anthocyanin and attached substituent groups. R^1, R^2, are –H, -OH or $–OCH_3$ (refer to inset table); R^3 is –H or a sugar moiety; R^4 is –OH or a sugar moiety [adapted from (Kong et al., 2003)].

Anthocyanins are responsible for the pigmentation of many fruits and vegetables (Keppler and Humpf, 2005), owing to a chromophore formed by eight conjugated double bonds and a positively charged oxygen in the heterocyclic C ring (Wallace, 2011). However, the stability of this flavylium cation form is significantly influenced by pH, and within aqueous solutions several molecular forms of anthocyanins exist which are in a dynamic equilibrium (McGhie and Walton, 2007) (Figure 1.4). At pH values of <2, the flavylium cation is the predominant form present, giving rise to a characteristic red colour (McGhie and Walton, 2007, Wallace, 2011). However, rapid de-protonation occurs with increasing pH, to generate a quinonoidal structure (pH 6-8) and blue colouration (Fleschhut et al., 2006, McGhie and Walton, 2007). A concurrent but substantially slower hydration of the flavylium cation also ensues, to generate a colourless hemiketal form (pH 4-5), which then tautomerises through opening of the C-ring to yield colourless *cis* and *trans* chalcone forms (pH 7-8) (Fleschhut et al., 2006, McGhie and Walton, 2007).

Aglycone anthocyanidins, formed by hydrolysis of the glycoside linkage, are stable under acidic conditions; but likewise undergo similar structural changes with increasing pH (Keppler and Humpf, 2005, Fleschhut et al., 2006). This results in the formation of a highly reactive α-diketone structure (pH >4) and decomposition into monomeric phenolic acid and aldehyde compounds (Keppler and Humpf, 2005) (Figure 1.5). The presence of a sugar moiety confers a degree of stability on anthocyanin glycosides (Fleschhut et al., 2006), but degradation also occurs at more alkaline pH (Woodward et al., 2009, Kay et al., 2009).

Figure 1.4 **Molecular structures of anthocyanin generated under varying pH conditions.**

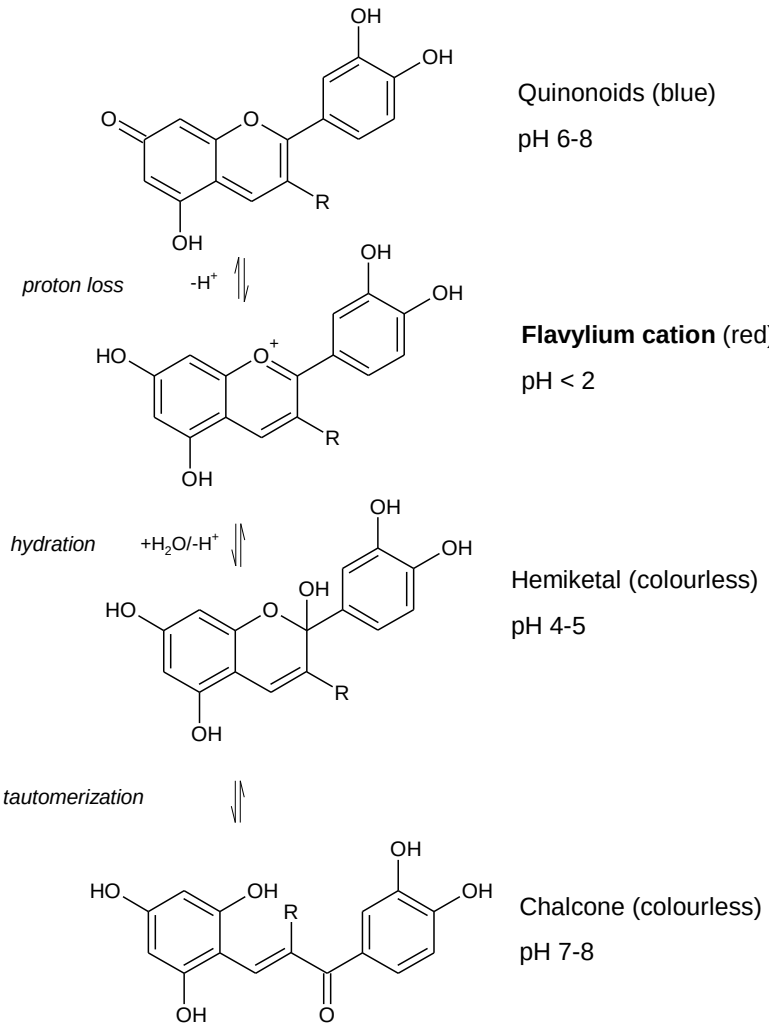

Derived from (Fleschhut et al., 2006, McGhie and Walton, 2007, Del Rio et al., 2010).

Figure 1.5 **Monomeric phenolic acids and aldehyde formed by anthocyanidin degradation.**

Anthocyanidin	B-ring degradation product (phenolic acid)
Cyanidin	Protocatechuic acid
Delphinidin	Gallic aid
Malvidin	Syringic acid
Pelargonidin	4-hydroxybenzoic acid
Peonidin	Vanillic acid
Petunidin	3-methylgallic acid

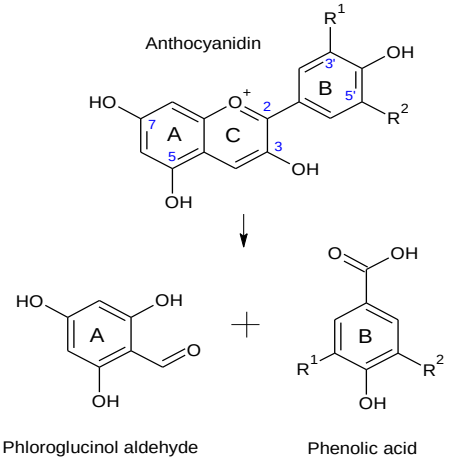

Derived from (Keppler and Humpf, 2005, Fleschhut et al., 2006, Forester and Waterhouse, 2008, Williamson and Clifford, 2010).

A recent study demonstrated that in physiological buffer (pH 7.4), cyanidin, delphinidin and pelargonidin anthocyanidins undergo rapid degradation with generation of phenolic acid/aldehyde, to the extent that no anthocyanidin could be detected after two hours (Woodward et al., 2009). Decomposition of the 3-glucoside conjugates of these anthocyanins was also examined in physiological buffer, and total losses of 20%, 40% and 100% over the first 12 hours of study were recorded for pelargonidin-3-glucoside, cyanidin-3-glucoside and delphinidin-3-glucoside respectively; with phenolic acid/aldehyde formation (Woodward et al., 2009). Moreover, Kay *et al* (2009) examined the stability of cyanidin and cyanidin-3-glucoside during incubation in phosphate buffer and cell culture media (Kay et al., 2009), and reported losses of 96% and 57% for cyanidin and its 3-glucoside respectively after a four incubation period in cell-free Dulbecco's Modified Eagle Medium (DMEM; pH 7). No significant difference was observed in the level of cyanidin-3-glucoside during incubation in DMEM with cultured caco-2 (intestinal epithelial) cells, suggesting anthocyanin degradation was spontaneous; and degradation products were identified as protocatechuic acid (PCA) and phloroglucinol aldehyde (PGA) (Kay et al., 2009).

Thus, and with regard to anthocyanin disposition *in vivo*, the flavylium cation is likely to be the predominant form in the acidic gastric environment (Crozier et al., 2009). However, in the more neutral pH conditions of the small and large intestines (and subsequently plasma), other molecular forms will predominate (McGhie and Walton, 2007, Del Rio et al., 2010), with concomitant effects on anthocyanin and anthocyanidin stability. Several *in vitro* studies have demonstrated deglycosylation of anthocyanins by intestinal microflora (Keppler and Humpf, 2005, Fleschhut et al., 2006), with subsequent degradation of liberated aglycones into phenolic acids and aldehydes; which may be subject to further microbial metabolism and/or absorption (Williamson and Clifford, 2010). Therefore anthocyanin bioactivity *in vivo* may be mediated by phenolic acid/aldehyde metabolites, as opposed to parent glycosides (Woodward et al., 2009, Williamson and Clifford, 2010, Del Rio et al., 2013), and indeed these have been reported to be the predominant forms in the systemic circulation (Czank et al., 2013).

1.3.3 Metabolism and bioavailability of anthocyanins

Manach *et al* (2005), Kay (2006), McGhie & Walton (2007), and Del Rio *et al* (2010, 2013) have published summaries of human bioavailability of anthocyanins, based on previously reported studies (Manach et al., 2005, Kay, 2006, McGhie and Walton, 2007, Del Rio et al., 2010, Del Rio et al., 2013). Such studies usually involved ingestion of red wine, grape or berry juices, berries, or berry extracts or concentrates; with anthocyanin dose (in terms of total intake) ranging from 50mg to 2g (McGhie and Walton, 2007). In terms of physiological relevance, a dose of several hundred milligrams of anthocyanin in a serving would not be deemed unreasonable (Manach et al., 2005); although anthocyanin bioavailability from extracts or concentrates may not be directly comparable to that

from normal dietary components (Wiczkowski et al., 2010, Wallace, 2011). Moreover, bioavailability studies invariably involve fasted subjects [for example (Kay et al., 2004, Kay et al., 2005, Wiczkowski et al., 2010)] and ingestion of significant bolus doses (Manach et al., 2005); as opposed to consumption of anthocyanin-containing foodstuffs as part of a normal diet (and with potential influence of other dietary components).

Low bioavailability of anthocyanin glycosides has been reported across many human studies (Table 1.4), with rapid excretion (6-8 hours) and little of the ingested dose appearing in urine (McGhie and Walton, 2007). Moreover, the time to maximal plasma concentration is relatively short, and has been suggested to reflect absorption of anthocyanins across the gastric mucosa (Passamonti et al., 2002, Passamonti et al., 2003). Recently, Czank *et al* (2013) have reported bioavailability data from an isotope tracer human study, wherein 500mg of ^{13}C-labelled cyandin-3-glucoside was consumed as a single bolus by eight healthy male volunteers (Czank et al., 2013); and excretion of ^{13}C-labelled anthocyanin and metabolites in urine, faeces, and breath was monitored over a 48 hour period. In this study, Czank *et al* (2013) described a C_{max} of 0.14µmol/L for ^{13}C-labelled cyanidin-3-glucoside at 1.8 hours post ingestion (Czank et al., 2013).

Anthocyanin glycosides are apparently absorbed and excreted intact (Manach et al., 2005), but glucuronidated, methylated and sulphated metabolites have been detected (Kay et al., 2004, Kay et al., 2005, Wiczkowski et al., 2010, Wallace, 2011) and phenolic acid/aldehyde degradation products and/or metabolites are reported at levels exceeding the parent glycoside (Vitaglione et al., 2007, de Pascual-Teresa et al., 2010, Azzini et al., 2010, Czank et al., 2013). After ingestion of 500mg ^{13}C-labelled cyanidin-3-glucoside by fasted volunteers, the serum concentration of degradants of the parent anthocyanin (protocatechuic acid and phloroglucinol aldehyde) peaked at 0.72µmol/L (T_{max} 6 hours), whilst phase II conjugates of the degradant protocatechuic acid (including methylated, glucuronidated and sulphated metabolites) reached a collective C_{max} of 2.35µmol/L (T_{max} 13 hours) (Czank et al., 2013).

Possible mechanisms of flavonoid absorption in the small intestine have been summarised previously; namely transport of intact glucoside through the active sodium-dependent glucose transporter (SGLT1) with subsequent hydrolysis by cytosolic B-glucosidase; or hydrolysis by brush-border lactase phloridzin hydrolase (LPH) and aglycone entry by passive diffusion (Kay, 2006, Crozier et al., 2009, Del Rio et al., 2013). Similar mechanisms are thought to be involved in the absorption of the large, polar anthocyanin molecules (McGhie and Walton, 2007), although this has yet to be fully elucidated (Kay, 2006), and the instability of liberated aglycones (anthocyanidins) at alkaline (intestinal) pH must also be considered (Fleschhut et al., 2006, McGhie and Walton, 2007, Woodward et al., 2009). Faria *et al* (2009) have reported transport of anthocyanins extracted from red grape skin through cultured caco-2 cells potentially involving the GLUT2 glucose transporter, though with

low efficiency (Faria et al., 2009). Moreover, anthocyanins have been shown *in vitro* to interact with the organic anion membrane transporter bilitranslocase, which is expressed in gastric epithelium and the basolateral region of liver plasma membrane (Passamonti et al., 2002). Gastric absorption of anthocyanins has been demonstrated from the stomach of anesthetised rats, potentially mediated by bilitranslocase (Passamonti et al., 2003), but direct evidence for a similar mechanism in humans is as yet unavailable (Kay, 2006).

Table 1.4 Summary of key pharmacokinetic data derived from selected human bioavailability studies of anthocyanins.

Material consumed	Anthocyanin dose (total intake; mg)	Maximal plasma concentration/ C_{max} (nmol/L)	Time to maximal plasma concentration/ T_{max} (hours)	Urinary excretion (% of intake)	Reference
Blackcurrant	236	115[a]	1.25 - 1.75	0.11 (8 hours)	(Matsumoto et al., 2001)
Blackcurrant juice (330 ml)	1000	3.5 - 51[b]	1.0	0.032 – 0.046[b]	(Rechner et al., 2002)
Blood orange juice	~26.5	0.63[c]	0.96[c]	-	(Giordano et al., 2012)
Blueberry powder (100 g)	1200	29	4.0	-	(Mazza et al., 2002)
Chokeberry extract (7.1 g)	721	96	2.8	0.15 (24 hours)	(Kay et al., 2004)
Chokeberry juice	60[d]	32.7	1.3	0.25 (24 hours)	(Wiczkowski et al., 2010)
Elderberry extract (12 g)	720	97	1.2	0.06 (24 hours)	(Milbury et al., 2002)
Grape juice	238µM	1.0 - 2.0[e]	1.3 - 3.3[e]	0.26 (24 hours)	(Stalmach et al., 2012)
Red grape juice (500 ml)	117[f]	2.8	2.0	0.02 (6 hours)	(Bub et al., 2001)
Strawberries (fresh)	~9.57	0.0[g]	-	0.9 (24 hours)	(Azzini et al., 2010)

[a]Total for four anthocyanin species. [b]According to anthocyanin considered in mixture. [c]Data tabulated for cyanidin-3-glucoside only. [d]Dose of 0.8mg anthocyanins per kg, estimated for 75kg body weight. [e]Range for four anthocyanin species detected in plasma. [f]Malvidin-3-glucoside. [g]No traces of parent anthocyanins or conjugated metabolites detected in plasma samples.

Whilst uptake of nutrients is typically associated with the small intestine, the colon is also capable of absorption of compounds, and is likely to be of particular relevance to anthocyanins (McGhie and Walton, 2007, Williamson and Clifford, 2010). Studies involving individuals who have undergone an ileostomy (where the colon has been excised and the ileum is drained into an affixed exterior pouch) suggest that a proportion of ingested anthocyanins transit the small intestine unchanged, and

therefore reach the colon (Williamson and Clifford, 2010, Gonzalez-Barrio et al., 2010, Stalmach et al., 2012). Moreover, the colon contains an extensive microbial population, as the majority of microorganisms populating the gastrointestinal tract are located in the distal region (Williamson and Clifford, 2010). Therefore unabsorbed anthocyanins may be degraded by colonic microflora to generate smaller aromatic molecules, which are then absorbed (Williamson and Clifford, 2010). Czank *et al* (2013) have estimated elimination half-lives of between 12.44 ± 4.22h and 51.62 ± 22.55h for ^{13}C-labelled phenolic metabolites of cyanidin-3-glucoside, which could partly reflect prolonged colonic production and absorption of these species (Czank et al., 2013). Potential enterocyte pathways of anthocyanin absorption are illustrated in Figure 1.6.

Figure 1.6 Putative mechanisms for intestinal absorption of anthocyanins into portal circulation.

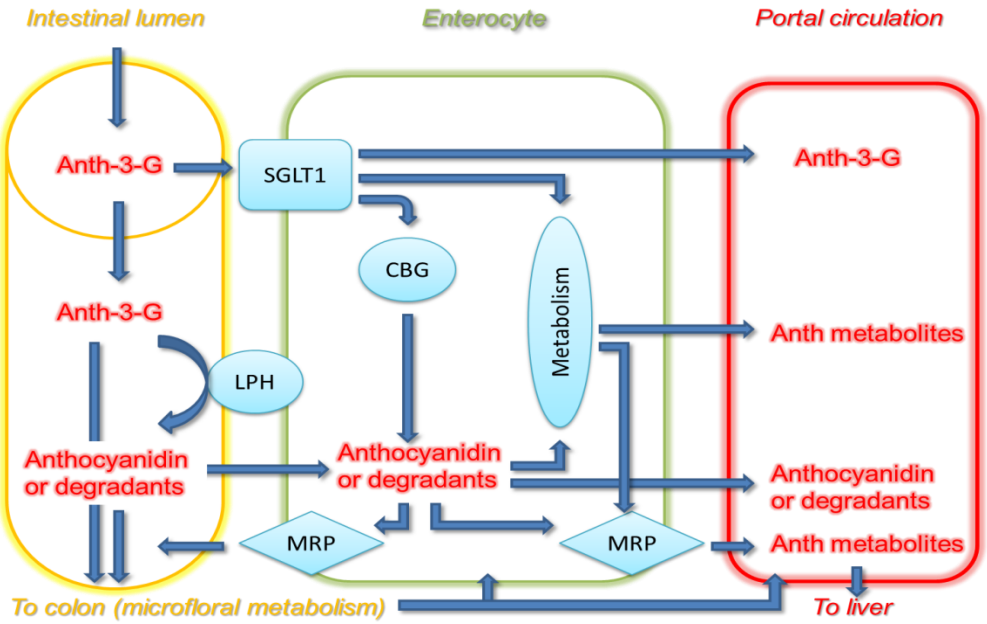

Putative mechanisms of anthocyanin-3-glycoside (**Anth-3-G**) intestinal absorption, based on (Walle, 2004, Kay, 2006). **SGLT1**, sodium-dependent glucose transporter; **LPH**, lactase phloridzin hydrolase; **CBG**, cytosolic-B-glucosidase; **MRP**, multi-drug resistance protein; **Anthocyanidin or degradants**; aglycone or phenolic acid/aldehyde degradation products; **Anth metabolites**, sulphated, glucuronidated or methylated metabolites of parent glycoside or degradation products.

Hepatic, and subsequently renal, biotransformation may further modify absorbed compounds, for example methylation or conjugation with glucuronic acid or sulphate (McGhie and Walton, 2007, Grassi et al., 2009). Czank *et al* (2013) identified 24 isotope-labelled metabolites following ingestion of ^{13}C-labelled cyanidin-3-glucoside by healthy volunteers; including phase II conjugates of cyanidin and cyanidin-3-glucoside, phenolic degradants of cyanidin (protocatechuic acid and phloroglucinol aldehyde), and phase II metabolites of protocatechuic acid (including vanillic acid, isovanillic acid, glucuronides & sulphates of protocatechuic acid, and glucuronides & sulphates of vanillic and

isovanillic acid) (Czank et al., 2013). Phase II conjugates of cyanidin-3-glucoside were only detected in urine (Czank et al., 2013).

Human elimination of anthocyanins has also been described by Czank *et al* (2013) as part of the aforementioned tracer study, with excretion of the ^{13}C label detected in urine (~5% of ^{13}C dose recovered), faeces (~32% of ^{13}C dose recovered), and breath (~7% of ^{13}C dose recovered) over a 48 hour period (Czank et al., 2013). A minimum relative bioavailability of ~12% for cyanidin-3-glucoside was calculated based upon these elimination data for breath and urine (Czank et al., 2013). Urinary excretion of anthocyanins has been reported by a number of other human intervention studies, and as already noted low urinary recovery of ingested dose is documented (typically < 1%) (Perez-Jimenez et al., 2010). This may reflect substantial conversion of ingested anthocyanins to unmeasured phenolic or aromatic metabolites (Kay, 2006) as discussed above. Any compounds subject to biliary excretion [more probable for large conjugates (Wang and Ho, 2009)] may be metabolised by intestinal microflora and subsequently reabsorbed, leading to enterohepatic recycling and continued presence within the body; as described for quercetin (Wang and Ho, 2009, Grassi et al., 2009) (Figure 1.7).

Figure 1.7 Scheme of pathways for anthocyanin absorption, metabolism and excretion.

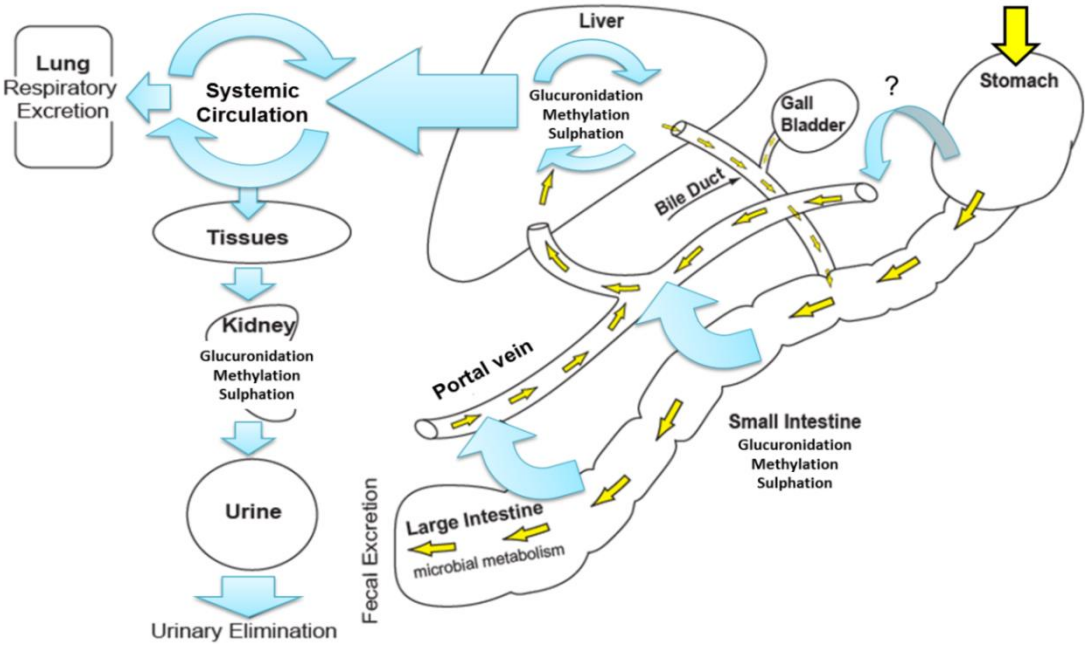

Routes of anthocyanin absorption and biotransformation within the body, adapted from (Kay, 2006). '**?**' denotes unconfirmed pathways in humans.

In summary, low bioavailability of parent anthocyanin glycosides is likely to reflect *in vivo* degradation and/or colonic metabolism to previously unmeasured phenolic and aromatic metabolites; and these metabolites may be responsible for the perceived bioactivity of anthocyanins (Williamson and Clifford, 2010, Wallace, 2011, Czank et al., 2013).

1.4 Bioactivity of anthocyanins and metabolites

1.4.1 Background and experimental data

Whilst molecular species mediating potential anthocyanin bioactivity *in vivo* are not yet fully elucidated, epidemiological studies suggest dietary consumption of anthocyanins is associated with beneficial effects on cardiovascular function (Erdman et al., 2007, Mink et al., 2007, Cassidy et al., 2010, Wallace, 2011, Jennings et al., 2012). Indeed, a considerable body of epidemiological data indicates an inverse association between intake of flavonoid-rich dietary components and CVD risk (Hertog et al., 1993, Geleijnse et al., 2002, Erdman et al., 2007); and a substantial intake of anthocyanins might be achieved by daily consumption of grapes and berries, or derived beverages (Manach et al., 2005, Wu et al., 2006b). Biological activity of anthocyanins has been investigated in a number of *in vitro* and animal studies with relevance to mechanisms of cardiovascular disease, such as effects on eNOS and endothelial function/reactivity (de Pascual-Teresa et al., 2010, Wallace, 2011). For example, Andriambeloson *et al* (1997, 1998) reported endothelium-dependent vasorelaxation of rat thoracic aortic rings elicited by red wine polyphenolic compounds (Andriambeloson et al., 1997), and anthocyanin-enriched fractions of red wine polyphenolic compounds (Andriambeloson et al., 1998). A similar study was conducted by Fitzpatrick *et al*, which demonstrated endothelium-dependent vasorelaxant activity of grape skin extracts, grape juice, and several wines (Fitzpatrick et al., 1993).

Experimental data in support of cardioprotective effects of anthocyanins is elucidated below; however, the physiological relevance of compounds and dose thereof utilised for *in vitro* investigations must always be considered (Crozier et al., 2009). In particular, prolonged incubation of cultured cells with anthocyanin glycosides at physiological pH is likely to result in formation of degradation products (Kay et al., 2009, Woodward et al., 2009), which may mediate observed bioactivity. Likewise, phenolic and aromatic metabolites may constitute the bioactive form of anthocyanins *in vivo* (de Pascual-Teresa et al., 2010, Czank et al., 2013, Del Rio et al., 2013).

Endothelium-derived NO is a key mediator of vascular homeostasis, most significantly through its role as endothelium-derived relaxing (vasodilatation) factor (EDRF); impairment of which is a critical step in the development of atherosclerosis (Kawashima and Yokoyama, 2004, Higashi et al., 2009). Bell and Gochenaur reported dose-dependent relaxation of isolated porcine coronary arterial rings elicited by chokeberry and bilberry extracts (using concentrations of 0.005 - 5mg total anthocyanins/L), in an endothelium-dependent response which was ablated by inhibition of eNOS (Bell and Gochenaur, 2006). Moreover, impairment of endothelium-dependent vasorelaxation, caused by pre-incubation with a superoxide-generating agent, was attenuated with concurrent pre-incubation using chokeberry, bilberry and elderberry extracts (0.05mg total anthocyanins/L) (Bell and

Gochenaur, 2006). More recently, Ziberna *et al* (2013) examined the importance of the bilitranslocase membrane transporter for anthocyanin-induced endothelium- and NO-dependent vasorelaxation (as confirmed by removal of endothelium or NOS inhibition) in excised rat thoracic aortic rings (Ziberna et al., 2013). Pre-incubation of aortic rings with rabbit polyclonal anti-bilitranslocase antibodies elicited a significant reduction in vasorelaxation induced by cyanidin-3-glucoside (1nM - 10μM), and a bilberry anthocyanin extract (0.01 - 20mg/L as equivalents of cyanidin-3-glucoside) (Ziberna et al., 2013). These data suggest a potential role for bilitranslocase-mediated membrane transport in the mechanism of anthocyanin-induced NO-dependent vasorelaxation (Ziberna et al., 2013).

Upregulation of eNOS by anthocyanins in bovine artery endothelial cells (BAECs) has also been described for malvidin-3-glucoside (Paixão et al., 2012) and cyanidin-3-glucoside (Xu et al., 2004b, Xu et al., 2004a). Incubation of BAECs with 25μM malvidin-3-glucoside for 14 hours resulted in significantly increased eNOS mRNA levels (Paixão et al., 2012); whilst cyanidin-3-glucoside at 1 - 100nM elicited a dose-dependent upregulation in eNOS protein expression, with the maximal increase measured after treatment with 100nM cyanidin-3-glucoside for eight hours (Xu et al., 2004b). Activation of cell signalling proteins Src kinase and ERK 1/2 kinase [ERK, extracellular signal regulated protein kinase (Robinson and Cobb, 1997)] was involved in eNOS upregulation, as measured by cyanidin-3-glucoside stimulated phosphorylation of these kinases and use of kinase inhibitors (Xu et al., 2004b). Moreover, 500nM cyanidin-3-glucoside was shown to rapidly regulate eNOS activity through phosphorylation of eNOS at Serine 1179, and dephosphorylation at Serine 116, in BAECs (Xu et al., 2004a).

With regard to anthocyanin bioactivity in human cells, Lazzè *et al* (2006) have described the effects of aglycone cyanidin and delphinidin on the expression of eNOS, and the vasoconstrictor protein ET-1, in cultured HUVECs (Lazze et al., 2006). Significant decreases in ET-1 secretion, and increases in eNOS protein level, were measured following 24 hour incubations with 100μM cyanidin, and 50μM or 100μM delphinidin (Lazze et al., 2006). However, the instability of anthocyanidins at physiological pH must be noted (Woodward et al., 2009), in conjunction with the supraphysiological or pharmacological levels of anthocyanidins to which cells were exposed (Crozier et al., 2009). Malvidin (at 0.1μM) (Quintieri et al., 2013), cyanidin-3-glucoside (2.3μg/ml; ~5μM), and delphinidin-3-glucoside (5.8μg/ml; ~12μM) (Edirisinghe et al., 2011) have also been reported to activate eNOS in HUVECs, as determined by phosphorylation of Serine 1177. Therefore anthocyanins, or their degradation products and/or metabolites *in vivo*, could increase both eNOS expression and activity; with enhanced endothelial function resulting from increased NO production (Wallace, 2011).

It is interesting to note that for dietary flavanols, inhibition of NADPH oxidase activity, with reduced scavenging of NO by generated superoxide anion, has been suggested as a 'short-term' mechanism

for enhanced NO bioavailability (Schewe et al., 2008); based upon structure-activity studies of (-)-epicatechin and its metabolites in a HUVEC model of angiotensin II-stimulated superoxide production (Steffen et al., 2007b, Steffen et al., 2008). Mono-*O*-methylation of a flavonoid catechol B-ring, or presence of a 4'-OH group only at the B-ring (refer to Figure 1.1 and Figure 1.2), are reported to confer NADPH oxidase inhibitory activity (Steffen et al., 2008). This is of structural significance for anthocyanins containing a catechol B-ring susceptible to methylation (cyanidin), or an existing mono-methylated catechol B-ring (peonidin), or a 4'-OH B-ring (pelargonidin) (refer to Figure 1.3 and Figure 1.5) (Cassidy et al., 2010). Moreover, the vasoactive compound apocynin, which incorporates a mono-methylated catechol group, is reported to decrease NOX activity by inhibiting the association of the $p47^{phox}$ subunit (refer to section 1.4.5) with membrane-associated subunits (Stolk et al., 1994, Drummond et al., 2011). Downregulation of $p47^{phox}$ by the flavonol quercetin, which contains a catechol B-ring, has been described in aortic rings from spontaneously hypertensive rats (Sanchez et al., 2006); and in rat aortic rings following stimulation with ET-1 (Romero et al., 2009), and angiotensin II (Sanchez et al., 2007). It should also be noted that cyanidin-3-glucoside (at 6.25nM - 6.25µM, and 62.5 - 250µM) upregulated expression of the enzyme haem oxygenase isoform 1 (HO-1), which demonstrates protective activities against cellular oxidative stress [(Ryter et al., 2002), refer to section 1.4.6], in human iliac artery endothelial cells following a 24 hour incubation period with this anthocyanin (Sorrenti et al., 2007).

Expression and/or activation of adhesion molecules on endothelial cells and circulating inflammatory cells is a key process in the recruitment of leucocytes to sites of inflammation (Granger et al., 2004); and anthocyanins may act to modulate this response to pro-inflammatory stimuli (Wallace, 2011, Chen et al., 2011a). For example, blueberry and cranberry anthocyanins have been reported to reduce tumour necrosis factor-alpha (TNF-α)-induced expression of intercellular adhesion molecule 1 (ICAM-1) by human microvascular endothelial cells (Youdim et al., 2002); whilst cyanidin-3-glucoside inhibited gene expression of endothelial cell adhesion molecules ICAM-1, vascular cell adhesion molecule 1 (VCAM-1), and E-selectin, in a TNF-α-stimulated HUVEC model (Speciale et al., 2010). Wang *et al* (2010) have also investigated the effects of protocatechuic acid on monocyte adhesion to murine endothelial cells, and atherosclerotic development in a mouse model (Wang et al., 2010a). Pre-treatment of mouse aortic endothelial cells (MAECs) with protocatechuic acid for 24 hours elicited a significant reduction in human monocyte adhesion to TNF-α activated MAECs. In addition, protocatechuic acid partially inhibited TNF-α-stimulated expression of VCAM-1 and ICAM-1 expression by MAECs (Wang et al., 2010a).

Overall, data from both animal studies and cell culture experiments suggest a variety of biological mechanisms by which anthocyanins, or their degradation products/metabolites, could elicit cardioprotective effects *in vivo*; with effects on NO bioavailability of particular significance.

Anthocyanin bioactivity *in vivo* is likely to be mediated by derivatives of ingested parent compounds, and as noted *in vitro* studies may not reflect physiologically relevant doses - or exposures - to bioactive molecules.

1.4.2 Anthocyanins and cardiovascular disease

Cardiovascular disease arises from disorders of the heart and vasculature, as manifested in pathophysiologies such as peripheral arterial disease, cerebrovascular disease (stroke), and CHD (de Pascual-Teresa et al., 2010, WHO, 2013). It is responsible for almost half of all deaths in Europe annually (Chong et al., 2010), and it is estimated that approximately 23.3 million people will die owing to CVDs by 2030 (WHO, 2013). Epidemiological data have associated consumption of flavonoid-rich foodstuffs with decreased risk of CVD (Vita, 2005, Wallace, 2011); and anthocyanin intake has been inversely related to mortality owing to CHD and CVD (Mink et al., 2007, McCullough et al., 2012, Cassidy et al., 2013) and relative risk of hypertension (Cassidy et al., 2010). A review of human dietary intervention studies by Chong *et al* (2010) indicated that fruits such as berries and purple grapes (with relatively high content of anthocyanins, flavonols and procyanidins) appeared more effective, as compared to other fruits studied, at reducing CVD risk; particularly with regard to anti-hypertensive activity, elevation of endothelium-dependent vasodilatation, and inhibition of platelet aggregation (Chong et al., 2010). In a recent study, consumption of a blueberry drink by healthy volunteers elicited increased endothelial-dependent vasodilation (measured as flow-mediated dilatation) relative to control, in a biphasic and dose-dependent response (Rodriguez-Mateos et al., 2013). Moreover, ingestion of a daily supplement of 320mg anthocyanins over 12 weeks by hypercholesterolaemic individuals was reported to significantly enhance endothelial function compared to placebo treatment, in a double-blind parallel group intervention (Zhu et al., 2011). However, not all studies support this protective association (Curtis et al., 2009, Jin et al., 2011, Hassellund et al., 2012, Riso et al., 2013, Del Bo et al., 2013); for example, Del Bo *et al* (2013) found no improvement in peripheral vascular function one hour after consumption of a single portion of blueberries (~348mg anthocyanins) by healthy subjects in a randomised cross-over intervention; which the authors noted may be partly attributable to the population studied (Del Bo et al., 2013).

In order to appreciate potential mechanisms of anthocyanin bioactivity in CVD, it is necessary to review briefly the pathophysiology of atherosclerosis, which underlies atherosclerotic cardiovascular disease and the concomitant morbidity and mortality arising from complications of this disease (Leopold and Loscalzo, 2009). Endothelial dysfunction forms an early part of the development of atherosclerosis (Vita and Keaney, 2002, Widlansky et al., 2003, Higashi et al., 2009), and anthocyanins or their *in vivo* bioactive derivatives may act to modulate molecular mechanisms underlying this disordered function.

1.4.3 Atherosclerosis, endothelial dysfunction, and effects of anthocyanins

Atherosclerosis is a chronic inflammatory disease (Libby et al., 2002), which occurs principally in medium and large-sized elastic and muscular arteries (Ross, 1999, Vita, 2005), and has been associated with areas of disturbed blood flow such as arterial bifurcations (Ross, 1999, Libby et al., 2002, Leopold and Loscalzo, 2009). The disease is characterised by localised thickening within the sub-intimal (endothelial) region of the arterial wall (Figure 1.8) (Ross, 1999, Bonomini et al., 2008) giving rise to progressive lesions termed plaques, which ultimately intrude into the arterial lumen (Bonomini et al., 2008). Advanced lesions may be of sufficient size to impair blood flow; but rupture of the fibrous cap of such lesions, or ulceration of the plaque, can lead to platelet-rich thrombosis [as the thrombogenic sub-endothelium is exposed to circulating blood (Vita, 2005)] and partial or total arterial occlusion (Ross, 1999, Vita, 2005, Bonomini et al., 2008). This is manifested clinically as infarction or ischaemia, such as myocardial infarction or stroke (Vita, 2005, Bonomini et al., 2008).

Figure 1.8 Overview of structure of the arterial wall

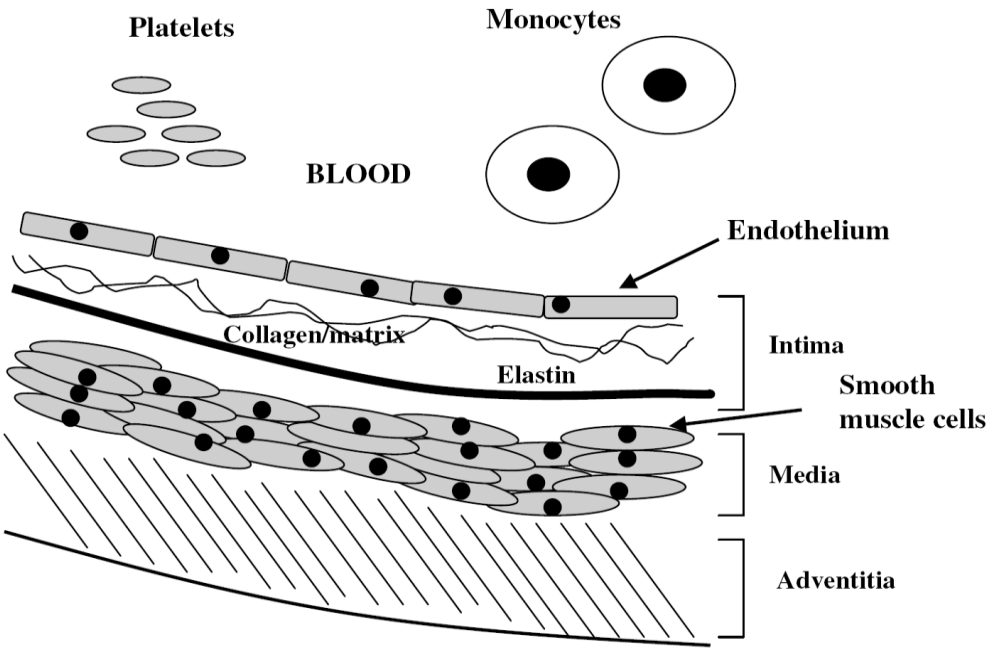

Structure of the arterial wall, and key cell types involved in the development of atherosclerosis [adapted from (Naseem, 2005)].

Dysfunction of the vascular endothelium is the initial process in the development of atherosclerosis (Landmesser et al., 2004, Higashi et al., 2009); in particular reduced bioavailability of NO from eNOS and impairment of endothelium-dependent relaxation (Kawashima and Yokoyama, 2004) through stimulation of soluble guanylate cyclase in vascular smooth muscle cells by NO (Hobbs et al., 1999, Michel and Vanhoutte, 2010). Nitric oxide also inhibits expression of cell surface adhesion molecules VCAM-1 (located on endothelium), ICAM-1 (located on endothelium and leucocytes) and P-selectin

(located on endothelium and platelets) and monocyte chemoattractant protein-1 (derived from endothelial cells); thereby reducing leucocyte recruitment, adhesion and extravasation (Ross, 1999, Granger et al., 2004, Naseem, 2005, Michel and Vanhoutte, 2010). Furthermore, NO acts to inhibit platelet activation and aggregation, proliferation of vascular smooth muscle cells (VSMC), and oxidation of low density lipoprotein (LDL; by scavenging of lipid radicals); all of which are important processes in atherogenesis (Kawashima and Yokoyama, 2004, Naseem, 2005, Michel and Vanhoutte, 2010). Experimental data suggest that loss of NO is linked to increased adhesion of leucocytes to vascular endothelium, and subsequent infiltration into the arterial wall; representing an essential step in the formation of atherosclerotic lesions (Wever et al., 1998, Landmesser et al., 2004, Granger et al., 2004). Likewise, clinical data indicate an association between coronary endothelial dysfunction (as assessed by endothelium-dependent vasodilatation) and cardiovascular events in patients with coronary artery diseases (Vita and Keaney, 2002, Higashi et al., 2009).

Endothelium-derived NO thus has anti-atherosclerotic activity (Wever et al., 1998, Naseem, 2005, Förstermann and Sessa, 2012), and any reduction in NO bioavailability can enhance inflammatory processes underlying atherosclerosis (Landmesser et al., 2004, Michel and Vanhoutte, 2010). This may arise from decreased production of NO by eNOS (whether by down-regulation of enzyme expression or loss of activity); or increased reaction of NO with ROS leading to loss of NO signalling [(Landmesser et al., 2004, Naseem, 2005, Higashi et al., 2009), refer also to section 1.2.3]. The primary mechanism for loss of NO in many vascular pathologies is thought to be by reaction with $O_2^{\cdot-}$, to form the potent oxidant $^{-}$ONOO (Wever et al., 1998, Naseem, 2005). The rate of this reaction is nearly diffusion-limited (6.7×10^{-9} M/s), and is approximately three times faster than the dismutation of $O_2^{\cdot-}$ by SOD (2.0×10^{-9} M/s) (Wever et al., 1998). Under normal physiological conditions, the estimated concentration of $O_2^{\cdot-}$ (10^{-9} - 10^{-12} M) relative to NO (10 - 300nM) is insufficient to drive formation of $^{-}$ONOO (Wever et al., 1998, Naseem, 2005); but increased vascular superoxide production has been associated with risk factors for atherogenesis (such as hypertension and hypercholesterolaemia) and cardiovascular disease states (Wever et al., 1998, Landmesser et al., 2004, Kawashima and Yokoyama, 2004, Naseem, 2005, Higashi et al., 2009). NADPH oxidase enzymes constitute a major source of ROS in the vasculature (Zalba et al., 2000, Touyz, 2004, Bedard and Krause, 2007, Bonomini et al., 2008), and inhibition of NOX may serve to enhance NO levels in an acute effect (Steffen et al., 2008, Schewe et al., 2008).

The activity of eNOS and NOX is thus of great importance in the development of endothelial dysfunction (Kawashima and Yokoyama, 2004, Landmesser et al., 2004, Higashi et al., 2009); and modulation of these enzymes by anthocyanins, or their *in vivo* metabolites, may underlie reported cardioprotective activity (Wallace, 2011). Given the importance of NO in maintenance of vascular homeostasis (Higashi et al., 2009), improving NO bioavailability should enhance vascular function

(Cassidy et al., 2010), and anthocyanins may act to upregulate eNOS expression and activity (Xu et al., 2004b, Xu et al., 2004a, Edirisinghe et al., 2011, Paixão et al., 2012). Moreover, anthocyanins and/or metabolites could attenuate superoxide production by NOX; with reduced scavenging of NO by generated ROS (Schewe et al., 2008), based on structural similarities with other flavonoids demonstrating inhibition of NOX activity (Schewe et al., 2008, Cassidy et al., 2010).

1.4.4 Activity of endothelial nitric oxide synthase & effects of anthocyanins

Nitric oxide is generated by the family of haem-containing NOS enzymes, through the oxidation of L-arginine (Arg) to produce NO and L-citrulline, in an oxygen- and NADPH-dependent reaction (Hobbs et al., 1999). Three mammalian isoforms of NOS have been characterised, namely neuronal (nNOS or NOS I), inducible (iNOS or NOS II) and endothelial (eNOS or NOS III) (Michel and Vanhoutte, 2010, Förstermann and Sessa, 2012). Endothelial NOS is constitutively expressed in most endothelial cells (particularly in conductance arteries) (Fleming and Busse, 2003) and a number of other cell types, including fibroblasts, lymphocytes and neutrophils (Villanueva and Giulivi, 2010). Functional eNOS is a homodimer of approximately 260 kDa, and requires binding of Ca^{2+}/calmodulin (CaM) [an allosteric effector (Michel and Vanhoutte, 2010)] for activation (Hobbs et al., 1999, Fleming and Busse, 2003), in addition to the essential cofactors tetrahydrobiopterin (BH_4), flavin mononucleotide (FMN) and flavin adenine dinucleotide (FAD) (Fleming and Busse, 2003) (Figure 1.9). An N-terminus consensus sequence for myristoylation/palmitoylation confers membrane association on eNOS, particularly with plasma membrane caveolae [lipid microenvironments or 'rafts' containing caveolin integral membrane proteins (Simons and Toomre, 2000)] (Hobbs et al., 1999, Fleming and Busse, 2003).

Figure 1.9 Representation of eNOS homodimer and associated cofactors

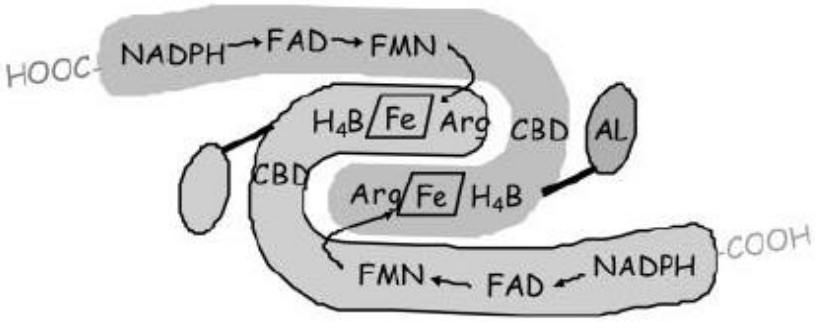

Structure of eNOS homodimer, with arrows indicating electron flow between monomers to haem (Fe) moiety [adapted from (Fleming and Busse, 2003)]. AL, auto-inhibitory loop; Arg, arginine; CBD, CaM binding domain; FAD, flavin adenine dinucleotide; FMN, flavin mononucleotide; H_4B, tetrahydrobiopterin; NADPH, reduced nicotinamide adenine dinucleotide phosphate.

Activity of eNOS is stimulated by agonists such as bradykinin or acetylcholine, which is coupled to increased intracellular Ca^{2+}/$[Ca^{2+}]_i$ (Shaul, 2002, Fleming and Busse, 2003); or by fluid shear stress resulting from the flow of blood over endothelial cells, which is apparently independent of a sustained increase in $[Ca^{2+}]_i$ (Shaul, 2002, Fleming and Busse, 2003, Higashi et al., 2009, Förstermann and Sessa, 2012). However, shear stress is reported to elicit differential effects on eNOS, according to the type of stress applied to blood vessels (Leopold and Loscalzo, 2009). Laminar (unidirectional) shear stress, which predominates in straight vessel segments, induces elevated eNOS activity and upregulation of enzyme expression, thereby limiting oxidative stress (Boo and Jo, 2003, Leopold and Loscalzo, 2009). In contrast, oscillatory shear stress, created by turbulent blood flow at arterial bifurcations, results in downregulation of eNOS; with upregulation and increased activation of NOX and xanthine oxidase (Hwang et al., 2003, McNally et al., 2003, Hsiai et al., 2007). Many of the physiological effects of generated NO result from binding of NO to the haem moiety of the soluble guanylate cyclase enzyme, causing increased enzyme activity and formation of the intracellular second messenger molecule cyclic guanosine monophosphate (cGMP) (Hobbs et al., 1999, Michel and Vanhoutte, 2010).

Two amino acid residues of the eNOS protein appear to be of particular importance as key regulatory sites through protein phosphorylation and/or dephosphorylation; specifically Ser (serine)^{1177} (human eNOS; Ser^{1179} bovine eNOS) in the C-terminal reductase domain [so called as this region of the protein closely resembles cytochrome P450 reductase (Hobbs et al., 1999)], and Thr (threonine)^{495} (human eNOS; Thr^{497} bovine eNOS) within the CaM binding domain (Fleming and Busse, 2003). Phosphorylation at Ser^{1177} is mediated by kinases including Akt/protein kinase B (PKB), protein kinase A (PKA), and the AMP-activated protein kinase (AMPK), according to stimuli applied to endothelial cells (Shaul, 2002); and results in increased NO production (two to three-fold over basal) by enhanced electron flow through the reductase domain (Fleming and Busse, 2003). By contrast, Thr^{495} appears to be constitutively phosphorylated in endothelial cells [probably by protein kinase C (PKC)], and acts as a negative regulatory site; in that phosphorylation interferes with CaM binding, and dephosphorylation [possibly by protein phosphatase-1 (PP1)] results in a significantly increased NO generation over basal levels (Fleming and Busse, 2003). Other sites of eNOS phosphorylation which may affect enzyme activity include Ser^{114}/Ser^{116} and Ser^{633}/Ser^{635} (human/bovine eNOS respectively) (Fleming and Busse, 2003).

Production of NO may be attenuated by increased levels of ROS, owing to oxidative degradation of the essential eNOS cofactor BH_4 (Landmesser et al., 2004), which leads to 'uncoupling' of eNOS, with reduced generation of NO and increased production of $O_2^{\cdot-}$ by the enzyme (Kawashima and Yokoyama, 2004, Naseem, 2005) (Figure 1.10). Endothelial NOS activity could also be reduced by a local deficiency of L-arginine (Förstermann and Sessa, 2012); or elevated levels of the circulating

endogenous NOS inhibitor asymmetric dimethylarginine (ADMA), owing to ROS-induced inhibition of the enzyme dimethylarginine dimethylaminohydrolase (DDAH) (Landmesser et al., 2004), which metabolises ADMA (Naseem, 2005). Oxidised LDL (oxLDL) may act to reduce expression of eNOS, although a consensus has yet to be reached given contradictory *in vivo* and *in vitro* data (Wever et al., 1998, Naseem, 2005), but there is evidence for lipoprotein-induced disruption of eNOS associated with caveolae and subsequent attenuation of signalling (Shaul, 2002, Naseem, 2005). Of interest, regenerated endothelial cells, which replace apoptotic endothelial cells following cell death, demonstrate diminished endothelium-dependent relaxations to agonists (such as thrombin and serotonin) which activate eNOS through a signalling cascade using the G_i G-protein [heterotrimeric GTP-dependent signal transduction protein (Tesmer, 2010)] (Michel and Vanhoutte, 2010). Regenerated endothelium may therefore exhibit selective dysfunction of eNOS signalling, which appears to be an initial step in the process of atherosclerosis (Michel and Vanhoutte, 2010).

Figure 1.10 Putative scheme for eNOS 'uncoupling' in conditions of oxidative stress

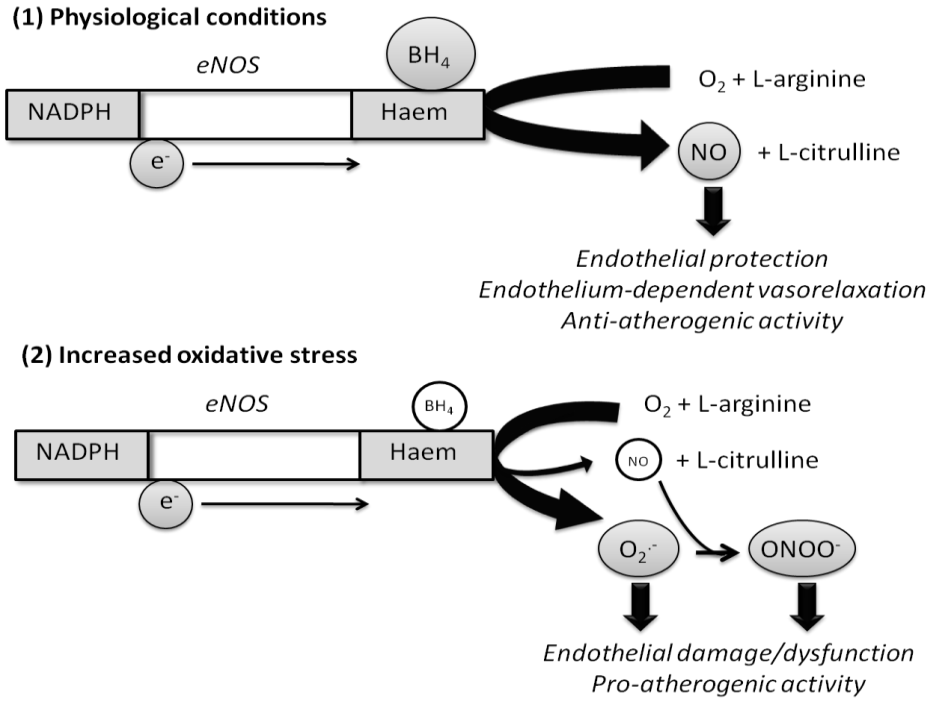

Possible mechanism for eNOS 'uncoupling' arising from increased oxidative stress. (1) Under physiological conditions, NO generated by eNOS mediates endothelial protection and vascular homeostasis. (2) When oxidative stress is increased, decreased tissue levels of the essential cofactor BH_4 results in uncoupling of eNOS, with reduced generation of NO and increased production of $O_2^{\cdot-}$. Superoxide, and peroxynitrite derived from scavenging of NO by $O_2^{\cdot-}$, can elicit deleterious effects on endothelial function [figure adapted from (Kawashima and Yokoyama, 2004)]. e^-, electron flow to haem moiety of eNOS.

With regard to anthocyanin modulation of eNOS activity, and as discussed in section 1.4.1, anthocyanins have demonstrated endothelium- and NO-dependent vasorelaxant activity in studies utilising excised porcine (Bell and Gochenaur, 2006) and rat (Ziberna et al., 2013) arterial rings.

Moreover, chokeberry, bilberry and elderberry extracts were able to attenuate impairment of endothelium-dependent vasorelaxation induced by a superoxide-generating agent (Bell and Gochenaur, 2006). Xu *et al* (2004) reported upregulation of eNOS expression by cyanidin-3-glucoside, involving activation of Src and ERK 1/2 kinases, in BAECs (Xu et al., 2004b); and stimulation of eNOS activity (through phosphorylation at Ser^{1179} and dephosphorylation at Ser^{116}) by cyanidin-3-glucoside in the same cell line (Xu et al., 2004a). Increased expression of eNOS protein was also demonstrated in HUVECs following incubation with cyanidin and delphinidin aglycones (Lazze et al., 2006), and both cyanidin-3-glucoside and delphinidin-3-glucoside elicited activation of eNOS in human vascular endothelial cells (Edirisinghe et al., 2011). Therefore anthocyanins, or their degradation products and/or metabolites *in vivo*, could increase both eNOS expression and activity; with enhanced endothelial function resulting from increased NO bioavailability (Wallace, 2011).

1.4.5 Activity of NADPH oxidase & effects of anthocyanins

The predominant source of ROS in the vasculature is, as previously noted, generally identified as the family of NADPH oxidase or NOX enzymes (Cai et al., 2003, Sumimoto et al., 2005, Leopold and Loscalzo, 2009); of which the original member is the phagocyte NADPH oxidase [$gp91^{phox}$/NOX2; 'phox' denotes **ph**agocyte **ox**idase (Lassegue and Clempus, 2003)] (Bedard and Krause, 2007). NADPH oxidase enzymes are transmembrane proteins which transfer electrons across biological membranes to an acceptor molecule, usually oxygen, thereby generating superoxide anion (Lassegue and Clempus, 2003, Bedard and Krause, 2007) although one NOX isoform produces mainly hydrogen peroxide (Altenhofer et al., 2012, Streeter et al., 2013) (Figure 1.11).

Six mammalian isoforms of the NOX2 protein have been identified and cloned, namely NOX1 (previously mox-1 or NOH-1), NOX3, NOX4, NOX5; and dual oxidases (DUOX) 1 and 2 (originally thyroid oxidases) (Sumimoto et al., 2005, Bedard and Krause, 2007). Assembly of a functional enzyme complex may require, according to the NOX isoform, association of additional protein components; however, all NOX isoforms share several conserved structural features (Bedard and Krause, 2007). These features comprise a cytoplasmic C-terminus with FAD and NADPH binding domains, six putative transmembrane domains (TMDs) (with an additional N-terminal TMD present in DUOX1 & 2), and two highly conserved histidine residues in both TMD III and TMD V (IV and VI for DUOX1 & 2) which bind two haem molecules between these domains (Bedard and Krause, 2007). The proposed topology of NOX subunits indicates that generated superoxide is released into intracellular vesicles or the extracellular space, although superoxide might pass into the cytoplasm through membrane organic anion channels (Lassegue and Clempus, 2003, Bedard and Krause, 2007).

Figure 1.11 Proposed transmembrane topology of NOX protein

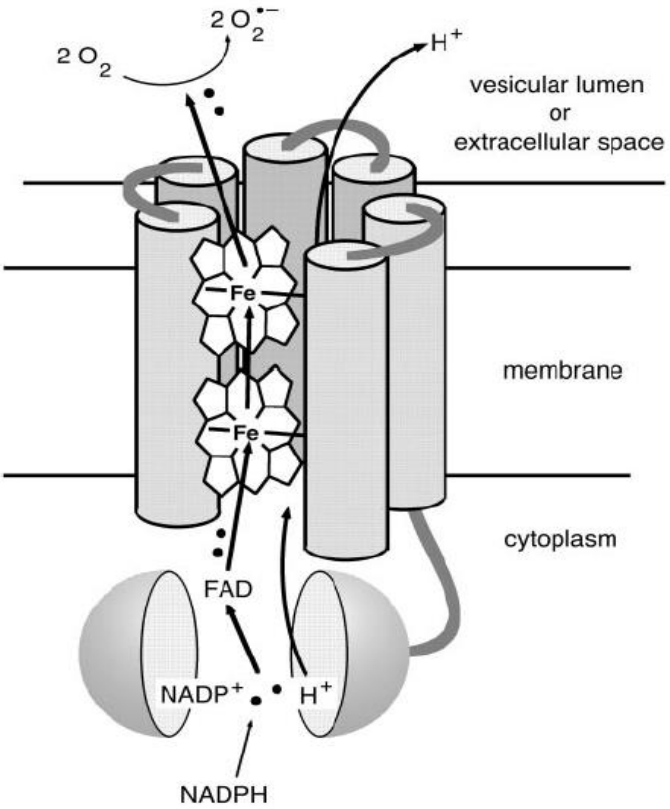

Proposed membrane topology for six transmembrane domain NOX protein, with C-terminal FAD and NADPH binding domains, and two haem (Fe) molecules bound between the third and fifth transmembrane domains (refer to text). '•' denotes electron transfer from electron donor (NADPH) to acceptor (O_2/oxygen) molecule; 'H^+' shows proton conductance to give electrical balance [adapted from (Lassegue and Clempus, 2003)].

NADPH oxidase isoform 2 represents the prototype NADPH oxidase, and has been extensively investigated (Lassegue and Clempus, 2003, Bedard and Krause, 2007). The relative molecular mass (RMM) for human NOX2 is ~ 70-90 kDa, and represents a highly glycosylated protein (Bedard and Krause, 2007). NOX2 constitutively associates with the integral membrane protein $p22^{phox}$, predicted to contain two TMDs, to form a stable complex termed cytochrome b_{558} (Sumimoto et al., 2005) (Figure 1.12). $p22^{phox}$ also serves as a site of interaction with cytoplasmic regulatory proteins (Bedard and Krause, 2007); specifically the 'organiser' subunit $p47^{phox}$ (Sumimoto et al., 2005). Phosphorylation of $p47^{phox}$ [by a number of serine kinases, including protein kinase C (PKC) (Brandes et al., 2010) or the c-Src tyrosine kinase (Cai et al., 2003)] is thought to induce a conformational change permitting association with $p22^{phox}$, and membrane localisation of $p47^{phox}$ elicits translocation of the cytoplasmic proteins $p67^{phox}$ (the NOX 'activator' subunit) and $p40^{phox}$ (an adaptor subunit which may not be essential for enzyme function) to the enzyme complex (Sumimoto et al., 2005, Bedard and Krause, 2007). The small cytoplasmic G-protein Rac forms the final part of the complex, initially interacting with NOX2 and subsequently with $p67^{phox}$, creating a functional enzyme

(Sumimoto et al., 2005, Bedard and Krause, 2007). As noted, NOX2 is the phagocyte NADPH oxidase; responsible for the microbicidal 'oxidative burst' of superoxide (and derived ROS) during phagocytosis by cells such as neutrophils and monocytes/macrophages (Lassegue and Clempus, 2003, Sumimoto et al., 2005). In addition to high levels of expression in phagocytes, NOX2 is expressed at lower levels in cardiovascular tissues including cardiomyocytes, endothelium, and smooth muscle (notably resistance vessel smooth muscle) (Bedard and Krause, 2007).

Figure 1.12 Proposed structure of NOX2 (gp91^{phox}) in association with p22^{phox}

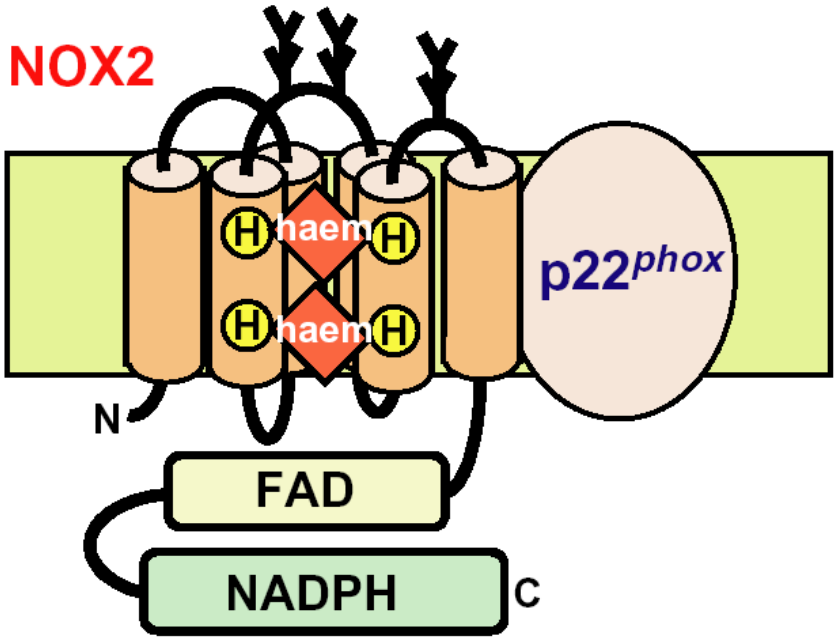

Proposed membrane topology of the glycosylated, haem-binding NOX2 protein (gp91^{phox}), shown in association with the integral membrane protein p22phox. 'H' denotes histidine residue, 'N' and 'C' refer to protein N- and C-termini respectively [adapted from (Sumimoto et al., 2005)].

Whilst NOX isoforms display a similar structure and function (Bedard and Krause, 2007), the mechanism of enzyme activation, and tissue distribution of protein, are distinct (Sumimoto et al., 2005, Bedard and Krause, 2007). Vascular ROS generation by NOX enzymes represents activity of several isoforms, and arterial expression of NOX1, NOX2, NOX4 and NOX5 has been reported; although relative abundance of isoforms varies according to cell type and location (Bedard and Krause, 2007). In contrast to the large quantities of superoxide produced by phagocytes during the oxidative burst (Cai et al., 2003), the rate of superoxide production in vascular cells has been estimated as ~ 1 – 10% of leucocyte activity (Lassegue and Clempus, 2003).

NOX1 is expressed at high levels in colon epithelial cells (Sumimoto et al., 2005); and at lower levels in both vascular endothelium, and smooth muscle cells (mainly in large conduit vessels) (Bedard and Krause, 2007). Activity of NOX1 requires the p22^{phox} subunit [though the enzyme may function in the

absence of this subunit (Sumimoto et al., 2005)], and the cytoplasmic proteins NOX organiser 1 (NOXO1; a homologue of $p47^{phox}$), NOX activator 1 (NOXA1; a homologue of $p67^{phox}$) and Rac (Sumimoto et al., 2005, Bedard and Krause, 2007). However, $p47^{phox}$ may act as a NOX1 subunit in the vasculature (Bedard and Krause, 2007). By contrast NOX4, which is abundantly expressed in the kidney and vascular endothelium (Sumimoto et al., 2005), does not require cytosolic subunits for enzyme activity (Brown and Griendling, 2009); but is associated with $p22^{phox}$ (Bedard and Krause, 2007) and may be regulated by polymerase δ-interacting protein 2 (POLDIP2) (Drummond et al., 2011). NOX4 appears to be constitutively active (Brandes et al., 2010), generating predominantly hydrogen peroxide (Sumimoto et al., 2005, Bedard and Krause, 2007, Brown and Griendling, 2009, Brewer et al., 2011); and immunoblotting has detected two bands for NOX4 protein at 75-80 kDa and 65 kDa, perhaps indicating protein glycosylation (Bedard and Krause, 2007). Finally, NOX5 [~ 85 kDa protein by immunoblotting (Bedard and Krause, 2007)] appears to form a functional enzyme without additional subunits, and is activated by Ca^{2+}; possibly by association with Ca^{2+}-binding sites ('EF-hands') present in an extended N-terminal region [though several variants of NOX5 have been described, one of which lacks this motif (Bedard and Krause, 2007)] (Sumimoto et al., 2005). NOX5 is highly expressed in lymphocytes, and to a lesser extent in vascular endothelium (Sumimoto et al., 2005, Bedard and Krause, 2007). Figure 1.13 illustrates the formation of a functional enzyme complex for NOX1, NOX2, NOX4 and NOX5 [adapted from (Drummond et al., 2011)].

In summary, NOX isoforms 1, 2, 4 and 5 are reported to be expressed in vascular endothelium (Leopold and Loscalzo, 2009), with NOX4 apparently the predominant isoform (Ago et al., 2004); by contrast, NOX1 and NOX4 are the principal isoforms in vascular smooth muscle cells (Bedard and Krause, 2007). Activity of NOX can be induced by a variety of stimuli, including mechanical forces and hormones (Cai et al., 2003), several of which may have relevance in the development of atherosclerosis; such as vascular oscillatory shear stress, inflammatory cytokines, and angiotensin II (Ang II) (Leopold and Loscalzo, 2009). Angiotensin II, an octapeptide hormone, is an important stimulus for activation of vascular NOXs (Cai et al., 2003); and subsequent oxidative stress with loss of NO activity (Dzau, 2001). The Ang II receptor [AT_1 receptor (Cai et al., 2003)] and Ang II are localised in regions of inflammation in human atherosclerotic lesions (Dzau, 2001); and Ang II induced NOX activity is one of the major sources of ROS in atherosclerosis (Higashi et al., 2009). Furthermore, increased expression of NOX subunits ($p22^{phox}$, $p47^{phox}$, and $p67^{phox}$) and NOX5 has been described in isolated coronary arteries from patients with established atherosclerosis (Guzik et al., 2006, Guzik et al., 2008).

Figure 1.13 **Proposed transmembrane structure, and associated proteins forming enzyme complex, for NOX isoforms 1, 2 4 and 5**

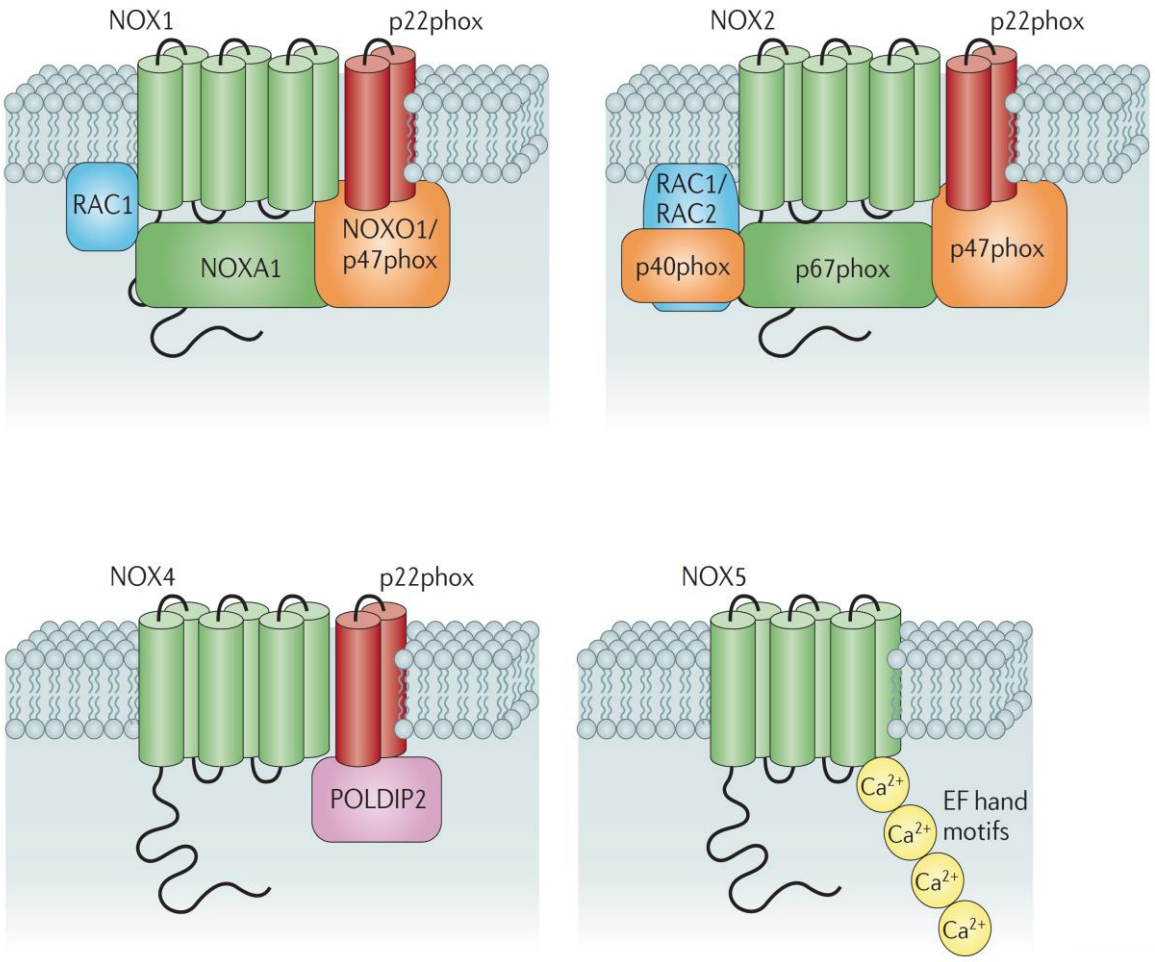

Proposed membrane topology, and associated proteins forming enzyme complex, for NOX isoforms 1, 2, 4 and 5. Both NOX1 and NOX2 associate with $p22^{phox}$ and cytoplasmic proteins, as detailed in text, to produce a functional enzyme complex; phosphorylation of the 'organiser' subunit $p47^{phox}$ is required for NOX2 activity. NOX4 associates with $p22^{phox}$ and may be regulated by POLDIP2; whereas NOX5 appears to be functional without additional subunits and is activated by Ca^{2+} [figure adapted from (Drummond et al., 2011)].

However, it should be noted that NOX isoforms may have distinct functions *in vivo* (Anilkumar et al., 2008, Schroder, 2010, Brandes et al., 2011, Touyz and Montezano, 2012); in that overexpression of endothelium-targeted NOX4 in transgenic mice resulted in enhanced histamine and acetylcholine-induced vasodilatation, through increased production and activity of H_2O_2 (Ray et al., 2011). Indeed, a recent study has suggested a key role for NOX4-derived hydrogen peroxide in eliciting eNOS activation in response to laminar shear stress in bovine aortic endothelial cells (Breton-Romero et al., 2012). Furthermore, Brewer *et al* (2011) have reported that overexpression of NOX4 in cardiomyocytes (using a transgenic mouse model) elicited activation of the transcription factor Nrf2 [nuclear factor-erythroid 2-related factor 2 (Pendyala et al., 2011), refer also to section 1.4.6], and

subsequent upregulation of transcription of a number of antioxidant/detoxification enzymes (Brewer et al., 2011). By contrast, superoxide anions generated through the activity of NOX1 and NOX2 in vascular pathophysiologies can react with NO to form peroxynitrite [a reaction which cannot occur with H_2O_2 (Brandes et al., 2011)], reducing NO bioavailability and leading to uncoupling of eNOS through oxidation of BH_4 by peroxynitrite [(Schroder, 2010, Brandes et al., 2011), refer also to section 1.4.4]. Elevated NOX2 activation, in association with impaired endothelial function (as measured by flow-mediated dilatation), has been reported for patients with peripheral artery disease as compared to control subjects (Loffredo et al., 2013); whereas inherited mutations in the *CYBB* gene encoding NOX2, which underlie most cases of the immunodeficiency pathology termed chronic granulomatous disease/CGD (Drummond et al., 2011), have been associated with enhanced flow-mediated dilatation in a multi-centre study involving 25 CGD patients (Violi et al., 2009).

As discussed in section 1.4.1, inhibition of NOX activity, with decreased scavenging of NO by generated $O_2^{\cdot-}$, has been proposed as a 'short-term' mechanism by which dietary flavanols may enhance NO bioavailability and thereby improve vascular function (Schewe et al., 2008). Structure-activity studies of (-)-epicatechin, and its metabolites, in a HUVEC model of angiotensin II-stimulated superoxide production (Steffen et al., 2007b, Steffen et al., 2008) identified a mono-*O*-methylated flavonoid catechol B-ring (refer to section 1.2.2), or a B-ring with a 4'-OH group only, as structural configurations conferring NOX inhibitory activity [(Steffen et al., 2008, Cassidy et al., 2010), Figure 1.1 and Figure 1.2]. This is of particular significance for anthocyanins, or their B-ring phenolic acid degradation products (refer to Figure 1.5), which contain a catechol B-ring subject to methylation by COMT (such as cyanidin) or an existing mono-methylated catechol B-ring (peonidin); or a 4'-OH B-ring (pelargonidin) [(Cassidy et al., 2010), Figure 1.3 and Figure 1.5]. Thus, anthocyanins could potentially act to increase NO bioavailability *in vivo* by both direct (upregulation/activation of eNOS) and indirect [NOX inhibition with reduced scavenging of NO by $O_2^{\cdot-}$, and possibly decreased oxidative degradation of eNOS cofactor BH_4 (Kawashima and Yokoyama, 2004)] mechanisms; thus improving vascular endothelium function (refer to sections 1.4.3 and 1.4.4). It is interesting to note that methylation of protocatechuic acid (the B-ring degradation product of cyanidin-3-glucoside) by COMT has also been reported as a key process for perceived bioactivity, in a study of potential anti-anginal mechanisms in the rat heart (Cao et al., 2009). Moreover, downregulation of the key $p47^{phox}$ subunit, as elicited by quercetin (containing a catechol B-ring) and its mono-methylated metabolite (Sanchez et al., 2006, Sanchez et al., 2007, Romero et al., 2009, Davalos et al., 2009), may represent a potential mechanism by which anthocyanins or their phenolic degradants could inhibit NOX activity. Indeed, a recent report by Lim *et al* (2013) has described inhibition of ultraviolet light (UV) subtype B-induced $p47^{phox}$ membrane translocation by the anthocyanidin delphinidin (at 10 or 20µM) in human dermal fibroblasts (Lim et al., 2013).

1.4.6 Activity of haem oxygenase & effects of anthocyanins

Haem oxygenase (HO) catalyses the oxidative catabolism of haem in an oxygen- and NADPH-dependent reaction (Ryter et al., 2002, Ryter et al., 2006), and constitutes the rate-limiting enzyme in the haem degradation pathway (Abraham and Kappas, 2008). Activity of HO generates equimolar quantities of the bile pigment biliverdin-IXα (rapidly reduced to bilirubin-IXα by cytosolic biliverdin reductase), free ferrous (Fe^{2+}) iron (immediately bound by the protein ferritin), and carbon monoxide (CO) (Siow et al., 1999, Ryter et al., 2002, Ryter et al., 2006, Abraham and Kappas, 2008) (Figure 1.14). Haem oxygenase is expressed as inducible (HO-1) and constitutive (HO-2) isoenzymes, with molecular masses of 32 kDa and 34 kDa respectively (Abraham and Kappas, 2008). With regard to subcellular localisation, HO-1 is known to associate with the endoplasmic reticulum, and both isoenzymes may be localised to the rough endoplasmic reticulum and membrane caveolae (Ryter et al., 2006).

Figure 1.14 Oxidative catabolism of haem by haem oxygenase

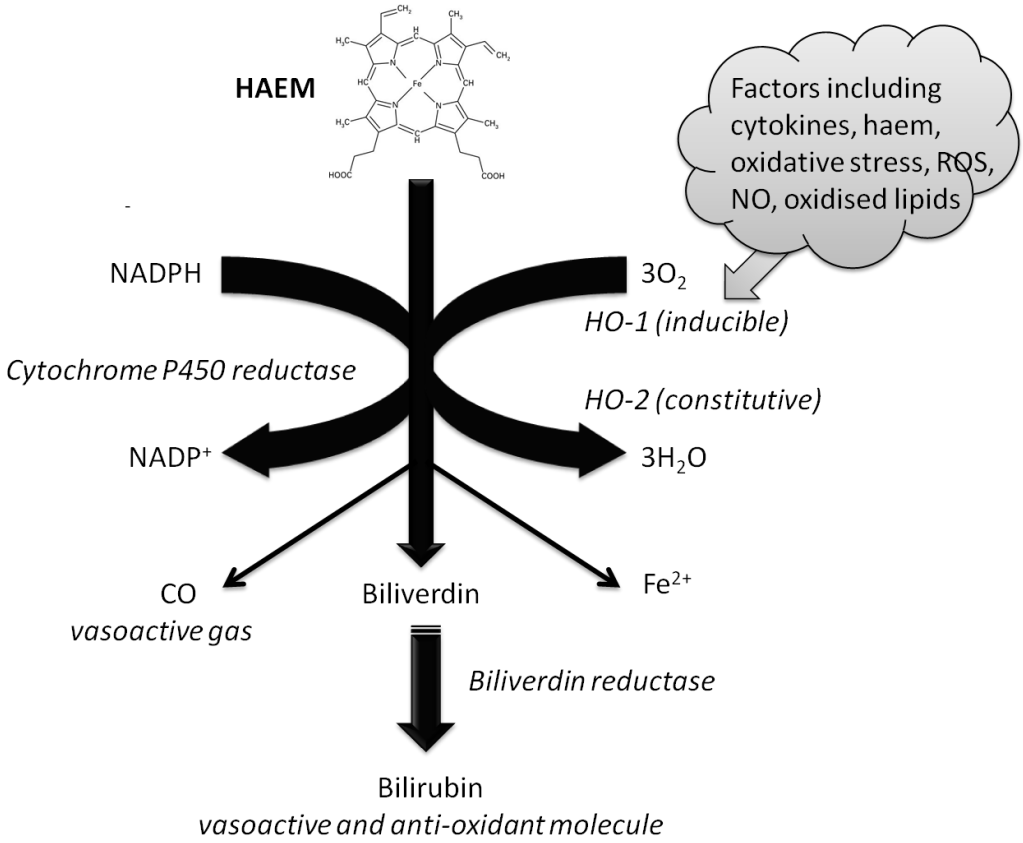

Degradation of haem by haem oxygenase (inducible and constitutive isoforms) yielding biliverdin (converted to bilirubin), ferrous iron (sequestered by ferritin) and CO gas [figure adapted from (Abraham and Kappas, 2008)].

Expression of HO-1 is activated by binding of the transcription factor Nrf2 to antioxidant response elements (AREs) or electrophile response elements (EpREs) located in the promoter regions of genes encoding antioxidant or detoxification enzymes such as HO-1, in response to oxidative stress (Pi et

al., 2010, Maher and Yamamoto, 2010). HO-1 demonstrates protective activity against cellular oxidative stress (Siow et al., 1999, He et al., 2010), which may be mediated in part by activity of generated CO (Chan et al., 2011). Moreover, biliverdin and bilirubin display potent antioxidant activity *in vitro* (Ryter et al., 2002). Induction of HO-1 can be stimulated in both animal tissues, for example vascular endothelium and smooth muscle (Siow et al., 1999), and many types of cells in culture (including endothelial cells), by exposure to haem and factors such as metals, pro-inflammatory cytokines and growth factors, xenobiotics, NO, oxidised lipids and oxidative stress (Ryter et al., 2002, Abraham and Kappas, 2008). Agents capable of inducing HO-1 expression may modulate intracellular redox balance, and/or elicit formation of ROS, by direct or indirect mechanisms; thus elevated HO-1 levels could serve as a marker of cellular oxidative stress (Ryter et al., 2002).

Carbon monoxide derived from HO activity [representing approximately 80% of CO produced *in vivo* (Abraham and Kappas, 2008)] is reported to have anti-inflammatory, anti-apoptotic, and anti-proliferative effects (Ryter et al., 2002, Abraham and Kappas, 2008, Chan et al., 2011). Akin to NO, CO can interact with soluble guanylate cyclase, resulting in enhanced generation of the intracellular second messenger cGMP (Siow et al., 1999); though CO is considerably less potent relative to NO (Chan et al., 2011). This signalling pathway may underlie subsequent vasodilatory (Idriss et al., 2008, Chan et al., 2011) and anti-thrombotic activity attributed to HO-derived CO (Ryter et al., 2006). Vasodilatation might also be effected by CO through stimulation of K^+ channel activity (Chan et al., 2011). Furthermore, CO can inhibit lipopolysaccharide (LPS)-induced expression of inflammatory cytokines such as TNF-α, by activation of p38 MAPK (Ryter et al., 2002), and may influence the activity of haemoproteins such as NOX and iNOS (Ryter et al., 2002, Abraham and Kappas, 2008). Bilirubin generated from haem degradation, by reduction of HO-1 derived biliverdin, is reported to inhibit NOX activity (Jiang et al., 2006, Datla et al., 2007) possibly by interruption of enzyme assembly and activation (refer also to section 1.4.5); and to preserve eNOS expression in human aortic endothelial cells following stimulation with oxLDL or TNF-α (Kawamura et al., 2005). In addition, bilirubin can act to inhibit expression of cell adhesion molecules and adhesion of neutrophils (Ryter et al., 2006, Abraham and Kappas, 2008), of significance with regard to the development of atherosclerosis (Granger et al., 2004). It should be noted that pro-atherogenic stimuli (such as angiotensin II and oxidised LDL) can induce HO-1 in endothelial and vascular smooth muscle cells (Ryter et al., 2006); and evidence from both animal models and clinical studies indicates that HO-1 activity may have protective effects on the cardiovascular system (Idriss et al., 2008, Chan et al., 2011). For example, Yet *et al* (2003) examined the formation of hypercholesterolaemia-induced atherosclerotic lesions in HO-1 and apolipoprotein E (ApoE)-deficient mice, and observed increased size and severity of lesions compared with those induced in ApoE-deficient mice expressing HO-1 (Yet et al., 2003). Additionally, in a cross-sectional study of 91 healthy subjects, Erdogan *et al* (2006)

reported an association between reduced serum bilirubin levels, and decreased flow-mediated dilatation (indicating impaired endothelial function) and increased carotid artery intima-media thickness (an index of atherosclerosis); suggesting lower bilirubin concentrations were inversely associated with an elevated risk of atherosclerosis (Erdogan et al., 2006).

Regarding activity of anthocyanins on HO expression, cyanidin-3-glucoside has been reported to upregulate expression of HO-1 in human iliac artery endothelial cells (Sorrenti et al., 2007), and serum samples obtained from healthy subjects following ingestion of 160mg purified anthocyanins elicited Nrf2 nuclear translocation and HO-1 expression in cultured HUVECs (Cimino et al., 2013). Moreover, delphindin-3-glucoside has previously been reported to enhance survival of murine hepatocytes exposed to a cytotoxic concentration of epigallocatechin-3-gallate through upregulation of HO-1 mRNA levels (Inoue et al., 2012); and Hwang *et al* (2011) have described protection against dimethylnitrosamine-induced hepatic fibrosis in rats elicited by an anthocyanin fraction purified from purple sweet potato, mediated in part through expression of Nrf2-regulated genes including HO-1 (Hwang et al., 2011). Therefore, activation of Nrf2-mediated expression of HO-1 and other antioxidant enzymes by anthocyanins could enhance protection against oxidative stress in endothelial cells.

1.5 Summary and concluding remarks

It is hoped that the foregoing review has illustrated not only current knowledge regarding anthocyanin availability in foodstuffs, dietary intake, and bioavailability/bioactivity; but also areas where, to date, limited or no data are available. As discussed in section 1.3.1, the high content of anthocyanins found in berries and grapes suggests a substantial daily intake of anthocyanins might be achieved by consumption of these foods, and derived beverages (such as fruit juices) (Manach et al., 2005, Zamora-Ros et al., 2011). Indeed, 400 - 500mg of anthocyanins could be consumed in one serving (Kay et al., 2009). Moreover, epidemiological data indicate consumption of flavonoid-rich foodstuffs is inversely associated with CVD risk (Erdman et al., 2007, Geleijnse and Hollman, 2008, Wallace, 2011); whilst dietary intake of anthocyanins has been inversely related to arterial stiffness (Jennings et al., 2012), hypertension (Cassidy et al., 2010), and CHD & CVD morbidity and mortality [(Mink et al., 2007, McCullough et al., 2012, Cassidy et al., 2013), refer also to section 1.4.2]. Data from animal and *in vitro* studies, as discussed in sections 1.4.1 and 1.4.2 - 1.4.5, suggest anthocyanins may act to increase NO bioavailability; for example as measured by endothelium- and NO-dependent vasorelaxation (Bell and Gochenaur, 2006, Ziberna et al., 2013). This could be effected directly by upregulation/stimulation of eNOS (Xu et al., 2004b, Xu et al., 2004a, Lazze et al., 2006, Edirisinghe et al., 2011, Paixão et al., 2012), or potentially indirectly by inhibition of endothelial NOX and reduced scavenging of NO by generated superoxide [(Cassidy et al., 2010), refer also to sections 1.4.4 & 1.4.5]; with beneficial effects on vascular endothelial (and thus cardiovascular) function, given the role of

endothelium-derived NO as a key mediator of vascular homeostasis (Kawashima and Yokoyama, 2004). Anthocyanins, or derived species, might also act to increase expression of haem oxygenase-1 (Sorrenti et al., 2007, Cimino et al., 2013) with resultant protection against cellular oxidative stress (He et al., 2010).

However, and as noted previously, the physiological relevance of compounds and doses examined in animal and *in vitro* studies must always be considered (Crozier et al., 2009, Wallace, 2011). Phenolic acid/aldehyde degradation products and/or metabolites have been reported in human plasma/serum at higher levels than parent glycoside(s) following ingestion of anthocyanins (Vitaglione et al., 2007, Azzini et al., 2010, Czank et al., 2013), and are likely to mediate the observed bioactivity (Wallace, 2011). Indeed, Czank *et al* (2013) have reported a 42-fold greater abundance of metabolites in the systemic circulation relative to the parent anthocyanin in a human tracer study (Czank et al., 2013).

In conclusion, future research into vascular bioactivity of anthocyanins must use not only parent glycosides, but also identified *in vivo* degradants and metabolites, and all species should be assayed at physiologically relevant concentrations. The capacity of anthocyanins and derived species to inhibit NOX activity and upregulate eNOS at physiologically relevant levels should be examined in a vascular endothelial cell model (as described in Chapters 2 & 3 respectively), as structurally similar compounds have demonstrated NOX inhibitory activity (Steffen et al., 2008, Cassidy et al., 2010). Investigating the molecular mechanisms by which anthocyanins, or their bioactive derivatives, may modulate key vascular enzymes is essential in understanding the potential cardioprotective effects of anthocyanins, as increased consumption of dietary anthocyanins might represent a simple measure to reduce the relative risk of CVD.

1.6 Hypothesis and aims of present thesis

It is hypothesised that the reported vasoprotective properties of anthocyanins may be elicited by their *in vivo* degradation products and metabolites, which act by directly stimulating eNOS expression and activity, and/or indirectly through inhibiting NOX function and reducing scavenging of NO by generated ROS; ultimately elevating NO levels and enhancing vascular function. The aims of the current thesis were therefore as follows: firstly, to compare the *in vitro* vascular bioactivity of selected parent anthocyanins with their phenolic acid degradation products, by screening physiologically relevant concentrations (0.1, 1, 10μM) for effects on eNOS expression and activity, and angiotensin II-stimulated superoxide production by NOX, in human vascular endothelial cells (Chapters 2 & 3); secondly, to explore the potential for interactions between a parent anthocyanin, or its phenolic acid degradation product, with other dietary bioactive compounds often present in sources of anthocyanins such as berries and berry-derived juices, by screening treatment

combinations (at cumulative concentrations of 0.1, 1, 10μM) for effects on eNOS expression and activity, and angiotensin II-stimulated superoxide production by NOX, in human vascular endothelial cells (Chapters 2 & 3); thirdly, to investigate cellular and molecular mechanisms potentially underlying observed reductions in stimulated endothelial superoxide production (Chapter 2) by using a selected degradation product (vanillic acid, at 0.1, 1, 10μM) to explore modulation of stimulated expression of NOX isoforms and subunits, and expression of HO-1 (as a possible indirect mechanism of NOX inhibition), in human venous and arterial endothelial cells (Chapters 4 - 6).

2 Modulation of angiotensin II-induced superoxide production by anthocyanin glucosides and phenolic acid degradants

2.1 Background

Impairment of vascular endothelial function, in particular reduced bioavailability of nitric oxide (NO), is a critical stage in the development of atherosclerosis (Kawashima and Yokoyama, 2004, Higashi et al., 2009). Loss of NO in vascular pathologies may be primarily mediated by reaction with superoxide anion ($O_2^{\cdot-}$) (Wever et al., 1998, Naseem, 2005), an important source of which is vascular NADPH oxidase or NOX enzymes (Bonomini et al., 2008, Higashi et al., 2009). NOX4 is reported to be the predominant isoform expressed in the vascular endothelium (Bedard and Krause, 2007) and appears to generate hydrogen peroxide (Brown and Griendling, 2009); whilst NOX2 generates superoxide anion (Brandes et al., 2010), and is thought to be of considerable importance in the regulation of human vascular function by reducing NO bioavailability (Brown and Griendling, 2009, Schroder, 2010). Inhibition of NOX activity has been proposed as a mechanism by which specific flavonoids may increase NO bioavailability, thereby improving vascular function (Schewe et al., 2008).

Anthocyanins, or their phenolic acid degradants, which contain a catechol or mono-*O*-methylated B-ring (Figure 2.1) might demonstrate NOX inhibitory activity; based upon structural similarities with the vasoactive compound apocynin (Cassidy et al., 2010), and structure-activity studies of the flavanol (-)-epicatechin (Steffen et al., 2007b, Steffen et al., 2008). In the current investigation, selected anthocyanin glucosides and their phenolic acid degradants (Figure 2.1 A) were screened to examine their effect on angiotensin II-stimulated superoxide production by endothelial NOX, using a previously reported assay (Rueckschloss et al., 2002, Steffen et al., 2007a, Steffen et al., 2007b, Steffen et al., 2008) which was optimised as detailed herein. Anthocyanins which contained a 3', 4'-catechol B-ring susceptible to methylation [cyanidin, Figure 2.1 A **(1)**, and its B-ring degradant protocatechuic acid, **(2)**], or an existing 3'-mono-methylated catechol B-ring [peonidin, **(3)** and its B-ring degradant vanillic acid, **(4)**], or a modified methylated catechol B-ring structure [petunidin, **(5)**, malvidin, **(6)**, and the B-ring degradant of malvidin, syringic acid, **(7)**] were selected for bioactivity screening. Two combination treatments of cyanidin-3-glucoside, or protocatechuic acid, in combination with the flavonol quercetin [Figure 2.1 B **(8)**], epicatechin **(9)**, and ascorbic acid [vitamin C, **(10)**] were also examined; representing commonly occurring bioactive compounds in foods and derived juices (Levine et al., 1999, Manach et al., 2005) and thus reflecting dietary intake of a range of flavonoids.

Cytotoxicity of the selected treatment compounds was assessed prior to bioactivity screening, to confirm that these compounds were not cytotoxic at the concentrations utilised. The production of

superoxide anion by endothelial NOX was stimulated using angiotensin II, and quantified by concomitant one electron reduction of ferricytochrome c reagent; in the absence and presence of superoxide dismutase [which catalyses dismutation of superoxide to hydrogen peroxide (Forman et al., 2002)] to determine the level of cytochrome c reduced by generated superoxide. Finally, endothelial cell lysates generated during bioactivity screening were analysed by immunoblotting to investigate possible modulation of expression of NOX2 and NOX4 isoforms by anthocyanin phenolic acid degradants; as degradants or metabolites may mediate at least part of anthocyanin bioactivity *in vivo* (Williamson and Clifford, 2010).

Figure 2.1 Treatment compounds for vascular bioactivity screening.

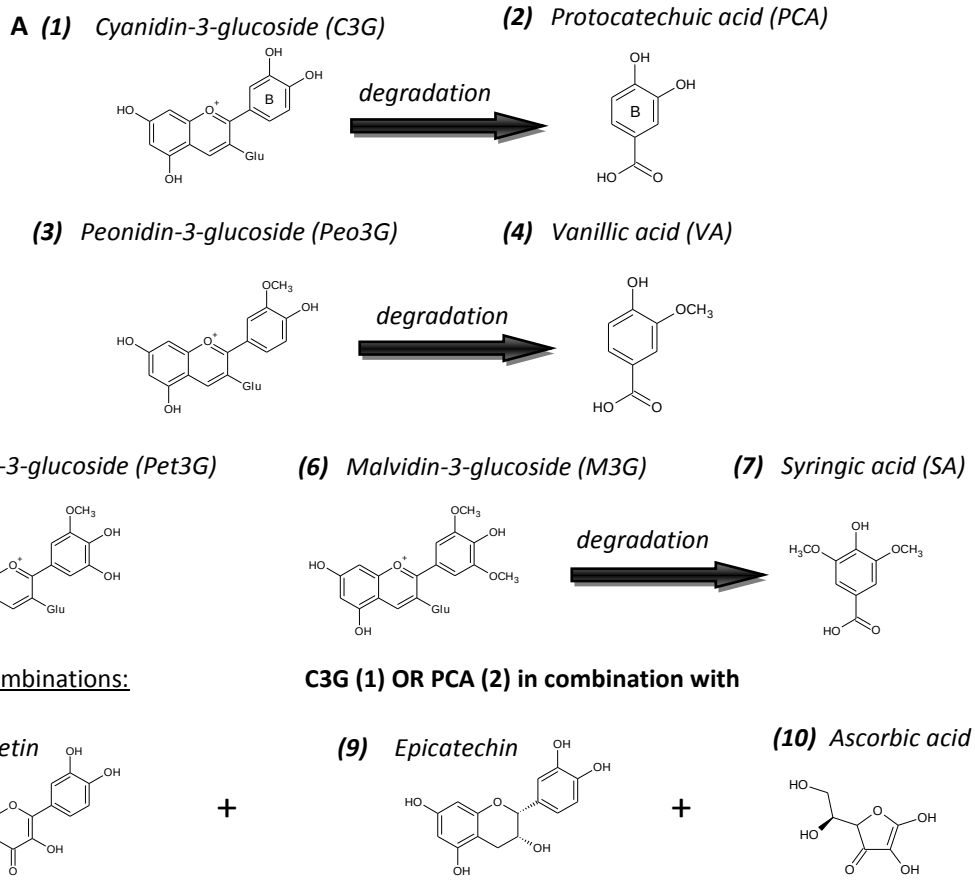

2.2 Materials and methods

Standards and reagents. Cyanidin-3-glucoside, peonidin-3-glucoside and malvidin-3-glucoside were purchased from Extrasynthese (Genay Cedex, France); petunidin-3-glucoside from Polyphenols Laboratories AS (Sandnes, Norway); VAS2870 from Enzo Life Sciences [Exeter, United Kingdom (UK)]; and protocatechuic acid, vanillic acid, syringic acid, (-)-epicatechin, quercetin and L-ascorbic acid from Sigma-Aldrich [Poole, United Kingdom (UK)]. Standard solutions were prepared in 100% dimethylsulphoxide (DMSO) from Sigma-Aldrich (molecular biology grade) at concentrations of 40mM for anthocyanins and 200mM for all other treatment compounds. Cell proliferation reagent

WST-1 was obtained from Roche Applied Science (Burgess Hill, UK). Human angiotensin II (synthetic), bovine serum albumin (BSA), (octylphenoxy)polyethoxyethanol (IGEPAL® CA-630), bovine erythrocyte superoxide dismutase (SOD), bovine heart cytochrome c, fibronectin, and Medium 199 were purchased from Sigma-Aldrich, and Medium 199 phenol-red free from Sigma-Aldrich and Invitrogen (Paisley, UK). Foetal bovine serum (FBS, heat-inactivated) was purchased from Biosera (Ringmer, UK), safe-lock microcentrifuge tubes from Qiagen (Crawley, UK), and acid-washed glass beads (~0.5mm diameter) from Sigma-Aldrich. All water utilised was of Milli-Q grade (18.2 MΩ cm^{-1}).

NuPAGE sample reducing agent and LDS sample buffer were purchased from Invitrogen, and Precision Plus Protein Dual Colour standards from Bio-Rad Laboratories, Inc (Hemel Hempstead, UK). Protein-Free T20 (TBS) blocking buffer was obtained from Fisher Scientific (Loughborough, UK); Immobilon-FL PVDF membrane from Millipore (Watford, UK), and Instant*Blue* protein gel stain from Expedeon Protein Solutions (Harston, UK). Tween® 20 was purchased from Sigma-Aldrich. Chicken polyclonal anti-glyceraldehyde-3-phosphate dehydrogenase (GAPDH; AB2302) and rabbit polyclonal anti-gp91phox (NOX2; 07-024) were obtained from Millipore; goat polyclonal anti-actin (sc-1615) from Santa Cruz Biotechnology, Inc. (California, USA), and rabbit polyclonal anti-NOX4 (ab81967) from Abcam (Cambridge, UK). Donkey anti-chicken IgG (IR dye 680 LT), donkey anti-goat IgG (IR dye 680), goat anti-rabbit IgG (IR dye 800 CW) and donkey anti-rabbit IgG (IR dye 800 CW) were supplied by Li-Cor (Cambridge, UK). Antibodies were prepared in a diluent of 50% T20 blocking buffer:50% phosphate-buffered saline (PBS) with 0.5% Tween® 20; and including 0.02% sodium dodecyl sulphate for solutions of IR dye 680 LT anti-IgG antibodies.

Cell culture. Cryo-preserved, early passage, pooled human umbilical vein endothelial cells (HUVECs) were purchased from TCS CellWorks (Buckingham, UK) and used between passages two to four. Cells were routinely cultured in Nunclon™ Δ 75cm^2 flasks in large vessel endothelial cell growth medium [TCS CellWorks; proprietary basal medium formulation supplemented with growth factor and antibiotic (gentamicin & amphotericin B) supplements, final concentration of 2% v/v foetal bovine serum] at 37°C and 5% CO_2. HUVECs were sub-cultured using 0.025% trypsin and 0.01% EDTA (TCS CellWorks).

Cytotoxicity assay. Cell viability was determined using cell proliferation reagent WST-1 [(4-[3-(4-Iodophenyl)-2-(4-nitrophenyl)-2H-5-tetrazolio]-1,3-benzene disulphonate)] (Berridge et al., 1996); whereby metabolically active cells cleave this tetrazolium salt to a water-soluble formazan dye, through the activity of mitochondrial succinate-tetrazolium reductase (Ngamwongsatit et al., 2008). Cytotoxicity assay method development was conducted as detailed in Appendix 9.1. The optimised cytotoxicity assay was conducted using 96-well microplates (BD Falcon®) coated with fibronectin (0.42μg/cm^2), which were seeded with HUVECs at a density of ~10,000 cells/well. Cells were subsequently grown to confluence (~24-48 hours at 37°C and 5% CO_2). Culture medium was then

aspirated, and solutions of the treatment compounds (0.5, 1, 10, 50 or 100µM; maximum 0.25% DMSO) prepared in supplemented large vessel endothelial cell growth medium were added to relevant wells at a volume of 100µl/well. The assay controls consisted of wells with media only (control), wells with DMSO in media (vehicle control), and blank wells (vehicle control only, no cells). Four replicate wells were used for each control and treatment solution. The microplates were incubated for 24 hours at 37°C and 5% CO_2; after which 10µl WST-1 reagent was added to each well, and plates were incubated for a further four hours prior to brief agitation. Absorbance was then measured at 440-450nm using a microplate reader [Fluostar Omega or Polarstar Optima, BMG Labtech (Aylesbury, UK)].

2.2.1 Method development: stimulated superoxide production assay

Preliminary experiments conducted in 6-well plates, using a cell seeding density of 47,500-57,000 cells/well, yielded inconsistent results and indicated a need for further method development. Ten key research papers selected for review were analysed, and data were summarised for nine method parameters; including cell seeding density, assay medium utilised, percentage of serum in the assay medium, stress agent and incubation time with the stress agent (Appendix Table 9.2.2). Figure 2.2 summarises the method development process.

Figure 2.2 Stimulated superoxide production assay method development flow chart.

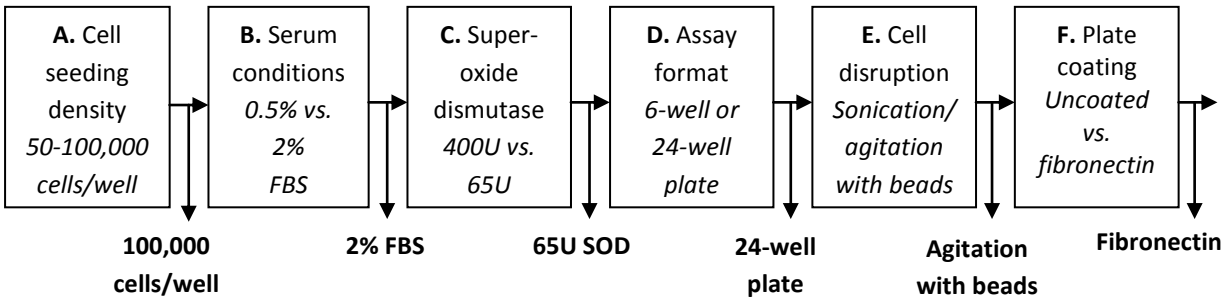

Cell seeding density (A). Whilst not all reports reviewed provided full details of assay methodology, the previously utilised cell seeding density was below that used in several other studies. Therefore, the effect of an elevated cell seeding density (100,000 cells/well for 6-well plate) was evaluated with basal (treatment media only), angiotensin II and vanillic acid (phenolic acid degradant of peonidin glycoside) treatments (Figure 2.2 A). A substantial increase in superoxide levels following angiotensin II stimulation was observed at a seeding density of 100,000 cells/well, as compared with unstimulated cells (~718% of basal superoxide levels) (Figure 2.3). Superoxide levels were reduced following exposure of cells to vanillic acid in conjunction with angiotensin II (~536% of basal superoxide levels). Therefore, a cell seeding density of 100,000 cells/well was utilised for subsequent method development.

Figure 2.3 Modulation of superoxide production by HUVECs after treatment with angiotensin II/Ang II (0.1µM), and Ang II (0.1µM) with vanillic acid/VA (1µM).

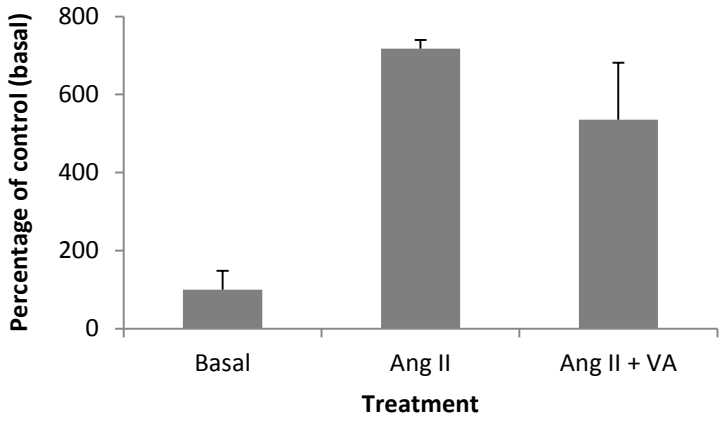

SOD-corrected mean absorbance (OD) ratio (550/620nm) normalised to protein, expressed as percentage of control (basal; designated as 100%) in stimulated superoxide production assay (6-well plate format). Data are graphed as mean ± SD (n=2).

Serum (B) and superoxide dismutase (C) conditions. Experiments were performed to investigate the use of low-serum (0.5%) conditions during the six-hour incubation with angiotensin II and treatment compounds ('serum starved'; Figure 2.2 B), or an elevated level of superoxide dismutase (400U, with 20 µM cytochrome c; Figure 2.2 C). However, poor cell viability was observed during these experiments, and therefore no changes were made to the assay methodology.

Assay format (D). In order to establish if screening efficiency could be increased, treatment compounds were tested in a 24-well plate format (Figure 2.2 D) as opposed to a 6-well plate format. HUVEC seeding density was adjusted in accordance with reduced well surface area (~20,000 cells/well for 2cm^2 surface area). It was determined that screening could be conducted in 24-well plates, and therefore this format was utilised in subsequent method development.

Cell disruption (E). Optimisation was conducted for cell disruption methodology following harvesting of cells from culture plates (Figure 2.2 E), for protein quantitation and normalisation of the absorbance data. Initially cell solutions were subject to probe sonication, but in order to improve efficiency cell disruption was performed by rapid agitation with acid-washed glass beads (~0.5mm diameter). Aliquots of a sample HUVEC lysate were subject to cell disruption by each method, and the total protein was measured to confirm comparable recovery from each method. No significant difference was observed between the two methods based on calculated protein concentration (1.11 ± 0.19 mg/ml with sonication versus 1.04 ± 0.03 mg/ml after agitation with beads; mean ± SD, n=3 for protein assay). As such, cell disruption was performed by rapid agitation with glass beads in the subsequent stages of method development.

Plate coating (F). Initial screening data for treatment compounds, generated using the parameters identified above, demonstrated considerable variance in corrected absorbance measurements; particularly for phenolic acid degradants. In order to improve assay reliability and reproducibility, the use of a fibronectin-coated surface for HUVEC culture (Baudin et al., 2007) was investigated as described previously (Figure 2.2 F).

24-well plates were washed with warm PBS, and incubated with 100µl/well of 5µg/ml fibronectin (in PBS) for 60 minutes at room temperature. Plates were then rinsed with PBS, dried, and stored at 4°C until use. Syringic acid was screened for bioactivity using HUVECs cultured on fibronectin-coated plates, as opposed to uncoated plates, which resulted in reduced variation in assay data (Figure 2.4); particularly for 0.1µM syringic acid (coefficient of variation 110% with uncoated plate versus 19% with fibronectin coating). Thus, the use of fibronectin-coated plates enhanced the reliability of the stimulated superoxide production assay, and was incorporated into the optimised methodology.

Figure 2.4 Effect of uncoated (A) and fibronectin-coated (B) 24-well plates upon variation in corrected mean absorbance for syringic acid screened in stimulated superoxide production assay.

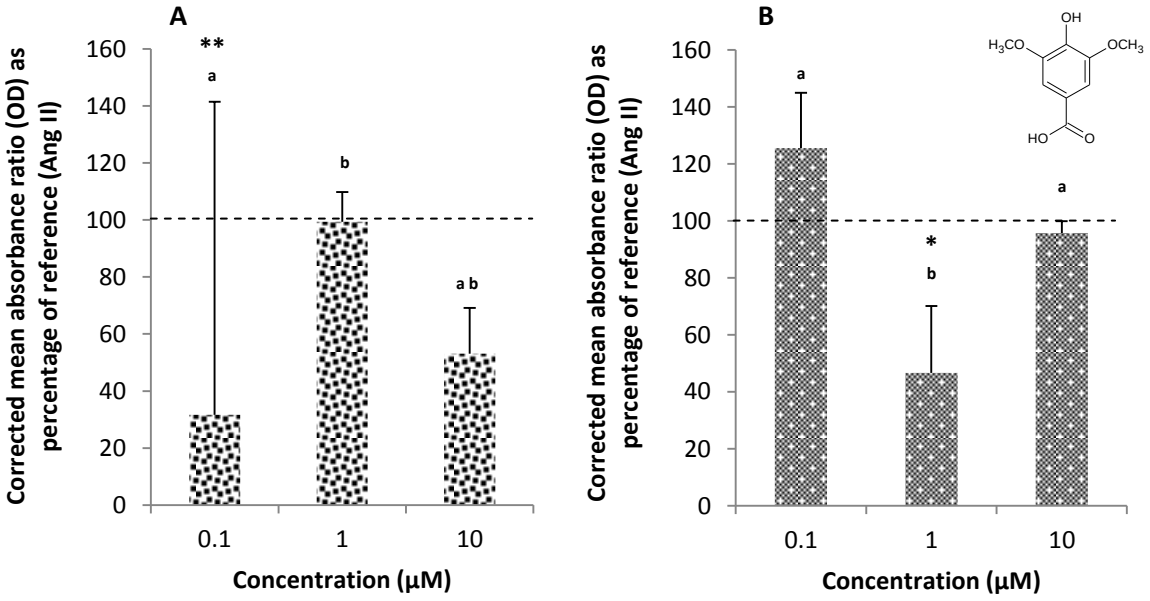

SOD-corrected mean absorbance (OD) ratio (550/620nm), expressed as percentage of reference (angiotensin II; designated as 100% and denoted by dashed line), for syringic acid (structure inset) screened in stimulated superoxide production assay (24-well plate format) at 0.1, 1 and 10µM; using uncoated (A) and fibronectin-coated (B) 24-well plates. Data are graphed as mean ± SD (n=3). *Significant difference versus angiotensin II reference (*$p < 0.05$ and **$p < 0.01$ respectively); columns with different superscript letters are significantly different ($p < 0.05$).

2.2.2 Method development: endothelial NOX expression

Seven research reports detailing immunoblot analysis of cell lysates for the expression of NOX isoforms and/or endothelial nitric oxide synthase (eNOS) were reviewed (Appendix Table 9.2.3); as modulation of eNOS expression by anthocyanins & phenolic acid degradants was to be examined in

related studies (refer to Chapter 3). Data were extracted for eleven key parameters, including amount of protein loaded for sodium dodecyl sulphate polyacrylamide gel electrophoresis (SDS-PAGE), primary antibody utilised and concentration, and loading control antibody used and concentration (Figure 2.5). Glyceraldehyde-3-phosphate dehydrogenase (GAPDH) and actin served as ubiquitously expressed loading control proteins (Appendix Table 9.2.3).

Figure 2.5 Immunoblotting method optimisation flow chart.

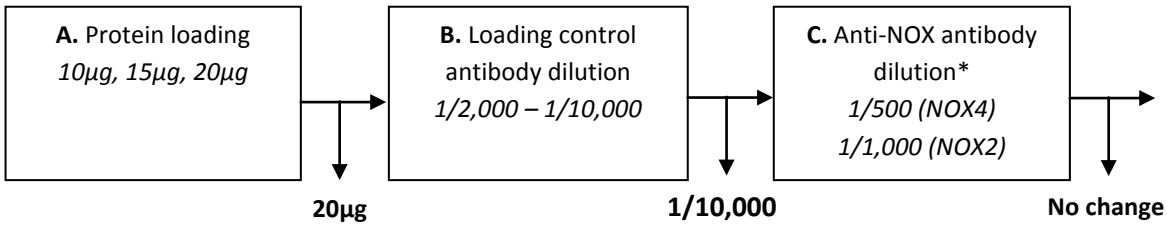

*based on manufacturer's recommendations

Protein loading (A). Expression of two loading controls, GAPDH and actin, was examined in lysates from unstimulated HUVECs using 10, 15 and 20µg of total protein (Figure 2.5 A). Distinct bands were visualised at all protein loading levels (Figure 2.6); however, 20µg of protein was selected as the optimum amount of cell lysate to load for gel electrophoresis and immunoblotting owing to the reported low expression of NOX proteins (Brandes et al., 2010).

Loading control antibody dilution (B). Two concentrations of each antibody (Figure 2.5 B) were used to detect the loading control protein (1/2,000 & 1/10,000 for anti-GAPDH; 1/5,000 & 1/10,000 for anti-actin). Clear bands were visualised in all cases (Figure 2.6); thus the loading control antibodies were used at a dilution of 1/10,000, since a more concentrated solution was not required for detection of protein.

Figure 2.6 Effect of protein loading and primary antibody concentration on detection of loading controls by Western blotting.

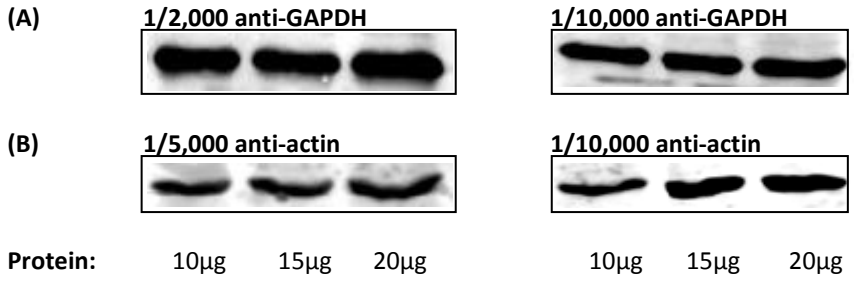

Detection of GAPDH (A) and actin (B) in lysates from unstimulated HUVECs by immunoblotting, at varying primary antibody concentrations and amount of total protein loaded for electrophoresis.

Anti-NOX antibody dilution (C). Endothelial expression of NOX2 and NOX4 was examined using lysates from unstimulated HUVECs, and from cells harvested following a six hour incubation with 0.1µM angiotensin II; using anti-NOX antibodies at dilutions based on manufacturer's

recommendations (1/1,000 for anti-NOX2, 1/500 for anti-NOX4; Figure 2.5 C). NOX4 expression was detected after angiotensin II stimulation, in accordance with previous reports (Bedard and Krause, 2007, Brown and Griendling, 2009); whilst a band identified as NOX2 (Jiang et al., 2006) was visualised more faintly following angiotensin II treatment (Figure 2.7). However, imaged NOX bands were of diminished intensity relative to the loading control (actin), and no signal was detected when anti-NOX4 was used at a concentration of 1/1,000 (data not shown). Therefore, anti-NOX antibodies were used at initially selected concentrations.

Figure 2.7 Detection of NOX2 and NOX4 protein in HUVEC lysates.

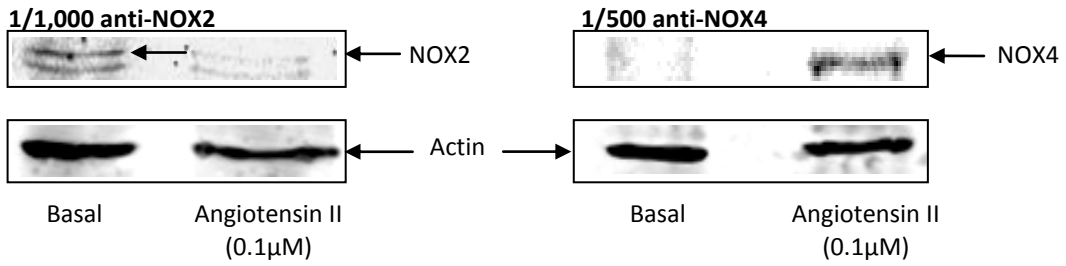

Detection of NOX2 and NOX4 protein (with actin loading control) in cell lysates from unstimulated HUVECs (basal) and following 6h incubation with angiotensin II.

2.2.3 Final methodology

Stimulated superoxide production assay: optimised parameters. The optimised angiotensin II stimulated superoxide production assay utilised 24-well plates (Nunclon™ Δ) coated with fibronectin (0.25μg/cm^2), which were seeded with HUVECs at a density of ~50,000 cells/well, and the cells grown to confluence (~48 hours at 37°C and 5% CO_2). Culture medium was then aspirated, and the cells were washed once with warm Medium 199 (supplemented with 2% FBS), prior to a 16 - 18 hour incubation in this medium (at 37°C and 5% CO_2). Thereafter, the cells were washed once with warm PBS, and incubated for six hours in Medium 199 (2% FBS) with 0.1μM angiotensin II, 30μM ferricytochrome c, and 0.1, 1 or 10μM of the treatment compounds or 5μM VAS2870 [selective NOX inhibitor (Stielow et al., 2006, Altenhofer et al., 2012)]; in the presence or absence of 65U superoxide dismutase. Four replicate wells were plated for each treatment. After incubation, aliquots of the cell supernatants from each well were transferred to a 96-well microplate, for measurement of absorbance at 550nm (reference wavelength 620nm) using a microplate reader (Fluostar Omega, BMG Labtech).

After aspiration of the remaining supernatant, 24-well plates were subsequently frozen at -80°C for protein extraction. Cells were harvested and lysed in 1% (octylphenoxy)polyethoxyethanol, 150mM NaCl, 20mM Tris and 10% glycerol (pH 8.0), supplemented with protease inhibitors (Complete Protease Inhibitor Cocktail). Briefly, 24-well plates were incubated with lysis buffer (120μl/well) for 30 minutes at 4°C, prior to removal of cells by scraping. Recovered solutions were subject to cell

disruption by rapid agitation (50Hz for 5 minutes using Qiagen TissueLyser LT) with acid-washed glass beads in safe-lock microcentrifuge tubes. After centrifugation at 13,000 rpm (15 minutes at 4°C), the protein content of the supernatants was assayed using the Pierce BCA Protein Assay Kit according to manufacturer's instructions.

Immunoblot analysis of endothelial NOX expression: optimised parameters. Cell lysates from the superoxide production assay were generated as described above. Briefly, 6-well plates (Nunclon™ Δ) were seeded with HUVECs at a density of 100,000 cells/well and cells grown to confluence, prior to a 16 - 18 hour incubation in Medium 199 (2% FBS) at 37°C and 5% CO_2. Thereafter, cells were incubated for six hours in Medium 199 (2% FBS) with 0.1µM angiotensin II, 30µM ferricytochrome c, and 0.1, 1 or 10µM of the treatment compounds; in the presence or absence of 65U superoxide dismutase. Cells were harvested and lysed, and recovered solutions were then subject to cell disruption by rapid agitation with glass beads. After centrifugation at 13,000 rpm (15 minutes at 4°C), the protein content of the supernatants was assayed using the Pierce BCA Protein Assay kit.

For gel electrophoresis, samples were reduced using NuPAGE sample reducing agent (50 mM dithiothreitol) prior to gel loading in NuPAGE LDS sample buffer. Precision Plus Protein Dual Colour standards were loaded as comparative molecular weight markers. Normally 20µg of protein was loaded onto a 4% polyacrylamide stacking gel, and separated across a 10% resolving gel (at 25mA for approximately one hour) prior to semi-dry transfer to Immobilon-FL PVDF membrane (at 200mA for approximately 90 minutes). Equal protein transfer was confirmed by Instant*Blue* staining of the gels. Membranes were blocked with T20 blocking buffer for one hour at room temperature, and incubated overnight (at 4°C) in the appropriate concentration of primary and loading control antibody. Membranes were washed using PBS with 0.1% Tween® 20 (PBST 0.1%), after which secondary antibody incubations were performed for one hour at room temperature, using IR dye-conjugated (680 and 800) secondary antibodies at a concentration of 1 in 10,000. Membranes were washed with PBST 0.1%, and subsequently imaged using an Odyssey Infrared Imaging System (Li-Cor). Immunoblots were quantified by densitometry using Odyssey Infrared Imaging System Application Software (Li-Cor, version 3.0.21).

Statistical analysis. Analysis of variance (ANOVA) with Tukey post-hoc test, or independent samples t-test as appropriate, was performed using SPSS software (IBM, New York, USA) version 18 for Windows. Significance was determined at the 5% level, and expressed relative to control (culture medium only) or angiotensin II (positive control). Three biological replicates for each control/treatment were utilised for analysis unless otherwise noted.

For each control or treatment in the stimulated superoxide production assay, mean absorbance ratio (550nm/620nm) in the presence of superoxide dismutase (n=3) was subtracted from individual

absorbance ratio values in the absence of superoxide dismutase (n=3); to correct for cytochrome c reduction owing to generated superoxide anion. Mean SOD-corrected absorbance ratio was then represented graphically; error bars in figures denote one standard deviation (SD) from the mean. Data for mean reduction of cytochrome c measured at 550nm (with and without SOD correction), and expressed as mM [molar extinction coefficient/ε = 21.1mM^{-1} cm^{-1} (Steffen et al., 2007b, Steffen et al., 2008)], for controls and treatment compounds/combinations are provided in Appendix 9.3 (Figure 9.3.1 - Figure 9.3.4).

2.3 Results

Cytotoxicity assay. Seven unique treatments and two treatment combinations (Figure 2.1) were screened for cytotoxicity at a concentration of 10µM, representing the highest concentration used in subsequent bioactivity investigations, using optimised methodology. For the two treatment combinations, a cumulative concentration of 10µM was utilised, consisting of an equimolar ratio of all compounds. No significant effects ($p > 0.05$) on endothelial cell viability were observed following a 24h incubation of HUVECs with 10µM of any treatment, or with the vehicle control (0.25% DMSO) (Figure 2.8).

Figure 2.8 Assessment of cytotoxicity of anthocyanins, phenolic degradants and treatment combinations following 24h incubation with cultured HUVECs.

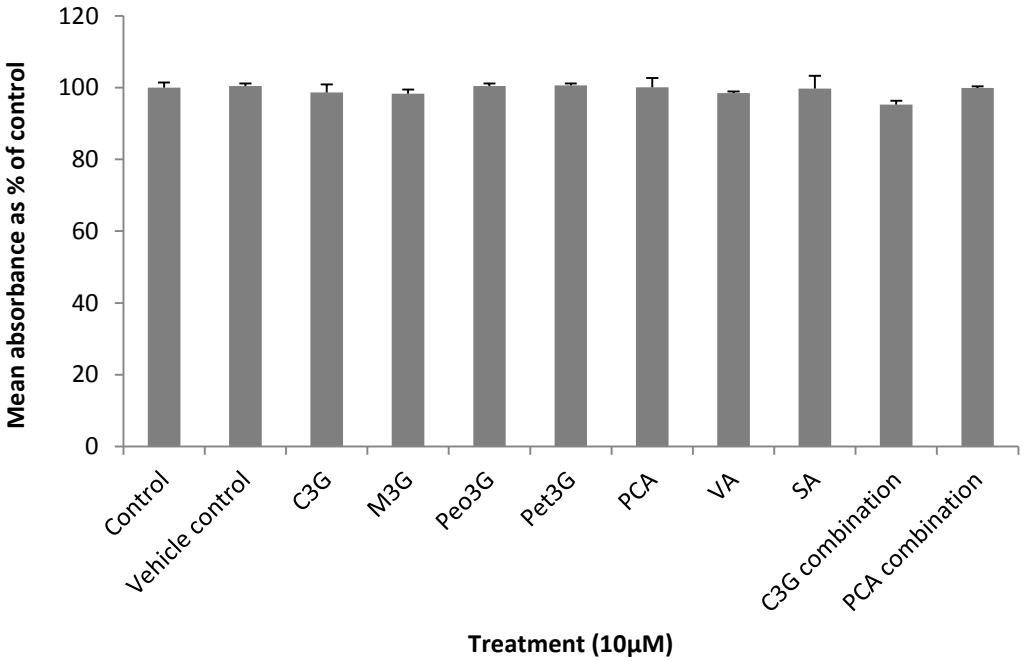

Cell viability (mean absorbance as percentage of mean control absorbance) for control (supplemented culture medium), vehicle control (culture medium with 0.25% DMSO), and 10µM cyanidin-3-glucoside (C3G), malvidin-3-glucoside (M3G), peonidin-3-glucoside (Peo3G), petunidin-3-glucoside (Pet3G), protocatechuic acid (PCA), vanillic acid (VA), syringic acid (SA), cyanidin-3-glucoside combination (C3G + epicatechin + quercetin + ascorbic acid) or protocatechuic acid combination (PCA + epicatechin + quercetin + ascorbic acid). Data are graphed as mean ± SD (n=3).

Stimulated superoxide production assay. Incubation of HUVECs with 0.1µM angiotensin II for six hours resulted in increased superoxide levels relative to basal (unstimulated) cells (Figure 2.9); moreover this increase was abolished by co-incubation with superoxide dismutase (Ang II + SOD), such that superoxide levels were not significantly different from basal ($p > 0.05$) but significantly lower than angiotensin II alone ($p < 0.05$).

Figure 2.9 **Elevation of superoxide levels by angiotensin II (0.1µM) following 6h incubation in HUVEC model.**

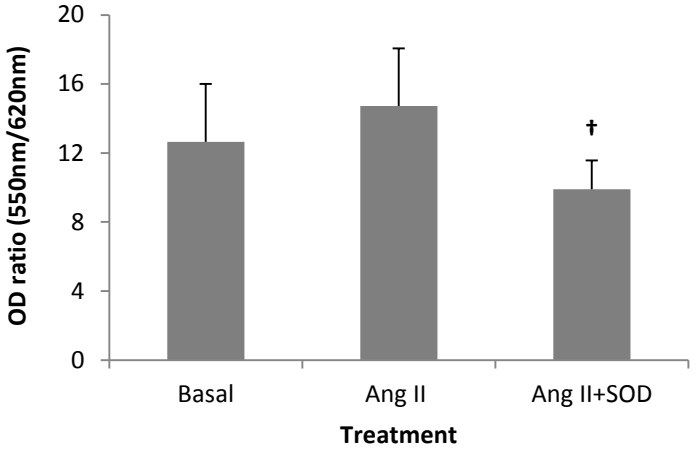

Mean absorbance (OD) ratio (550nm/620nm), for basal (unstimulated) cells, angiotensin II control (Ang II, 0.1µM) and Ang II with superoxide dismutase (SOD) correction in stimulated superoxide production assay (24-well plate format). Data are graphed as mean ± SD (n=8). †Significant difference versus angiotensin II ($p < 0.05$).

The generation of superoxide anion by endothelial NOX following angiotensin II stimulation was confirmed using an established NOX inhibitor, VAS2870 (Stielow et al., 2006, Altenhofer et al., 2012), at 5µM in the presence and absence of angiotensin II. Following co-incubation of HUVECs with angiotensin II and VAS2870, superoxide levels were significantly reduced relative to incubation with angiotensin II alone ($p < 0.05$); moreover 5µM VAS2870 was without effect on basal superoxide levels (Figure 2.10).

With regard to bioactivity of treatment compounds, significantly elevated superoxide levels were observed following incubation of cells with 0.1µM and 1µM cyanidin-3-glucoside (catechol B-ring; Figure 2.11 A), as compared with angiotensin II alone. In contrast, statistically significant reductions in superoxide were elicited by the anthocyanins peonidin-3-glucoside (mono-*O*-methylated catechol B-ring; Figure 2.11 B) at 0.1µM and 10µM; malvidin-3-glucoside (methylated catechol B-ring with 5'-methoxy group; Figure 2.11 C) at 10µM; and petunidin-3-glucoside (methylated catechol B-ring with 5'-hydroxy group; Figure 2.11 D) at 1µM and 10µM. In addition, decreased superoxide levels with 10µM peonidin-3-glucoside were significantly different from those following 0.1µM exposure levels (Figure 2.11 B).

Figure 2.10 Modulation of angiotensin II-stimulated endothelial superoxide production by NOX inhibitor VAS2870.

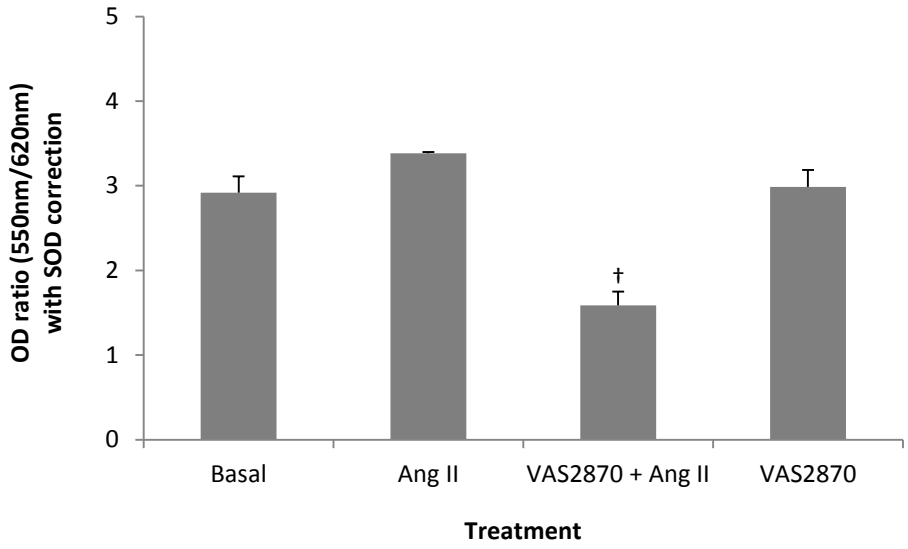

SOD-corrected mean absorbance (OD) ratio (550nm/620nm), for basal (unstimulated) cells, angiotensin II control (Ang II, 0.1µM), 5µM VAS2870 (NOX inhibitor) with 0.1µM Ang II (VAS2870 + Ang II), and 5µM VAS2870 in stimulated superoxide production assay (24-well plate format). Data are graphed as mean ± SD (n=3). †Significant difference versus angiotensin II ($p < 0.05$).

Statistically significant reductions in superoxide levels were also elicited by anthocyanin B-ring degradants. In contrast to the parent anthocyanin cyanidin-3-glucoside, a substantial decrease in superoxide was observed with the B-ring degradant protocatechuic acid at 10µM (Figure 2.11 E); to levels significantly below those measured for basal (unstimulated) HUVECs in the same assay (data not shown). Vanillic acid (B-ring degradant of peonidin-3-glucoside) elicited reductions in superoxide levels at all concentrations examined, with a statistically significant decrease observed at 1µM (Figure 2.11 F). Moreover, following treatment with angiotensin II and vanillic acid, superoxide levels were not significantly different from basal cells (data not shown). Finally, a significant decrease in superoxide was elicited by 1µM syringic acid (Figure 2.11 G); and after treatment with angiotensin II and 1µM or 10µM syringic acid, superoxide levels were not significantly different from basal cells (data not shown).

Figure 2.11 **Modulation of superoxide levels by cyanidin-3-glucoside (A), peonidin-3-glucoside (B), malvidin-3-glucoside (C), petunidin-3-glucoside (D), protocatechuic acid (E), vanillic acid (F), and syringic acid (G) following 6h incubation in angiotensin II-stimulated HUVEC model.**

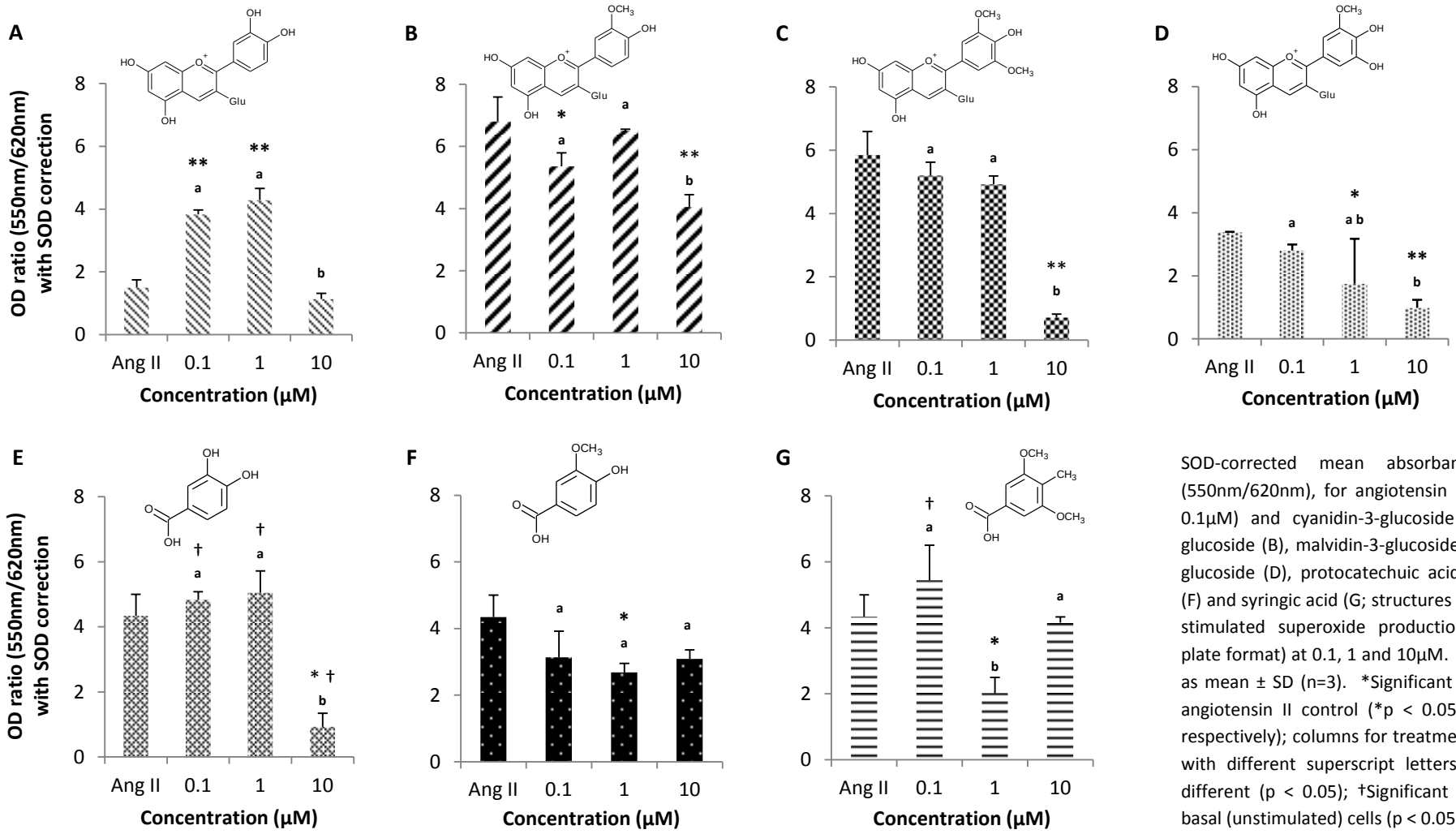

SOD-corrected mean absorbance (OD) ratio (550nm/620nm), for angiotensin II control (Ang II, 0.1µM) and cyanidin-3-glucoside (A), peonidin-3-glucoside (B), malvidin-3-glucoside (C), petunidin-3-glucoside (D), protocatechuic acid (E), vanillic acid (F) and syringic acid (G; structures inset) screened in stimulated superoxide production assay (24-well plate format) at 0.1, 1 and 10µM. Data are graphed as mean ± SD (n=3). *Significant difference versus angiotensin II control (*$p < 0.05$ and **$p < 0.01$ respectively); columns for treatment concentrations with different superscript letters are significantly different ($p < 0.05$); †Significant difference versus basal (unstimulated) cells ($p < 0.05$).

No significant changes in superoxide levels were elicited with cyanidin-3-glucoside in combination with epicatechin, quercetin and ascorbic acid (Figure 2.12 A); whereas a statistically significant reduction was observed with protocatechuic acid in combination with these compounds, at a cumulative concentration of 10µM (Figure 2.12 B).

Figure 2.12 **Modulation of superoxide levels by cyanidin-3-glucoside (A) or protocatechuic acid (B) in combination with epicatechin, quercetin and ascorbic acid following 6h incubation in angiotensin II-stimulated HUVEC model.**

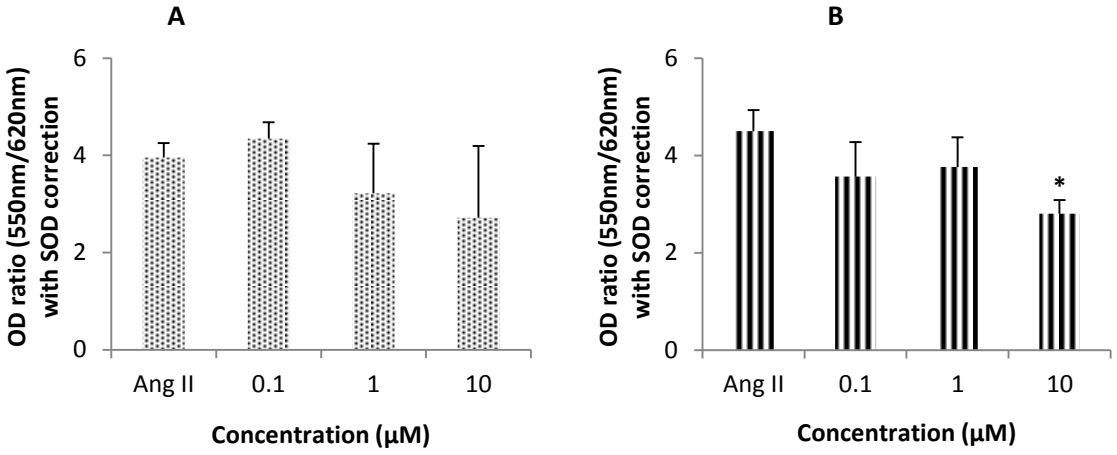

SOD-corrected mean absorbance (OD) ratio (550nm/620nm), for angiotensin II control (Ang II, 0.1µM) and equimolar ratio of cyanidin-3-glucoside (A) or protocatechuic acid (B) with epicatechin, quercetin and ascorbic acid, screened in stimulated superoxide production assay (24-well plate format) at 0.1, 1 and 10µM. Data are graphed as mean ± SD (n=3). *Significant difference versus angiotensin II control ($p < 0.05$).

Immunoblot analysis of endothelial NOX expression. Following angiotensin II stimulation, weak immunoreactive bands corresponding to NOX2 were visualised by immunoblotting of endothelial lysates, although no substantial modulation of NOX2 expression was observed after incubation with angiotensin II and either protocatechuic acid (Figure 2.13 A) or syringic acid (Figure 2.13 C). NOX2 protein was poorly detected following incubation of cells with angiotensin II and vanillic acid (Figure 2.13 B), such that quantification of bands by densitometry was not possible. Statistical analysis of densitometric data from replicate immunoblots was also precluded by poor detection of NOX2 protein.

Figure 2.13 Effect of protocatechuic acid (A), vanillic acid (B) and syringic acid (C) on NOX2 expression by HUVECs following angiotensin II stimulation.

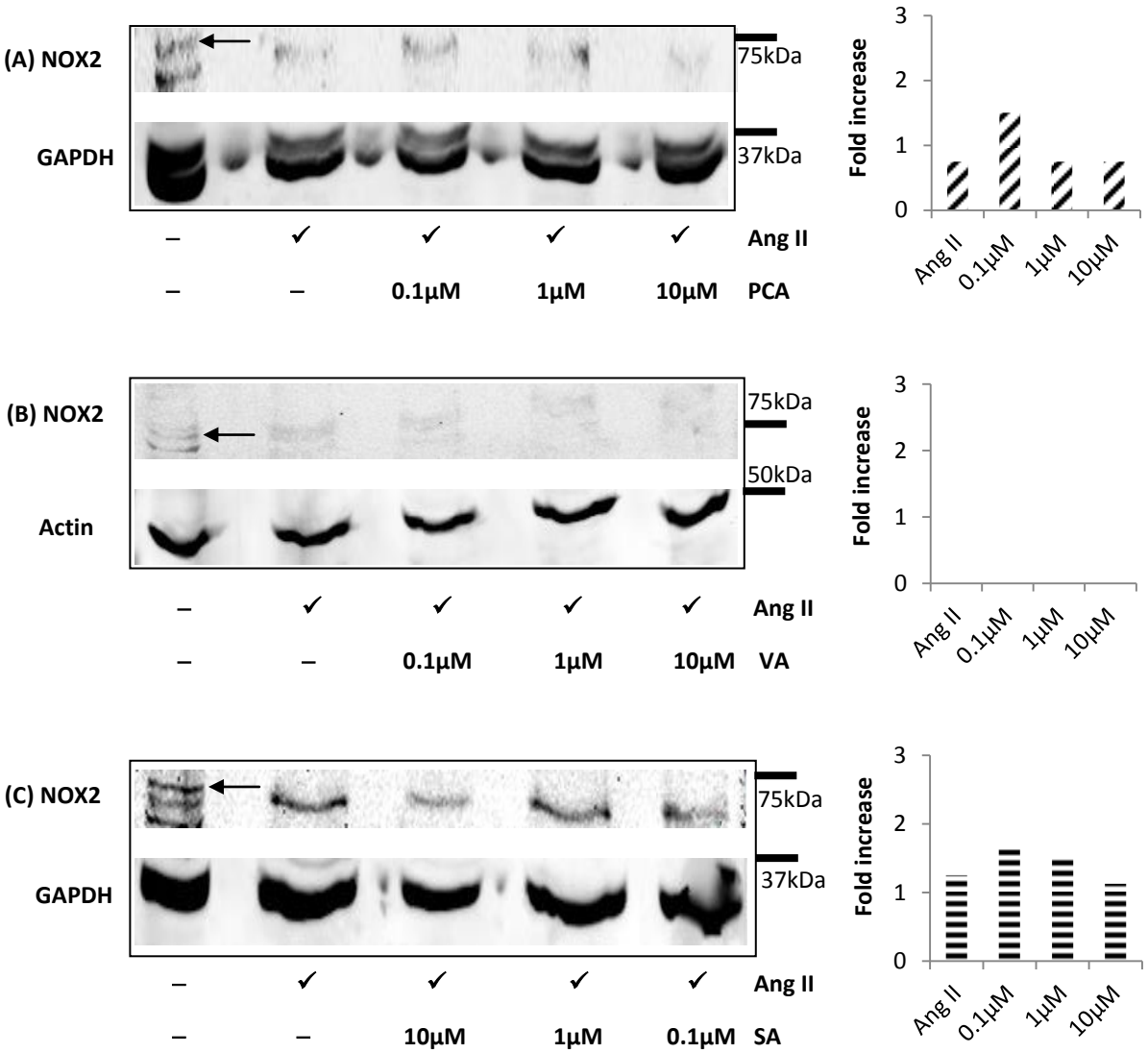

Expression of NOX2 protein (with actin or GAPDH loading control) in cell lysates from unstimulated HUVECs (basal) and following 6h incubation with angiotensin II 0.1µM (Ang II), or angiotensin II with 0.1µM, 1µM or 10µM protocatechuic acid/PCA (A), vanillic acid/VA (B) or syringic acid/SA (C). Relative molecular weight markers (kDa) are indicated at right-hand side of immunoblots. Inset graphs show fold increase in NOX2 expression relative to basal (designated as 1), after quantification by densitometry and normalisation to corresponding loading control (n=1; statistical analysis across replicate immunoblots was precluded by poor detection of NOX2 protein).

By contrast, upregulation of NOX4 expression after incubation of HUVECs with angiotensin II was clearly visualised by immunoblotting (Figure 2.14). However, the observed increase in NOX4 protein levels was not significantly modulated ($p > 0.05$) by co-incubation of cells with angiotensin II and either protocatechuic acid (Figure 2.14 A), vanillic acid (Figure 2.14 B) or syringic acid (Figure 2.14 C) at any concentration examined (0.1 - 10µM).

Figure 2.14 Effect of protocatechuic acid (A), vanillic acid (B) and syringic acid (C) on NOX4 expression by HUVECs following angiotensin II stimulation.

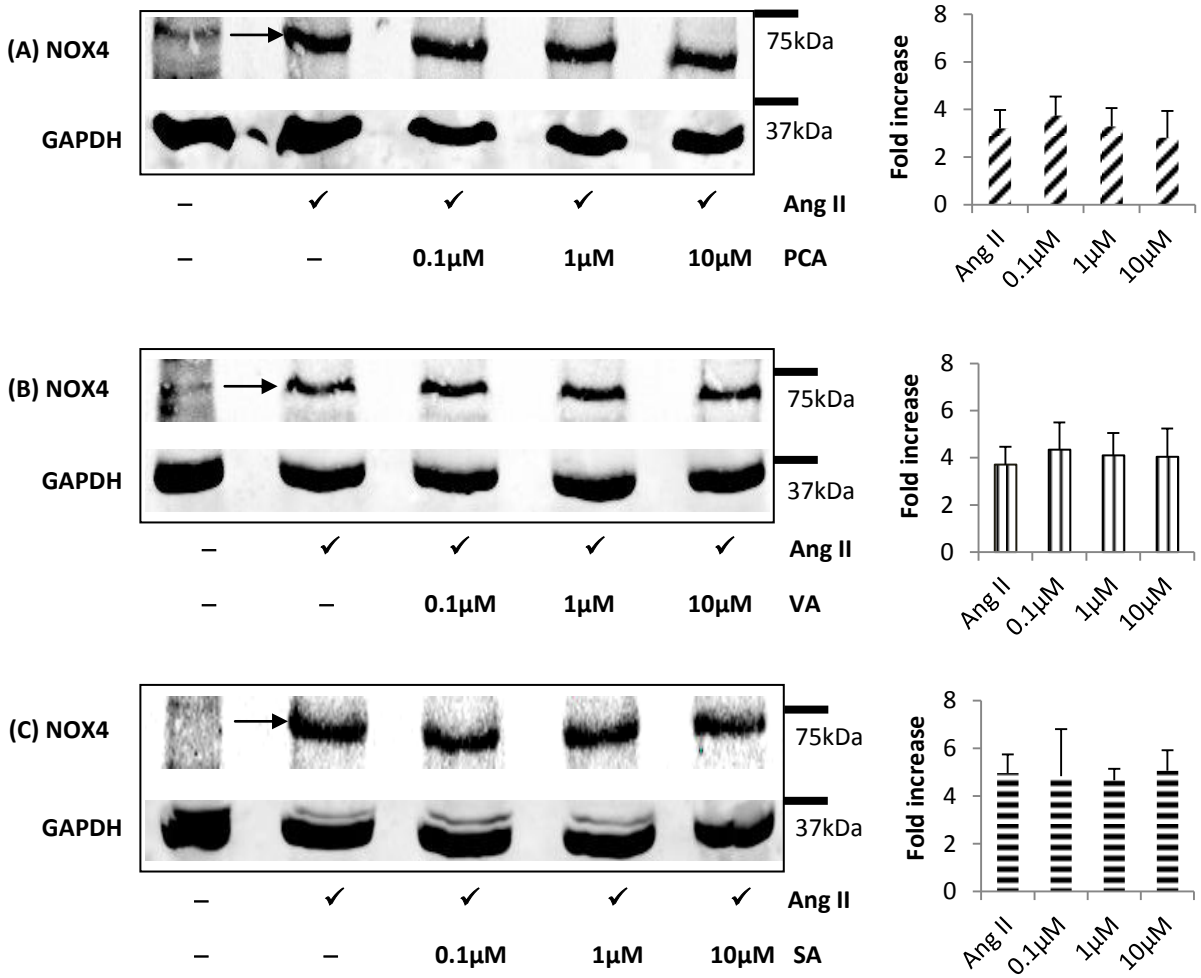

Expression of NOX4 protein (with GAPDH loading control) in cell lysates from unstimulated HUVECs (basal) and following 6h incubation with angiotensin II 0.1µM (Ang II), or angiotensin II with 0.1µM, 1µM or 10µM protocatechuic acid/PCA (A), vanillic acid/VA (B) or syringic acid/SA (C). Relative molecular weight markers (kDa) are indicated at right-hand side of immunoblots. Inset graphs show fold increase in NOX4 expression relative to basal (designated as 1), after quantification by densitometry and normalisation to corresponding loading control (mean ± SD, n=5).

2.4 Discussion

Cytotoxicity assessment of selected treatment compounds was necessary to ensure endothelial cell viability was not affected by these compounds at levels utilised in subsequent vascular bioactivity investigations; specifically 0.1, 1, & 10µM. The maximal level of total dietary flavonoids and related compounds reported in the systemic circulation is generally below 10µM (Crozier et al., 2009), thus this concentration was used to represent the maximum *in vivo* concentration. By contrast, ~0.1µM/100nM of anthocyanins in plasma has been described in some human bioavailability studies, and phenolic acid/aldehyde degradation products or metabolites may be present at levels in excess of the parent compound(s) (Vitaglione et al., 2007, Williamson and Clifford, 2010, Azzini et al., 2010).

For example, Czank *et al* (2013) recently reported a serum C_{max} of 0.14μM for cyanidin-3-glucoside following consumption of 500mg ^{13}C-labelled cyanidin-3-glucoside by healthy volunteers; whereas C_{max} values for ^{13}C-labelled phenolic degradants (protocatechuic acid and phloroglucinol aldehyde) and phase II conjugates of protocatechuic acid (including vanillic acid) were 0.72μM and 2.35μM respectively (Czank et al., 2013).

Initial cytotoxicity data indicated all treatment compounds tested were cytotoxic between concentrations of 0.5μM and 100μM; but no dose-response relationship was evident. In contrast, method development data (Appendix 9.1) indicated a cytotoxic effect of the phenolic degradant protocatechuic acid at 100μM but not 1μM in cultured HUVECs. Cytotoxicity of anthocyanins *in vitro*, at micromolar concentrations, has previously been reported using human vascular endothelial cells; for example cyanidin-3-glucoside at ≥62.5μM (Sorrenti et al., 2007), but cytotoxicity at low micromolar levels has not been indicated. Subsequent screening of all treatment compounds at a concentration of 10μM (the highest concentration used in bioactivity investigations) using optimised methodology revealed no significant reductions in endothelial cell viability with any treatment. Therefore no cytotoxicity was observed for the proposed treatment compounds at low micromolar levels, which is in accordance with both prior laboratory work, and previously published data (Sorrenti et al., 2007).

Overall, physiologically relevant doses (≤ 10μM) of selected anthocyanin glucosides, and phenolic acid degradants, are not cytotoxic to human vascular endothelial cells over a 24 hour period; and thus these concentrations were utilised during subsequent assessment of vascular biological activity in a HUVEC model of angiotensin II-stimulated superoxide production. Screening of treatment compounds in this model suggested several might act as NOX inhibitors, since significantly reduced superoxide levels were observed with 0.1μM & 10μM peonidin-3-glucoside (mono-*O*-methylated catechol B-ring), 10μM malvidin-3-glucoside (methylated catechol B-ring with 5'-methoxy group), and 1μM & 10μM petunidin-3-glucoside (methylated catechol B-ring with 5'-hydroxy group). In contrast, a significant elevation in superoxide levels was elicited by 0.1μM and 1μM cyanidin-3-glucoside (catechol B-ring susceptible to methylation), as compared with angiotensin II alone; although this may reflect a low angiotensin II reference within the cyanidin-3-glucoside screen (Figure 9.3.3 A). Interestingly, no significant changes in levels of superoxide were elicited in the experiments where cyanidin-3-glucoside was added in combination with epicatechin, quercetin and ascorbic acid, though data suggested a possible trend for decreasing superoxide with increasing treatment concentration (Figure 2.12).

Anthocyanin bioactivity *in vivo* may be mediated by phenolic and aromatic metabolites as opposed to parent glycosides (Williamson and Clifford, 2010, Wallace, 2011); moreover, low micromolar levels of phenolic degradants/metabolites in human plasma have been reported following ingestion of

anthocyanin glucosides (Vitaglione et al., 2007, Azzini et al., 2010, Czank et al., 2013). Significant decreases in superoxide levels were elicited by 10μM protocatechuic acid (B-ring degradant of cyanidin-3-glucoside), and 1μM vanillic acid or syringic acid (B-ring degradants of peonidin- and malvidin-3-glucosides respectively). Furthermore, following incubation with vanillic acid at 0.1-10μM, or syringic acid at 1 & 10μM, superoxide levels were not significantly different from basal (unstimulated) HUVECs; and were significantly below basal after treatment with 10μM protocatechuic acid. Superoxide levels were also significantly reduced by a cumulative concentration of 10μM of protocatechuic acid, epicatechin, quercetin and ascorbic acid; though the reduction observed with this combination treatment was smaller than that for protocatechuic acid alone.

A limitation of the stimulated superoxide production assay was the variable response in superoxide generation observed following angiotensin II stimulation of the cultured HUVEC. Previous studies using this methodology generally do not report induction of superoxide production by angiotensin II relative to basal levels, possibly for this reason (Steffen et al., 2007b, Steffen et al., 2008). Alvarez *et al* (2010) have described limited induction of superoxide production by angiotensin II relative to the control in HUVEC cultures (Alvarez et al., 2010). A limited and variable response has also been observed for upregulation of NOX4 mRNA following exposure of HUVEC to 0.1μM angiotensin II [(Yamagishi et al., 2005, Alvarez et al., 2010); refer also to Chapter 4], again suggesting inherent variability in the response of HUVEC to angiotensin II, and representing a possible limitation of this cell type. Whilst HUVEC are an established *in vitro* research model for human endothelial cells (Baudin et al., 2007), an arterial cell type may be more relevant for investigating potential modulation of NOX activity (as explored in Chapter 5).

In summary, anthocyanin-3-glucosides, and their phenolic acid degradants, appeared to reduce superoxide levels following stimulation of HUVECs by angiotensin II. Screening of three phenolic degradants suggested reductions with a catechol B-ring at 10μM (protocatechuic acid), a mono-*O*-methylated catechol B-ring at 1μM (vanillic acid), and a methylated catechol B-ring with 5'-methoxy group at 1μM (syringic acid); although methylation of a catechol B-ring by endothelial catechol-*O*-methyltransferase has been described previously for the flavonoid (-)-epicatechin (Steffen et al., 2008), yielding monomethyl metabolites which display NOX inhibitory activity [at a concentration range around 10μM (Steffen et al., 2007b, Steffen et al., 2008)]. Inhibition of NOX by anthocyanin glycosides or derived molecules *in vivo*, with decreased scavenging of NO by generated superoxide, could potentially enhance the function of the vascular endothelium. Therefore, phenolic degradants which appeared to be bioactive in the current investigation were further examined for effects on endothelial expression of NOX protein; which represents a potential mechanism by which NOX activity, and thus superoxide production, could be reduced.

No significant modulation of angiotensin II-induced NOX4 expression was discerned after incubation of HUVECs with angiotensin II and protocatechuic acid, vanillic acid or syringic acid; indicating that these phenolic acids do not affect enzyme activity at the level of protein expression. By contrast, NOX2 expression was more difficult to discern by immunoblotting of cell lysates, which may reflect low protein expression in vascular cells, and/or poor antibody specificity (Brandes et al., 2010), although upregulation of NOX2 in HUVECs following angiotensin II stimulation has been reported previously (Rueckschloss et al., 2002). Quantification of immunoblots indicated no consistent effect of anthocyanin degradants on NOX2 expression, although owing to poor detection statistical analysis was not possible. The use of a monoclonal anti-NOX2 antiserum, in conjunction with increased protein loading for SDS-PAGE, may resolve these issues.

In conclusion, the anthocyanin degradants protocatechuic acid, vanillic acid, and syringic acid do not appear to alter expression of endothelial NOX2 or NOX4 proteins following stimulation of HUVECs with angiotensin II. Therefore, any modulation of NOX activity elicited by these compounds may occur at the post-translational level. NOX2, unlike NOX4, requires additional cytosolic subunits for enzyme activity (Schroder, 2010), and the putative NOX inhibitor apocynin is reported to act by inhibiting assembly of these subunits (Drummond et al., 2011). Moreover, vanillic acid contains a mono-*O*-methylated catechol B-ring structure, which is similar to that of apocynin, and might therefore affect post-translational regulation of the superoxide-generating NOX2 isoform as discussed in Chapters 3 & 5.

3 Effect of anthocyanin glucosides and phenolic degradants on endothelial nitric oxide synthase expression and nitric oxide production

3.1 Background

Nitric oxide (NO) is a key mediator of vascular homeostasis, notably through its vasodilatory activity as the endothelium-derived relaxing factor (Michel and Vanhoutte, 2010); in addition to inhibiting platelet aggregation, oxidation of low density lipoprotein, and expression of cell surface adhesion molecules (Wever et al., 1998, Granger et al., 2004, Naseem, 2005). Most vascular endothelial cells constitutively express endothelial nitric oxide synthase (eNOS) (Fleming and Busse, 2003), which generates NO in response to fluid shear stress (arising from blood flow over endothelial cells) or agonists including bradykinin and oestradiol (Shaul, 2002, Fleming and Busse, 2003).

A number of *in vitro* studies have previously reported bioactivity of anthocyanins, or anthocyanin-rich berry extracts, on endothelium-dependent vasorelaxation; or directly on eNOS expression/activation. Chokeberry and bilberry extracts elicited endothelial- and NOS-dependent relaxation of porcine coronary arterial rings (Bell and Gochenaur, 2006); whilst bilberry extract, and cyanidin-3-glucoside (1nM - 10µM), induced NO- and endothelium-dependent relaxation of rat thoracic aortic rings (Ziberna et al., 2013). Moreover, 0.1µM cyanidin-3-glucoside upregulated expression of eNOS in bovine artery endothelial cells (BAECs) (Xu et al., 2004b), and 0.5µM of this anthocyanin elicited regulation of eNOS in BAECs through phosphorylation and dephosphorylation at residues Serine 1179 and Serine 116 respectively (Xu et al., 2004a). Upregulation of eNOS has also been reported following incubation of human umbilical vein endothelial cells (HUVECs) with the anthocyanidins cyanidin (at 100µM) and delphinidin (at 50 and 100µM) (Lazze et al., 2006); furthermore cyanidin-3-glucoside (2.3µg/ml; ~5µM) and delphinidin-3-glucoside (5.8µg/ml; ~12µM) activated eNOS in HUVECs, as determined by phosphorylation of Serine 1177 (Edirisinghe et al., 2011). Thus upregulation and/or activation of eNOS, and increased endothelial NO production, represent mechanisms by which anthocyanins, or their degradants/metabolites *in vivo*, could enhance vascular function through elevated NO bioavailability (Erdman et al., 2007, Wallace, 2011)

In the current investigation, selected anthocyanin glucosides and their phenolic acid degradants (Figure 3.1 A) were screened for their effect on expression of eNOS in cultured HUVECs, and endothelial nitric oxide production, to assess relative vascular bioactivity of these compounds. Two combination treatments of cyanidin-3-glucoside or protocatechuic acid, in an equimolar ratio with epicatechin, quercetin and ascorbic acid (Figure 3.1 B) were also examined; to represent

consumption of a mixture of flavonoids and other bioactive compounds which would be present in the habitual diet.

Figure 3.1 Treatment compounds for vascular bioactivity screening.

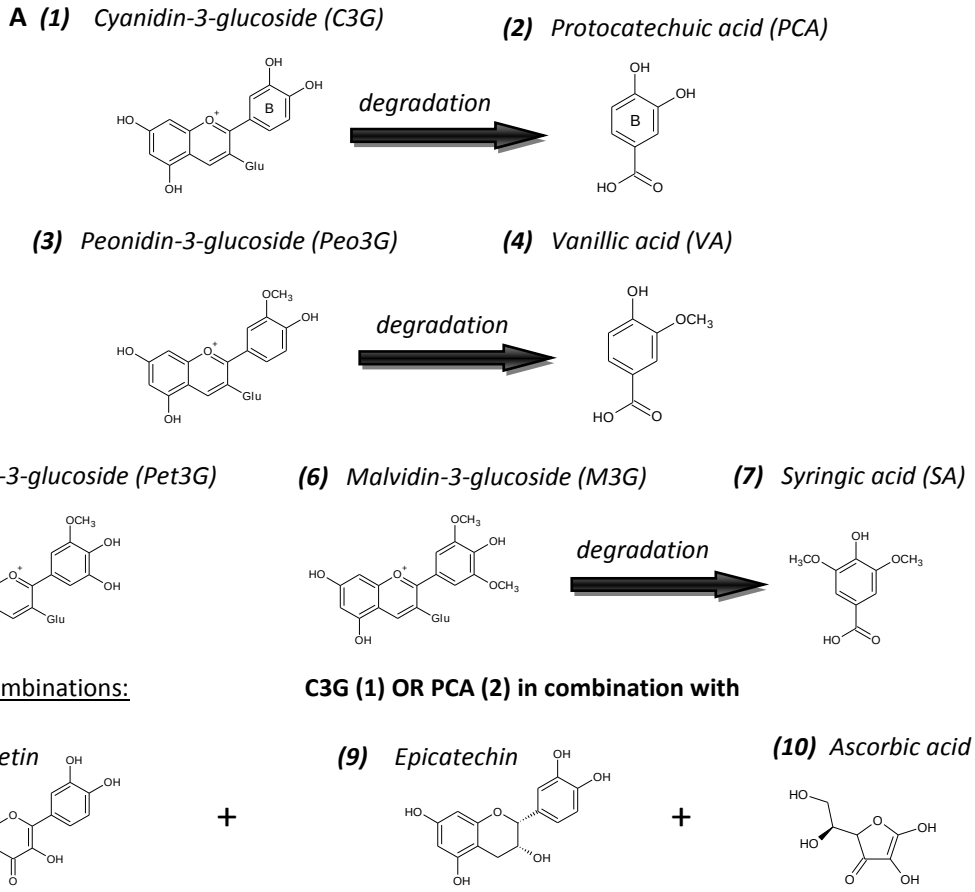

3.2 Materials and methods

Standards and reagents. Cyanidin-3-glucoside, peonidin-3-glucoside and malvidin-3-glucoside were purchased from Extrasynthese (Genay Cedex, France); petunidin-3-glucoside from Polyphenols Laboratories AS (Sandnes, Norway); and protocatechuic acid, vanillic acid, syringic acid, (-)-epicatechin, quercetin and L-ascorbic acid from Sigma-Aldrich [Poole, United Kingdom (UK)]. Standard solutions were prepared in 100% dimethylsulphoxide (DMSO) from Sigma-Aldrich (molecular biology grade) at concentrations of 40mM for anthocyanins and 200mM for all other treatment compounds. Quantikine Human eNOS Immunoassay was purchased from R&D Systems (Abingdon, UK) and Nitrate/Nitrite Colourimetric Assay Kit from Cambridge Bioscience (Cambridge, UK). Resveratrol, tumour necrosis factor-α (TNF-α), and fibronectin were purchased from Sigma-Aldrich. All water utilised was of Milli-Q grade (18.2 MΩ cm^{-1}).

Cell culture. Cryo-preserved, early passage, pooled human umbilical vein endothelial cells (HUVECs) were purchased from TCS CellWorks (Buckingham, UK) and used between passages two to four. Cells were routinely cultured in 75cm^2 flasks (SPL Life Sciences) with fibronectin coating (0.27µg/cm^2) in

large vessel endothelial cell growth medium [TCS CellWorks; proprietary basal medium formulation supplemented with growth factor and antibiotic (gentamicin & amphotericin B) supplements, final concentration of 2% v/v foetal bovine serum] at 37°C and 5% CO_2. HUVECs were sub-cultured using 0.025% trypsin and 0.01% EDTA (TCS CellWorks).

Cell treatments. 24-well plates (SPL Life Sciences) were coated with fibronectin (0.25µg/cm^2), and seeded with HUVECs at a density of ~30,000 cells/well. Cells were subsequently grown to confluence (~24 - 48 hours at 37°C and 5% CO_2). Culture medium was then aspirated, and solutions of the treatment compounds (0.1, 1, or 10µM) prepared in supplemented large vessel endothelial cell growth medium (phenol-red free) were added to relevant wells at a volume of 500µl/well. The assay controls included wells with media only (basal), and wells with DMSO in media (vehicle control). Three replicate wells were used for each control and treatment solution. The plates were incubated for 24 hours at 37°C and 5% CO_2; after which supernatants were removed and stored at -80°C. Cells were washed once with warm phosphate-buffered saline (PBS), and then harvested in 250µl trypsin/EDTA and 250µl trypsin-blocking solution (TCS CellWorks). Cell suspensions were stored at -80°C until analysis.

eNOS enzyme-linked immunosorbent assay (ELISA). Quantification of eNOS in HUVEC lysates was performed with a commercially available ELISA (Quantikine, R&D Systems), using a microplate pre-coated with monoclonal anti-eNOS. Briefly, cell suspensions were thawed, prior to centrifugation at 10,000rpm for 10 minutes and supernatant removal. Cells were then lysed at 2-8°C using assay lysis buffer, and centrifuged at 5000rpm for five minutes; the resultant supernatants were subsequently assayed in duplicate (100µl per well). One hundred microlitres of assay diluent was added to each well, and the microplate incubated for two hours at room temperature with agitation (500rpm). After washing with assay wash buffer, 200µl polyclonal anti-eNOS (conjugated to horseradish peroxidase) was added to each well, and the microplate incubated for a further two hours. Unbound antibody was removed by washing; and 200µl/well substrate solution added prior to a 30 minute incubation. After addition of 50µl/well stop solution, end-point absorbance was measured at 450nm (reference 540nm) with a microplate reader [Fluostar Omega, BMG Labtech (Aylesbury, UK)]; and eNOS quantified based upon a standard curve generated using recombinant human eNOS standard. Tumour necrosis factor-α (20ng/ml) was screened as a negative control for eNOS expression (Anderson et al., 2004). The intra-assay coefficient of variation (CV) was 4.67% ± 1.86% [mean ± standard deviation (SD), n=3] and the inter-assay CV was 6.10% (n=3).

Nitrate/nitrite assay. Nitric oxide production was assessed by quantification of the levels of nitrite (NO_2^-) and nitrate (NO_3^-) decomposition products (Tsikas, 2007) in cell supernatants using a colourimetric microplate assay (Nitrate/Nitrite Colourimetric Assay Kit, Cayman Chemical Company). Briefly, cell supernatants were thawed, and particulate matter removed by centrifugation at

10,000rpm for 10 minutes. The supernatants were then assayed in duplicate (50µl per well). Thirty microlitres of assay buffer was added to each well, followed by 10µl/well enzyme cofactor mixture and 10µl/well nitrate reductase mixture. The microplate was incubated for two hours at room temperature, prior to addition of Griess Reagents R1 and R2 (both at 50µl/well). End-point absorbance was measured at 540nm (reference 690nm) with a microplate reader (Fluostar Omega, BMG Labtech) and total NO decomposition products quantified based upon a nitrate standard curve generated using nitrate standard. Resveratrol (100µM) was screened as a positive control for endothelial NO production (Wallerath et al., 2002). The intra-assay CV was 6.63% ± 1.10% (mean ± SD, n=3) and the inter-assay CV was 2.38% (n=3).

Statistical analysis. Analysis of variance (ANOVA) with Tukey post-hoc test was performed using SPSS software (IBM, New York, USA) version 18 for Windows. Significance was determined at the 5% level, and expressed relative to DMSO (vehicle control). Three biological replicates for each control or treatment were utilised for analysis unless otherwise noted, and means of replicates represented graphically. Error bars in figures represent one SD from the mean.

3.3 Results

Significant upregulation of eNOS, as compared with vehicle control ($p < 0.05$), was observed following a 24h incubation of HUVECs with 0.1-10µM cyanidin-3-glucoside (Figure 3.2 A), 10µM peonidin-3-glucoside (Figure 3.2 B) and 0.1µM petunidin-3-glucoside (Figure 3.2 C). However, no significant alteration in eNOS levels was observed with any concentration of malvidin-3-glucoside (Figure 3.2 D).

No significant modulation of eNOS levels was elicited by the phenolic degradants protocatechuic acid (Figure 3.3 A), vanillic acid (Figure 3.3 B) and syringic acid (Figure 3.3 C); although a trend towards elevated eNOS relative to vehicle control was observed with 1µM syringic acid ($p = 0.177$). Incubation of HUVECs with cyanidin-3-glucoside, or protocatechuic acid, in combination with epicatechin, quercetin and ascorbic acid (in an equimolar ratio) did not significantly alter eNOS expression (Figure 3.4). Tumour necrosis factor-α (negative control) elicited reduced eNOS expression relative to basal (220.2 ± 89.3pg/ml versus 419.4 ± 88.0pg/ml respectively; mean ± SD), although the reduction was not significant ($p > 0.05$). Normalisation of measured eNOS protein levels to the total protein concentration of cell lysates assayed may help to reduce variability between biological replicates, and should be incorporated into future analyses.

Figure 3.2 Modulation of HUVEC eNOS expression by cyanidin-3-glucoside (A), peonidin-3-glucoside (B), petunidin-3-glucoside (C) and malvidin-3-glucoside (D) following 24h incubation.

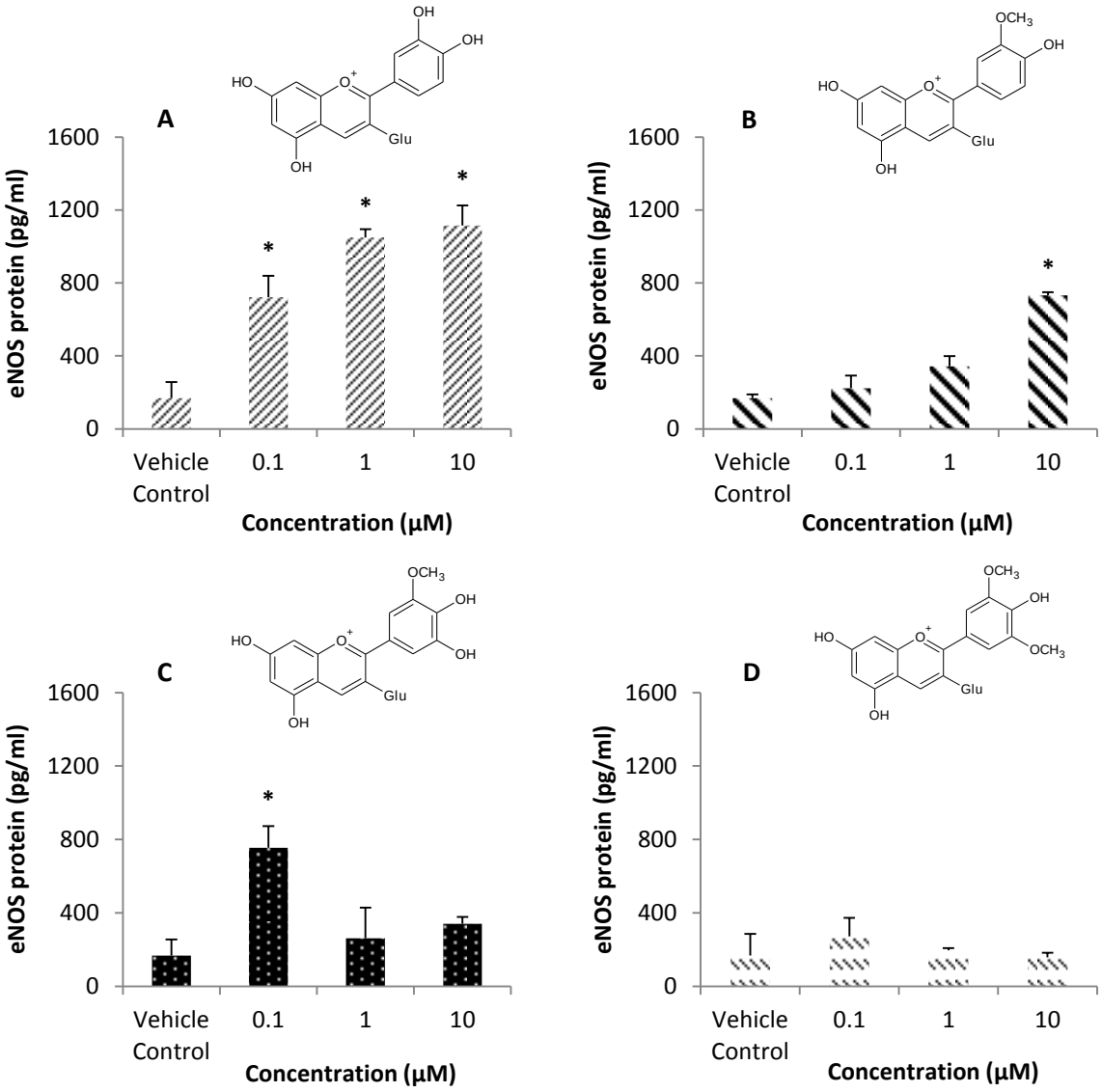

eNOS expression (pg/ml) following 24h incubation of HUVECs with vehicle control (0.05% DMSO in supplemented culture medium) or 0.1-10µM of cyanidin-3-glucoside (A), peonidin-3-glucoside (B), petunidin-3-glucoside (C), or malvidin-3-glucoside (D; structures inset). Data are graphed as mean ± SD, n=3. *Significant difference versus vehicle control ($p < 0.05$).

Figure 3.3 Modulation of HUVEC eNOS expression by protocatechuic acid (A), vanillic acid (B), and syringic acid (C) following 24h incubation.

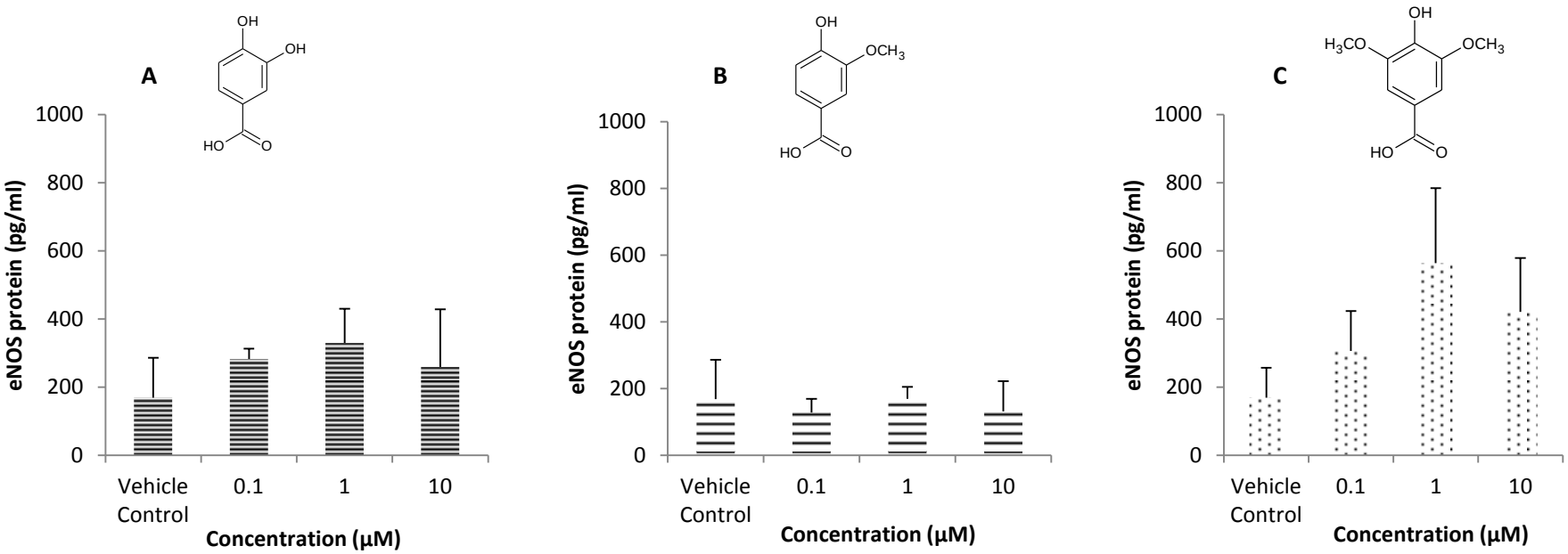

eNOS expression (pg/ml) following 24h incubation of HUVECs with vehicle control (0.05% DMSO in supplemented culture medium) or 0.1-10µM of protocatechuic acid (A), vanillic acid (B), or syringic acid (C, structures inset). Data are graphed as mean ± SD, n=3.

Figure 3.4 **Modulation of HUVEC eNOS expression by cyanidin-3-glucoside (A) or protocatechuic acid (B) in combination with epicatechin, quercetin and ascorbic acid following 24h incubation.**

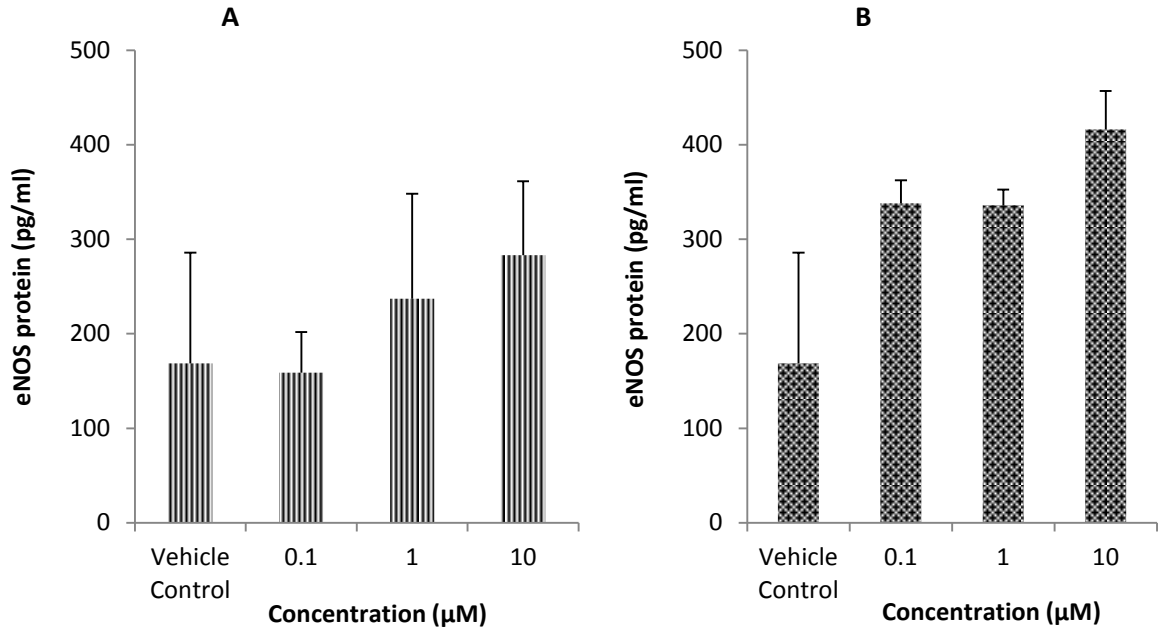

eNOS expression (pg/ml) following 24h incubation of HUVECs with vehicle control (0.05% DMSO in supplemented culture medium) or 0.1-10µM of equimolar ratio of cyanidin-3-glucoside (A) or protocatechuic acid (B) with epicatechin, quercetin and ascorbic acid. Data are graphed as mean ± SD, n=3.

With regard to effects of treatment compounds on endothelial NO production, anthocyanin-3-glucosides did not significantly alter levels of NO decomposition products in HUVEC supernatants (Figure 3.5), although an apparent elevation in nitrite & nitrate concentrations ($p = 0.082$) was elicited by 1µM malvidin-3-glucoside (Figure 3.5 D).

No significant modulation of endothelial NO production was observed with 0.1-10µM anthocyanin phenolic degradants (Figure 3.6), though all degradants appeared to reduce nitrite and nitrate levels relative to vehicle control. Equally, no significant changes in NO production were detected following incubation of HUVECs with cyanidin-3-glucoside, or protocatechuic acid, in combination with epicatechin, quercetin and ascorbic acid (Figure 3.7). Resveratrol (positive control) elicited increased levels of NO decomposition products relative to basal (6.39 ± 0.39µM versus 5.34 ± 2.22µM), although this increase was not significant ($p > 0.05$).

Figure 3.5 Modulation of endothelial NO production by cyanidin-3-glucoside (A), peonidin-3-glucoside (B), petunidin-3-glucoside (C) and malvidin-3-glucoside (D) following 24h incubation.

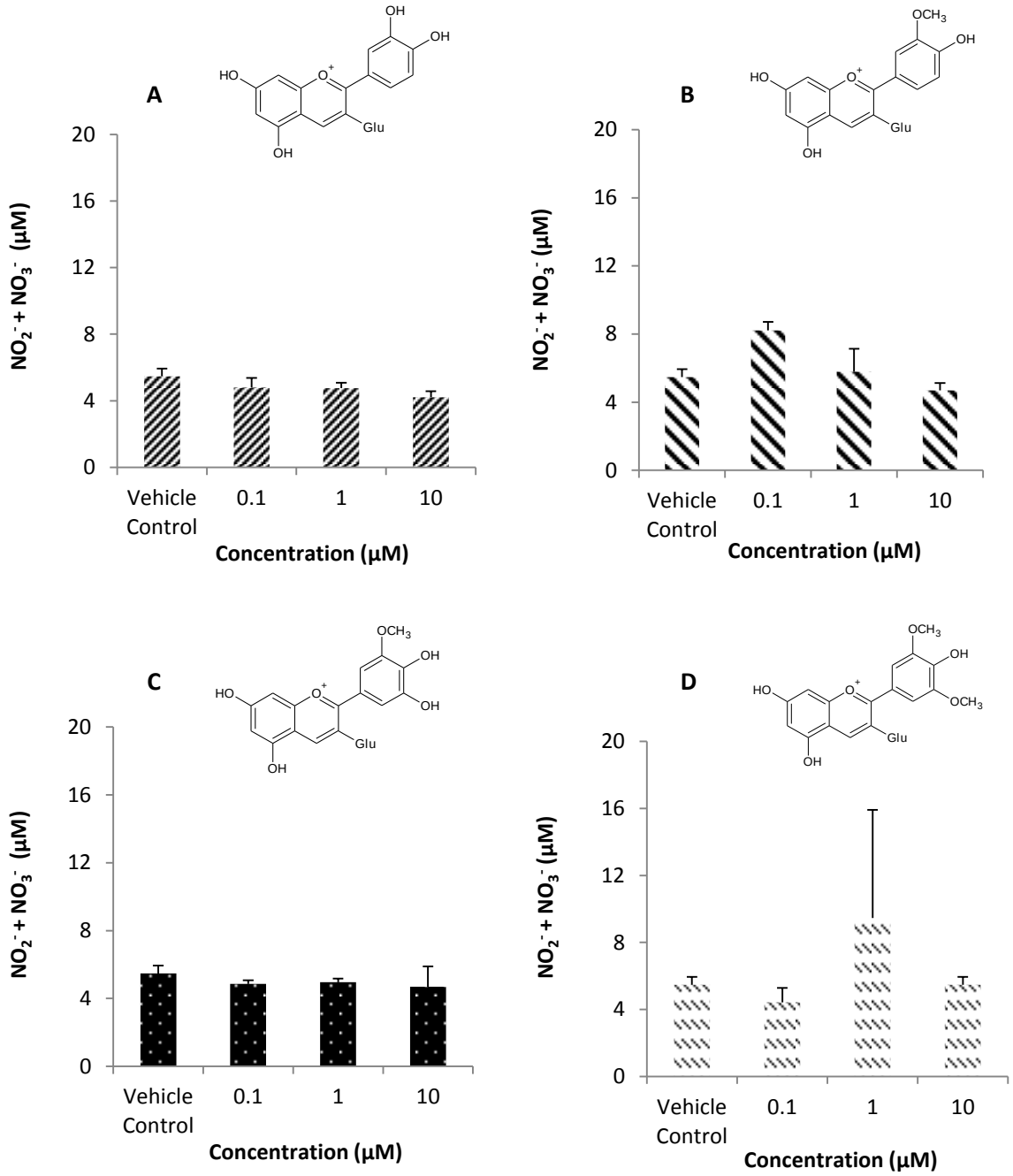

Concentration of nitrite & nitrate (µM) in cell supernatant following 24h incubation of HUVECs with vehicle control (0.05% DMSO in supplemented culture medium) or 0.1-10µM of cyanidin-3-glucoside (A), peonidin-3-glucoside (B), petunidin-3-glucoside (C), or malvidin-3-glucoside (D; structures inset). Data are graphed as mean ± SD, n=3.

Figure 3.6 Modulation of endothelial NO production by protocatechuic acid (A), vanillic acid (B), and syringic acid (C) following 24h incubation.

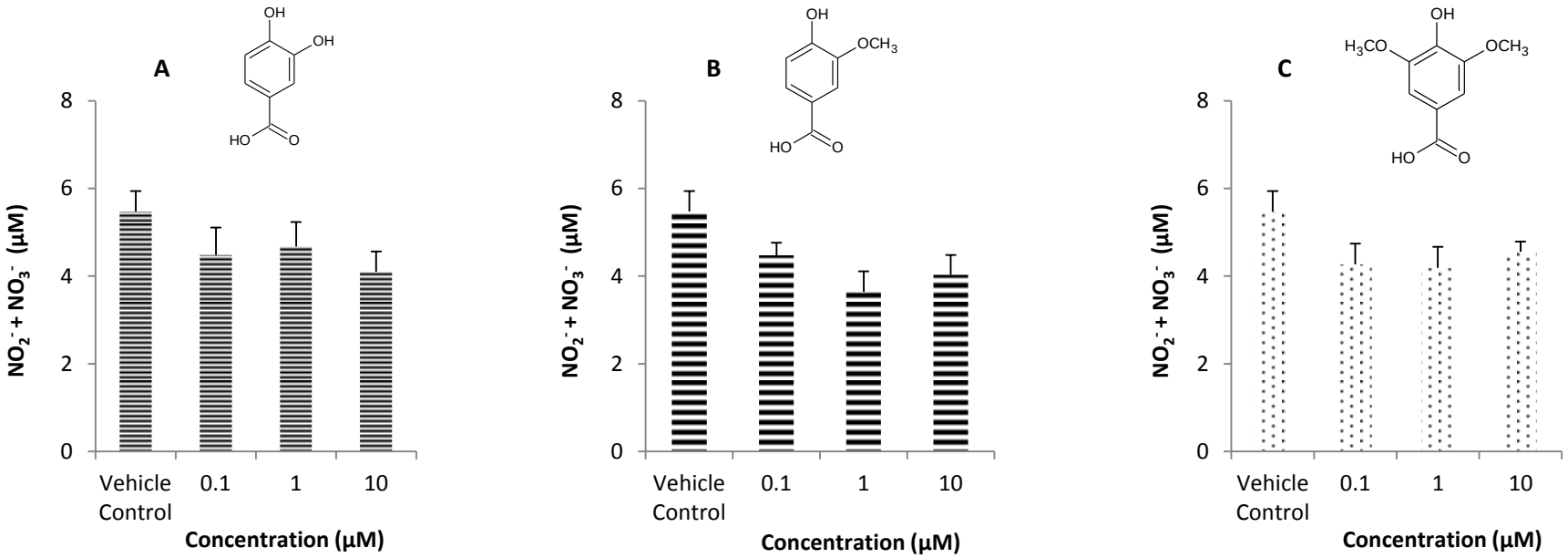

Concentration of nitrite & nitrate (µM) in cell supernatant following 24h incubation of HUVECs with vehicle control (0.05% DMSO in supplemented culture medium) or 0.1-10µM of protocatechuic acid (A), vanillic acid (B), or syringic acid (C, structures inset). Data are graphed as mean ± SD, n=3.

Figure 3.7 Modulation of endothelial NO production by cyanidin-3-glucoside (A) or protocatechuic acid (B) in combination with epicatechin, quercetin and ascorbic acid following 24h incubation.

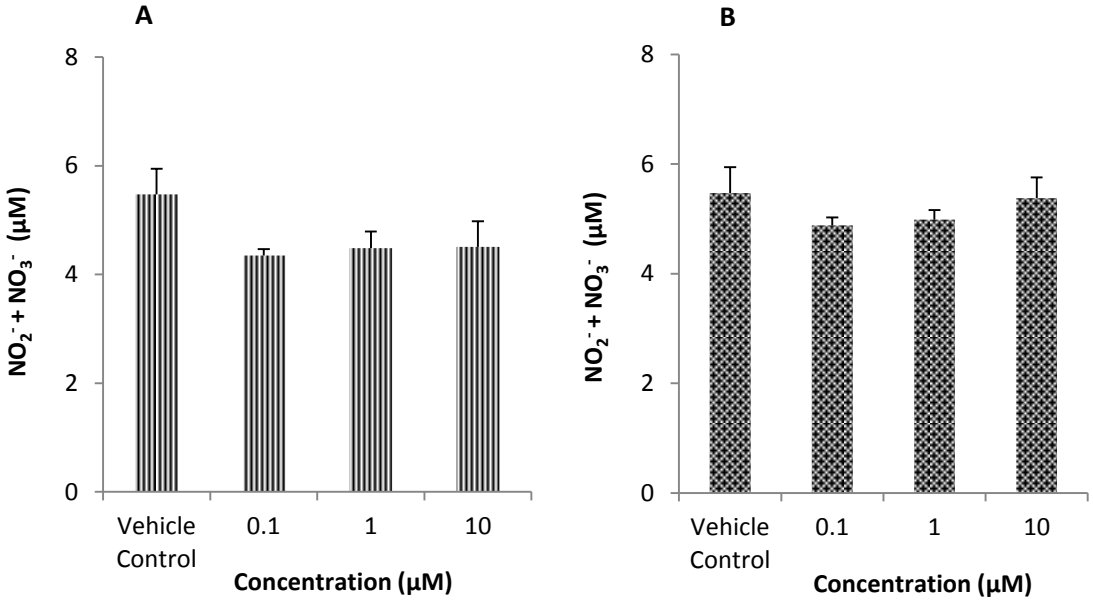

Concentration of nitrite & nitrate (µM) in cell supernatant following 24h incubation of HUVECs with vehicle control (0.05% DMSO in supplemented culture medium) or 0.1-10µM of equimolar ratio of cyanidin-3-glucoside (A) or protocatechuic acid (B) with epicatechin, quercetin and ascorbic acid. Data are graphed as mean ± SD, n=3.

3.4 Discussion

Bioactivity screening of selected anthocyanins and B-ring degradants, for effects upon HUVEC eNOS expression and endothelial NO production, indicates differential bioactivity of parent anthocyanins as compared to their phenolic degradants. Cyanidin-3-glucoside has been reported to upregulate eNOS in BAECs at 1 - 100nM (Xu et al., 2004b), although not in human iliac artery endothelial cells (HIAEC) at ≤ 10µM (Sorrenti et al., 2007); and in the current investigation cyanidin-3-glucoside (at 0.1 - 10µM), peonidin-3-glucoside (at 10µM) and petunidin-3-glucoside (at 0.1µM), but not malvidin-3-glucoside, elicited significant upregulation of eNOS protein in HUVECs. By contrast, the phenolic degradants protocatechuic acid (B-ring degradant of cyanidin-3-glucoside), vanillic acid (B-ring degradant of peonidin-3-glucoside) and syringic acid (B-ring degradant of malvidin-3-glucoside) did not significantly modulate eNOS expression. Moreover, no significant changes in eNOS levels were induced by cyanidin-3-glucoside or protocatechuic acid in combination with quercetin, epicatechin and ascorbic acid (at 1 - 10µM in an equimolar ratio). It should be noted that Steffen *et al* (2005) previously reported no modulation of basal eNOS levels by 40µM epicatechin in both BAECs and the endothelial cell line Ea.hy926 (Steffen et al., 2005). In contrast to eNOS expression, no treatment compounds or combinations significantly modulated endothelial NO production, as assessed by levels of nitrite and nitrate decomposition products (Tsikas, 2007) in cell supernatants.

A limitation of the current investigation was the use of HUVECs, which are extensively used for general research concerning human endothelial cells; however, an arterial cell type may be more relevant for assessing the potential modulation of endothelial function predisposing to development of atherosclerosis (Baudin et al., 2007). Moreover, no significant effects of treatment compounds upon endothelial NO production were detected in this study, yet activation of eNOS by cyanidin-3-glucoside (through alteration of phosphorylation status at key serine residues) has been described in BAECs (Xu et al., 2004a) and HUVECs (Edirisinghe et al., 2011). Furthermore, significant increases in nitrite levels were reported following incubation of HUVECs with malvidin and syringic acid (Simoncini et al., 2011), and epicatechin (Persson et al., 2006, Brossette et al., 2011, Simoncini et al., 2011). However, in the current investigation nitrite and nitrate decomposition products were detected within a range of 3 - 17μM, and it is possible that the modified Griess reaction utilised to quantify these products was not sufficiently sensitive to detect submicromolar changes in eNOS activity (Granger et al., 1996). The use of an alternative detection methodology such as reductive chemiluminescence (MacArthur et al., 2007), possibly in combination with nitrite- and nitrate-free culture medium (Brossette et al., 2011), might address this issue. In addition, extra time points could be included in both eNOS expression and NO production screening assays (for example six, 18 and 36 hour incubations with treatment compounds or combinations) to ensure detection of bioactivity.

Overall, only parent anthocyanin glucosides, as opposed to their phenolic degradants or combinations of flavonoids with other bioactive compounds, significantly upregulated endothelial expression of eNOS. Bioactivity of anthocyanins was observed in the concentration range 0.1 - 10μM; and whilst anthocyanin plasma concentrations of ~0.1μM/100nM have been reported in some human bioavailability studies, C_{max} values are often below 100nM (Manach et al., 2005, McGhie and Walton, 2007, Milbury et al., 2010, Wiczkowski et al., 2010). Indeed, following ingestion of 71mg of cyanidin glucosides, C_{max} values for cyanidin-3-glucoside and protocatechuic acid in human serum were 1.9nM and 492nM (0.5μM) respectively (Vitaglione et al., 2007); and a plasma C_{max} of 2.5μM for the B-ring degradant 4-hydroxybenzoic acid was reported after ingestion of the parent anthocyanin pelargonidin-3-glucoside in 300g fresh strawberries, whilst no anthocyanins were detectable (Azzini et al., 2010). More recently, Czank *et al* (2013) described a serum C_{max} of 0.14μM for cyanidin-3-glucoside following consumption of 500mg ^{13}C-labelled cyanidin-3-glucoside by healthy volunteers, as compared with C_{max} values of 0.72μM and 2.35μM for ^{13}C-labelled phenolic degradants (protocatechuic acid and phloroglucinol aldehyde) and phase II conjugates of protocatechuic acid (including vanillic acid) respectively (Czank et al., 2013). Therefore, the observed upregulation of eNOS in HUVECs by anthocyanins at ≥ 0.1μM may not be biologically relevant *in vivo*; but as detailed in Chapter 2, anthocyanin phenolic degradants appeared to reduce superoxide levels in a HUVEC stimulated superoxide production model, with significant decreases ($p < 0.05$) elicited by vanillic acid and syringic acid at 1μM. Moreover, degradants which contain a catechol (protocatechuic acid) or

mono-*O*-methylated (vanillic acid) B-ring might act as inhibitors of NADPH oxidase/NOX (Steffen et al., 2007b, Steffen et al., 2008); thereby reducing superoxide production and scavenging of NO *in vivo*, and indirectly enhancing vascular endothelial function (Schewe et al., 2008, Cassidy et al., 2010), as opposed to direct stimulation of NO production. Vanillic acid elicited an apparent decrease in superoxide levels at all concentrations examined, such that these levels were not significantly different from basal (unstimulated) cells in the same assay.

Given the observed bioactivity of vanillic acid at a physiologically relevant concentration for phenolic degradants, and the structural relationship between vanillic acid and reported NOX inhibitors, this compound was selected to investigate the mechanisms by which anthocyanin degradants could inhibit NOX activity and therefore reduce vascular superoxide production. Modulation of endothelial NOX2 and NOX4 protein expression by anthocyanin degradants (at 0.1 - 10μM), following angiotensin II stimulation, has been assessed previously (as detailed in Chapter 2). NOX4 is reported to be the predominant vascular endothelial isoform (Bedard and Krause, 2007); whilst NOX2, which requires additional cytosolic proteins for enzyme activity (Lassegue and Griendling, 2010), is thought to play a key role in regulating vascular function through reduction of bioavailable NO (Brown and Griendling, 2009, Schroder, 2010). Vanillic acid did not appear to alter expression of either of these isoforms; suggesting any modulation of NOX activity may occur at the post-translational level, or through effects on expression of other subunits of the NOX enzyme complex.

In conclusion, inhibition of NOX activity and thus superoxide production by vanillic acid, with reduced scavenging of endothelial NO, could indirectly elevate NO levels and therefore enhance vascular function *in vivo*; and the cellular mechanisms potentially underlying this activity should be further investigated (as detailed in Chapters 4, 5 and 6).

4 Regulation of stimulated endothelial NOX gene expression by the anthocyanin phenolic acid degradation product vanillic acid

4.1 Background

Endothelium-derived nitric oxide (NO) is a mediator of vascular homeostasis (Higashi et al., 2009, Förstermann and Sessa, 2012), eliciting vasodilation through activation of soluble guanylate cyclase in vascular smooth muscle cells (Hobbs et al., 1999). In addition, NO acts to inhibit activation and aggregation of platelets, expression of cell surface adhesion molecules, and oxidation of low density lipoprotein; which are all important processes in atherogenesis (Kawashima and Yokoyama, 2004, Naseem, 2005, Michel and Vanhoutte, 2010). Nitric oxide therefore has anti-atherosclerotic activity (Wever et al., 1998), and decreased NO bioavailability can impair endothelial function (Higashi et al., 2009), which is a critical process in atherosclerotic development (Kawashima and Yokoyama, 2004). Reduced NO bioavailability may result from inactivation of NO by reactive oxygen species (ROS) (Landmesser et al., 2004), and the NADPH oxidase, or NOX, family of transmembrane enzymes constitute a major source of ROS in the vasculature (Touyz, 2004, Bedard and Krause, 2007, Leopold and Loscalzo, 2009). Structure-activity studies of (-)-epicatechin and its metabolites (Steffen et al., 2007b, Steffen et al., 2008) have suggested inhibition of NOX activity may be a mechanism by which certain flavonoids could increase NO levels and improve vascular function (Schewe et al., 2008).

NADPH oxidase proteins transfer electrons across biological membranes to an acceptor molecule, usually oxygen (Lassegue and Clempus, 2003, Bedard and Krause, 2007); and of seven identified mammalian isoforms (Sumimoto et al., 2005, Bedard and Krause, 2007), NOX1, 2, 4 and 5 are expressed in the cardiovascular system (Brandes et al., 2010, Takac et al., 2011). With regard to the vascular endothelium, expression of NOX2, NOX4 and NOX5 has been described previously (Bedard and Krause, 2007, Brandes and Schröder, 2008). NOX4 appears to be the major vascular endothelial isoform (Bedard and Krause, 2007, Takac et al., 2011) producing predominantly hydrogen peroxide (Brown and Griendling, 2009), whereas NOX2 generates superoxide (Brandes et al., 2010) and may have a key role in regulating vascular function by limiting NO bioavailability (Brown and Griendling, 2009, Schroder, 2010). Assembly of a functional enzyme complex can require additional protein components depending upon the NOX isoform (Brown and Griendling, 2009), and both NOX2 and 4 associate with the integral membrane protein $p22^{phox}$ (Sumimoto et al., 2005). However, whereas NOX4 is reported to be constitutively active (Takac et al., 2011), activation of NOX2 follows recruitment of additional cytosolic proteins including $p47^{phox}$ ('organiser' subunit), $p67^{phox}$ ('activator' subunit), $p40^{phox}$, and the small G-protein Rac1/2 (Sumimoto et al., 2005, Drummond et al., 2011).

During an earlier investigation (Chapter 2), selected anthocyanin glucosides and phenolic acid degradants were screened for their effect on angiotensin II-stimulated superoxide production by endothelial NOX. Based upon the generated bioactivity screening data, and structural similarities with reported NOX inhibitors such as apocynin, the anthocyanin B-ring degradant vanillic acid (Figure 4.1) was selected to elucidate cellular mechanisms potentially underlying previously observed reductions in superoxide levels elicited by anthocyanins and their degradants (Chapter 2). As noted above, inhibition of superoxide production by endothelial NOX may result in enhanced NO availability, with beneficial effects on vascular endothelial function *in vivo* (Schewe et al., 2008, Förstermann, 2010).

Figure 4.1 **Anthocyanin degradant vanillic acid selected for investigation of the potential mechanisms of NOX inhibition by anthocyanins.**

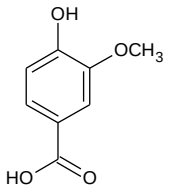

In the current investigation, the effect of vanillic acid at physiologically relevant concentrations (Czank et al., 2013) on endothelial mRNA levels of selected NOX isoforms and associated proteins following cell stimulation was examined by reverse transcription – quantitative polymerase chain reaction (RT-qPCR), to assess whether NOX function was affected by vanillic acid at the transcriptional level. Both NOX2 and NOX4 isoforms were chosen for analysis, in addition to their common membrane partner $p22^{phox}$, and the cytosolic subunits $p47^{phox}$ and $p67^{phox}$ required for NOX2 activity.

4.2 Materials and methods

Standards and reagents. Vanillic acid was purchased from Sigma-Aldrich [Poole, United Kingdom (UK)] and a 200mM standard solution prepared in 100% dimethylsulphoxide (DMSO; Sigma-Aldrich molecular biology grade). All water utilised was of Milli-Q grade (18.2 MΩ cm^{-1}).

Recombinant human transforming growth factor-beta 1 (TGF-β1) was purchased from R&D Systems (Abingdon, UK). Tumour necrosis factor-alpha (TNF-α), TRIzol® reagent, RNase-free water, oligo (dT) primer (50µM), SuperScript® II Reverse Transcriptase (with 5x first strand buffer and 100mM dithiothreitol/DTT), and MicroAmp™ optical microplates were obtained from Life Technologies (Paisley, UK). RiboLock RNase inhibitor, DNase I (with 10x reaction buffer with $MgCl_2$, and 50mM EDTA), dNTP PCR mix (10mM), oligo (dT) primer (100µM), chloroform (molecular biology grade), and isopropanol were purchased from Thermo Fisher Scientific (Fisher Scientific, Loughborough, UK); and

ethanol (molecular biology grade), human angiotensin II (synthetic), fibronectin, and Medium 199 from Sigma-Aldrich. Foetal bovine serum (FBS; heat-inactivated) was purchased from Biosera (Ringmer, UK). Precision 2x real-time PCR MasterMix with SYBR®Green was obtained from PrimerDesign Ltd (Southampton, UK), and custom primer sets for human NOX2, NOX4, $p22^{phox}$, $p47^{phox}$ and $p67^{phox}$ were designed, pre-validated and supplied by PrimerDesign Ltd. Primer sequences are tabulated below.

Table 4.1 Sense/anti-sense primers sequences (5' to 3') for qPCR (real time).

Gene	Symbol/accession number	Sense Primer	Anti-sense Primer
NOX2	CYBB/NM_000397	AAGAAGAAGGGGTTCAAAATGGA	GGGGCGGATGTCAGTGTAA
NOX4	NOX4/NM_016931	CACAGACTTGGCTTTGGATTTC	GGATGACTTATGACCGAAATGATG
$p22^{phox}$	CYBA/NM_000101	GTTTGTGTGCCTGCTGGAG	CCGAACATAGTAATTCCTGGTAAAG
$p47^{phox}$	NCF1/NM_000265	GCGGTTGGTGGTTCTGTCAG	TAGTTGGGCTCAGGGTCTTCC
$p67^{phox}$	NCF2/NM_000433	CCTCCACCCAGACCGAAAA	TCTCAGGCACAAACCCAAATAG

CYBA/CYBB, cytochrome b-245 alpha/beta polypeptide; NCF1/NCF2, neutrophil cytosolic factor 1/2; NOX2/4, NADPH oxidase isoform 2/4.

Cell culture. Cryo-preserved, early passage, pooled human umbilical vein endothelial cells (HUVEC) were purchased from TCS CellWorks (Buckingham, UK) and used between passages two to four. Cells were routinely cultured in 75cm^2 flasks (SPL Life Sciences) coated with fibronectin (0.27µg/cm^2), using large vessel endothelial cell growth medium [TCS CellWorks; proprietary basal medium formulation supplemented with growth factor and antibiotic (gentamicin & amphotericin B) supplements, final concentration of 2% v/v foetal bovine serum] at 37°C and 5% CO_2. HUVECs were sub-cultured using 0.025% trypsin and 0.01% EDTA (TCS CellWorks).

4.2.1 Method development – RT-qPCR

Reverse-transcription – quantitative polymerase chain reaction: method development (Figure 4.2). Method development was conducted to confirm specificity of PCR products generated using custom primer sets for NOX isoforms and subunits (Figure 4.2 A), and to select optimal endogenous reference genes for normalisation of C_t data for genes of interest (Figure 4.2 B). A time course experiment was also conducted to identify the optimum incubation time with angiotensin II for stimulated gene expression (Figure 4.2 C), as based upon reviewed reports (Appendix Table 9.2.4) and previous investigations (Chapters 2 & 3), 0.1µM angiotensin II (or 10ng/ml TGF-β1; Figure 4.2 D) was utilised to stimulate endothelial cells.

Figure 4.2 **RT-qPCR analysis of stimulated endothelial NOX isoform/subunit expression: method development flow chart.**

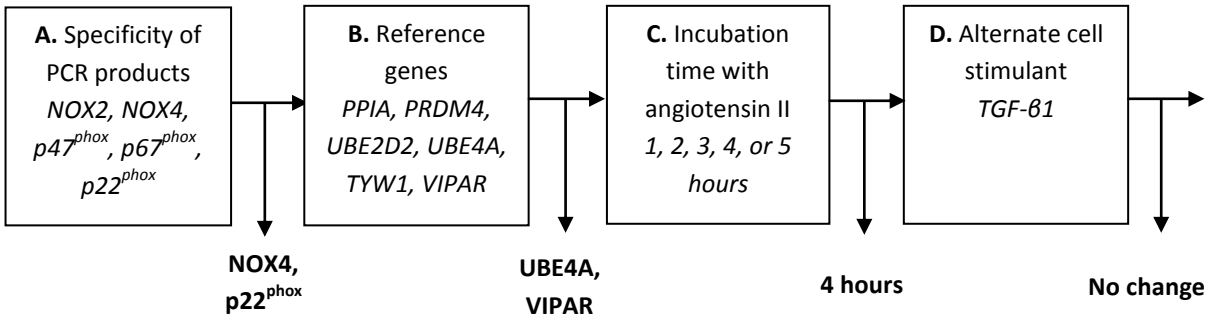

Specificity of PCR products (Figure 4.2 A). Analysis of melt curve data for NOX custom primer sets, to confirm specificity of PCR product prior to relative quantification of gene expression levels, indicated non-specific amplification for NOX2 (Appendix Figure 9.4.1 A), $p47^{phox}$ (Appendix Figure 9.4.1 B), and $p67^{phox}$ (Appendix Figure 9.4.1 C) primer sets generating multiple T_m peaks. Amplification of multiple amplicons for NOX2, $p47^{phox}$ and $p67^{phox}$ was not resolved by either redesign of custom primers by the supplier, or conducting gene-specific reverse transcription to select for specific mRNA transcripts. Melt curve analysis for NOX4 and $p22^{phox}$ primer sets indicated specific amplification of a single PCR product (Appendix Figure 9.4.2 A & B), permitting relative quantification of gene expression levels for these transcripts.

Reference/housekeeping genes (Figure 4.2 B). Identification of optimal reference genes for normalisation of C_t data was conducted using a geNorm^{PLUS} kit (PrimerDesign Ltd). Primer sets for six stably expressed human reference genes (Table 4.2) were designed, pre-validated and supplied by PrimerDesign Ltd, and used to evaluate expression of these genes in both unstimulated and stimulated HUVEC. Real-time PCR data were analysed using the geNorm function in qbase^{PLUS} software (version 2.3, Biogazelle NV, Zwijnaarde, Belgium) to assess reference gene stability across samples, and optimal number of reference genes (Vandesompele et al., 2002).

Table 4.2 **Reference/housekeeping genes evaluated during method development.**

Gene	Description
PPIA	Peptidylprolyl isomerase A (cyclophilin A)
PRDM4	PR domain containing 4
UBE2D2	Ubiquitin-conjugating enzyme E2D 2
UBE4A	Ubiquitination factor E4A
TYW1	tRNA-yW synthesizing protein 1 homologue (*S. cerevisiae*)
VIPAR/C14orf133/VIPAS39	VPS33B interacting protein, apical-basolateral polarity regulator, spe-39 homologue

Cultured HUVEC were incubated for five hours with culture medium only (basal), 0.1µM angiotensin II, or 0.1µM angiotensin II with 10µM vanillic acid. A five hour time point was selected as approximating to the mid-point of the range of four to seven hours used in previous studies with HUVEC reporting upregulation of NOX4 and $p22^{phox}$ mRNA induced by 0.1µM angiotensin II (Rueckschloss et al., 2002, Yamagishi et al., 2005, Alvarez et al., 2010). Following RNA extraction and first strand cDNA synthesis, reference gene expression was assessed by real-time PCR, and the generated C_t data were analysed using $qbase^{PLUS}$. The average expression stability of reference targets across treatment conditions (geNorm M value) was investigated by geNorm analysis (Figure 4.3; targets plotted in order of increasing stability from left to right); and optimal number of targets was also confirmed (Figure 4.4). UBE4A and VIPAR were identified as the optimum reference genes, and their geometric mean used as the normalisation factor in the final assay.

Figure 4.3 Average reference gene expression stability (geNorm M graph) for untreated HUVEC and following 5h incubation with 0.1µM angiotensin II and 10µM vanillic acid.

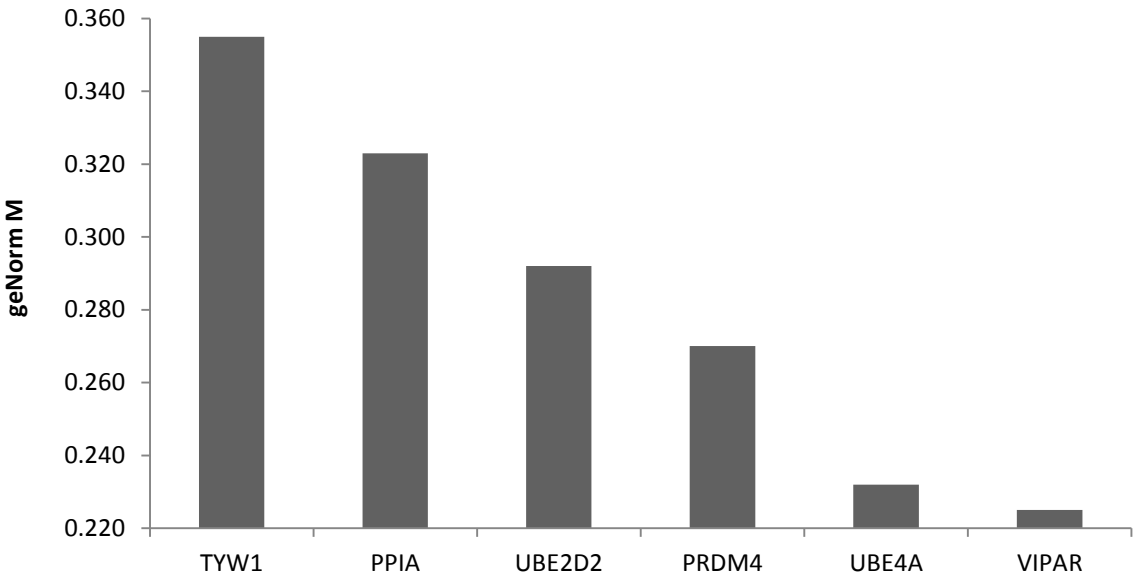

geNorm M graph demonstrating average reference gene expression stability (geNorm M value, y-axis) across experimental conditions (ie untreated, 0.1µM angiotensin II, & 10µM vanillic acid). Reference genes (x-axis) are arranged in order of increasing stability from left to right (refer to Table 4.2. for gene descriptions).

Incubation time with angiotensin II (Figure 4.2 C). The optimal incubation time for HUVEC with 0.1µM angiotensin II to elicit upregulation of NOX isoform/subunit mRNA was confirmed by a time course experiment. Tumour-necrosis factor-alpha was selected for use as a positive control in this investigation, based upon a review of 12 research reports (Appendix Table 9.2.5). Cultured HUVEC were incubated for one, two, three, four or five hours with 0.1µM angiotensin II, or 20ng/ml TNF-α; prior to RNA extraction and first strand cDNA synthesis. The additional time points of one hour to four hours were chosen based on reported upregulation of NOX4 and $p22^{phox}$ mRNA by ~1.4-fold and

3-fold respectively following incubation of HUVECs for only four hours with 0.1µM angiotensin II (Yamagishi et al., 2005).

Figure 4.4 Determination of optimal number of reference genes (geNorm V graph) for untreated HUVEC and following 5h incubation with 0.1µM angiotensin II and 10µM vanillic acid.

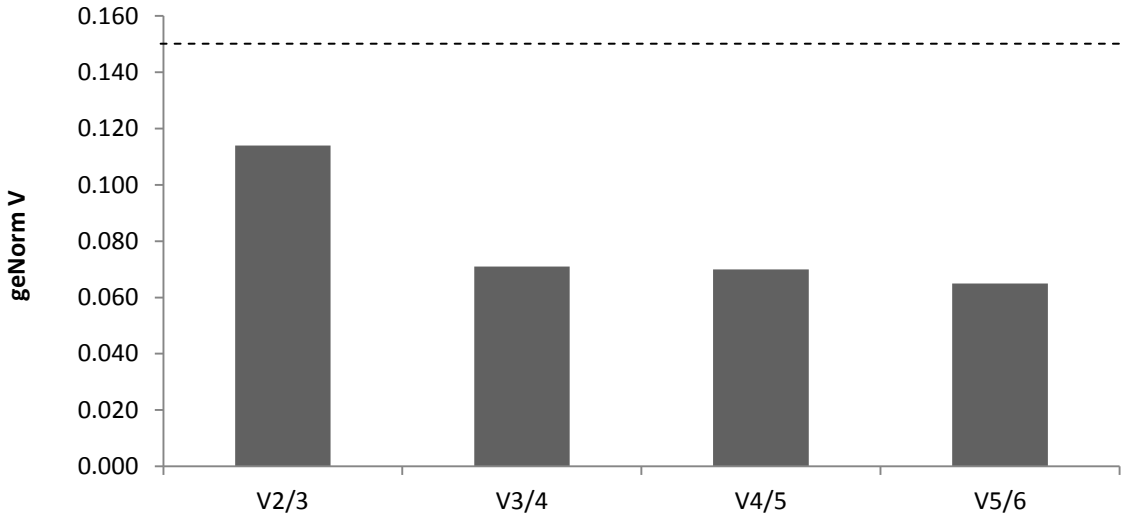

geNorm V graph determining optimal number of reference genes. 'V2/3' denotes comparison between 2 genes and 3 genes, 'V3/4' compares 3 genes versus 4 genes etc. across untreated (basal) and treated (0.1µM angiotensin II & 10µM vanillic acid) samples. Where the geNorm V value is below 0.15 (ie below dashed line), no additional benefit is derived from using a further reference gene.

Expression of NOX4 and $p22^{phox}$, in addition to six reference genes (Table 4.2), was compared against unstimulated (basal) cells by real-time PCR. Owing to the inclusion of a positive control (TNF-α), a geNorm analysis was performed to identify the optimal reference genes across treatments used in this time course experiment (data not shown). UBE2D2 and PRDM4 were identified as the optimum reference genes, and their geometric mean was used as the normalisation factor in this assay. Based on fold change in NOX4 mRNA levels versus basal [1.86 fold ± 0.98; mean ± SD (Figure 4.5 A)], a four hour incubation was identified as the optimum time point for subsequent assays. Endothelial mRNA levels for $p22^{phox}$ (Figure 4.5 B) showed the greatest fold change versus basal following five hours incubation with angiotensin II (1.80 ± 0.14); however, as upregulation was also indicated at the four hour time point (1.63 ± 1.10), four hours was selected as the optimum incubation period for upregulation of both NOX4 and $p22^{phox}$ mRNA levels in the final assay.

Following stimulation of HUVEC with TNF-α (positive control), significant upregulation of NOX4 mRNA was detected at the three hour time point (1.63 ± 0.39; Figure 4.6 A) as compared with the one hour time point (0.75 ± 0.19), and significantly elevated levels of $p22^{phox}$ mRNA were observed after two hours incubation with TNF-α (1.32 ± 0.11; Figure 4.6 B) relative to all other time points.

Figure 4.5 **Modulation of endothelial NOX4 (A) and p22^{phox} (B) mRNA levels following stimulation of HUVEC with 0.1μM angiotensin II for 1-5 hours.**

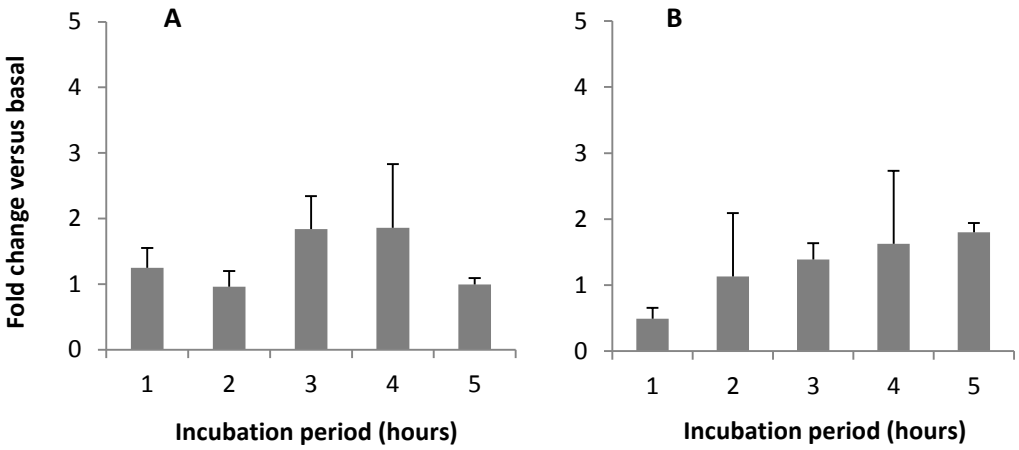

Fold change in HUVEC NOX4 (A) and p22^{phox} (B) mRNA levels versus unstimulated cells (basal) following incubation with 0.1μM angiotensin II for 1, 2, 3, 4 or 5 hours. Relative quantification was performed using the comparative C_t method, incorporating the geometric mean of reference genes PRDM4 and UBE2D2 as the normalisation factor. Data are graphed as mean ± SD (n=3); no significant differences between time points ($p > 0.05$).

Figure 4.6 **Modulation of endothelial NOX4 (A) and p22^{phox} (B) mRNA levels following stimulation of HUVEC with 20ng/ml TNF-α for 1-5 hours.**

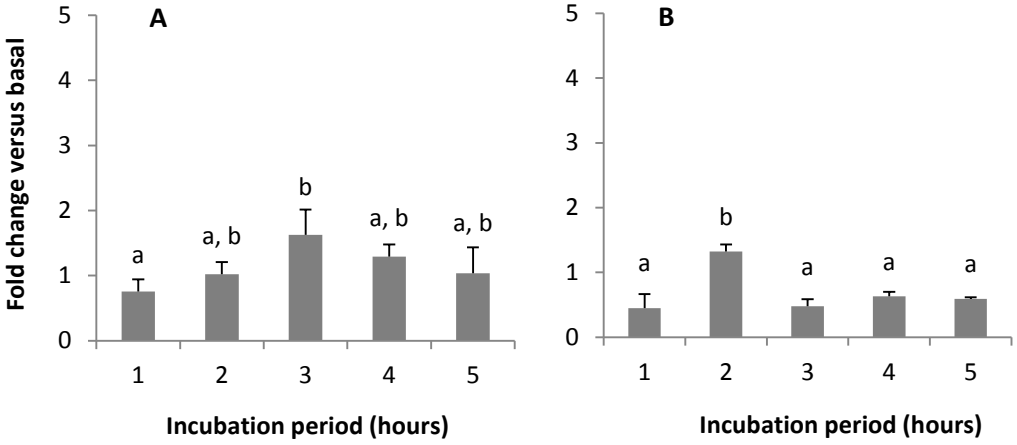

Fold change in HUVEC NOX4 (A) and p22^{phox} (B) mRNA levels versus basal (unstimulated) cells following incubation with 20ng/ml TNF-α for 1, 2, 3, 4 or 5 hours. Relative quantification was performed using the comparative C_t method, incorporating the geometric mean of reference genes PRDM4 and UBE2D2 as the normalisation factor. Data are graphed as mean ± SD (n=3); columns with different superscript letters are significantly different ($p < 0.05$).

Alternate cell stimulant (Figure 4.2 D). Upregulation of gene expression levels following cell stimulation was less than two-fold of basal values (Figure 4.5 & Figure 4.6), therefore an alternate cell stimulant was investigated to increase upregulation of NOX isoform/subunit mRNA, and improve assay sensitivity. TGF-β1 was selected for use in this experiment, following a review of potential positive controls for NOX expression (Appendix Table 9.2.5). Cultured HUVEC were incubated for four hours with TGF-β1 at a concentration of 10ng/ml, prior to RNA extraction and cDNA synthesis. Real-time PCR analysis indicated modest fold changes in gene expression versus basal with decreased levels of NOX4 mRNA (NOX4 mRNA, 0.80 ± 0.14; $p22^{phox}$ mRNA, 1.14 ± 0.19), and therefore angiotensin II was retained as the cell stimulant.

4.2.2 Final methodology

Stimulated NOX isoform/subunit gene expression assay: optimised parameters. The angiotensin II stimulated NOX gene expression assay utilised 24-well plates (SPL Life Sciences) coated with fibronectin (0.25μg/cm^2), which were seeded with HUVEC at a density of ~30,000 cells/well, and the cells grown to confluence (~48 hours at 37°C and 5% CO_2). Culture medium was then aspirated, and the cells incubated for 16 - 18 hours in Medium 199 (M199) supplemented with 2% FBS (at 37°C and 5% CO_2). Thereafter, the cells were incubated for four hours in supplemented M199 alone (basal), or media with 0.1μM angiotensin II in the presence or absence of 0.1, 1 or 10μM vanillic acid. After incubation, media was aspirated from all wells, and the plates were either frozen at -80°C or utilised for RNA extraction.

RNA extraction and mRNA reverse transcription. RNA was extracted from cultured cells by phenol-based organic extraction. Briefly, cells were homogenised using TRIzol reagent (500μl per well), and homogenates incubated for five minutes at room temperature. Following addition of 100μl chloroform, samples were agitated vigorously and subject to centrifugation at 12,000*g* for 15 minutes at 4°C. Two hundred microlitres of the aqueous phase was removed and mixed with 250μl isopropanol, prior to a ten minute incubation at room temperature. Cellular RNA was pelleted by centrifugation at 12,000*g* for 10 minutes at 4°C, and washed with 500μl of 75% ethanol by centrifugation at 7500*g* for 5 minutes at 4°C. After removal of supernatants, pellets were partially dried and resuspended in 20μl RNase-free water, prior to a 15 minute incubation at 57.5°C. Quantification of RNA was performed using a NanoDrop 2000 (Thermo Fisher Scientific).

One microgram of each RNA sample was utilised in a 20μl reverse transcription reaction with oligo (dT) primers. Prior to reverse transcription, RNA was incubated for 30 minutes at 37°C with DNase I and RiboLock RNase inhibitor, to remove any residual genomic DNA from extracted RNA. Following addition of EDTA, oligo (dT) primers (final concentration 5μM), and dNTP PCR mix, DNase was inactivated by a 10 minute incubation at 65°C. First strand buffer, RiboLock, and DTT were then

added to each sample, prior to a two minute incubation at 42°C to allow annealing of primers. After the addition of SuperScript® II (or RNase-free water for a no reverse-transcriptase control), samples were incubated at 42°C for 50 minutes for first strand cDNA synthesis, followed by a 15 minute incubation at 70°C to inactivate the reverse transcriptase enzyme.

Real-time PCR. Analysis of gene expression was performed using the Applied Biosystems 7500 Real time PCR System (Life Technologies; 7500 software version 2.0) with SYBR®Green detection. Typically, 25ng cDNA (or RNase-free water for a 'no template' control) was amplified with 300nM of the appropriate primer set (Table 4.1 & Table 4.2), and 8.33µl Precision 2x real-time PCR MasterMix with SYBR®Green (Primer Design Ltd) in a total volume of 20µl. Following enzyme activation at 95°C for 10 minutes, 50 cycles of denaturation (15 seconds at 95°C) and data collection (60 seconds at 60°C) were performed, prior to melt curve analysis to confirm specificity of amplification. Relative changes in gene expression following cell treatment were quantified using the comparative C_t method (Dorak, 2006, Schmittgen and Livak, 2008), incorporating the geometric mean of the reference genes UBE4A and VIPAR (as identified during method development; refer to section 4.2.1) as the normalisation factor.

Statistical analysis. Analysis of variance (ANOVA) with Tukey post-hoc test was performed using SPSS software (IBM, New York, USA) version 18 for Windows. Significance was determined at the 5% level, and expressed relative to angiotensin II treatment. Three biological replicates for each control/treatment were used for analysis unless otherwise noted.

4.3 Results

Following incubation of HUVECs with 0.1µM angiotensin II for four hours, NOX4 mRNA levels showed little change relative to unstimulated cells (1.04 ± 0.03 fold change; mean ± SD). Co-incubation of angiotensin II with vanillic acid at concentrations of 0.1, 1 and 10µM elicited little alteration in NOX4 mRNA, with no significant differences compared to angiotensin II alone ($p > 0.05$, Figure 4.7).

A reduction in HUVEC $p22^{phox}$ mRNA levels, relative to basal cells (fold change 0.63 ± 0.44), was observed following a four hour incubation with angiotensin II. However, co-incubation of angiotensin II with vanillic acid at 0.1µM and 1µM increased $p22^{phox}$ mRNA levels relative to angiotensin II [fold changes 2.19 ± 0.81, $p = 0.2$ and 2.30 ± 0.33, $p = 0.1$ (respectively) versus angiotensin II control] (Figure 4.8). No changes were significant relative to angiotensin II control ($p > 0.05$).

Figure 4.7 **Modulation of endothelial NOX4 mRNA levels by vanillic acid following stimulation of HUVEC with 0.1µM angiotensin II.**

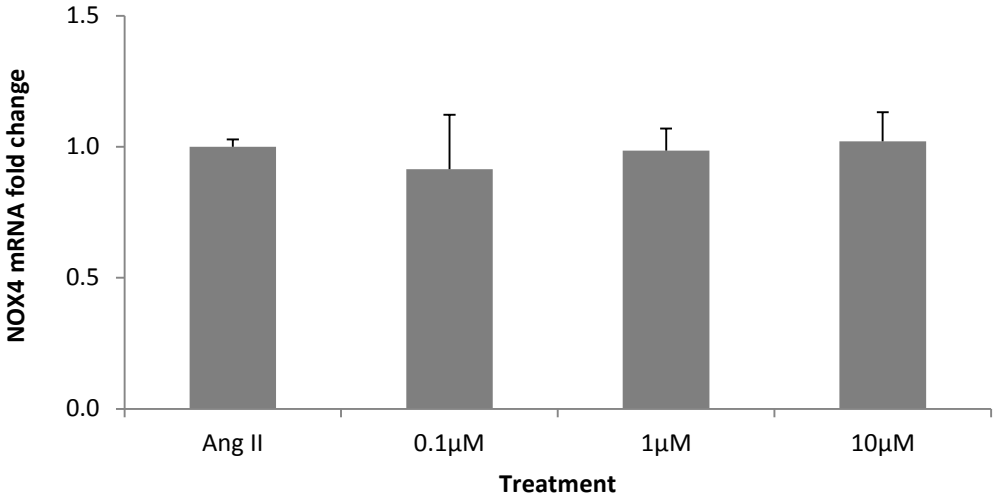

Fold change in HUVEC NOX4 mRNA levels relative to angiotensin II following 4 hour incubation with 0.1µM angiotensin II control (Ang II), or Ang II with 0.1µM, 1µM or 10µM vanillic acid. Relative quantification was performed using the comparative C_t method, incorporating the geometric mean of reference genes UBE4A and VIPAR as the normalisation factor. Data are graphed as mean ± SD (n=3).

Figure 4.8 **Modulation of endothelial $p22^{phox}$ mRNA levels by vanillic acid following stimulation of HUVEC with 0.1µM angiotensin II.**

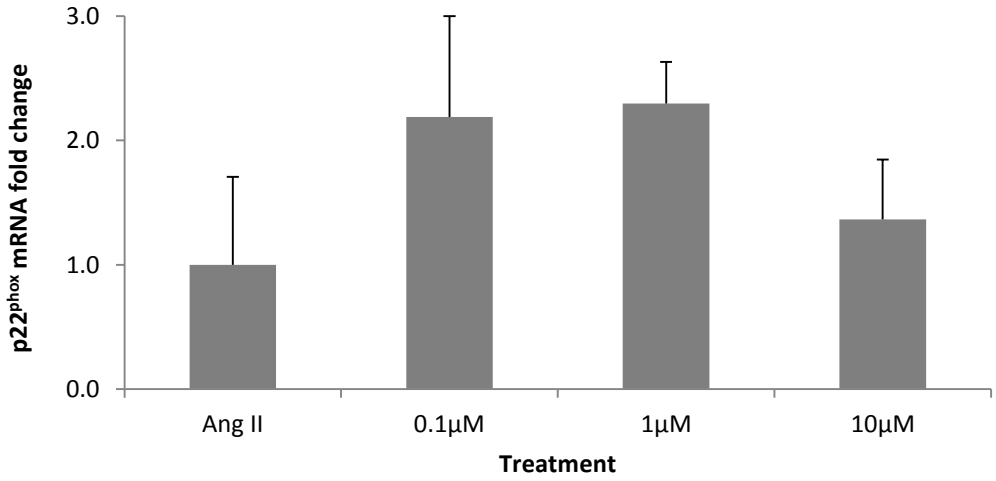

Fold change in HUVEC $p22^{phox}$ mRNA levels relative to angiotensin II following 4 hour incubation with 0.1µM angiotensin II control (Ang II), or Ang II with 0.1µM, 1µM or 10µM vanillic acid. Relative quantification was performed using the comparative C_t method, incorporating the geometric mean of reference genes UBE4A and VIPAR as the normalisation factor. Data are graphed as mean ± SD (n=3).

4.4 Discussion

The present study aimed to investigate potential mechanisms of NOX inhibition, and thus regulation of vascular endothelial ROS production, by the anthocyanin degradant vanillic acid (Figure 4.1); through examining the effects of vanillic acid on endothelial NOX isoform/subunit mRNA levels following cell stimulation. NADPH oxidase or NOX enzymes are generally identified as the predominant source of ROS in the vasculature (Cai et al., 2003, Sumimoto et al., 2005, Leopold and Loscalzo, 2009), and NOX activity in response to stimulation by the hormone angiotensin II is a major source of ROS in atherosclerosis (Cai et al., 2003, Higashi et al., 2009). In a prior investigation (Chapter 2), vanillic acid appeared to reduce endothelial superoxide levels following activation of NOX by angiotensin II; suggesting vanillic acid might enhance vascular function by reducing inactivation of NO by superoxide, as previously proposed for certain dietary flavonoids (Schewe et al., 2008). Therefore the current study examined angiotensin II-stimulated NOX expression in HUVEC as a model of NOX activity, in the context of endothelial dysfunction preceding atherosclerotic development, to elucidate cellular mechanisms potentially underlying the observed activity of vanillic acid.

Following incubation of cultured HUVECs with 0.1µM angiotensin II, observed changes in NOX4 and $p22^{phox}$ mRNA ranged from 0.95 - 1.86-fold increase relative to basal for NOX4 (Figure 4.5 A), and 0.49 - 1.80-fold for $p22^{phox}$ (Figure 4.5 B), with the greatest fold increases detected after four and five hours incubation with angiotensin II respectively. Previous reports have described upregulation of endothelial NOX4 mRNA by ~1.2 - 1.6-fold, and $p22^{phox}$ mRNA by ~1.1 - 3-fold, after stimulation of HUVEC with 0.1µM angiotensin II for four to seven hours (Rueckschloss et al., 2002, Yamagishi et al., 2005, Alvarez et al., 2010), and incubation of human aortic endothelial cells (HAEC) with 1µM angiotensin II for six hours (Richard et al., 2009). Therefore the maximal transcriptional response to angiotensin II stimulation in the current investigation was comparable to previous reports, suggesting adequate sensitivity of the HUVEC model used in the present study to the effects of a known vasoactive stimulant.

Co-incubation of angiotensin II with 0.1, 1 or 10µM of the anthocyanin degradant vanillic acid elicited no significant changes in NOX4 or $p22^{phox}$ mRNA levels relative to angiotensin II alone. NOX4 mRNA levels showed minimal change (Figure 4.7), whereas increased $p22^{phox}$ mRNA levels were observed when HUVEC were co-incubated with angiotensin II and 0.1 or 1µM vanillic acid (Figure 4.8). Interestingly, the apparent upregulation of $p22^{phox}$ mRNA did not display a linear dose - response relationship across the range of concentrations of vanillic acid tested, which reflects previous reports suggesting differential bioactivity of flavonoids across dose ranges (Chirumbolo et al., 2010, Kay et al., 2012). However, vanillic acid demonstrated no statistically significant modulation of angiotensin II-stimulated gene expression for NOX4 and $p22^{phox}$, thereby appearing to preclude an effect of this

degradant upon NOX4 activity at the transcriptional level. These data reflect previous findings (Chapter 2) where vanillic acid (at 0.1 - 10µM) did not significantly alter angiotensin II-stimulated NOX4 protein expression in cultured HUVEC, and suggest vanillic acid does not modulate the function of the predominant vascular endothelial NOX isoform, which produces mainly hydrogen peroxide (Brown and Griendling, 2009). Whilst NOX4-derived hydrogen peroxide would not act to limit NO bioavailability (Brandes et al., 2011), it may induce vasodilation through hyperpolarisation independently of NO activity (Ray et al., 2011); however the current study indicates that the anthocyanin phenolic degradant vanillic acid is unlikely to enhance vascular function *in vivo* by this mechanism.

A limitation of the current investigation was the poor specificity of amplification observed with custom primer sets for NOX2, $p47^{phox}$ and $p67^{phox}$ (Appendix Figure 9.4.1), which could not be resolved by redesigning primers or gene-specific reverse-transcription; and thus prevented determination of relative changes in gene expression for the superoxide-generating NOX2 isoform, and the cytosolic 'organiser' and 'activator' proteins $p47^{phox}$ and $p67^{phox}$ respectively. This is of particular consequence given the observed reduction in stimulated endothelial superoxide production elicited by vanillic acid (Chapter 2). Previously reported studies have suggested low or no endothelial expression of NOX2 mRNA (Ago et al., 2004, Jiang et al., 2006, Xu et al., 2008, Alvarez et al., 2010), and low expression of $p47^{phox}$ and $p67^{phox}$ mRNA in HUVEC (Ago et al., 2004); therefore the poor specificity of amplification in the current investigation is likely to reflect low mRNA copy number, which might be addressed by the use of hydrolysis probe detection chemistry for real time PCR in future studies. In contrast, specific amplification of NOX4 and $p22^{phox}$ amplicons (Appendix Figure 9.4.2) permitted relative quantification of transcript levels, reflecting the ~100-fold higher expression of NOX4 in HUVEC (Xu et al., 2008).

In the current investigation, variation was noted in the stimulatory effect of angiotensin II after a four hour incubation, although time course experiments conducted during method development identified this time point as optimal for upregulation of NOX4 and $p22^{phox}$ mRNA levels (Figure 4.5). Moreover, the use of TGF-β1 to enhance upregulation of HUVEC NOX isoform/subunit mRNA was without effect, yet TGF-β1 is known to elicit NOX4 expression in vascular smooth muscle and endothelial cells (Montezano et al., 2011); and approximately six-fold upregulation of NOX4 mRNA in response to a four hour incubation with TGF-β1 has been reported in human cardiac fibroblasts (Cucoranu et al., 2005). Therefore, data generated during the current investigation may indicate a relative lack of NOX transcriptional response in HUVEC following acute cell stimulation. Whilst HUVEC are widely used for research concerning general properties of endothelial cells (Baudin et al., 2007), an arterial endothelial cell type may be more appropriate for future studies investigating the potential modulation of NOX activity in relation to endothelial dysfunction preceding atherosclerosis;

the lesions of which occur primarily in medium to large-sized muscular and elastic arteries (Ross, 1999). As such, an alternative cell type, namely human arterial endothelial cells, should be used for subsequent *in vitro* studies investigating modulation of NOX subunit expression (as explored in Chapter 5). A strength of the current investigation was the selection of optimal endogenous reference genes for relative quantification of mRNA levels (Figure 4.3 & Figure 4.4), ensuring their suitability for normalising qPCR data to account for non-treatment related sources of variation between samples (Bustin et al., 2009).

The current study represents the first stage in elucidating possible mechanisms of action for vanillic acid, and suggests this phenolic acid degradant does not alter stimulated expression of the constitutively active NOX4 isoform at the transcriptional level; thus vanillic acid is unlikely to modulate vascular endothelial function through effects on NOX4 activity. However, the vasoactive compound apocynin, which in common with vanillic acid (Figure 4.1) incorporates a mono-methylated catechol group, has previously been reported to inhibit NOX function by inhibiting $p47^{phox}$ association with membrane components (Stolk et al., 1994, Drummond et al., 2011); indicating a possible mechanism by which vanillic acid could inhibit NOX2-mediated endothelial superoxide production (Chapters 2 & 3). Inhibition of NOX-mediated superoxide production by anthocyanin degradants or metabolites *in vivo*, resulting in elevated vascular NO bioavailability and enhanced endothelial function, could explain at least part of the reported vasoprotective activity of ingested anthocyanins (Mink et al., 2007, Zhu et al., 2011, Cassidy et al., 2013).

5 Modulation of stimulated endothelial p47^{phox} expression and activation by the anthocyanin B-ring degradant vanillic acid

5.1 Background

Dietary consumption of anthocyanins has been associated with reduced risk of cardiovascular disease (CVD) (Wallace, 2011) according to data from several epidemiological studies [for example (Mink et al., 2007, McCullough et al., 2012, Cassidy et al., 2013)]. Anthocyanins could enhance vascular endothelial function by modulating levels of the vasodilator nitric oxide (NO), through upregulation of the endothelial NO synthase (eNOS) enzyme or activation of eNOS; based on studies using cultured bovine (Xu et al., 2004a, Xu et al., 2004b, Paixão et al., 2012) and human (Lazze et al., 2006, Edirisinghe et al., 2011, Quintieri et al., 2013) endothelial cells, and excised porcine (Bell and Gochenaur, 2006) and rat (Ziberna et al., 2013) arterial rings. Reduced NO bioavailability may underlie the development of endothelial dysfunction and subsequent atherothrombotic cardiovascular disease (Kawashima and Yokoyama, 2004, Leopold and Loscalzo, 2009, Higashi et al., 2009, Drummond et al., 2011), and loss of NO in many vascular pathologies is thought to be mediated by reaction with the reactive oxygen species (ROS) superoxide. A major source of ROS in the vasculature is the NADPH oxidase (NOX) family of transmembrane enzymes (Bonomini et al., 2008, Brandes et al., 2010), of which the superoxide-generating NOX2 isoform is the prototype and best characterised member (Lassegue and Clempus, 2003, Sumimoto et al., 2005, Bedard and Krause, 2007, Brown and Griendling, 2009). Vascular expression of NOX2 has been reported in endothelial cells, smooth muscle, and adventitial fibroblasts (Takac et al., 2011, Schramm et al., 2012), and NOX2 function may contribute to the limitation of NO availability in the vasculature (Brandes and Schröder, 2008, Violi et al., 2009, Schroder, 2010); whereas the predominant endothelial isoform NOX4 (Ago et al., 2004) produces mainly hydrogen peroxide (Brown and Griendling, 2009), and therefore vascular NOX4 activity is unlikely to result in scavenging of NO (Brandes et al., 2011).

Formation of a functional NOX2 enzyme complex requires the association of NOX2 with a second transmembrane protein, p22^{phox} (forming the cytochrome b_{558} complex), and recruitment of additional cytosolic subunits upon enzyme activation; specifically p47^{phox} ('organiser' subunit), p67^{phox} ('activator' subunit), p40^{phox}, and the small G-protein Rac1/2 (Sumimoto et al., 2005, Bedard and Krause, 2007, Brandes and Schröder, 2008, Drummond et al., 2011). Following cell stimulation by agonists such as angiotensin II (Cai et al., 2003), the p47^{phox} subunit is subject to serine phosphorylation mediated by kinases including protein kinase C (PKC), Akt, or c-Src (el Benna et al., 1994, Cai et al., 2003, Drummond et al., 2011). Phosphorylation of p47^{phox} results in membrane translocation and association of p47^{phox}, p67^{phox} and p40^{phox} with the NOX2/p22^{phox} complex (Sumimoto et al., 2005, Drummond et al., 2011, El-Benna et al., 2012). The vasoactive compound

apocynin, which is structurally similar to certain anthocyanins and anthocyanin degradants or metabolites (as it incorporates a mono-methylated catechol functional group), has been reported to decrease NOX activity by inhibiting the association of $p47^{phox}$ with transmembrane components (Stolk et al., 1994, Drummond et al., 2011).

Recent research reports suggest that $p47^{phox}$ may represent a target of flavonoid bioactivity in decreasing NOX activity and improving endothelial function (Sanchez et al., 2006, Sanchez et al., 2007, Romero et al., 2009, Davalos et al., 2009). For example, in a spontaneously hypertensive rat model, the flavonol quercetin (which contains a catechol B-ring) enhanced endothelium-dependent vasorelaxation and decreased NOX activity, in conjunction with downregulation of $p47^{phox}$ protein (Sanchez et al., 2006). Moreover, quercetin and its metabolite isorhamnetin (containing a mono-methylated catechol B-ring) decreased angiotensin II- and endothelin-1-stimulated $p47^{phox}$ expression in rat aortic rings (Sanchez et al., 2007, Romero et al., 2009). In a prior investigation (Chapter 2), anthocyanins (namely peonidin-, petunidin-, and malvidin-3-glucoside) and anthocyanin phenolic acid degradants (protocatechuic, vanillic, and syringic acid) significantly decreased stimulated endothelial superoxide production, possibly through inhibition of NOX activity. However, as low human bioavailability of parent anthocyanins suggests bioactivity *in vivo* is likely to be mediated by their degradation products or metabolites (Vitaglione et al., 2007, Azzini et al., 2010, Czank et al., 2013), an anthocyanin phenolic degradant was selected to investigate cellular pathways potentially underlying the observed reductions in superoxide levels (Chapters 2 & 3). The B-ring degradant vanillic acid has been chosen for this study, as it significantly reduced endothelial superoxide levels (Chapter 2) at a physiologically relevant concentration [1µM; (Czank et al., 2013)], and in common with isorhamnetin and apocynin vanillic acid incorporates a mono-methylated catechol group (Figure 5.1). Therefore in the current investigation the effect of vanillic acid on endothelial $p47^{phox}$ expression and activation was explored, as a possible mechanism to explain at least part of the vasoprotective effects of anthocyanins described in epidemiological (Mink et al., 2007, Jennings et al., 2012, Cassidy et al., 2013), human (Zhu et al., 2011, Zhu et al., 2012) and animal (Fitzpatrick et al., 1993, Andriambeloson et al., 1997) studies.

Figure 5.1 Chemical structures of the anthocyanin degradant vanillic acid (A), the quercetin metabolite isorhamnetin (B), and the reported NOX inhibitor apocynin (C).

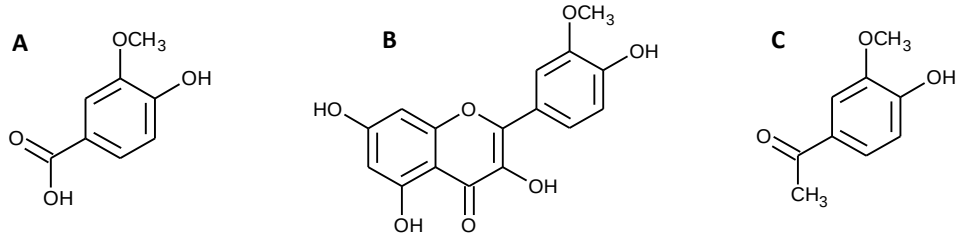

Experiments were conducted using human umbilical vein endothelial cells (HUVEC), which represent a widely-used model for research on general properties of endothelial cells (Baudin et al., 2007); and human coronary artery endothelial cells (HCAEC) as a more physiologically representative model of endothelial function in the context of atherosclerotic development, which is a disease of medium and large-sized arteries (Bonomini et al., 2008).

5.2 Materials and methods

Standards and reagents. Vanillic acid was purchased from Sigma-Aldrich [Poole, United Kingdom (UK)], and a 200mM standard solution prepared in 100% dimethylsulphoxide (DMSO; Sigma-Aldrich molecular biology grade). IGEPAL (octylphenoxy polyethoxyethanol, CA-630), fibronectin, & Medium 199 were purchased from Sigma-Aldrich, and recombinant human tumour necrosis factor-α (TNF-α) from Invitrogen (Paisley, UK). Foetal bovine serum (FBS; heat-inactivated) was purchased from Biosera (Ringmer, UK), safe-lock microcentrifuge tubes from Qiagen (Crawley, UK), acid-washed glass beads (~0.5mm diameter) from Sigma-Aldrich, and polycarbonate ultracentrifuge tubes (230µl) from Beckman Coulter (High Wycombe, UK). Complete Protease Inhibitor Cocktail Tablets and PhosSTOP Phosphatase Cocktail Inhibitor Tablets were obtained from Roche Applied Science (Burgess Hill, UK). All water utilised was of Milli-Q grade (18.2 MΩ cm^{-1}).

NuPAGE sample reducing agent and LDS sample buffer were purchased from Invitrogen, and Precision Plus Protein Dual Colour standards from Bio-Rad Laboratories, Inc (Hemel Hempstead, UK). Protein-Free T20 (TBS) blocking buffer was obtained from Fisher Scientific (Loughborough, UK); Immobilon-FL PVDF membrane from Millipore, and Instant*Blue* protein gel stain from Expedeon Protein Solutions (Harston, UK). Tween® 20 was purchased from Sigma-Aldrich. Chicken polyclonal anti-glyceraldehyde-3-phosphate dehydrogenase (GAPDH; AB2302) was obtained from Millipore (Watford, UK); rabbit polyclonal anti-$p47^{phox}$ was purchased from Santa Cruz Biotechnology, Inc. (California, USA) and Abcam (Cambridge, UK) (sc-14015 and ab63361 respectively), and rabbit polyclonal anti-phospho (S304) $p47^{phox}$ from Abcam (ab63554). Donkey anti-chicken IgG (IR dye 680 LT) and goat anti-rabbit IgG (IR dye 800 CW) were supplied by Li-Cor (Cambridge, UK). Antibodies were prepared in a diluent of 50% T20 blocking buffer:50% phosphate-buffered saline (PBS) with 0.5% Tween® 20; and including 0.02% sodium dodecyl sulphate for solutions of IR dye 680 LT anti-IgG antibodies.

Cell culture. Cryo-preserved, early passage, HUVEC were purchased from TCS CellWorks (Buckingham, UK) and used between passages two to four. Cells were routinely cultured in 75cm^2 flasks (SPL Life Sciences) coated with fibronectin (0.27µg/cm^2), using large vessel endothelial cell growth medium [TCS CellWorks; proprietary basal medium formulation supplemented with growth factor and antibiotic (gentamicin & amphotericin B) supplements, final concentration of 2% v/v foetal

bovine serum] at 37°C and 5% CO_2. HUVECs were sub-cultured using 0.025% trypsin and 0.01% EDTA (TCS CellWorks).

Cryo-preserved, second passage, single donor HCAEC were purchased from PromoCell GmbH (Heidelberg, Germany) and used between passages three to six (Figure 5.2). Cells were routinely cultured in 75cm^2 flasks (SPL Life Sciences) coated with fibronectin (0.27µg/cm^2), using endothelial cell medium MV (PromoCell GmbH; proprietary basal medium formulation supplemented with foetal calf serum, endothelial cell growth supplement, recombinant human epidermal growth factor, heparin, and hydrocortisone, final concentration of 5% v/v foetal calf serum) at 37°C and 5% CO_2. HCAEC were sub-cultured using 0.04% trypsin and 0.03% EDTA (PromoCell GmbH).

Figure 5.2 **Light microscopy image of sub-confluent HCAEC at sixth passage (cultured on fibronectin coating).**

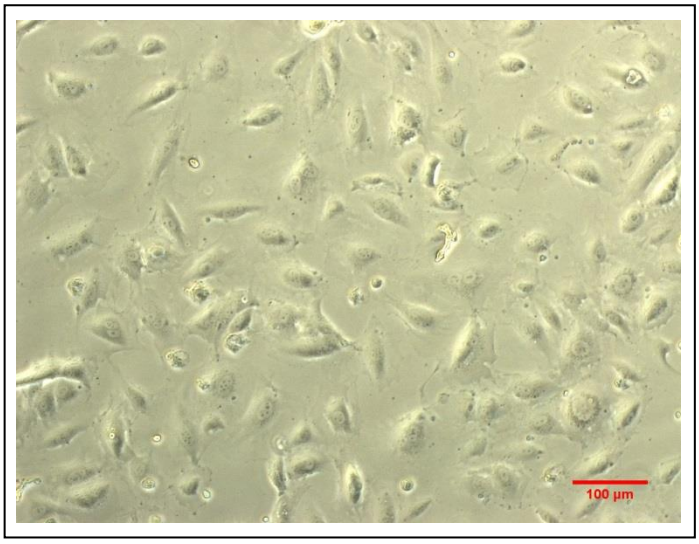

5.2.1 Method development – HUVEC p47^{phox} activation

Stimulated p47^{phox} activation in HUVEC: method development (Figure 5.3). Method development was conducted to optimise cell fractionation methodology (Figure 5.3 A & Appendix Table 9.2.6), including buffer composition (Figure 5.3 B), as a means of assessing movement of endothelial p47^{phox} from cytosolic to membrane fractions following stimulation of HUVEC with TNF-α (Appendix Table 9.2.7). The optimal cell stimulation time for detection of activated p47^{phox} using an anti-phospho p47^{phox} antibody was subsequently investigated (Figure 5.3 C).

Figure 5.3 Stimulated p47^{phox} activation in HUVEC: method development flow chart.

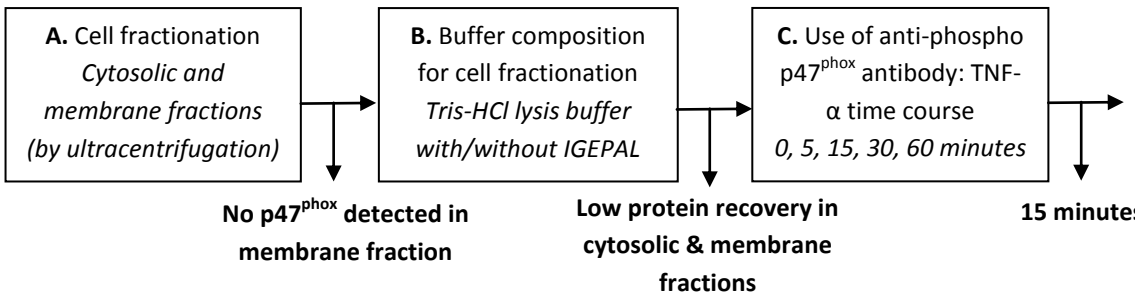

Cell fractionation (Figure 5.3 A). Immunodetection of p47^{phox} was assessed in cytosolic and membrane fractions prepared by ultracentrifugation following HUVEC stimulation. Cultured HUVEC were seeded in fibronectin-coated 6-well plates at a density of 100,000 cells/well and cells grown to confluence, prior to a 16 - 18 hour incubation in Medium 199 (supplemented with 2% FBS) at 37°C and 5% CO_2. Confluent cells were then incubated for a further five hours in supplemented Medium 199, in the presence or absence of 20ng/ml TNF-α. Prior NOX bioactivity and/or expression studies (Appendix Table 9.2.7) described incubation periods with TNF-α ranging from five minutes to 24 hours; therefore five hours was selected for the current study, as comparable to the six hour period used in the previously reported stimulated superoxide production assay (Chapter 2). Cells were subsequently lysed in 1% IGEPAL® CA-630, 150mM NaCl, 20mM Tris and 10% glycerol (pH 8.0), supplemented with protease inhibitors (Complete Protease Inhibitor Cocktail), and recovered solutions homogenised by probe sonication on ice (3 x 10 seconds) before centrifugation at 3000*g* at 4°C for ten minutes to pellet nuclei and unbroken cells/debris. The resulting supernatants were then subject to ultracentrifugation at 100,000*g* for 60 minutes at 4°C, using a Beckman Coulter Optima TLX with rotor TLA-100 (Beckman Coulter). Supernatants were subsequently removed and designated as the cytosolic fraction, whilst pellets were resuspended in 125µl cell lysis buffer and ultracentrifuged as noted above. Supernatants from the second ultracentrifugation were designated as the membrane-enriched fraction; and the protein content of both fractions quantified prior to gel electrophoresis and immunoblotting (section 5.2.2).

A weak immunoreactive band for p47^{phox} was observed in cytosolic fractions (Figure 5.4 A), whereas no p47^{phox} could be detected in membrane fractions (Figure 5.4 B), and GAPDH loading control was present in both fractions (Figure 5.4 A & B). Owing to low protein content of membrane-enriched fractions, the effect of lysis buffer composition upon protein recovery was investigated (Figure 5.3 B).

Figure 5.4 Immunodetection of endothelial p47^{phox} in cytosolic (A) and membrane (B) fractions following stimulation of HUVEC with 20ng/ml TNF-α.

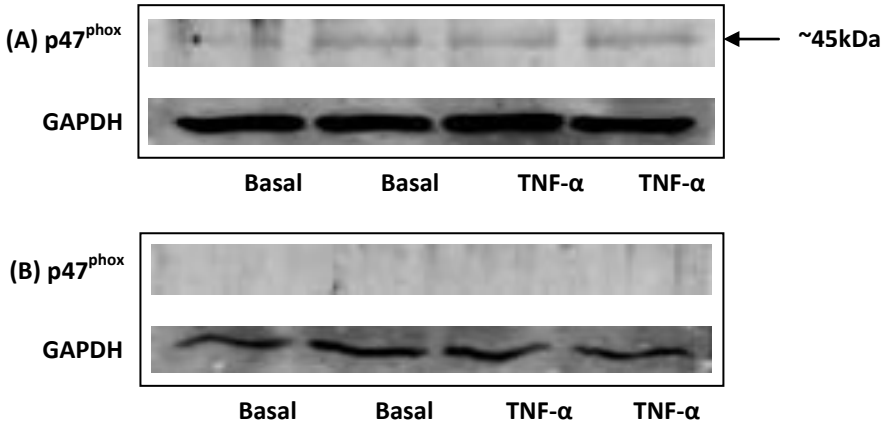

Detection of p47^{phox} protein (with GAPDH loading control) in cytosolic (A) and membrane-enriched (B) fractions prepared from unstimulated HUVEC (basal) and following a 5 hour incubation with TNF-α.

Buffer composition for cell fractionation (Figure 5.3 B). The effect of buffer composition on protein content of cellular fractions was explored using the HUVEC stimulation assay outlined above. Following cell treatment, HUVEC were harvested in a 20mM Tris-HCl buffer without IGEPAL [pH 7.5, supplemented with protease inhibitors; (Deng et al., 2012)], and cytosolic fractions prepared as described previously. Pellets were then resuspended in Tris-HCl buffer with 1% IGEPAL prior to ultracentrifugation and collection of supernatants as membrane-enriched fractions (refer to Appendix Table 9.2.6).

Low protein content (<1mg/ml) was measured for all fractions, and no immunoreactive bands for p47^{phox} were detected after gel electrophoresis/immunoblotting of membrane fractions (data not shown). An alternative methodology was therefore identified to detect p47^{phox} activation following HUVEC stimulation (Figure 5.3 C).

Anti-phospho-p47^{phox} antibody: TNF-α time course (Figure 5.3 C). Activation of p47^{phox} occurs through phosphorylation of serine (S) residues (Sumimoto et al., 2005, Drummond et al., 2011), including S304 (el Benna et al., 1994), and detection of phospho-(S304) p47^{phox} following cell stimulation has been described recently (Leverence et al., 2011). As such, p47^{phox} activation in the current study was investigated by immunoblotting of HUVEC lysates with a rabbit polyclonal anti-phospho-(S304) p47^{phox} antibody. Previous scientific reports have described peak phosphorylation of p47^{phox} following stimulation with TNF-α for five minutes in human pulmonary artery endothelial cells (Frey et al., 2002) and 30 minutes in human dermal microvascular endothelial cells (Li et al., 2005); therefore method optimisation was conducted to establish the optimal incubation time with TNF-α.

A time course experiment was performed to assess p47^{phox} phosphorylation following incubation of cultured HUVEC with TNF-α for 0, 5, 15, 30, and 60 minutes; based on the HUVEC stimulation assay described above. Incubation with TNF-α for 5 - 30 minutes appeared to elicit a minimal increase in phosphorylated p47^{phox} relative to basal (0 minutes exposure), although after 60 minutes incubation with TNF-α phospho-p47^{phox} decreased below basal levels (Figure 5.5). As p47^{phox} phosphorylation was sustained between the 5 and 30 minute time points, the mid-point (15 minutes) was selected as the optimal incubation time with TNF-α.

Figure 5.5 Immunodetection of phospho-p47^{phox} protein following stimulation of HUVEC with 20ng/ml TNF-α for 5-60 minutes.

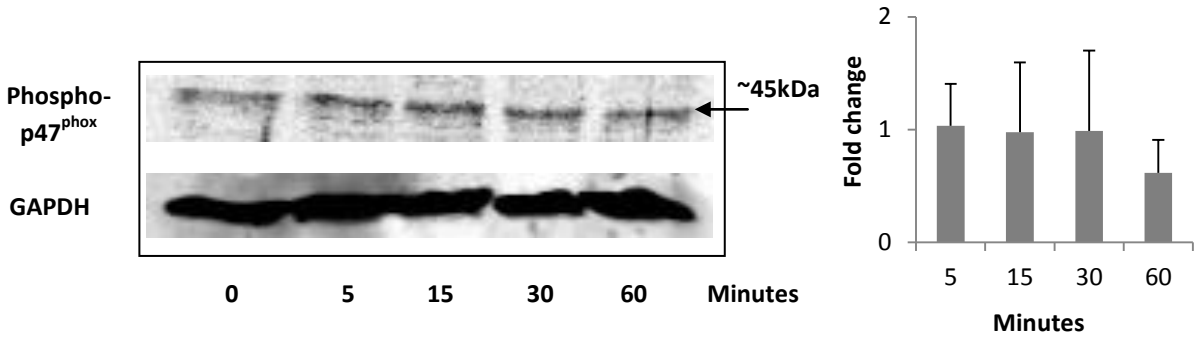

Levels of phospho-p47^{phox} protein (with GAPDH loading control) in cell lysates from unstimulated HUVEC (0 minutes) and following incubation with 20ng/ml TNF-α for 5, 15, 30, or 60 minutes. Inset graph shows fold change in phospho-p47^{phox} levels relative to basal (designated as 1), after quantification by densitometry and normalisation to loading control (mean ± SD, n=4). No significant differences in fold change were observed between time points ($p > 0.05$).

5.2.2 Final methodology

Stimulated p47^{phox} activation: optimised parameters. Cell lysates for immunoblotting were generated from cultured HUVEC pre-incubated with vanillic acid for five hours prior to stimulation with TNF-α. Briefly, 6-well plates (SPL Life Sciences) coated with fibronectin (0.25µg/cm^2) were seeded with HUVEC at a density of 100,000 cells/well and cells grown to confluence, prior to a 16 - 18 hour incubation in Medium 199 (2% FBS) at 37°C and 5% CO_2. Thereafter, cells were pre-incubated for five hours with 0.1, 1, or 10µM vanillic acid and subsequently stimulated with TNF-α for 15 minutes. Cells were harvested and lysed in 1% IGEPAL® CA-630, 150mM NaCl, 20mM Tris and 10% glycerol (pH 8.0), supplemented with protease inhibitors (Complete Protease Inhibitor Cocktail), and phosphatase inhibitors (PhosSTOP Phosphatase Cocktail Inhibitor). Six-well plates were incubated with lysis buffer (120µl/well) for 30 minutes at 4°C, prior to removal of cells by scraping. Recovered solutions were subject to cell disruption by rapid agitation (50Hz for 5 minutes with Qiagen TissueLyser LT) with acid-washed glass beads in safe-lock microcentrifuge tubes. After centrifugation at 13,000 rpm (15 minutes at 4°C), the protein content of the supernatants was assayed using the Pierce BCA Protein Assay Kit according to manufacturer's instructions.

Stimulated p47^{phox} expression. Cell lysates for immunoblotting were generated from cultured HUVEC or HCAEC co-incubated with TNF-α and vanillic acid for five hours. Briefly, 6-well plates (SPL Life Sciences) coated with fibronectin (0.25µg/cm^2) were seeded with HUVEC or HCAEC at a density of 100,000 cells/well and cells grown to confluence, prior to a 16 - 18 hour incubation in Medium 199 (2% FBS) at 37°C and 5% CO_2 (HUVEC only). Thereafter, cells were incubated for five hours in Medium 199 (2% FBS) with 0.1, 1, or 10µM vanillic acid and 20ng/ml TNFα. Cells were harvested and lysed in 1% IGEPAL® CA-630, 150mM NaCl, 20mM Tris and 10% glycerol (pH 8.0), supplemented with protease inhibitors (Complete Protease Inhibitor Cocktail), as described for the p47^{phox} activation assay.

Immunoblot analysis. For gel electrophoresis, samples were reduced using NuPAGE sample reducing agent (50mM dithiothreitol) prior to gel loading in NuPAGE LDS sample buffer. Precision Plus Protein Dual Colour standards were loaded as comparative molecular weight markers. Normally 20 - 25µg of protein was loaded onto a 4% polyacrylamide stacking gel, and separated across a 10% resolving gel (at 25mA for approximately one hour) prior to semi-dry transfer to Immobilon-FL PVDF membrane (at 200mA for approximately 90 minutes). Equal protein transfer was confirmed by Instant*Blue* staining of the gels. Membranes were blocked with T20 blocking buffer for one hour at room temperature, and incubated overnight (at 4°C) in the appropriate concentration of primary and loading control antibody (anti-GAPDH, 1 in 10,000; anti-p47^{phox}; 1 in 200 to 1 in 500, anti-phospho p47^{phox}, 1 in 500). Membranes were washed using PBS with 0.1% Tween® 20 (PBST 0.1%), after which secondary antibody incubations were performed for one hour at room temperature, using IR dye-conjugated (680 and 800) secondary antibodies at a concentration of 1 in 10,000. Membranes were washed with PBST 0.1%, and subsequently imaged using an Odyssey Infrared Imaging System (Li-Cor). Immunoblots were quantified by densitometry using Odyssey Infrared Imaging System Application Software (Li-Cor, version 3.0.21).

Statistical analysis. Analysis of variance (ANOVA) with Tukey post-hoc test was performed using SPSS software (IBM, New York, USA) version 18 for Windows. Significance was determined at the 5% level and expressed relative to TNF-α treatment. Four biological replicates for each control/treatment were utilised for analysis unless otherwise noted.

5.3 Results

Minimal upregulation of p47^{phox} was detected following stimulation of cultured HUVEC with TNF-α for five hours, as compared with unstimulated (basal) cells (1.04 ± 0.32 fold increase from basal, mean ± SD; Figure 5.6). Co-incubation of cells with TNF-α and increasing concentrations of vanillic acid (0.1, 1, or 10µM) resulted in a trend towards decreased p47^{phox} expression relative to TNF-α alone (with a maximal response of 0.57 ± 0.41 fold of basal expression at 1µM and 10µM vanillic

acid), although these changes were not statistically significant (p = 0.2 at 1µM and 10µM vanillic acid; Figure 5.6).

Figure 5.6 Modulation of HUVEC p47^{phox} protein expression by vanillic acid following stimulation with 20ng/ml TNF-α.

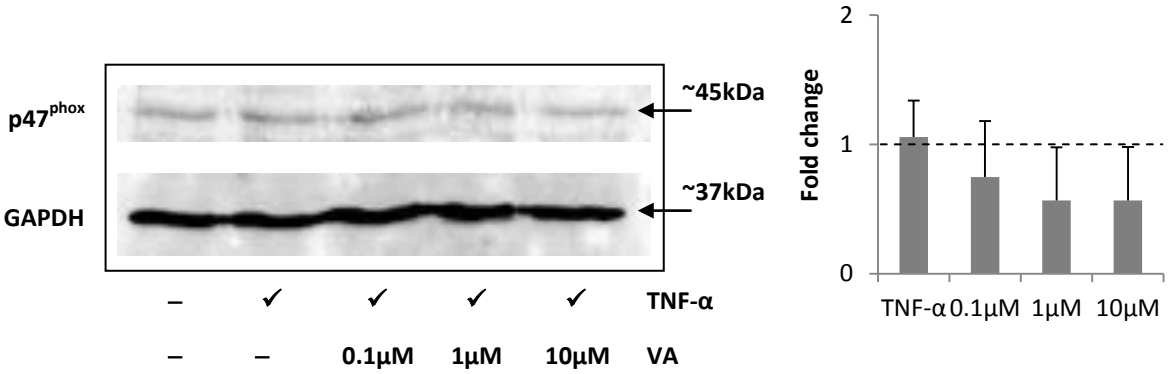

Expression of p47^{phox} protein (with GAPDH loading control) in cell lysates from unstimulated HUVEC (basal) and following incubation with 20ng/ml TNF-α in the presence or absence of 0.1, 1, or 10µM vanillic acid (VA) for 5 hours. Inset graph shows fold change in p47^{phox} expression relative to basal (designated as 1 and marked by dashed line), after quantification by densitometry and normalisation to loading control (mean ± SD, n=5). No significant differences in fold change were observed between treatments (p > 0.05).

A weak immunoreactive band was detected for phospho-p47^{phox} following stimulation of cultured HUVECs with TNF-α for 15 minutes (Figure 5.7). Pre-incubation of HUVECs with 0.1, 1, or 10µM vanillic acid for five hours prior to cell stimulation elicited no discernible effect on phospho-p47^{phox} protein levels; however densitometric quantification of detected bands, and statistical analysis of densitometric data from replicate immunoblots, were precluded by poor immunodetection of phospho-p47^{phox} (Figure 5.7).

Figure 5.7 Modulation of HUVEC phospho-p47^{phox} protein levels by pre-incubation with vanillic acid prior to stimulation with 20ng/ml TNF-α.

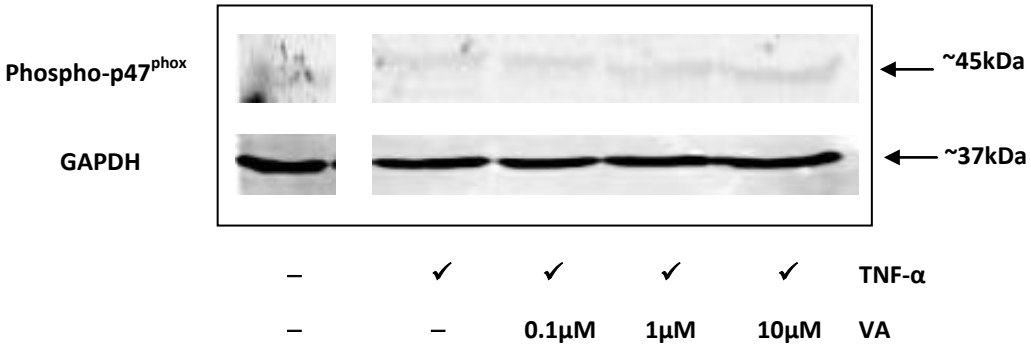

Levels of phospho-p47^{phox} protein (with GAPDH loading control) in cell lysates from unstimulated HUVEC (basal) and following stimulation with 20ng/ml TNF-α for 15 minutes, with or without 5 hours pre-incubation in the presence of 0.1, 1, or 10µM vanillic acid (VA).

In order to characterise the effect of vanillic acid on p47^{phox} expression in a more physiologically representative cell line, a study was conducted using cultured HCAEC. Here, no significant modulation of p47^{phox} expression was detected after cells were co-incubated with 20ng/ml TNF-α in the presence of increasing concentrations (0.1, 1, or 10μM) of vanillic acid ($p > 0.05$; Figure 5.8), although incubation of HCAEC with TNF-α alone again elicited minimal increases in p47^{phox} protein levels relative to unstimulated cells (Figure 5.8).

Figure 5.8 Modulation of HCAEC p47^{phox} protein expression by vanillic acid following stimulation with 20ng/ml TNF-α.

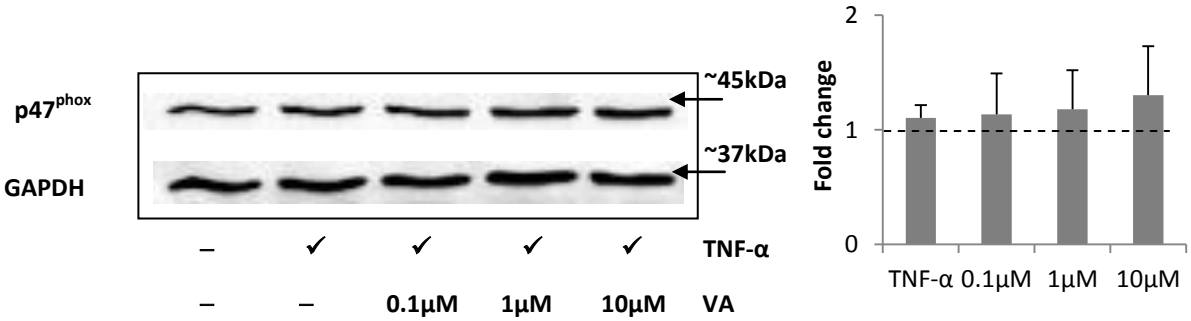

Expression of p47^{phox} protein (with GAPDH loading control) in cell lysates from unstimulated HCAEC (basal) and following 5h incubation with 20ng/ml tumour necrosis factor-alpha (TNF-α), or TNF-α with 0.1, 1, or 10μM vanillic acid. Inset graph shows fold change in p47^{phox} expression relative to basal (designated as 1 and marked by dashed line), after quantification by densitometry and normalisation to loading control (n=4; mean ± SD). No significant differences from TNF-α were observed ($p > 0.05$).

5.4 Discussion

The current study aimed to explore modulation of stimulated endothelial p47^{phox} expression, or activation, by the anthocyanin degradant vanillic acid, as a mechanism potentially underlying observed bioactivity of anthocyanins and their phenolic degradants in reducing stimulated endothelial superoxide production (Chapter 2). Translocation of p47^{phox} protein between cellular fractions was examined to assess NOX activation, based upon previous reports (Li et al., 2005, Deng et al., 2012), although in the present investigation low protein content of membrane-enriched fractions precluded immunodetection of p47^{phox} protein (Figure 5.4). Activation of p47^{phox} was therefore detected by immunoblotting for serine-phosphorylated protein (Figure 5.5), as phosphorylation of p47^{phox} precedes membrane translocation of this subunit and NOX-mediated superoxide production (el Benna et al., 1994).

A trend was observed towards decreased p47^{phox} protein levels after co-incubation of HUVEC for five hours with TNF-α and increasing concentrations of the anthocyanin B-ring degradant vanillic acid (Figure 5.6). Following ingestion of ^{13}C-labelled cyanidin-3-glucoside, low micromolar levels of phase II conjugates of the B-ring degradant protocatechuic acid, including vanillic acid, have been reported

in human serum within six hours [~0.8μM (Czank et al., 2013)]; therefore both the concentrations of vanillic acid (0.1 - 10μM) and duration of exposure (five hours) used in the current investigation were of physiological relevance. Whilst the observed reductions in $p47^{phox}$ protein were not statistically significant ($p \geq 0.2$), they reflect previously published reports detailing downregulation of $p47^{phox}$ mRNA and/or protein by quercetin and its metabolite isorhamnetin, which contain a catechol and a mono-methylated catechol B-ring respectively (Sanchez et al., 2006, Sanchez et al., 2007, Romero et al., 2009, Davalos et al., 2009). In contrast, no effect of vanillic acid was detected on levels of phospho-$p47^{phox}$ protein following a five hour pre-incubation of HUVECs with vanillic acid prior to acute stimulation by TNF-α (Figure 5.7); suggesting that vanillic acid does not modulate phosphorylation status of $p47^{phox}$ following cell stimulation and thus inhibit NOX activity by this mechanism.

Given the absence of statistically significant effects on $p47^{phox}$ protein expression, the activity of vanillic acid was further explored in an alternative primary human endothelial cell model; as atherosclerosis is principally a disease of medium and large-sized arteries (Ross, 1999, Bonomini et al., 2008), and thus umbilical vein endothelial cells may not represent the most physiologically representative model for examining altered endothelial function preceding development of atherosclerotic lesions (Baudin et al., 2007). Several previous research reports have investigated stimulated $p47^{phox}$ expression in cultured HCAEC (Yun et al., 2006, Dandapat et al., 2007, Yoshida and Tsunawaki, 2008, Chen et al., 2011b), therefore this cell type was selected for a confirmatory study of vanillic acid bioactivity. Here, no significant modulation of TNF-α stimulated $p47^{phox}$ expression was detected after co-incubation of HCAEC with 0.1 - 10μM vanillic acid (Figure 5.8), and in contrast to HUVEC data (Figure 5.6) there was no trend towards downregulation of this protein; indicating HUVEC may not be an appropriate model for investigating modulation of $p47^{phox}$ levels in the context of arterial endothelial function.

The current investigation therefore suggests vanillic acid is unlikely to affect activity of the superoxide-generating NOX2 isoform by decreasing protein expression of the key $p47^{phox}$ subunit, and apparent reductions in stimulated endothelial superoxide production elicited by anthocyanins and their degradants (Chapter 2) may not be attributable to this mechanism of action. However, it is interesting to note that the anthocyanidin delphinidin has recently been reported to inhibit $p47^{phox}$ translocation and NOX activity in human dermal fibroblasts (Lim et al., 2013), suggesting that anthocyanins and/or their degradation products at cellular pH might modulate NOX function by this mechanism. Moreover, vanillic acid is structurally similar to the vasoactive compound apocynin, which is reported to inhibit association of $p47^{phox}$ with membrane-bound components of the NOX complex (Drummond et al., 2011). Activity of the NOX2 isoform may limit bioavailability of the key vascular mediator NO (Schroder, 2010), resulting in disruption of vascular homeostasis and

endothelial dysfunction; therefore decreasing NOX-generated superoxide production by preventing enzyme assembly could enhance NO levels and preserve vascular endothelial function *in vivo*.

A limitation of the present investigation was the minimal change detected in both total $p47^{phox}$ expression (Figure 5.6 & Figure 5.8) and levels of phosphorylated $p47^{phox}$ (Figure 5.7) relative to unstimulated cells following stimulation of cultured endothelial cells with 20ng/ml TNF-α; although a time course experiment was conducted to identify the optimal incubation period with TNF-α for immunodetection of phospho-$p47^{phox}$ in HUVEC (Figure 5.5). Previously published reports have described elevations in membrane-associated $p47^{phox}$ (Massaro et al., 2006, Carluccio et al., 2007, Deng et al., 2012), $p47^{phox}$ protein levels (Yoshida and Tsunawaki, 2008, Chen et al., 2011b), or phospho-$p47^{phox}$ levels (Frey et al., 2002, Li et al., 2005) following stimulation of human endothelial cells. This may be partly attributable to the use of alternative cell types, for example pulmonary artery endothelial cells (Frey et al., 2002) or saphenous vein endothelial cells (Massaro et al., 2006). Equally, prior studies have used alternative cell stimulants, such as homocysteine (Carluccio et al., 2007), or treatment conditions, for instance 40ng/ml TNF-α for 24 hours (Deng et al., 2012); which might also explain the limited response to cell stimulation observed in the current study relative to previous reports. Furthermore, low expression of $p47^{phox}$ mRNA has been reported in HUVEC (Jones et al., 1996, Ago et al., 2004), which may contribute to poor immunodetection of the expressed protein; as observed previously for NOX2 following angiotensin II stimulation of cultured HUVEC (Chapters 2 & 4). Another potential limitation of the current study was that the ratio of phosphorylated $p47^{phox}$ to total $p47^{phox}$ protein in HUVEC was not examined, although levels of total protein may not represent an appropriate reference as these were apparently affected by vanillic acid; and any changes in phosphorylated protein were compared to baseline or basal values (Figure 5.5 & Figure 5.7).

In summary, the current study has indicated that the anthocyanin degradant vanillic acid does not inhibit stimulated endothelial superoxide production by downregulating a key component of the NOX2 enzyme complex. Both anthocyanin glucosides and their phenolic acid degradants appeared to decrease endothelial superoxide levels in a prior investigation (Chapter 2); suggesting a mechanism for reducing NO scavenging by superoxide anion and enhancing vascular function *in vivo* following ingestion of anthocyanins, where phenolic degradants and metabolites are likely to constitute the major circulating forms (Czank et al., 2013). By contrast, direct upregulation and/or activation of endothelial nitric oxide synthase (eNOS) previously described for parent anthocyanins *in vitro* [Chapter 3, also (Xu et al., 2004b, Xu et al., 2004a, Sorrenti et al., 2007, Edirisinghe et al., 2011)] may not contribute to elevated NO levels *in vivo*; given the low human bioavailability reported for parent anthocyanins relative to their degradant products/metabolites (Vitaglione et al., 2007, Azzini et al., 2010). However, data from the present investigation and prior studies (Chapter 2) do not indicate a

direct inhibition of NOX2 function by vanillic acid, suggesting an indirect effect on stimulated superoxide production; potentially through upregulation of the cytoprotective haem oxygenase-1 (HO-1) enzyme, which has been reported to inhibit NOX function in human microvascular endothelial cells (Jiang et al., 2006) and apolipoprotein E-deficient mice (Datla et al., 2007); and should form a focus of future research (as detailed in Chapter 6).

6 Effect of the anthocyanin phenolic degradant vanillic acid on endothelial haem oxygenase-1 expression

6.1 Background

Increased dietary intake of anthocyanins has been associated with decreased risk of cardiovascular disease (CVD) (Mink et al., 2007, Cassidy et al., 2013), which might in part reflect improved vascular endothelial function (Wallace, 2011) owing to enhanced availability of the key mediator nitric oxide (NO) (Xu et al., 2004b, Xu et al., 2004a, Bell and Gochenaur, 2006, Edirisinghe et al., 2011, Zhu et al., 2011). However, the molecular mechanisms underlying potential cardioprotective activity of anthocyanin degradation products and/or metabolites, which are likely to mediate anthocyanin bioactivity *in vivo* (Azzini et al., 2010, Czank et al., 2013), are not yet fully elucidated with regard to effects on the vascular endothelium. Vascular endothelial dysfunction, and particularly reduced NO activity, forms an initial stage of atherosclerotic development (Landmesser et al., 2004, Kawashima and Yokoyama, 2004, Higashi et al., 2009), and loss of NO can arise through scavenging by superoxide anion, generating the potent oxidant peroxynitrite (Wever et al., 1998, Naseem, 2005). The NADPH oxidase (NOX) transmembrane enzyme family constitutes a major source of reactive oxygen species in the vasculature (Bedard and Krause, 2007, Bonomini et al., 2008), moreover activity of the superoxide-generating NOX2 isoform could contribute to reduced vascular availability of NO (Brandes and Schröder, 2008, Violi et al., 2009, Schroder, 2010). However, bilirubin derived from haem degradation by the haem oxygenase-1 (HO-1) enzyme may inhibit NOX activity (Jiang et al., 2006, Datla et al., 2007), and bilirubin has also been reported to preserve expression of eNOS in stimulated endothelial cells (Kawamura et al., 2005).

Haem oxygenase (HO) enzymes catalyse the oxidative degradation of cellular haem, yielding carbon monoxide (CO) gas, free ferrous (Fe^{2+}) iron, and the bile pigment biliverdin IXα (subsequently reduced to bilirubin IXα by biliverdin reductase) (Ryter et al., 2002, Ryter et al., 2006). Two isoenzymes of HO have been characterised, an inducible form (HO-1, molecular mass ~32,000 Da) and a constitutively expressed form (HO-2, molecular mass ~34,000 Da) (Abraham and Kappas, 2008); localised to subcellular compartments such as the rough endoplasmic reticulum and plasma membrane caveolae (Ryter et al., 2006). Upregulation of HO-1 can be induced in both tissues and cultured cells by a range of chemical or physical agents, including nitric oxide (NO), pro-inflammatory cytokines, heavy metals, oxidised low-density lipoprotein (LDL), ultraviolet A radiation, and both hypo- and hyperoxia (Siow et al., 1999, Ryter et al., 2002, Ryter et al., 2006, Abraham and Kappas, 2008). In the absence of cellular stress, HO-1 is normally present at low or undetectable levels in most cell types or tissues (Ryter et al., 2002, Ryter et al., 2006), and upregulation of HO-1 confers protection against oxidative stress *in vivo* and *in vitro* (Ryter et al., 2002). Carbon monoxide

produced by HO displays anti-inflammatory (Ryter et al., 2002) and vasodilatory (Siow et al., 1999) activity; and HO-1-derived bilirubin can scavenge reactive oxygen species *in vitro*, inhibit NOX function, and enhance vascular reactivity (Abraham and Kappas, 2008). Indeed, upregulation of HO-1 with subsequent inhibition of NOX activity has been described in human microvascular endothelial cells (Jiang et al., 2006) and apolipoprotein-E deficient mice (Datla et al., 2007).

Anthocyanins and/or their metabolites (in *ex vivo* serum incubation) have previously been reported to upregulate expression of HO-1 in human vascular endothelial cells (Sorrenti et al., 2007, Cimino et al., 2013), and thus could potentially decrease endothelial NOX activity through induction of HO-1. Inhibition of NOX may represent a mechanism by which certain flavonoids enhance vascular function by increasing NO bioavailability (Schewe et al., 2008); and elevated CO production through upregulation of HO-1 might also mediate a vasodilatory effect (Chan et al., 2011). Based upon earlier investigations (Chapters 2 & 3) the anthocyanin B-ring degradant vanillic acid (Figure 6.1) was selected to elucidate cellular mechanisms potentially underlying the reductions in superoxide levels observed previously with anthocyanins and their degradants (Chapter 2).

Figure 6.1 **Anthocyanin degradant (vanillic acid) selected for investigation of potential mechanisms of NOX inhibition.**

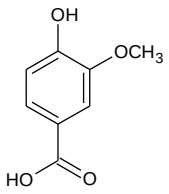

In the current study, the effect of vanillic acid (at 0.1 - 10μM) on endothelial mRNA and protein levels of HO-1 was examined by reverse transcription – quantitative polymerase chain reaction (RT-qPCR) and immunoblotting respectively; to assess whether basal HO-1 expression was modulated by vanillic acid, as a potential indirect mechanism of NOX inhibition. Experiments were conducted using human umbilical vein endothelial cells (HUVEC), which represent an experimental model of endothelial cells (Baudin et al., 2007); and human coronary artery endothelial cells (HCAEC) as a more physiologically representative model of endothelial function in the context of atherosclerotic development within medium and large-sized arteries (Bonomini et al., 2008).

6.2 Materials and methods

Standards and reagents. Vanillic acid was purchased from Sigma-Aldrich [Poole, United Kingdom (UK)] and a 200mM standard solution was prepared in 100% dimethylsulphoxide (DMSO; Sigma-Aldrich molecular biology grade). All water utilised was of Milli-Q grade (18.2 MΩ cm^{-1}).

Tumour necrosis factor-alpha (TNF-α), TRIzol® reagent, RNase-free water, oligo (dT) primer (50μM), SuperScript® II Reverse Transcriptase (with 5x first strand buffer and 100mM dithiothreitol/DTT), and MicroAmp™ optical microplates were obtained from Life Technologies (Paisley, UK). RiboLock RNase inhibitor, DNase I (with 10x reaction buffer with $MgCl_2$, and 50mM EDTA), dNTP PCR mix (10mM), oligo (dT) primer (100μM), chloroform (molecular biology grade), and isopropanol were purchased from Thermo Fisher Scientific (Fisher Scientific, Loughborough, UK); and ethanol (molecular biology grade), (octylphenoxy)polyethoxyethanol (CA-630), phorbol 12-myristate 13-acetate (PMA), and fibronectin from Sigma-Aldrich. Precision 2x real-time PCR MasterMix with SYBR®Green was obtained from PrimerDesign Ltd (Southampton, UK), and custom primers for human HO-1 (HMOX-1, accession number NM_002133.2) were supplied by Life Technologies. The primer sequences (5' to 3') used were ATGGCCTCCCTGTACCACATC (forward) and TGTTGCGCTCAATCTCCTCCT (reverse).

Safe-lock microcentrifuge tubes were purchased from Qiagen (Crawley, UK), acid-washed glass beads (~0.5mm diameter) from Sigma-Aldrich, and Complete Protease Inhibitor Cocktail Tablets were obtained from Roche Applied Science (Burgess Hill, UK). NuPAGE sample reducing agent and LDS sample buffer were purchased from Invitrogen, and Precision Plus Protein Dual Colour standards from Bio-Rad Laboratories, Inc (Hemel Hempstead, UK). Protein-Free T20 (TBS) blocking buffer was obtained from Fisher Scientific (Loughborough, UK); Immobilon-FL PVDF membrane from Millipore, and Instant*Blue* protein gel stain from Expedeon Protein Solutions (Harston, UK). Tween® 20 was purchased from Sigma-Aldrich. Chicken polyclonal anti-glyceraldehyde-3-phosphate dehydrogenase (GAPDH; AB2302) was obtained from Millipore (Watford, UK) and rabbit polyclonal anti-HO-1 (ab13243) from Abcam (Cambridge, UK). Donkey anti-chicken IgG (IR dye 680 LT) and goat anti-rabbit IgG (IR dye 800 CW) were supplied by Li-Cor (Cambridge, UK). Antibodies were prepared in a diluent of 50% T20 blocking buffer:50% phosphate-buffered saline (PBS) with 0.5% Tween® 20; and including 0.02% sodium dodecyl sulphate for solutions of IR dye 680 LT anti-IgG antibodies.

Cell culture. Cryo-preserved, early passage, pooled HUVEC were purchased from TCS CellWorks (Buckingham, UK) and used between passages two to four. Cells were routinely cultured in 75cm^2 flasks (SPL Life Sciences) coated with fibronectin (0.27μg/cm^2), using large vessel endothelial cell growth medium [TCS CellWorks; proprietary basal medium formulation supplemented with growth factor and antibiotic (gentamicin & amphotericin B) supplements, final concentration of 2% v/v foetal bovine serum] at 37°C and 5% CO_2. HUVECs were sub-cultured using 0.025% trypsin and 0.01% EDTA (TCS CellWorks).

Cryo-preserved, second passage, single donor HCAEC were purchased from PromoCell GmbH (Heidelberg, Germany) and used between passages three to six (Figure 6.2). Cells were routinely cultured in 75cm^2 flasks (SPL Life Sciences) coated with fibronectin (0.27μg/cm^2), using endothelial cell medium MV (PromoCell GmbH; proprietary basal medium formulation supplemented with foetal

calf serum, endothelial cell growth supplement, recombinant human epidermal growth factor, heparin, and hydrocortisone, final concentration of 5% v/v foetal calf serum) at 37°C and 5% CO_2. HCAEC were sub-cultured using 0.04% trypsin and 0.03% EDTA (PromoCell GmbH).

Figure 6.2 **Light microscopy image of sub-confluent HCAEC at sixth passage (cultured on fibronectin coating).**

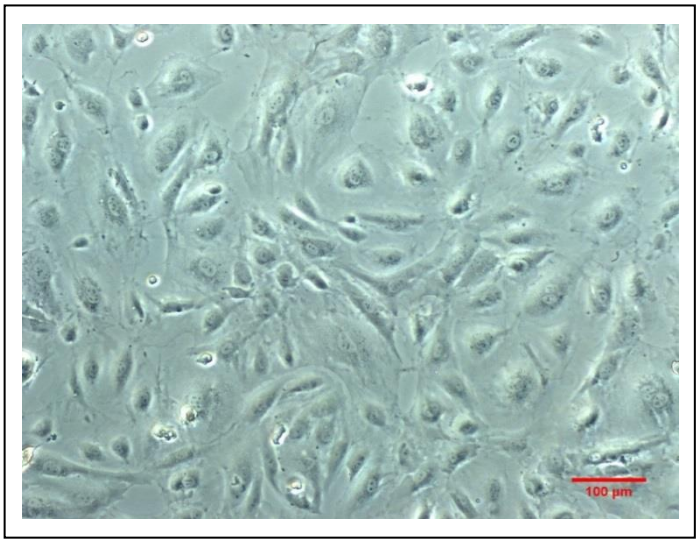

6.2.1 Method development – HUVEC RT-qPCR

Reverse-transcription – quantitative polymerase chain reaction: method development for HUVEC model (Figure 6.3 & Appendix Table 9.2.8). Method development was conducted to identify a positive control for upregulation of HO-1 expression (Figure 6.3 A); and to select endogenous reference genes for normalisation of C_t data for genes of interest (Figure 6.3 B).

Figure 6.3 **Analysis of HUVEC HO-1 expression: RT-qPCR method development flow chart.**

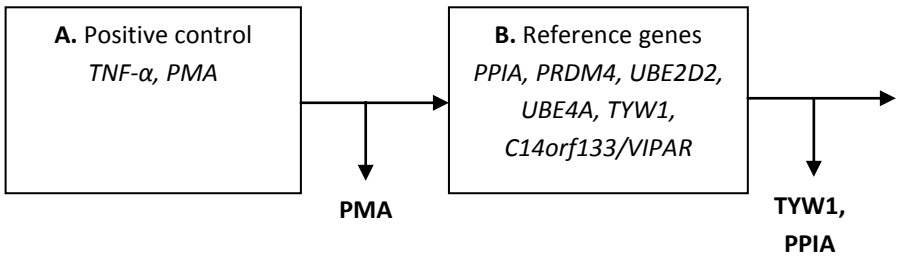

Cell stimulant (Figure 6.3 A). A positive control for induction of HO-1 expression was identified using 20ng/ml TNF-α with or without serum starvation (Terry et al., 1998, Terry et al., 1999), and 10ng/ml PMA. Cultured HUVEC (~70 - 80% confluent) were incubated for five or six hours with TNF-α or PMA respectively, as comparable to the six hour period used in the previously reported stimulated superoxide production assay (Chapters 2 & 5); prior to RNA extraction and first strand cDNA synthesis. For the serum-starved condition, HUVEC were pre-incubated for three hours in basal (non-supplemented) endothelial cell growth medium, prior to incubation with TNF-α in the same

medium. Expression of HO-1, in addition to six reference genes (Table 6.1), was compared against unstimulated (basal) cells by real-time PCR. PMA elicited optimal upregulation of HO-1 expression, and was used as the positive control.

Reference/housekeeping genes (Figure 6.3 B). Reference genes for normalisation of C_t data were selected using a geNorm^{PLUS} kit (PrimerDesign Ltd). Primer sets for six stably expressed human reference genes (Table 6.1) were designed, pre-validated and supplied by PrimerDesign Ltd, and used to evaluate expression of these genes in both unstimulated and stimulated HUVEC. Real-time PCR data were analysed using the geNorm function in qbase^{PLUS} software (version 2.3, Biogazelle NV, Zwijnaarde, Belgium) to assess reference gene stability across samples, and optimal number of reference genes (Vandesompele et al., 2002).

Table 6.1 Reference/housekeeping genes evaluated during method development.

Gene	Description
PPIA	Peptidylprolyl isomerase A (cyclophilin A)
PRDM4	PR domain containing 4
UBE2D2	Ubiquitin-conjugating enzyme E2D 2
UBE4A	Ubiquitination factor E4A
TYW1	tRNA-yW synthesizing protein 1 homologue (*S. cerevisiae*)
VIPAR/C14orf133/VIPAS39	VPS33B interacting protein, apical-basolateral polarity regulator, spe-39 homologue

Cultured HUVEC were incubated for six hours with culture medium only (basal), 10ng/ml PMA, vehicle control (0.005% DMSO), or 10µM vanillic acid. Following RNA extraction and first strand cDNA synthesis, reference gene expression was assessed by real-time PCR, and the generated C_t data were analysed using qbase^{PLUS}. The average expression stability of reference targets across treatment conditions (geNorm M value) was investigated by geNorm analysis (Figure 6.4; targets plotted in order of increasing stability from left to right); and optimal number of targets was also confirmed (Figure 6.5). TYW1 and PPIA were identified as the optimum reference genes, and their geometric mean used as the normalisation factor in the final assay.

Figure 6.4 **Average reference gene expression stability (geNorm M graph) for untreated HUVEC and following 6h incubation with 10ng/ml PMA, vehicle control (0.005% DMSO), or 10µM vanillic acid.**

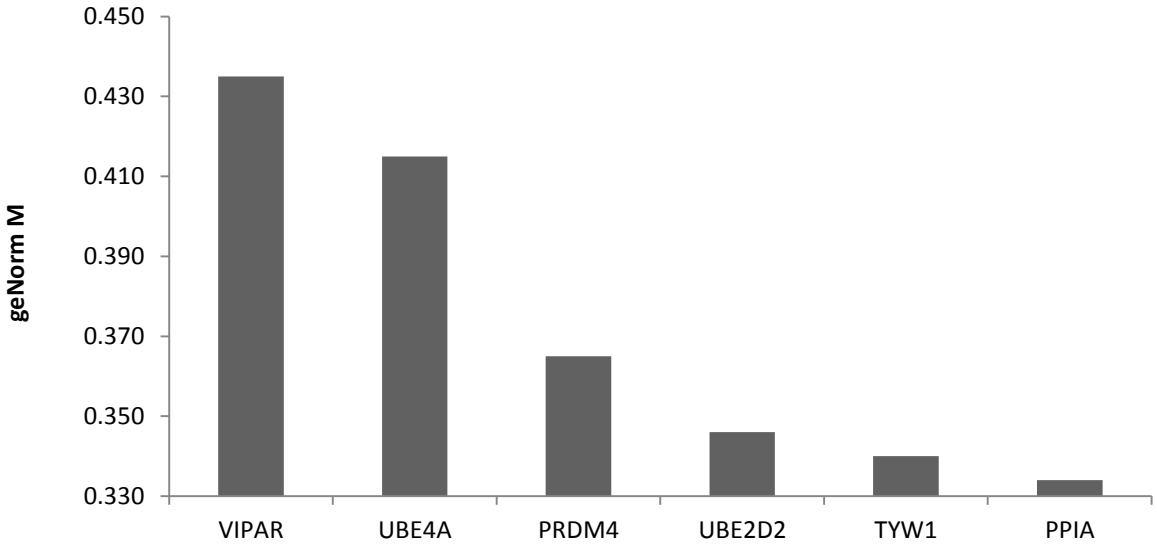

geNorm M graph demonstrating average reference gene expression stability (geNorm M value, y-axis) across experimental conditions (ie untreated, PMA, vehicle control, or 10µM vanillic acid). Reference genes (x-axis) are arranged in order of increasing stability from left to right (refer to Table 6.1 for gene descriptions).

Figure 6.5 **Determination of optimal number of reference genes (geNorm V graph) for untreated HUVEC and following 6h incubation with 10ng/ml PMA, vehicle control (0.005% DMSO), or 10µM vanillic acid.**

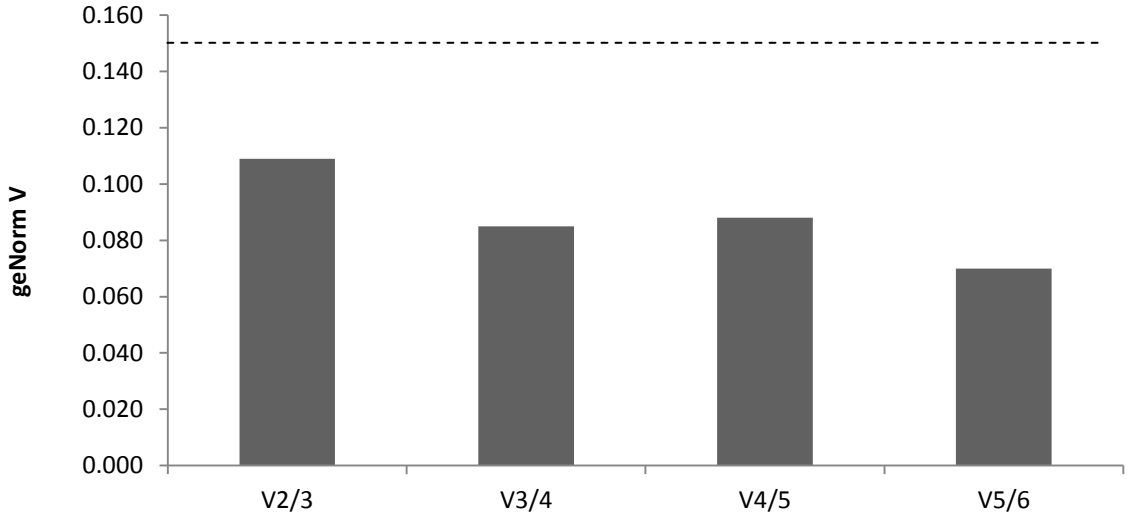

geNorm V graph determining optimal number of reference genes. 'V2/3' denotes comparison between 2 genes and 3 genes, 'V3/4' compares 3 genes versus 4 genes etc. across untreated (basal) and treated (PMA, vehicle control, or 10µM vanillic acid) samples. Where the geNorm V value is below 0.15 (ie below dashed line), no additional benefit is derived using a further reference gene.

6.2.2 Final methodology

HO-1 gene expression assay: optimised parameters. The optimised HO-1 gene expression assay used 6-well plates (SPL Life Sciences) coated with fibronectin (0.25µg/cm^2), which were seeded with HUVEC at a density of ~100,000 cells/well, and the cells grown to ~70% confluence (~24 hours at 37°C and 5% CO_2). Culture medium was then aspirated, and the cells were incubated for six hours in supplemented culture medium alone (basal), or media with 10ng/ml PMA, 0.005% DMSO, or 0.1, 1 or 10µM vanillic acid. After incubation, media was aspirated from all wells, and the plates were either frozen at -80°C or utilised for RNA extraction.

RNA extraction and mRNA reverse transcription. RNA was extracted from cultured cells by phenol-based organic extraction. Briefly, cells were homogenised using TRIzol reagent (1ml per well), and homogenates incubated for ten minutes at room temperature. Following addition of 200µl chloroform, samples were agitated vigorously, incubated for ten minutes at room temperature, and then subject to centrifugation at 12,000*g* for 20 minutes at 4°C. Four hundred microlitres of the aqueous phase was removed and mixed with 500µl isopropanol, prior to a ten minute incubation at room temperature. Cellular RNA was pelleted by centrifugation at 12,000*g* for 15 minutes at 4°C, and washed with 1000µl of 75% ethanol by centrifugation at 12,000*g* for ten minutes at 4°C. After removal of supernatants, pellets were partially dried and resuspended in 20µl RNase-free water, prior to a 15 minute incubation at 57.5°C. Quantification of RNA was performed using a NanoDrop 2000 (Thermo Fisher Scientific).

One microgram of each RNA sample was utilised in a 20µl reverse transcription reaction with oligo (dT) primers. Prior to reverse transcription, RNA was incubated for 30 minutes at 37°C with DNase I and RiboLock RNase inhibitor, to remove any residual genomic DNA from extracted RNA. Following addition of EDTA, oligo (dT) primers (final concentration 5µM), and dNTP PCR mix, DNase was inactivated by a 10 minute incubation at 65°C. First strand buffer, RiboLock, and DTT were then added to each sample, prior to a two minute incubation at 42°C to allow annealing of primers. After the addition of SuperScript® II (or RNase-free water for a no reverse-transcriptase control), samples were incubated at 42°C for 50 minutes for first strand cDNA synthesis, followed by a 15 minute incubation at 70°C to inactivate the reverse transcriptase enzyme.

Real-time PCR. Analysis of gene expression was performed using the Applied Biosystems 7500 Real time PCR System (Life Technologies; 7500 software version 2.0) with SYBR®Green detection. Typically, 25ng cDNA (or RNase-free water for a 'no template' control) was amplified with 300nM of the appropriate primer set, and 8.33µl Precision 2x real-time PCR MasterMix with SYBR®Green (Primer Design Ltd) in a total volume of 20µl. Following enzyme activation at 95°C for 10 minutes, 50 cycles of denaturation (15 seconds at 95°C) and data collection (60 seconds at 60°C) were performed,

prior to melt curve analysis to confirm specificity of amplification. Relative changes in gene expression following cell treatment, as compared with basal (unstimulated) cells, were quantified using the comparative C_t method (Dorak, 2006, Schmittgen and Livak, 2008), incorporating the geometric mean of reference genes TYW1 and PPIA as the normalisation factor.

Immunoblot analysis of HO-1 protein. Cell lysates for immunoblotting were generated from cultured HUVEC or HCAEC incubated with culture medium only (basal), or PMA, vehicle control (HUVEC only), or vanillic acid (0.1 - 10μM). Briefly, 6-well plates (SPL Life Sciences) coated with fibronectin (0.25μg/cm^2) were seeded with HUVEC or HCAEC at a density of 100,000 cells/well, and cells were grown to ~70% confluence. Thereafter, cells were incubated for six hours in supplemented culture medium only, or media with 10ng/ml PMA, 0.005% DMSO (HUVEC only), or 0.1, 1, or 10μM vanillic acid (in ≤ 0.005% DMSO for HUVEC, or without DMSO for HCAEC). Cells were harvested and lysed in 1% (octylphenoxy)polyethoxyethanol (CA-630), 150mM NaCl, 20mM Tris and 10% glycerol (pH 8.0), supplemented with protease inhibitors (Complete Protease Inhibitor Cocktail). Six-well plates were incubated with lysis buffer (120μl/well) for 30 minutes at 4°C, prior to removal of cells by scraping. Recovered solutions were subject to cell disruption by rapid agitation (50Hz for 5 minutes with Qiagen TissueLyser LT) with acid-washed glass beads in safe-lock microcentrifuge tubes. After centrifugation at 13,000 rpm (15 minutes at 4°C), the protein content of the supernatants was assayed using the Pierce BCA Protein Assay Kit according to manufacturer's instructions.

For gel electrophoresis, samples were reduced using NuPAGE sample reducing agent (50mM dithiothreitol) prior to gel loading in NuPAGE LDS sample buffer. Precision Plus Protein Dual Colour standards were loaded as comparative molecular weight markers. Normally 15μg (HUVEC) or 20μg (HCAEC) of protein was loaded onto a 4% polyacrylamide stacking gel, and separated across a 10% resolving gel (at 25mA for approximately one hour) prior to semi-dry transfer to Immobilon-FL PVDF membrane (at 25V for 60 minutes). Equal protein transfer was confirmed by Instant*Blue* staining of the gels. Membranes were blocked with T20 blocking buffer for one hour at room temperature, and incubated overnight (at 4°C) in the appropriate concentration of primary and loading control antibody (anti-GAPDH, 1 in 10,000; anti-HO-1; 1 in 2000). Membranes were washed using PBS with 0.1% Tween® 20 (PBST 0.1%), after which secondary antibody incubations were performed for one hour at room temperature, using IR dye-conjugated (680 and 800) secondary antibodies at a concentration of 1 in 10,000. Membranes were washed with PBST 0.1%, and subsequently imaged using an Odyssey Infrared Imaging System (Li-Cor). Immunoblots were quantified by densitometry using Odyssey Infrared Imaging System Application Software (Li-Cor, version 3.0.21).

Statistical analysis. Analysis of variance (ANOVA) with Tukey post-hoc test was performed using SPSS software (IBM, New York, USA) version 18 for Windows. Significance was determined at the 5%

level and expressed relative to DMSO (vehicle control) or PMA (positive control). Three biological replicates for each control/treatment were used for analysis unless otherwise noted.

6.3 Results

Following incubation of HUVEC with 10ng/ml PMA for six hours, HO-1 mRNA levels were significantly elevated (6.42 ± 1.63 fold increase from basal; mean ± SD), as compared with the vehicle control 0.001% DMSO (0.62 ± 0.12 fold change from basal). Exposure to vanillic acid at concentrations of 0.1µM, 1µM, and 10µM appeared to elicit a concentration-dependent increase in endothelial HO-1 mRNA, with fold changes from basal of 0.53 ± 0.12, 1.03 ± 0.21, and 1.59 ± 0.29 respectively; although there were no significant differences compared to vehicle control (p = 1.0 for 0.1µM vanillic acid, p = 1.0 for 1µM vanillic acid, and p = 0.5 for 10µM vanillic acid; Figure 6.6).

Figure 6.6 Modulation of HUVEC HO-1 mRNA levels following six hour incubation with 0.1 - 10µM vanillic acid.

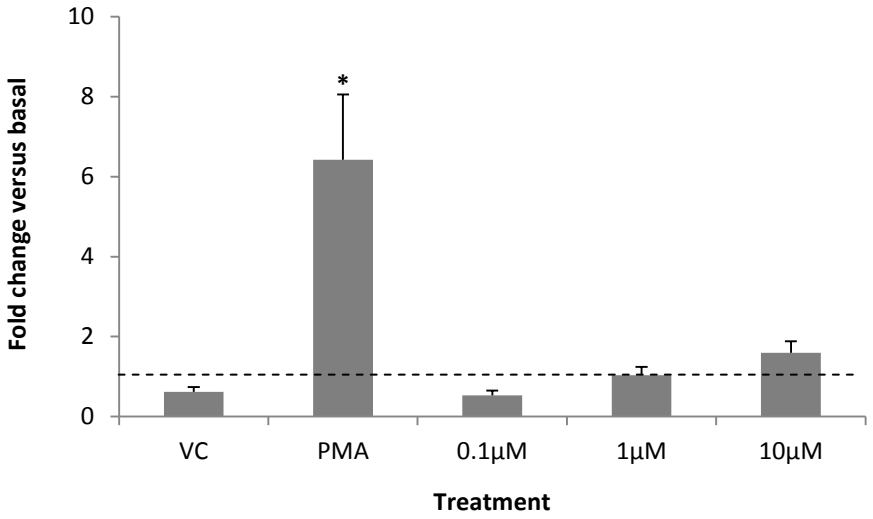

Fold change in HUVEC HO-1 mRNA levels versus unstimulated cells (basal; denoted by dashed line) following 6 hour incubation with vehicle control (VC, 0.005% DMSO), 10ng/ml phorbol 12-myristate 13-acetate (PMA), or 0.1µM, 1µM or 10µM vanillic acid. Relative quantification was performed using the comparative C_t method, incorporating the geometric mean of reference genes TYW1 and PPIA as the normalisation factor. Data are graphed as mean ± SD (n=3). *Significant difference versus vehicle control (*p < 0.01).

An apparent upregulation of HO-1 protein in HUVEC following a six hour incubation with vanillic acid was observed at all concentrations of vanillic acid tested, with a maximal response at 1µM (mean 1.83 ± 0.34 fold increase over basal), although the response was variable between biological replicates and no changes were significant relative to the vehicle control (p = 0.6 at 1µM vanillic acid, Figure 6.7). A non-significant increase in HO-1 protein was observed following treatment with the positive control PMA (mean 1.92 ± 0.36 fold increase) relative to the vehicle control (p = 0.3);

however, the vehicle control (0.005% DMSO) also increased levels of HO-1 protein from basal (Figure 6.7).

Figure 6.7 **Modulation of HUVEC HO-1 protein expression following six hour incubation with 0.1 - 10µM vanillic acid.**

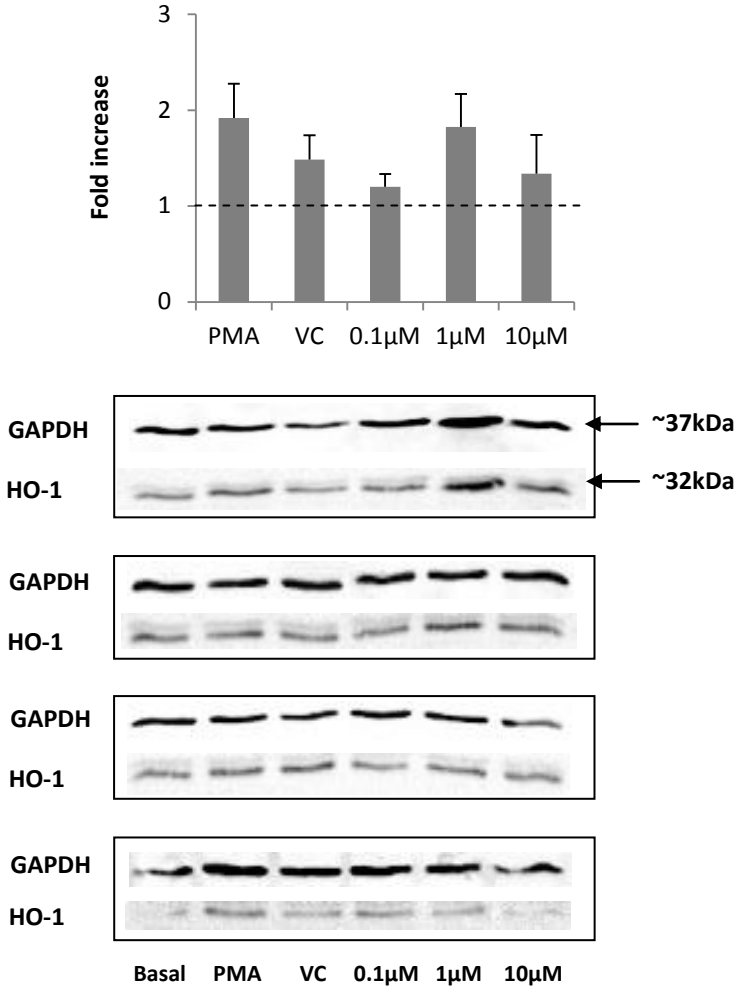

Expression of HO-1 protein (with GAPDH loading control) in cell lysates from unstimulated HUVEC (basal) and following 6h incubation with 10ng/ml phorbol 12-myristate 13-acetate (PMA), vehicle control (VC, 0.005% DMSO) or 0.1µM, 1µM or 10µM vanillic acid. Graph shows fold increase in HO-1 expression relative to basal (designated as 1 and marked by dashed line), after quantification by densitometry and normalisation to loading control (n=4; mean ± SD). No significant differences from vehicle control were observed ($p > 0.05$).

In order to characterise the observed effects of vanillic acid in a more physiologically relevant vascular endothelial cell model, a study was conducted using cultured HCAEC, with vanillic acid prepared directly in aqueous solution to exclude vehicle-related activity. Here, HO-1 protein appeared to be upregulated at all concentrations of vanillic acid tested, with a maximal effect at 1µM (mean 1.81 ± 0.63 fold increase over basal; Figure 6.8); although again, responses were variable between biological replicates and no changes were significant relative to unstimulated cells ($p \geq 0.3$).

Figure 6.8 **Modulation of HCAEC HO-1 protein expression following six hour incubation with 0.1 - 10µM vanillic acid.**

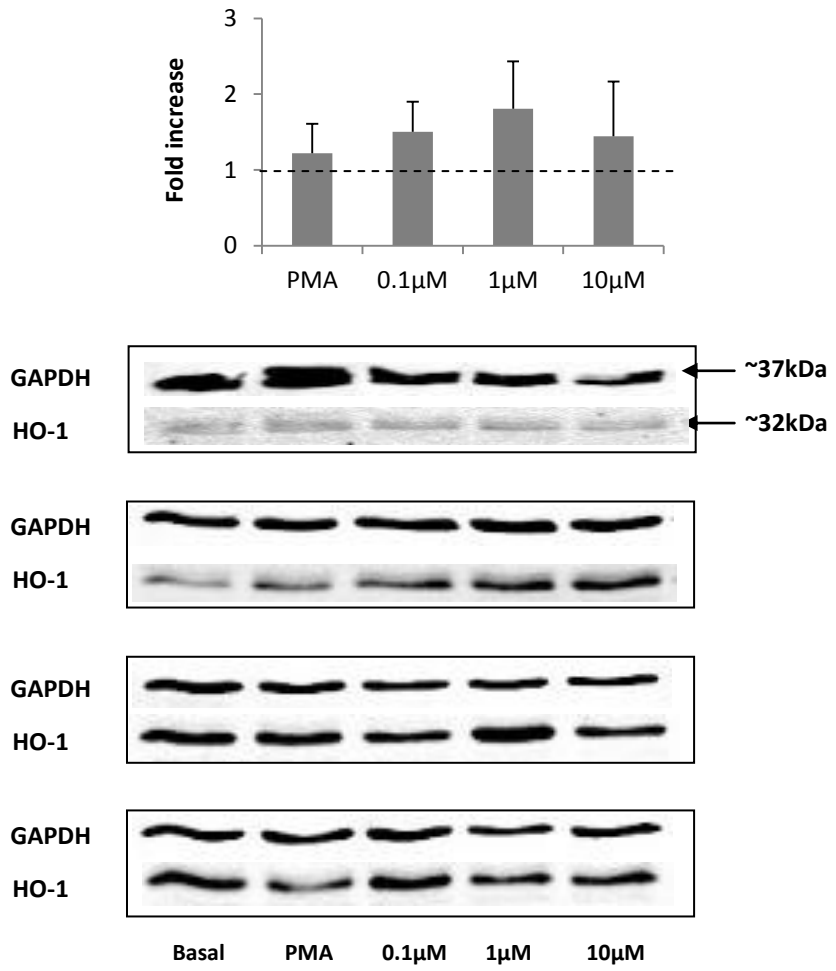

Expression of HO-1 protein (with GAPDH loading control) in cell lysates from unstimulated HCAEC (basal) and following 6h incubation with 10ng/ml phorbol 12-myristate 13-acetate (PMA), or 0.1µM, 1µM or 10µM vanillic acid. Graph shows fold increase in HO-1 expression relative to basal (designated as 1 and marked by dashed line), after quantification by densitometry and normalisation to loading control (n=4; mean ± SD). No significant differences from basal were observed ($p > 0.05$).

Given the limited induction of HO-1 protein by PMA in HCAEC (Figure 6.8), cultured HCAEC were incubated with 10ng/ml PMA for six hours and 24 hours, to assess whether an extended incubation period resulted in elevated upregulation of HO-1 from basal levels. However, the fold increase in HO-1 protein over basal following PMA stimulation was comparable at both time points (~1.5-fold increase; Figure 6.9).

Figure 6.9 Expression of HO-1 protein in HCAEC lysates following six hour or 24 hour incubation with PMA.

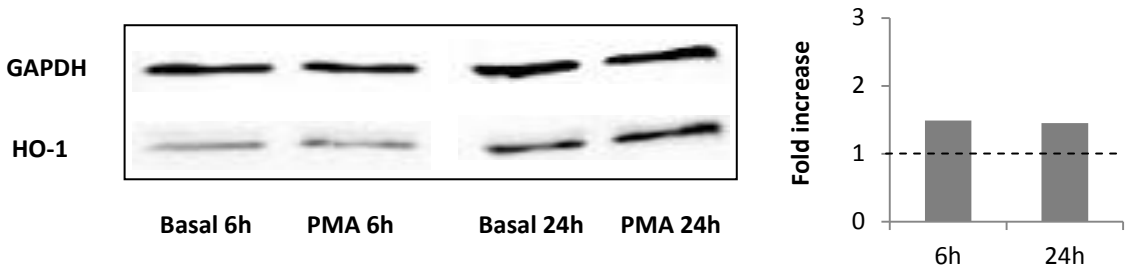

Expression of HO-1 protein (with GAPDH loading control) in lysates prepared from unstimulated HCAEC (basal) and following either a six hour (6h) or 24 hour (24h) incubation with 10ng/ml phorbol 12-myristate 13-acetate (PMA). Inset graph shows fold increase in HO-1 expression relative to basal (designated as 1 and marked by dashed line), after quantification by densitometry and normalisation to loading control (n=1).

6.4 Discussion

The current investigation aimed to explore a potential mechanism by which the anthocyanin degradant vanillic acid could indirectly inhibit NOX activity in vascular endothelium, specifically through upregulating the inducible isoform of haem oxygenase/HO-1 (Jiang et al., 2006, Wolin and Abraham, 2006, Datla et al., 2007). Inhibition of NOX-generated superoxide production may preserve bioavailability of the key meditator NO, with beneficial effects on vascular endothelial function, as suggested for certain flavonoids and their metabolites (Steffen et al., 2007b, Steffen et al., 2008, Schewe et al., 2008); as opposed to direct effects on endothelial NO synthase observed for parent anthocyanins but not phenolic acid degradation products including vanillic acid (Chapter 2). In a previous study, vanillic acid appeared to reduce endothelial superoxide levels following stimulation of NOX activity (Chapter 2); however, no significant modulation of endothelial expression of NOX2, NOX4, $p22^{phox}$ and $p47^{phox}$ mRNA and/or protein could be discerned following exposure to 0.1 - 10µM vanillic acid (Chapters 2, 4 & 5), nor was it possible to detect any effect of vanillic acid upon $p47^{phox}$ activation following cell stimulation (Chapter 5). These data therefore suggested an indirect effect of vanillic acid on NOX activity, which forms the basis of the present study examining endothelial HO-1 expression as a possible indirect mechanism of regulating NOX-mediated superoxide production and thereby enhancing NO levels in the vasculature.

Here, stimulation of cultured HUVEC with the positive control PMA [a protein kinase C activator (Terry et al., 1999)] elicited a six-fold increase in HO-1 mRNA from basal levels (Figure 6.6). This elevation was comparable to a reported four- to five-fold increase in HO-1 mRNA levels following incubation of HUVEC with 0.1µg/ml PMA for four hours (Terry et al., 1999), indicating that the cells used in the current study were sufficiently responsive to a known stimulant of HO-1 expression. Moreover, expression of HO-1 protein by HUVEC was apparently increased following PMA stimulation as compared with unstimulated cells (Figure 6.7), by an average of two-fold, and Li *et al* (2004) have described a similar response in perfused rat kidneys after a two hour exposure to 0.2µM PMA (Li et al., 2004). In the present study, the vehicle control (0.005% DMSO) slightly increased HO-1 protein relative to basal (1.49-fold increase), potentially reducing the sensitivity of the assay; however, this reflects previously reported induction of HO-1 protein in HUVECs by low concentrations of DMSO (Liang et al., 2011). Liang *et al* (2011) observed upregulation of HUVEC HO-1 mRNA and protein expression following a four hour incubation with 0.05% DMSO, in a time- and concentration-dependent response mediated partly through activity of c-Jun-N-terminal kinases (JNKs) and NF-E2-related factor 2 (Nrf2) (Liang et al., 2011); although interestingly no effect of DMSO on HUVEC HO-1 mRNA levels was observed in the current investigation (0.62-fold change versus basal; Figure 6.6).

Elevated endothelial HO-1 mRNA expression was observed following a six hour incubation of cultured HUVEC with 1µM and 10µM vanillic acid (1.03-fold and 1.59-fold increase versus basal respectively; Figure 6.6), in what appeared to be a concentration-dependent response, although the maximal response at 10µM vanillic acid was not significantly different from the vehicle control ($p = 0.5$). An apparent increase in protein levels of HO-1 was also detected following exposure of HUVEC to vanillic acid, where the maximal response at 1µM vanillic acid (1.83-fold increase versus basal, Figure 6.7) was similar to that elicited by the positive control PMA (1.92-fold increase); although the observed changes were variable across replicates and not significant as compared with the vehicle control ($p = 0.6$ and $p = 0.3$ respectively). However, vanillic acid appeared to induce endothelial HO-1 expression, which could potentially inhibit NOX activity thus preserving NO levels and ultimately vascular homeostasis. The induction of HO-1 protein elicited by both 1µM vanillic acid and PMA is of particular interest, given the significant elevation in HO-1 mRNA induced by PMA over the same period (Figure 6.6); suggesting no direct correlation between the magnitude of observed stimulatory effects on HO-1 mRNA relative to those on protein, and perhaps indicating an effect of vanillic acid at the translational/post-translational level as opposed to activation of gene transcription.

In order to characterise further the activity of vanillic acid on endothelial HO-1 expression, an additional study was conducted using a more physiologically relevant vascular endothelial cell type; specifically human coronary artery endothelial cells. Whilst HUVEC represent a widely used model

for research concerning general properties of endothelial cells (Baudin et al., 2007), a human arterial endothelial cell type may be more appropriate for studies investigating the potential modulation of NOX activity in relation to endothelial dysfunction preceding atherosclerosis, which is principally a disease of medium and large-sized arteries (Ross, 1999, Vita, 2005). A number of previously published research reports have employed HCAEC to assess the effect of treatment compounds on HO-1 expression (Kaga et al., 2005, Vidavalur et al., 2006, Ungvari et al., 2010, Khoo et al., 2010, Wu et al., 2012, Donovan et al., 2012), and as such the effect of vanillic acid at 0.1 - 10μM on HO-1 protein expression was investigated in cultured HCAEC. For this study, vanillic acid was prepared directly in cell culture medium to exclude any vehicle-related effects on HO-1 expression, owing to induction of HO-1 observed with low concentrations of DMSO as discussed above.

In the HCAEC model, an apparent upregulation of HO-1 protein was observed following exposure to increasing concentrations of vanillic acid (Figure 6.8), with a maximal increase of ~1.81-fold over basal at 1μM vanillic acid ($p = 0.3$), although again, the detected changes were variable between biological replicates. Similar observations suggesting elevated endothelial HO-1 protein levels (Figure 6.7 & Figure 6.8) were noted in both the HUVEC and HCAEC models following exposure to vanillic acid, as opposed to disparate effects between models on $p47^{phox}$ protein expression as described in Chapter 5; indicating HUVEC may represent an appropriate model for investigating modulation of HO-1 expression by anthocyanin phenolic degradants in the context of vascular endothelial cell function. Interestingly, no linear concentration-response relationship was observed for the effects of vanillic acid on HO-1 expression in either cell model, in accordance with previous reports describing differential bioactivity of flavonoids across a concentration range (Chirumbolo et al., 2010, Kay et al., 2012). Upregulation of HO-1 may indirectly inhibit endothelial NOX activity (Wolin and Abraham, 2006), and therefore reduce scavenging of the key vascular mediator NO by NOX-derived superoxide (Brandes et al., 2010), indicating a potential mechanism by which anthocyanin degradants or metabolites formed *in vivo* following anthocyanin intake (such as vanillic acid) (Czank et al., 2013) might act to enhance vascular function. Indeed, Cimino *et al* (2013) have reported Nrf2 nuclear translocation and HO-1 expression in cultured HUVEC elicited by serum samples obtained from healthy subjects following ingestion of 160mg purified anthocyanins; which may reflect activity of anthocyanin metabolites as opposed to parent compounds (Cimino et al., 2013). Increased HO-1 expression could also result in elevated levels of generated CO and subsequent vasodilatory activity (Siow et al., 1999), although CO is considerably less potent as a vasodilator relative to NO (Chan et al., 2011).

A limitation of the current investigation was the minimal increase detected in HO-1 protein following stimulation of HCAEC with the positive control PMA, as previous reports (Appendix Table 9.2.8) have described 2- to- 8-fold increases in HO-1 protein levels following stimulation of HCAEC with agents

such as haemin chloride, sildenafil, niacin, and Protandim (a marketed phytochemical dietary supplement). (Vidavalur et al., 2006, Zieger and Gupta, 2009, Wu et al., 2012, Donovan et al., 2012). Upregulation of HO-1 protein elicited by PMA in the current study ranged from ~1.2 - 1.5-fold (Figure 6.8 & Figure 6.9), and was not enhanced by an extended incubation period with PMA (Figure 6.9). These data suggest considerable variation in the response of cultured HCAEC to cell stimulation, which may constitute an inherent limitation of an endothelial cell culture model, as also reflected by the variability in response to vanillic acid observed between biological replicates in both models (Figure 6.7 & Figure 6.8). Equally, the limited effect of PMA in the current study could also reflect the use of a lower concentration (10ng/ml, ~16.2nM) to stimulate HCAEC as compared with studies using, for example, 100ng/ml (Zhao et al., 2004) or 100nM (Meyer et al., 2005) PMA. A strength of the HCAEC confirmatory study was the exclusion of any vehicle (DMSO)-related effects on HO-1 induction (Liang et al., 2011), as observed in the HUVEC model, by preparing vanillic acid in aqueous solution and therefore ensuring observed effects reflected the activity of vanillic acid alone. Moreover, and as described in a previous investigation (Chapter 4), optimal endogenous reference genes were identified for relative quantification of HUVEC HO-1 mRNA levels (Figure 6.4 & Figure 6.5); as selection of multiple reference genes stably expressed across experimental conditions ensures accurate normalisation of qPCR data to account for non-treatment related sources of variation between samples, such as RNA extraction and reverse transcription yields (Bustin et al., 2009).

In summary, the current study has indicated that the anthocyanin degradant vanillic acid might act to upregulate vascular endothelial expression of HO-1, as reported for cyanidin-3-glucoside (Sorrenti et al., 2007). A previous investigation (Chapter 3) has demonstrated that bioactivity of anthocyanin glycosides may not necessarily correspond to activity of phenolic degradation products or metabolites, but to date no studies have sought to characterise the vascular bioactivity *in vitro* of these compounds at physiologically relevant concentrations. Indeed, low human bioavailability of anthocyanin glycosides (Vitaglione et al., 2007, Azzini et al., 2010, Czank et al., 2013) suggests anthocyanin bioactivity *in vivo* is likely to be mediated by their degradants or metabolites present at levels in excess of the parent compound – for example Czank *et al* (2013) have reported a 42-fold greater abundance of metabolites in human serum relative to the administered parent anthocyanin cyanidin-3-glucoside, based on maximal serum concentrations (Czank et al., 2013). Moreover, anthocyanin degradants and metabolites may act by mechanisms different to those reported for the parent compounds, such as upregulation of eNOS expression observed with anthocyanin-3-glucosides (Chapter 3) and described by other studies (Xu et al., 2004b, Sorrenti et al., 2007, Paixão et al., 2012). In contrast, anthocyanin phenolic degradants/metabolites could indirectly elevate NO levels through HO-1-mediated NOX inhibition, with enhanced vascular function resulting from improved NO bioavailability. This should be explored further in an endothelial model by examining

modulation of HO-1 protein expression, and/or activity as assessed by bilirubin production (Datla et al., 2007); relative to NO levels [using reductive chemiluminescence methodology (MacArthur et al., 2007, Brossette et al., 2011)] and NOX-derived superoxide production quantified by, for example, electron spin resonance spectroscopy (Maghzal et al., 2012) in cell supernatants. Dysfunction of the vascular endothelium, and in particular reduced bioavailability of NO from eNOS with impaired endothelium dependent relaxation, is an initial process in the development of atherosclerosis (Landmesser et al., 2004, Kawashima and Yokoyama, 2004, Higashi et al., 2009); thus the current investigation suggests a mechanism by which anthocyanin degradants or metabolites may enhance vascular function *in vivo*, and thereby explain at least part of the reported cardioprotective activity of dietary anthocyanins observed following habitual intake in prospective studies (Mink et al., 2007, Cassidy et al., 2013).

7 Overview and future perspectives

7.1 General discussion

Consumption of anthocyanins may have beneficial effects on human vascular function, based upon data from both epidemiological studies (Mink et al., 2007, Cassidy et al., 2010, McCullough et al., 2012, Jennings et al., 2012, Cassidy et al., 2013) and randomised controlled trials (Qin et al., 2009, Broncel et al., 2010, Zhu et al., 2011, Zhu et al., 2012, Hassellund et al., 2013). For example, dietary anthocyanin intake has been inversely associated with risk of cardiovascular disease (CVD) morbidity or mortality (Mink et al., 2007, Cassidy et al., 2013), whilst daily ingestion of an anthocyanin supplement by hypercholesterolaemic subjects for up to 24 weeks improved blood lipid profile and endothelial function (Zhu et al., 2011, Zhu et al., 2012). However, the low human bioavailability reported for anthocyanin glycosides (Manach et al., 2005, McGhie and Walton, 2007), and presence of degradation products and/or metabolites in the systemic circulation at levels greatly exceeding those of ingested anthocyanins (Vitaglione et al., 2007, Azzini et al., 2010, Czank et al., 2013), suggests anthocyanin bioactivity *in vivo* is likely to be mediated by lower molecular weight derivatives of parent compounds. This is of particular relevance to *in vitro* or *ex vivo* investigations which seek to elucidate the cellular and molecular mechanisms underlying the observed bioactivity of anthocyanins, as for such studies to be physiologically relevant they must utilise compounds present *in vivo*, and at appropriate concentrations.

Modulation of vascular endothelial function by anthocyanins has been the subject of many studies, for example initial observations include endothelium-dependent vasorelaxation of rat thoracic aortic rings elicited by red wine polyphenolic compounds (Andriambeloson et al., 1997), and anthocyanin-enriched fractions of red wine (Andriambeloson et al., 1998). More recently, the effects of anthocyanin glucosides or anthocyanidins on expression and activity of the key vascular enzyme endothelial nitric oxide synthase (eNOS) have been characterised *in vitro* using cultured endothelial cells (Xu et al., 2004a, Xu et al., 2004b, Lazze et al., 2006, Edirisinghe et al., 2011, Paixão et al., 2012, Quintieri et al., 2013), yet as noted such compounds are unlikely to represent the bioactive forms of anthocyanins present *in vivo* (Williamson and Clifford, 2010, Del Rio et al., 2013). Therefore, whilst assessment of the vascular bioactivity of anthocyanins is essential to understanding potential cardioprotective effects of this important sub-class of flavonoids, there is a paucity of *in vitro* investigations examining biologically relevant compounds and doses on potential targets within the vasculature.

The current thesis has sought to address at least part of these deficiencies in the scientific literature, by investigating relative vascular bioactivity of both parent anthocyanins and phenolic acid degradants *in vitro*, and at physiologically relevant concentrations [0.1, 1, 10µM (Czank et al., 2013)]

(Figure 7.1). Moreover, two combination treatments of an anthocyanin, or its phenolic acid degradant, and additional bioactive dietary constituents (namely other sub-classes of flavonoids and vitamin C) commonly found in flavonoid-rich foods were screened for vascular activity, to explore the potential for interactions between bioactive compounds which may be consumed as part of a healthy diet. Selection of treatment compounds was based upon the presence of a 3', 4'-catechol B-ring, or methylated B-ring structure (Figure 7.1, 'Treatment compounds'), as these structural features may confer inhibitory activity towards NADPH oxidase (NOX) enzymes (Steffen et al., 2007b, Steffen et al., 2008) which represent predominant sources of reactive oxygen species (ROS) in the vasculature (Cai et al., 2003). Vascular function may therefore be enhanced by reducing the production of NOX-derived superoxide, and subsequent scavenging of the key vascular mediator nitric oxide (NO) (Schewe et al., 2008, Cassidy et al., 2010). Treatment compounds and combinations were initially confirmed to be non-cytotoxic (Figure 7.1 **(1)**; experimental flow diagram); then screened for inhibition of stimulated superoxide production by endothelial NOX, and direct effects on eNOS and NO production, in primary human vascular endothelial cells (Figure 7.1 **(2)**).

Vascular bioactivity screening of anthocyanin-3-glucosides and their phenolic acid degradants indicated differential bioactivity of degradants relative to parent compounds (Chapters 2 & 3). Both anthocyanins - with the exception of cyanidin-3-glucoside - and phenolic acid degradants appeared to reduce stimulated endothelial superoxide production (Chapter 2), in a modified form of a previously reported assay (Steffen et al., 2007b, Steffen et al., 2008); as did a combination treatment of the anthocyanin degradant protocatechuic acid with quercetin, epicatechin, and ascorbic acid. In contrast, three anthocyanins (cyanidin-, peonidin-, and petunidin-3-glucoside) upregulated endothelial expression of eNOS (Chapter 3), reflecting previous reports (Xu et al., 2004b, Paixão et al., 2012), yet the more physiologically relevant phenolic acid degradants were without effect on eNOS. Moreover, no treatments or combinations significantly modulated NO production (Chapter 3), although this may reflect insufficient sensitivity of the modified Griess reaction used to detect NO degradation products at submicromolar concentrations (Granger et al., 1996). However, data from the current study suggest that anthocyanin derivatives *in vivo* are unlikely to enhance vascular function by direct activity upon eNOS, which should be further investigated and confirmed across multiple time points (for example 0, 6, 12, 18, 24, 30 hours) in a human endothelial cell model using alternative NO detection methodology (MacArthur et al., 2007). Anthocyanins and their phenolic degradants might therefore indirectly elevate endothelial NO levels by reducing NOX-mediated generation of superoxide anion, and enhance vascular function through a similar mechanism as described previously for flavan-3-ols (Schewe et al., 2008).

Figure 7.1 **Experimental scheme for assessment of vascular bioactivity *in vitro***

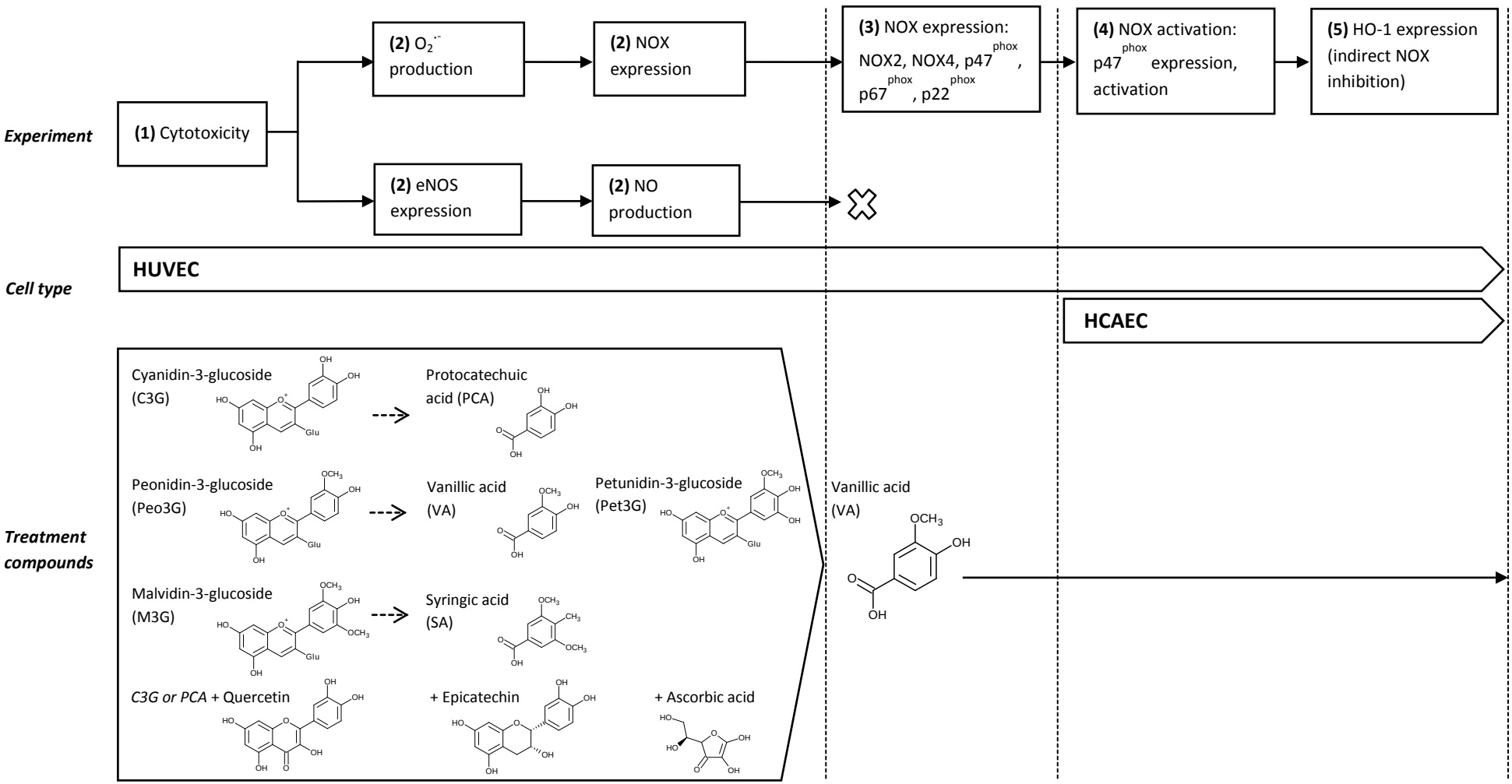

Work scheme for investigation of vascular bioactivity *in vitro*, in primary human endothelial cell model, of selected treatment compounds (1-2), and exploration of mechanisms potentially underlying observed bioactivity with identified lead compound (3-5). 'X' denotes possible bioactivity mechanism not selected for further investigation owing to lack of activity of anthocyanin degradants in previous experiments. eNOS, endothelial nitric oxide synthase; HO-1, inducible haem oxygenase; HCAEC, human coronary artery endothelial cell; HUVEC, human umbilical vein endothelial cell; NO, nitric oxide; NOX2/NOX4, NADPH oxidase isoform 2 or 4; $O_2^{\cdot-}$, superoxide.

Whilst the cytochrome c reduction assay used in the current investigation may be subject to interference by direct radical scavenging activity of polyphenols, the doses of the treatment compounds and combinations examined were in the high nanomolar to low micromolar range, as compared with concentrations of ~40 - 100µM used in previous reports describing superoxide scavenging activity of flavonoids (Taubert et al., 2003) or direct reduction of cytochrome c by anthocyanins (Skemiene et al., 2012). Indeed, vanillic acid has been reported to have no effect on superoxide levels generated by xanthine oxidase activity in a cell-free system (Steffen et al., 2008, Woodward, 2010). Moreover, a NOX-selective inhibitor (Stielow et al., 2006) was employed in the current study to ascertain the involvement of endothelial NOX in the production of superoxide (Chapter 2). Ideally, data from the stimulated superoxide production assay should be confirmed using an alternative detection methodology for reactive oxygen species (ROS), for example electron spin resonance spectroscopy (Maghzal et al., 2012). In addition, catalase controls could be incorporated into the cytochrome c assay to address possible interference by hydrogen peroxide (Nauseef, 2013). Interestingly, a combination of protocatechuic acid with two other flavonoids and ascorbic acid, but not the parent anthocyanin cyanidin-3-glucoside, appeared to reduce superoxide production at 10µM, but this decrease was smaller than that observed for protocatechuic acid alone. These data could reflect the lower individual concentrations of each component within an equimolar mixture, or may suggest the absence of additive effects (or potentially indicate antagonistic effects) between dietary bioactive compounds. Again, this supposition warrants further investigation, perhaps using all constituents at the same concentration (ie 10µM of each individual compound), and testing all constituents singly as well as in combination.

For the purposes of the current study, one treatment compound of those screened (cyanidin-, peonidin-, petunidin- & malvidin-3-glucoside; and protocatechuic, vanillic, & syringic acid), namely vanillic acid, was selected (Figure 7.1) to explore mechanisms potentially underlying the apparent reductions in stimulated superoxide production; and in particular effects on endothelial expression of NOX isoforms (Figure 7.1 **(3)**). NOX4 has been described as the major vascular endothelial isoform (Ago et al., 2004) producing predominantly hydrogen peroxide which may have vasodilatory activity (Ray et al., 2011), whereas NOX2 generates superoxide and could have an important role in regulation of vascular function (Violi et al., 2009, Schroder, 2010). Both NOX2 and NOX4 associate with the integral membrane protein $p22^{phox}$, although NOX2 activation requires recruitment of cytosolic proteins including $p47^{phox}$ and $p67^{phox}$ (Drummond et al., 2011); thus in the present study gene expression of NOX2, NOX4, $p22^{phox}$, $p47^{phox}$, and $p67^{phox}$ was examined in a primary human vascular endothelial cell model. Vanillic acid, the phenolic acid degradant of peonidin-3-glucoside, was chosen for this investigation (Figure 7.1); as vanillic acid elicited a significant reduction in endothelial superoxide levels (at 1µM; Chapter 2), and contains a mono-*O*-methylated catechol functional group which has been previously associated with NOX inhibitory activity (Steffen et al.,

2008, Cassidy et al., 2010). Moreover, vanillic acid has recently been described in human serum following ingestion of ^{13}C-labelled cyanidin-3-glucoside (Czank et al., 2013), where isotope-labelled phase II conjugates (including vanillic acid) of the degradant protocatechuic acid reached a collective C_{max} of 2.35μM; suggesting the presence of vanillic acid *in vivo* at concentrations similar to those associated with bioactivity *in vitro* in the current investigation (Chapter 2).

Vanillic acid (at 0.1 - 10μM) did not significantly modulate angiotensin II-stimulated gene expression of NOX4 and p22^{phox} (Chapter 4), in accordance with immunoblotting data indicating no effect of this degradant on NOX4 endothelial protein levels following cell stimulation (Chapter 2). However, gene expression analysis for NOX2, p47^{phox} and p67^{phox} was precluded by poor specificity of real time polymerase chain reaction (PCR) amplification (Chapter 4); which may reflect reported low or no endothelial expression of mRNA for this NOX isoform and subunits (Jones et al., 1996, Ago et al., 2004, Jiang et al., 2006, Xu et al., 2008, Alvarez et al., 2010) as manifested in poor immunodetection of NOX2 protein (Chapter 2). Another limitation of the current study was the relative lack of NOX transcriptional response to acute stimulation in the human umbilical vein endothelial cell (HUVEC) model used (Chapter 4), even in response to the more potent stimulus transforming growth factor-beta 1 (TGF-β1) (Cucoranu et al., 2005); thus a more physiologically representative cell type (namely human coronary artery endothelial cells/HCAEC) was used to confirm vanillic acid bioactivity on subsequent targets explored in a HUVEC model (Chapters 5 & 6; Figure 7.1 **(4)** & **(5)**). As vanillic acid appeared to be without effect on NOX4 activity at the level of transcription or translation, the next stage of the current research examined potential translational/post-translational mechanisms of NOX inhibition; specifically modulation of expression and activation of the cytosolic p47^{phox} subunit (Figure 7.1 **(4)**), as described for structurally similar compounds such as isorhamnetin and apocynin (Romero et al., 2009, Drummond et al., 2011).

The vasoactive compound apocynin, which in common with vanillic acid incorporates a mono-methylated catechol group, has been reported to inhibit p47^{phox} association with membrane components of the NOX complex (Stolk et al., 1994, Drummond et al., 2011), and both quercetin (containing a catechol B-ring) and its mono-methylated metabolite inhibited endothelin-1-stimulated p47^{phox} gene expression in rat aortic rings (Romero et al., 2009). Therefore the effect of vanillic acid on both total p47^{phox} expression, and activation of p47^{phox} [as assessed by levels of phosphorylated protein (Leverence et al., 2011)], was examined in a HUVEC model. Here, vanillic acid did not significantly modulate TNF-α stimulated p47^{phox} expression, although a trend towards decreased protein levels with increasing concentration of vanillic acid was observed (Chapter 5); but no effect was discerned upon levels of phosphorylated p47^{phox}. However, and as noted above, HUVEC were relatively unresponsive to acute cell stimulation, perhaps reflecting low p47^{phox} expression (Jones et al., 1996, Ago et al., 2004). Interestingly, a confirmatory study conducted as part of this investigation

using a more physiologically relevant HCAEC model (Figure 7.1 **(4)**) (Baudin et al., 2007) suggested vanillic acid was without effect on total $p47^{phox}$ protein expression (Chapter 5); although TNF-α again elicited minimal upregulation of $p47^{phox}$. Previously reported studies using HCAEC have described up regulation of $p47^{phox}$ by ~1.5-fold (Yoshida and Tsunawaki, 2008) and 5-fold (Chen et al., 2011b) following cell stimulation, and it is possible the observed variation in response to stimulation represents an inherent limitation of a static cell culture model. Indeed, the effect of vanillic acid on $p47^{phox}$ mRNA and protein expression may be better studied using an excised tissue model as reported for other flavonoids (Sanchez et al., 2006, Sanchez et al., 2007, Romero et al., 2009), and should be a focus of future investigations.

The final part of the current thesis examined upregulation of the cytoprotective enzyme haem oxygenase-1 (HO-1) as a possible indirect mechanism of NOX inhibition, resulting in decreased superoxide production (Figure 7.1 **(5)**). Induction of HO-1 has been reported to decrease NOX activity in studies using human microvascular endothelial cells (Jiang et al., 2006) and apolipoprotein-E deficient mice (Datla et al., 2007); and anthocyanins are reported to upregulate expression of HO-1 in human vascular endothelial cells (Sorrenti et al., 2007, Cimino et al., 2013) and murine hepatocytes (Inoue et al., 2012). The effect of the anthocyanin degradant vanillic acid on levels of HO-1 mRNA and protein was therefore examined in a HUVEC model (Chapter 6), using phorbol 12-myristate 13-acetate (PMA) as a positive control for HO-1 induction (Terry et al., 1999). In the current investigation, vanillic acid appeared to upregulate endothelial HO-1 mRNA (~1.6-fold increase at 10μM) and protein (~1.8-fold increase at 1μM); although these changes were not significant relative to the vehicle control (0.005% DMSO) which also upregulated HO-1 protein, but not mRNA (Chapter 6). Induction of HO-1 in HUVEC by low concentrations of DMSO has been described previously (Liang et al., 2011); and thus a confirmatory study was conducted to confirm the effect of vanillic acid, prepared in aqueous solution without vehicle, on HO-1 protein expression in cultured HCAEC (Figure 7.1 **(5)**). Here, a possible upregulation of HO-1 by vanillic acid was observed (~1.8-fold increase at 1μM), although this was not significant relative to PMA; and the response to cell treatments was variable between biological replicates in both HUVEC and HCAEC models (Chapter 6). Whilst limitations on time and available resources have precluded further investigation of these observations as part of the current thesis, the activity of vanillic acid on HO-1 expression could be further characterised in the HCAEC model. Such a study might incorporate an extended incubation period with PMA and include a time course experiment (for example protein levels at 0, 6, 12, 18, 24 hours) to establish the maximal response elicited by vanillic acid, or examine modulation of bilirubin production as a marker of HO-1 enzyme activity (Datla et al., 2007) and therefore potential NOX inhibition.

In summary, data presented in the current thesis suggest anthocyanin phenolic acid degradants might act to enhance vascular function by decreasing NOX-mediated endothelial superoxide production, and therefore reduce scavenging of the key vascular mediator NO *in vivo*; as opposed to direct stimulatory activity on eNOS described for parent anthocyanins. Vanillic acid, which contains a structural configuration previously associated with NOX inhibitory activity, could in theory elicit this effect by downregulating endothelial $p47^{phox}$ and/or upregulating HO-1. Although no statistically significant changes were observed in studies of these target proteins conducted using primary human vascular endothelial cells, immunoblotting data from HUVEC and HCAEC models suggest a possible induction of HO-1 expression by vanillic acid; which could potentially result in NOX inhibition and enhanced NO bioavailability, with beneficial effects on vascular regulation. However, the differential bioactivity observed for parent anthocyanins and their derivatives re-emphasises the need to conduct *in vitro* investigations of cellular activity using compounds likely to mediate *in vivo* bioactivity, and at physiologically relevant concentrations, in order to elucidate molecular mechanisms underlying cardioprotective activity associated with dietary anthocyanin intake (Jennings et al., 2012, Cassidy et al., 2013).

7.2 Future perspectives

Characterising the mechanisms by which anthocyanin derivatives *in vivo* may act to enhance vascular function is key to understanding reported vasoprotective effects of this sub-class of flavonoids, and therefore improvements in cardiovascular health associated with consumption of anthocyanin-rich dietary components. A major limitation of *in vitro* studies conducted using static cultures of endothelial cell monolayers is the absence of physiological fluid shear stress upon vascular cells, and concomitant effects on eNOS and NOX expression according to the type of stress applied (Boo and Jo, 2003, Hwang et al., 2003, Hsiai et al., 2007). Therefore the effect of anthocyanin degradants or metabolites on the activity of these important vascular enzymes should be investigated in endothelial cultures subjected to laminar or oscillatory shear stress, using equipment such as the ibidi Pump System[1] where cells can be cultured in flow chambers and subject to differential medium flow (for example unidirectional or oscillatory). Equally, effects of target compounds on vascular biomarkers could be examined in systems mimicking anatomical structure *in vivo* as a more representative model of the vascular endothelial environment, such as excised arterial rings (Bell and Gochenaur, 2006, Sanchez et al., 2006, Sanchez et al., 2007, Romero et al., 2009) or potentially co-culture models of endothelial and smooth muscle cells. The biomarkers to be targeted also require consideration, as prior *in vitro* investigations conducted using supraphysiological doses of parent anthocyanins may not necessarily reflect activity of *in vivo* derivatives (for example expression

[1] http://ibidi.com/xtproducts/en/Instruments-Accessories/Pump-Systems/ibidi-Pump-System; accessed 3rd July 2013.

and/or activation of eNOS); and therefore are unlikely to elucidate mechanisms underlying bioactivity *in vivo* mediated by anthocyanin degradation products and metabolites.

NOX2 represents an important putative target of anthocyanin bioactivity, given the reported inverse relationship between NOX2 and endothelial function (Violi et al., 2009, Loffredo et al., 2013), and previous studies of flavonoids targeting NOX activity (Steffen et al., 2007b, Sanchez et al., 2007, Steffen et al., 2008, Romero et al., 2009). However, and as described in the current thesis, low endothelial expression of NOX2 (Ago et al., 2004) may hinder assessment of treatment-induced modulations in mRNA and/or protein levels; although the effect of exposing endothelial cells to oscillatory shear stress (Leopold and Loscalzo, 2009) should be explored as noted above. Inhibition of NOX could be elicited by direct (for example reduced $p47^{phox}$ expression, activation, or translocation) or indirect (induction of HO-1) mechanisms; and modulation of HO-1 activity, relative to NOX function and ROS generation, should be investigated in a suitable endothelial cell model such as HCAEC, or if feasible excised human vascular tissue (for example from cardiovascular surgical procedures). As described in Chapter 1, HO-1 expression is regulated by the transcription factor Nrf2 (nuclear factor-erythroid 2-related factor 2) and nuclear localisation of Nrf2 in HUVEC, with increased expression of HO-1 mRNA, was enhanced by human serum derived from healthy subjects who had ingested 160mg purified anthocyanins (Cimino et al., 2013). Thus the effects of anthocyanin degradants and metabolites on both Nrf2 activity [possibly in a reporter gene assay system, for example (Kropat et al., 2013)], and endothelial expression of genes containing antioxidant response elements (AREs) in their promoter regions such as HO-1 and catalase (Pi et al., 2010), must be explored. Equally, given previous reports of inhibition of activity of the pro-inflammatory transcription factor NF-κB (nuclear factor kappa B) (Bremner and Heinrich, 2002) by anthocyanins (Karlsen et al., 2007, Haseeb et al., 2013), anthocyanin derivatives should also screened for modulation of NF-κB function and therefore transcription of regulated genes, such as NOX2 (Anrather et al., 2006) and NOX4 (Manea et al., 2010).

In addition to characterising bioactivity of anthocyanin degradants or metabolites at the cellular level, the activity of these compounds could be assessed in human intervention studies, to correlate identified mechanisms with effects on vascular function and ultimately disease outcomes. Several randomised controlled trials with anthocyanin supplements have described improved blood lipid profile (Qin et al., 2009, Zhu et al., 2011, Zhu et al., 2012, Hassellund et al., 2013), endothelial function (Zhu et al., 2011), and decreased levels of inflammatory cytokines (Zhu et al., 2012) compared to placebo; thus similar interventions could be performed using anthocyanin degradation products or metabolites, such as vanillic acid, as opposed to parent compounds. Vascular endothelial function, as determined by endothelial-dependent vasodilatation (Zhu et al., 2011, Riso et al., 2013, Del Bo et al., 2013, Rodriguez-Mateos et al., 2013), could be assessed as part of such an intervention,

in addition to measuring circulating levels of soluble NOX2 derived peptide (Pignatelli et al., 2009, Rodriguez-Mateos et al., 2013) as a marker of NOX2 activation (Loffredo et al., 2011).

In conclusion, this thesis has contributed to the current literature on the vascular biological activity of anthocyanins, by providing novel insights into potential mechanisms responsible for the vasoprotective activity of anthocyanin metabolites at physiologically relevant levels. However, further investigation of these mechanisms is required to explain fully the observed cardioprotective effects of anthocyanins in epidemiological and clinical studies. Increased dietary intake of anthocyanins, through consumption of grapes and berries or derived juices, could represent a simple measure to reduce the relative risk of cardiovascular disease (CVD); which is of particular relevance to public health as it is estimated that approximately 23.3 million people will die owing to CVD by 2030 (WHO, 2013).

8 Bibliography

ABRAHAM, N. G. & KAPPAS, A. 2008. Pharmacological and clinical aspects of heme oxygenase. *Pharmacol. Rev.,* 60**,** 79-127.

AFZAL-AHMED, I., MANN, G. E., SHENNAN, A. H., POSTON, L. & NAFTALIN, R. J. 2007. Preeclampsia inactivates glucose-6-phosphate dehydrogenase and impairs the redox status of erythrocytes and fetal endothelial cells. *Free Radic. Biol. Med.,* 42**,** 1781-90.

AGO, T., KITAZONO, T., OOBOSHI, H., IYAMA, T., HAN, Y. H., TAKADA, J., WAKISAKA, M., IBAYASHI, S., UTSUMI, H. & IIDA, M. 2004. Nox4 as the Major Catalytic Component of an Endothelial NAD(P)H Oxidase. *Circulation,* 109**,** 227-233.

AHERNE, S. A. & O'BRIEN, N. M. 2002. Dietary flavonols: chemistry, food content, and metabolism. *Nutrition,* 18**,** 75-81.

ALTENHOFER, S., KLEIKERS, P. W., RADERMACHER, K. A., SCHEURER, P., ROB HERMANS, J. J., SCHIFFERS, P., HO, H., WINGLER, K. & SCHMIDT, H. H. 2012. The NOX toolbox: validating the role of NADPH oxidases in physiology and disease. *Cell Mol. Life Sci.,* 69**,** 2327-43.

ALVAREZ, E., RODINO-JANEIRO, B. K., UCIEDA-SOMOZA, R. & GONZALEZ-JUANATEY, J. R. 2010. Pravastatin counteracts angiotensin II-induced upregulation and activation of NADPH oxidase at plasma membrane of human endothelial cells. *J Cardiovasc. Pharmacol.,* 55**,** 203-12.

ANDERSON, H. D., RAHMUTULA, D. & GARDNER, D. G. 2004. Tumor necrosis factor-alpha inhibits endothelial nitric-oxide synthase gene promoter activity in bovine aortic endothelial cells. *J Biol. Chem.,* 279**,** 963-9.

ANDRIAMBELOSON, E., KLESCHYOV, A. L., MULLER, B., BERETZ, A., STOCLET, J. C. & ANDRIANTSITOHAINA, R. 1997. Nitric oxide production and endothelium-dependent vasorelaxation induced by wine polyphenols in rat aorta. *Br. J Pharmacol.,* 120**,** 1053-8.

ANDRIAMBELOSON, E., MAGNIER, C., HAAN-ARCHIPOFF, G., LOBSTEIN, A., ANTON, R., BERETZ, A., STOCLET, J. C. & ANDRIANTSITOHAINA, R. 1998. Natural dietary polyphenolic compounds cause endothelium-dependent vasorelaxation in rat thoracic aorta. *J Nutr.,* 128**,** 2324-33.

ANILKUMAR, N., WEBER, R., ZHANG, M., BREWER, A. & SHAH, A. M. 2008. Nox4 and nox2 NADPH oxidases mediate distinct cellular redox signaling responses to agonist stimulation. *Arterioscler. Thromb. Vasc. Biol.,* 28**,** 1347-54.

ANRATHER, J., RACCHUMI, G. & IADECOLA, C. 2006. NF-κB Regulates Phagocytic NADPH Oxidase by Inducing the Expression of gp91phox. *J. Biol. Chem.,* 281**,** 5657-5667.

ARTS, I. C. & HOLLMAN, P. C. 2005. Polyphenols and disease risk in epidemiologic studies. *Am. J Clin. Nutr.,* 81**,** 317S-325S.

AZZINI, E., VITAGLIONE, P., INTORRE, F., NAPOLITANO, A., DURAZZO, A., FODDAI, M. S., FUMAGALLI, A., CATASTA, G., ROSSI, L., VENNERIA, E., RAGUZZINI, A., PALOMBA, L., FOGLIANO, V. &

MAIANI, G. 2010. Bioavailability of strawberry antioxidants in human subjects. *Br. J Nutr.,* 104**,** 1165-73.

BASU, A., RHONE, M. & LYONS, T. J. 2010. Berries: emerging impact on cardiovascular health. *Nutr. Rev.,* 68**,** 168-77.

BAUDIN, B., BRUNEEL, A., BOSSELUT, N. & VAUBOURDOLLE, M. 2007. A protocol for isolation and culture of human umbilical vein endothelial cells. *Nat. Protoc.,* 2**,** 481-5.

BEDARD, K. & KRAUSE, K. H. 2007. The NOX family of ROS-generating NADPH oxidases: physiology and pathophysiology. *Physiol. Rev.,* 87**,** 245-313.

BELL, D. R. & GOCHENAUR, K. 2006. Direct vasoactive and vasoprotective properties of anthocyanin-rich extracts. *J Appl. Physiol.,* 100**,** 1164-70.

BERRIDGE, M. V., TAN, A. S., MCCOY, K. D. & WANG, R. 1996. The Biochemical and Cellular Basis of Cell Proliferation Assays That Use Tetrazolium Salts. *Biochemica,* 4**,** 14-19.

BONOMINI, F., TENGATTINI, S., FABIANO, A., BIANCHI, R. & REZZANI, R. 2008. Atherosclerosis and oxidative stress. *Histol. Histopathol.,* 23**,** 381-90.

BOO, Y. C. & JO, H. 2003. Flow-dependent regulation of endothelial nitric oxide synthase: role of protein kinases. *Am. J Physiol. Cell Physiol.,* 285**,** C499-C508.

BRAND, W., SCHUTTE, M. E., WILLIAMSON, G., VAN ZANDEN, J. J., CNUBBEN, N. H., GROTEN, J. P., VAN BLADEREN, P. J. & RIETJENS, I. M. 2006. Flavonoid-mediated inhibition of intestinal ABC transporters may affect the oral bioavailability of drugs, food-borne toxic compounds and bioactive ingredients. *Biomed. Pharmacother.,* 60**,** 508-19.

BRANDES, R. P. & SCHRÖDER, K. 2008. Composition and Functions of Vascular Nicotinamide Adenine Dinucleotide Phosphate Oxidases. *Trends Cardiovasc. Med.,* 18**,** 15-19.

BRANDES, R. P., TAKAC, I. & SCHRODER, K. 2011. No Superoxide--No Stress?: Nox4, the Good NADPH Oxidase! *Arterioscler. Thromb. Vasc. Biol.,* 31**,** 1255-1257.

BRANDES, R. P., WEISSMANN, N. & SCHRODER, K. 2010. NADPH oxidases in cardiovascular disease. *Free Radic. Biol. Med.,* 49**,** 687-706.

BREMNER, P. & HEINRICH, M. 2002. Natural products as targeted modulators of the nuclear factor-kappaB pathway. *J Pharm. Pharmacol.,* 54**,** 453-72.

BRETON-ROMERO, R., DE ORDUNA, C. G., ROMERO, N., SANCHEZ, F. J., DE ALVARO, C., PORRAS, A., RODRIGUEZ-PASCUAL, F., LARANJINHA, J., RADI, R. & LAMAS, S. 2012. Critical role of hydrogen peroxide signaling in the sequential activation of p38 MAPK and eNOS in laminar shear stress. *Free Radic. Biol. Med.,* 52**,** 1093-100.

BREWER, A. C., MURRAY, T. V., ARNO, M., ZHANG, M., ANILKUMAR, N. P., MANN, G. E. & SHAH, A. M. 2011. Nox4 regulates Nrf2 and glutathione redox in cardiomyocytes in vivo. *Free Radic. Biol. Med.,* 51**,** 205-15.

BRONCEL, M., KOZIROG, M., DUCHNOWICZ, P., KOTER-MICHALAK, M., SIKORA, J. & CHOJNOWSKA-JEZIERSKA, J. 2010. Aronia melanocarpa extract reduces blood pressure, serum endothelin, lipid, and oxidative stress marker levels in patients with metabolic syndrome. *Med. Sci. Monit.,* 16**,** CR28-34.

BROSSETTE, T., HUNDSDORFER, C., KRONCKE, K. D., SIES, H. & STAHL, W. 2011. Direct evidence that (-)-epicatechin increases nitric oxide levels in human endothelial cells. *Eur. J Nutr.,* 50**,** 595-9.

BROWN, D. I. & GRIENDLING, K. K. 2009. Nox proteins in signal transduction. *Free Radic. Biol. Med.,* 47**,** 1239-53.

BUB, A., WATZL, B., HEEB, D., RECHKEMMER, G. & BRIVIBA, K. 2001. Malvidin-3-glucoside bioavailability in humans after ingestion of red wine, dealcoholized red wine and red grape juice. *Eur. J Nutr.,* 40**,** 113-20.

BUER, C. S., IMIN, N. & DJORDJEVIC, M. A. 2010. Flavonoids: new roles for old molecules. *J Integr. Plant. Biol.,* 52**,** 98-111.

BUSTIN, S. A., BENES, V., GARSON, J. A., HELLEMANS, J., HUGGETT, J., KUBISTA, M., MUELLER, R., NOLAN, T., PFAFFL, M. W., SHIPLEY, G. L., VANDESOMPELE, J. & WITTWER, C. T. 2009. The MIQE Guidelines: Minimum Information for Publication of Quantitative Real-Time PCR Experiments. *Clin. Chem.,* 55**,** 611-622.

CAI, H., GRIENDLING, K. K. & HARRISON, D. G. 2003. The vascular NAD(P)H oxidases as therapeutic targets in cardiovascular diseases. *Trends Pharmacol. Sci.,* 24**,** 471-8.

CAO, Y. G., ZHANG, L., MA, C., CHANG, B. B., CHEN, Y. C., TANG, Y. Q., LIU, X. D. & LIU, X. Q. 2009. Metabolism of protocatechuic acid influences fatty acid oxidation in rat heart: new anti-angina mechanism implication. *Biochem. Pharmacol.,* 77**,** 1096-104.

CARLUCCIO, M. A., ANCORA, M. A., MASSARO, M., CARLUCCIO, M., SCODITTI, E., DISTANTE, A., STORELLI, C. & DE CATERINA, R. 2007. Homocysteine induces VCAM-1 gene expression through NF-κB and NAD(P)H oxidase activation: protective role of Mediterranean diet polyphenolic antioxidants. *Am. J Physiol. Heart Circ. Physiol.,* 293**,** H2344-H2354.

CASSIDY, A., MUKAMAL, K. J., LIU, L., FRANZ, M., ELIASSEN, A. H. & RIMM, E. B. 2013. High anthocyanin intake is associated with a reduced risk of myocardial infarction in young and middle-aged women. *Circulation,* 127**,** 188-96.

CASSIDY, A., O'REILLY, E. J., KAY, C., SAMPSON, L., FRANZ, M., FORMAN, J., CURHAN, G. & RIMM, E. B. 2010. Habitual intake of flavonoid subclasses and incident hypertension in adults. *Am. J Clin. Nutr.,* 93**,** 338-47.

CHALOPIN, M., TESSE, A., MARTINEZ, M. C., ROGNAN, D., ARNAL, J. F. & ANDRIANTSITOHAINA, R. 2010. Estrogen receptor alpha as a key target of red wine polyphenols action on the endothelium. *PLoS One,* 5**,** e8554.

CHAN, K. H., NG, M. K. C. & STOCKER, R. 2011. Haem oxygenase-1 and cardiovascular disease: mechanisms and therapeutic potential. *Clin. Sci. (Lond),* 120**,** 493-504.

CHEN, C.-Y., YI, L., JIN, X., ZHANG, T., FU, Y.-J., ZHU, J.-D., MI, M.-T., ZHANG, Q.-Y., LING, W.-H. & YU, B. 2011a. Inhibitory Effect of Delphinidin on Monocyte–Endothelial Cell Adhesion Induced by Oxidized Low-Density Lipoprotein via ROS/p38MAPK/NF-κB Pathway. *Cell Biochem. Biophys.,* 61**,** 337-48.

CHEN, J., CHEN, W., ZHU, M., ZHU, Y., YIN, H. & TAN, Z. 2011b. Propofol attenuates angiotensin II-induced apoptosis in human coronary artery endothelial cells. *Br. J Anaesth.,* 107**,** 525-532.

CHEN, W.-L., QIAN, Y., MENG, W.-F., PANG, J.-Y., LIN, Y.-C., GUAN, Y.-Y., CHEN, S.-P., LIU, J., PEI, Z. & WANG, G.-L. 2009. A novel marine compound xyloketal B protects against oxidized LDL-induced cell injury in vitro. *Biochem. Pharmacol.,* 78**,** 941-950.

CHIRUMBOLO, S., MARZOTTO, M., CONFORTI, A., VELLA, A., ORTOLANI, R. & BELLAVITE, P. 2010. Bimodal action of the flavonoid quercetin on basophil function: an investigation of the putative biochemical targets. *Clin. Mol. Allergy,* 8**,** 13.

CHONG, M. F.-F., MACDONALD, R. & LOVEGROVE, J. A. 2010. Fruit polyphenols and CVD risk: a review of human intervention studies. *Br. J Nutr.,* 104**,** S28-S39.

CHUN, O. K., CHUNG, S. J. & SONG, W. O. 2007. Estimated dietary flavonoid intake and major food sources of U.S. adults. *J Nutr.,* 137**,** 1244-52.

CIMINO, F., SPECIALE, A., ANWAR, S., CANALI, R., RICCIARDI, E., VIRGILI, F., TROMBETTA, D. & SAIJA, A. 2013. Anthocyanins protect human endothelial cells from mild hyperoxia damage through modulation of Nrf2 pathway. *Genes Nutr.,* 8**,** 391-9.

CROZIER, A., JAGANATH, I. B. & CLIFFORD, M. N. 2009. Dietary phenolics: chemistry, bioavailability and effects on health. *Nat. Prod. Rep.,* 26**,** 1001-43.

CUCORANU, I., CLEMPUS, R., DIKALOVA, A., PHELAN, P. J., ARIYAN, S., DIKALOV, S. & SORESCU, D. 2005. NAD(P)H oxidase 4 mediates transforming growth factor-beta1-induced differentiation of cardiac fibroblasts into myofibroblasts. *Circ. Res.,* 97**,** 900-7.

CURTIS, P. J., KROON, P. A., HOLLANDS, W. J., WALLS, R., JENKINS, G., KAY, C. D. & CASSIDY, A. 2009. Cardiovascular disease risk biomarkers and liver and kidney function are not altered in postmenopausal women after ingesting an elderberry extract rich in anthocyanins for 12 weeks. *J Nutr.,* 139**,** 2266-71.

CZANK, C., CASSIDY, A., ZHANG, Q., MORRISON, D. J., PRESTON, T., KROON, P. A., BOTTING, N. P. & KAY, C. D. 2013. Human metabolism and elimination of the anthocyanin, cyanidin-3-glucoside: a ^{13}C-tracer study. *Am. J Clin. Nutr.,* 97**,** 995-1003.

DANDAPAT, A., HU, C., SUN, L. & MEHTA, J. L. 2007. Small Concentrations of oxLDL Induce Capillary Tube Formation From Endothelial Cells via LOX-1 Dependent Redox-Sensitive Pathway. *Arterioscler. Thromb. Vasc. Biol.,* 27**,** 2435-2442.

DATLA, S. R., DUSTING, G. J., MORI, T. A., TAYLOR, C. J., CROFT, K. D. & JIANG, F. 2007. Induction of Heme Oxygenase-1 In Vivo Suppresses NADPH Oxidase–Derived Oxidative Stress. *Hypertension,* 50**,** 636-642.

DAVALOS, A., DE LA PENA, G., SANCHEZ-MARTIN, C. C., TERESA GUERRA, M., BARTOLOME, B. & LASUNCION, M. A. 2009. Effects of red grape juice polyphenols in NADPH oxidase subunit expression in human neutrophils and mononuclear blood cells. *Br. J Nutr.,* 102**,** 1125-35.

DE PASCUAL-TERESA, S., MORENO, D. A. & GARCIA-VIGUERA, C. 2010. Flavanols and anthocyanins in cardiovascular health: a review of current evidence. *Int. J Mol. Sci.,* 11**,** 1679-703.

DEL BO, C., RISO, P., CAMPOLO, J., MOLLER, P., LOFT, S., KLIMIS-ZACAS, D., BRAMBILLA, A., RIZZOLO, A. & PORRINI, M. 2013. A single portion of blueberry (Vaccinium corymbosum L) improves protection against DNA damage but not vascular function in healthy male volunteers. *Nutr. Res.,* 33**,** 220-227.

DEL RIO, D., BORGES, G. & CROZIER, A. 2010. Berry flavonoids and phenolics: bioavailability and evidence of protective effects. *Br. J Nutr.,* 104**,** S67-S90.

DEL RIO, D., RODRIGUEZ-MATEOS, A., SPENCER, J. P., TOGNOLINI, M., BORGES, G. & CROZIER, A. 2013. Dietary (poly)phenolics in human health: structures, bioavailability, and evidence of protective effects against chronic diseases. *Antioxid. Redox Signal.,* 18**,** 1818-92.

DELL'AGLI, M., BUSCIALA, A. & BOSISIO, E. 2004. Vascular effects of wine polyphenols. *Cardiovasc. Res.,* 63**,** 593-602.

DENG, B., XIE, S., WANG, J., XIA, Z. & NIE, R. 2012. Inhibition of Protein Kinase C beta(2) Prevents Tumor Necrosis Factor-alpha-Induced Apoptosis and Oxidative Stress in Endothelial Cells: The Role of NADPH Oxidase Subunits. *J Vasc. Res.,* 49**,** 144-159.

DOMITROVIC, R. 2011. The molecular basis for the pharmacological activity of anthocyans. *Curr. Med. Chem.,* 18**,** 4454-69.

DONOVAN, E. L., MCCORD, J. M., REULAND, D. J., MILLER, B. F. & HAMILTON, K. L. 2012. Phytochemical activation of Nrf2 protects human coronary artery endothelial cells against an oxidative challenge. *Oxid. Med. Cell Longev.,* 2012**,** 132931.

DORAK, M. T. (ed.) 2006. *Real-Time PCR (Advanced Methods Series)*: Oxford: Taylor & Francis.

DRUMMOND, G. R., SELEMIDIS, S., GRIENDLING, K. K. & SOBEY, C. G. 2011. Combating oxidative stress in vascular disease: NADPH oxidases as therapeutic targets. *Nat. Rev. Drug Discov.,* 10**,** 453-71.

DZAU, V. J. 2001. Theodore Cooper Lecture: Tissue angiotensin and pathobiology of vascular disease: a unifying hypothesis. *Hypertension,* 37**,** 1047-52.

EDIRISINGHE, I., BANASZEWSKI, K., CAPPOZZO, J., MCCARTHY, D. & BURTON-FREEMAN, B. M. 2011. Effect of Black Currant Anthocyanins on the Activation of Endothelial Nitric Oxide Synthase (eNOS) in Vitro in Human Endothelial Cells. *J Agric. Food Chem.,* 59**,** 8616–8624.

EL-BENNA, J., DANG, P. M.-C. & PÉRIANIN, A. 2012. Towards specific NADPH oxidase inhibition by small synthetic peptides. *Cell. Mol. Life Sci.,* 69**,** 2307-14.

EL BENNA, J., FAUST, L. P. & BABIOR, B. M. 1994. The phosphorylation of the respiratory burst oxidase component p47phox during neutrophil activation. Phosphorylation of sites recognized by protein kinase C and by proline-directed kinases. *J Biol. Chem.,* 269**,** 23431-6.

ERDMAN, J. W., JR., BALENTINE, D., ARAB, L., BEECHER, G., DWYER, J. T., FOLTS, J., HARNLY, J., HOLLMAN, P., KEEN, C. L., MAZZA, G., MESSINA, M., SCALBERT, A., VITA, J., WILLIAMSON, G. & BURROWES, J. 2007. Flavonoids and heart health: proceedings of the ILSI North America Flavonoids Workshop, May 31-June 1, 2005, Washington, DC. *J Nutr.,* 137**,** 718S-737S.

ERDOGAN, D., GULLU, H., YILDIRIM, E., TOK, D., KIRBAS, I., CIFTCI, O., BAYCAN, S. T. & MUDERRISOGLU, H. 2006. Low serum bilirubin levels are independently and inversely related to impaired flow-mediated vasodilation and increased carotid intima-media thickness in both men and women. *Atherosclerosis,* 184**,** 431-437.

FARIA, A., PESTANA, D., AZEVEDO, J., MARTEL, F., DE FREITAS, V., AZEVEDO, I., MATEUS, N. & CALHAU, C. 2009. Absorption of anthocyanins through intestinal epithelial cells - Putative involvement of GLUT2. *Mol. Nutr. Food Res.,* 53**,** 1430-7.

FELICE, F., LUCCHESI, D., DI STEFANO, R., BARSOTTI, M. C., STORTI, E., PENNO, G., BALBARINI, A., DEL PRATO, S. & PUCCI, L. 2010. Oxidative stress in response to high glucose levels in endothelial cells and in endothelial progenitor cells: evidence for differential glutathione peroxidase-1 expression. *Microvasc. Res.,* 80**,** 332-8.

FENG, D., XIAOCHUN, Z., WOLD, L. E., QUN, R., ZHAOJIE, Z. & REN, J. 2005. Endothelin-1 enhances oxidative stress, cell proliferation and reduces apoptosis in human umbilical vein endothelial cells: role of ET_B receptor, NADPH oxidase and caveolin-1. *Br. J Pharmacol.,* 145**,** 323-333.

FITZPATRICK, D. F., HIRSCHFIELD, S. L. & COFFEY, R. G. 1993. Endothelium-dependent vasorelaxing activity of wine and other grape products. *Am. J Physiol.,* 265**,** H774-8.

FLEMING, I. & BUSSE, R. 2003. Molecular mechanisms involved in the regulation of the endothelial nitric oxide synthase. *Am. J Physiol. Regul. Integr. Comp. Physiol.,* 284**,** R1-12.

FLESCHHUT, J., KRATZER, F., RECHKEMMER, G. & KULLING, S. E. 2006. Stability and biotransformation of various dietary anthocyanins in vitro. *Eur. J Nutr.,* 45**,** 7-18.

FORESTER, S. C. & WATERHOUSE, A. L. 2008. Identification of Cabernet Sauvignon anthocyanin gut microflora metabolites. *J Agric. Food Chem.,* 56**,** 9299-304.

FORMAN, H. J., TORRES, M. & FUKUTO, J. 2002. Redox signaling. *Mol. Cell Biochem.,* 234-235**,** 49-62.

FÖRSTERMANN, U. 2010. Nitric oxide and oxidative stress in vascular disease. *Pflügers Arch.,* 459**,** 923-939.

FÖRSTERMANN, U. & SESSA, W. C. 2012. Nitric oxide synthases: regulation and function. *Eur. Heart J,* 33**,** 829-837.

FORTUÑO, A., BIDEGAIN, J., ROBADOR, P. A., HERMIDA, J., LÓPEZ-SAGASETA, J., BELOQUI, O., DÍEZ, J. & ZALBA, G. 2009. Losartan Metabolite EXP3179 Blocks NADPH Oxidase-Mediated Superoxide Production by Inhibiting Protein Kinase C. *Hypertension,* 54**,** 744-750.

FREY, R. S., RAHMAN, A., KEFER, J. C., MINSHALL, R. D. & MALIK, A. B. 2002. PKCzeta regulates TNF-alpha-induced activation of NADPH oxidase in endothelial cells. *Circ. Res.,* 90**,** 1012-9.

GALLEANO, M., VERSTRAETEN, S. V., OTEIZA, P. I. & FRAGA, C. G. 2010. Antioxidant actions of flavonoids: thermodynamic and kinetic analysis. *Arch. Biochem. Biophys.,* 501**,** 23-30.

GAZIANO, J. M., BURING, J. E., BRESLOW, J. L., GOLDHABER, S. Z., ROSNER, B., VANDENBURGH, M., WILLETT, W. & HENNEKENS, C. H. 1993. Moderate alcohol intake, increased levels of high-density lipoprotein and its subfractions, and decreased risk of myocardial infarction. *N. Engl. J Med.,* 329**,** 1829-34.

GELEIJNSE, J. M. & HOLLMAN, P. 2008. Flavonoids and cardiovascular health: which compounds, what mechanisms? *Am. J Clin. Nutr.,* 88**,** 12-3.

GELEIJNSE, J. M., LAUNER, L. J., VAN DER KUIP, D. A., HOFMAN, A. & WITTEMAN, J. C. 2002. Inverse association of tea and flavonoid intakes with incident myocardial infarction: the Rotterdam Study. *Am. J Clin. Nutr.,* 75**,** 880-6.

GIORDANO, L., COLETTA, W., TAMBURRELLI, C., D'IMPERIO, M., CRESCENTE, M., SILVESTRI, C., RAPISARDA, P., REFORGIATO RECUPERO, G., DE CURTIS, A., IACOVIELLO, L., DE GAETANO, G., ROTILIO, D., CERLETTI, C. & DONATI, M. B. 2012. Four-week ingestion of blood orange juice results in measurable anthocyanin urinary levels but does not affect cellular markers related to cardiovascular risk: a randomized cross-over study in healthy volunteers. *Eur. J Nutr.,* 51**,** 541-8.

GONZALEZ-BARRIO, R., BORGES, G., MULLEN, W. & CROZIER, A. 2010. Bioavailability of anthocyanins and ellagitannins following consumption of raspberries by healthy humans and subjects with an ileostomy. *J Agric. Food Chem.,* 58**,** 3933-9.

GONZÁLEZ-GALLEGO, J., GARCÍA-MEDIAVILLA, M. V., SÁNCHEZ-CAMPOS, S. & TUÑÓN, M. J. 2010. Fruit polyphenols, immunity and inflammation. *Br. J Nutr.,* 104**,** S15-S27.

GÖRLACH, A., BRANDES, R. P., NGUYEN, K., AMIDI, M., DEHGHANI, F. & BUSSE, R. 2000. A gp91phox Containing NADPH Oxidase Selectively Expressed in Endothelial Cells Is a Major Source of Oxygen Radical Generation in the Arterial Wall. *Circ. Res.,* 87**,** 26-32.

GRANGER, D. L., TAINTOR, R. R., BOOCKVAR, K. S. & HIBBS, J. B., JR. 1996. Measurement of nitrate and nitrite in biological samples using nitrate reductase and Griess reaction. *Methods Enzymol.,* 268**,** 142-51.

GRANGER, D. N., VOWINKEL, T. & PETNEHAZY, T. 2004. Modulation of the inflammatory response in cardiovascular disease. *Hypertension,* 43**,** 924-31.

GRASSI, D., DESIDERI, G., CROCE, G., TIBERTI, S., AGGIO, A. & FERRI, C. 2009. Flavonoids, vascular function and cardiovascular protection. *Curr. Pharm. Des.,* 15**,** 1072-84.

GUZIK, T. J., CHEN, W., GONGORA, M. C., GUZIK, B., LOB, H. E., MANGALAT, D., HOCH, N., DIKALOV, S., RUDZINSKI, P., KAPELAK, B., SADOWSKI, J. & HARRISON, D. G. 2008. Calcium-dependent NOX5 nicotinamide adenine dinucleotide phosphate oxidase contributes to vascular oxidative stress in human coronary artery disease. *J Am. Coll. Cardiol.,* 52**,** 1803-9.

GUZIK, T. J., SADOWSKI, J., GUZIK, B., JOPEK, A., KAPELAK, B., PRZYBYŁOWSKI, P., WIERZBICKI, K., KORBUT, R., HARRISON, D. G. & CHANNON, K. M. 2006. Coronary Artery Superoxide Production and Nox Isoform Expression in Human Coronary Artery Disease. *Arterioscler. Thromb. Vasc. Biol.,* 26**,** 333-339.

HALLIWELL, B. 2007. Dietary polyphenols: good, bad, or indifferent for your health? *Cardiovasc. Res.,* 73**,** 341-7.

HALLIWELL, B., RAFTER, J. & JENNER, A. 2005. Health promotion by flavonoids, tocopherols, tocotrienols, and other phenols: direct or indirect effects? Antioxidant or not? *Am. J Clin. Nutr.,* 81**,** 268S-276S.

HASEEB, A., CHEN, D. & HAQQI, T. M. 2013. Delphinidin inhibits IL-1beta-induced activation of NF-kappaB by modulating the phosphorylation of IRAK-1Ser376 in human articular chondrocytes. *Rheumatology (Oxford),* 52**,** 998-1008.

HASSELLUND, S. S., FLAA, A., KJELDSEN, S. E., SELJEFLOT, I., KARLSEN, A., ERLUND, I. & ROSTRUP, M. 2013. Effects of anthocyanins on cardiovascular risk factors and inflammation in pre-hypertensive men: a double-blind randomized placebo-controlled crossover study. *J Hum. Hypertens.,* 27**,** 100-6.

HASSELLUND, S. S., FLAA, A., SANDVIK, L., KJELDSEN, S. E. & ROSTRUP, M. 2012. Effects of anthocyanins on blood pressure and stress reactivity: a double-blind randomized placebo-controlled crossover study. *J Hum. Hypertens.,* 26**,** 396-404.

HE, M., SIOW, R. C., SUGDEN, D., GAO, L., CHENG, X. & MANN, G. E. 2010. Induction of HO-1 and redox signaling in endothelial cells by advanced glycation end products: A role for Nrf2 in vascular protection in diabetes. *Nutr. Metab. Cardiovasc. Dis.,* 21**,** 277-85.

HEINLOTH, A., HEERMEIER, K., RAFF, U., WANNER, C. & GALLE, J. 2000. Stimulation of NADPH oxidase by oxidized low-density lipoprotein induces proliferation of human vascular endothelial cells. *J Am. Soc. Nephrol.,* 11**,** 1819-25.

HERTOG, M. G., FESKENS, E. J., HOLLMAN, P. C., KATAN, M. B. & KROMHOUT, D. 1993. Dietary antioxidant flavonoids and risk of coronary heart disease: the Zutphen Elderly Study. *Lancet,* 342**,** 1007-11.

HEYWORTH, P. G., CURNUTTE, J. T., NAUSEEF, W. M., VOLPP, B. D., PEARSON, D. W., ROSEN, H. & CLARK, R. A. 1991. Neutrophil nicotinamide adenine dinucleotide phosphate oxidase

assembly. Translocation of p47-phox and p67-phox requires interaction between p47-phox and cytochrome b558. *J Clin. Invest.,* 87**,** 352-6.

HIDALGO, M., MARTIN-SANTAMARIA, S., RECIO, I., SANCHEZ-MORENO, C., DE PASCUAL-TERESA, B., RIMBACH, G. & DE PASCUAL-TERESA, S. 2012. Potential anti-inflammatory, anti-adhesive, anti/estrogenic, and angiotensin-converting enzyme inhibitory activities of anthocyanins and their gut metabolites. *Genes Nutr.,* 7**,** 295-306.

HIGASHI, Y., NOMA, K., YOSHIZUMI, M. & KIHARA, Y. 2009. Endothelial function and oxidative stress in cardiovascular diseases. *Circ. J,* 73**,** 411-8.

HOBBS, A. J., HIGGS, A. & MONCADA, S. 1999. Inhibition of nitric oxide synthase as a potential therapeutic target. *Annu. Rev. Pharmacol. Toxicol.,* 39**,** 191-220.

HOLLMAN, P. C., CASSIDY, A., COMTE, B., HEINONEN, M., RICHELLE, M., RICHLING, E., SERAFINI, M., SCALBERT, A., SIES, H. & VIDRY, S. 2011. The biological relevance of direct antioxidant effects of polyphenols for cardiovascular health in humans is not established. *J Nutr.,* 141**,** 989S-1009S.

HOOPER, L., KROON, P. A., RIMM, E. B., COHN, J. S., HARVEY, I., LE CORNU, K. A., RYDER, J. J., HALL, W. L. & CASSIDY, A. 2008. Flavonoids, flavonoid-rich foods, and cardiovascular risk: a meta-analysis of randomized controlled trials. *Am. J Clin. Nutr.,* 88**,** 38-50.

HSIAI, T. K., HWANG, J., BARR, M. L., CORREA, A., HAMILTON, R., ALAVI, M., ROUHANIZADEH, M., CADENAS, E. & HAZEN, S. L. 2007. Hemodynamics influences vascular peroxynitrite formation: Implication for low-density lipoprotein apo-B-100 nitration. *Free Radic. Biol. Med.,* 42**,** 519-529.

HU, T., RAMACHANDRARAO, S. P., SIVA, S., VALANCIUS, C., ZHU, Y., MAHADEV, K., TOH, I., GOLDSTEIN, B. J., WOOLKALIS, M. & SHARMA, K. 2005. Reactive oxygen species production via NADPH oxidase mediates TGF-β-induced cytoskeletal alterations in endothelial cells. *Am. J Physiol. Renal Physiol.,* 289**,** F816-F825.

HUXLEY, R. R. & NEIL, H. A. 2003. The relation between dietary flavonol intake and coronary heart disease mortality: a meta-analysis of prospective cohort studies. *Eur. J Clin. Nutr.,* 57**,** 904-8.

HWANG, J., ING, M. H., SALAZAR, A., LASSÈGUE, B., GRIENDLING, K., NAVAB, M., SEVANIAN, A. & HSIAI, T. K. 2003. Pulsatile Versus Oscillatory Shear Stress Regulates NADPH Oxidase Subunit Expression: Implication for Native LDL Oxidation. *Circ. Res.,* 93**,** 1225-1232.

HWANG, Y. P., CHOI, J. H., YUN, H. J., HAN, E. H., KIM, H. G., KIM, J. Y., PARK, B. H., KHANAL, T., CHOI, J. M., CHUNG, Y. C. & JEONG, H. G. 2011. Anthocyanins from purple sweet potato attenuate dimethylnitrosamine-induced liver injury in rats by inducing Nrf2-mediated antioxidant enzymes and reducing COX-2 and iNOS expression. *Food Chem. Toxicol.,* 49**,** 93-99.

IDRISS, N. K., BLANN, A. D. & LIP, G. Y. H. 2008. Hemoxygenase-1 in Cardiovascular Disease. *J Am. Coll. Cardiol.,* 52**,** 971-978.

INOUE, H., MAEDA-YAMAMOTO, M., NESUMI, A. & MURAKAMI, A. 2012. Delphinidin-3-O-galactoside protects mouse hepatocytes from (-)-epigallocatechin-3-gallate-induced cytotoxicity via up-regulation of heme oxygenase-1 and heat shock protein 70. *Nutr. Res.,* 32**,** 357-64.

JENNINGS, A., WELCH, A. A., FAIRWEATHER-TAIT, S. J., KAY, C., MINIHANE, A. M., CHOWIENCZYK, P., JIANG, B., CECELJA, M., SPECTOR, T., MACGREGOR, A. & CASSIDY, A. 2012. Higher anthocyanin intake is associated with lower arterial stiffness and central blood pressure in women. *Am. J Clin. Nutr.,* 96**,** 781-8.

JEON, J., LEE, J., KIM, C., AN, Y. & CHOI, C. 2010. Aqueous extract of the medicinal plant Patrinia villosa Juss. Induces angiogenesis via activation of focal adhesion kinase. *Microvasc. Res.,* 80**,** 303-9.

JIANG, F., ROBERTS, S. J., DATLA, S. & DUSTING, G. J. 2006. NO modulates NADPH oxidase function via heme oxygenase-1 in human endothelial cells. *Hypertension,* 48**,** 950-7.

JIN, Y., ALIMBETOV, D., GEORGE, T., GORDON, M. H. & LOVEGROVE, J. A. 2011. A randomised trial to investigate the effects of acute consumption of a blackcurrant juice drink on markers of vascular reactivity and bioavailability of anthocyanins in human subjects. *Eur. J Clin. Nutr.,* 65**,** 849-56.

JONES, S. A., O'DONNELL, V. B., WOOD, J. D., BROUGHTON, J. P., HUGHES, E. J. & JONES, O. T. 1996. Expression of phagocyte NADPH oxidase components in human endothelial cells. *Am. J Physiol. Heart Circ. Physiol.,* 271**,** H1626-H1634.

KAGA, S., ZHAN, L., MATSUMOTO, M. & MAULIK, N. 2005. Resveratrol enhances neovascularization in the infarcted rat myocardium through the induction of thioredoxin-1, heme oxygenase-1 and vascular endothelial growth factor. *J Mol. Cell. Cardiol.,* 39**,** 813-822.

KAMIYAMA, M., KISHIMOTO, Y., TANI, M., UTSUNOMIYA, K. & KONDO, K. 2009. Effects of equol on oxidized low-density lipoprotein-induced apoptosis in endothelial cells. *J Atheroscler. Thromb.,* 16**,** 239-49.

KAMIZATO, M., NISHIDA, K., MASUDA, K., TAKEO, K., YAMAMOTO, Y., KAWAI, T., TESHIMA-KONDO, S., TANAHASHI, T. & ROKUTAN, K. 2009. Interleukin 10 inhibits interferon gamma- and tumor necrosis factor alpha-stimulated activation of NADPH oxidase 1 in human colonic epithelial cells and the mouse colon. *J Gastroenterol.,* 44**,** 1172-84.

KARLSEN, A., RETTERSTØL, L., LAAKE, P., PAUR, I., KJØLSRUD-BØHN, S., SANDVIK, L. & BLOMHOFF, R. 2007. Anthocyanins Inhibit Nuclear Factor-κB Activation in Monocytes and Reduce Plasma Concentrations of Pro-Inflammatory Mediators in Healthy Adults. *J Nutr.,* 137**,** 1951-1954.

KAUR, J., DHAUNSI, G. S. & TURNER, R. B. 2004. Interleukin-1 and nitric oxide increase NADPH oxidase activity in human coronary artery smooth muscle cells. *Med. Princ. Pract.,* 13**,** 26-9.

KAWAMURA, K., ISHIKAWA, K., WADA, Y., KIMURA, S., MATSUMOTO, H., KOHRO, T., ITABE, H., KODAMA, T. & MARUYAMA, Y. 2005. Bilirubin From Heme Oxygenase-1 Attenuates Vascular Endothelial Activation and Dysfunction. *Arterioscler. Thromb. Vasc. Biol.,* 25**,** 155-160.

KAWASHIMA, S. & YOKOYAMA, M. 2004. Dysfunction of endothelial nitric oxide synthase and atherosclerosis. *Arterioscler. Thromb. Vasc. Biol.,* 24**,** 998-1005.

KAY, C. D. 2006. Aspects of anthocyanin absorption, metabolism and pharmacokinetics in humans. *Nutr. Res. Rev.,* 19**,** 137-46.

KAY, C. D., HOOPER, L., KROON, P. A., RIMM, E. B. & CASSIDY, A. 2012. Relative impact of flavonoid composition, dose and structure on vascular function: A systematic review of randomised controlled trials of flavonoid-rich food products. *Mol. Nutr. Food Res.,* 56**,** 1605-16.

KAY, C. D., KROON, P. A. & CASSIDY, A. 2009. The bioactivity of dietary anthocyanins is likely to be mediated by their degradation products. *Mol. Nutr. Food Res.,* 53 Suppl 1**,** S92-101.

KAY, C. D., MAZZA, G., HOLUB, B. J. & WANG, J. 2004. Anthocyanin metabolites in human urine and serum. *Br. J Nutr.,* 91**,** 933-42.

KAY, C. D., MAZZA, G. J. & HOLUB, B. J. 2005. Anthocyanins exist in the circulation primarily as metabolites in adult men. *J Nutr.,* 135**,** 2582-8.

KEPPLER, K. & HUMPF, H. U. 2005. Metabolism of anthocyanins and their phenolic degradation products by the intestinal microflora. *Bioorg. Med. Chem.,* 13**,** 5195-205.

KHOO, N. K. H., RUDOLPH, V., COLE, M. P., GOLIN-BISELLO, F., SCHOPFER, F. J., WOODCOCK, S. R., BATTHYANY, C. & FREEMAN, B. A. 2010. Activation of vascular endothelial nitric oxide synthase and heme oxygenase-1 expression by electrophilic nitro-fatty acids. *Free Radic. Biol. Med.,* 48**,** 230-239.

KIM, H. K., CHOI, Y. W., LEE, E. N., PARK, J. K., KIM, S. G., PARK, D. J., KIM, B. S., LIM, Y. T. & YOON, S. 2011. 5-Hydroxymethylfurfural from Black Garlic Extract Prevents TNFalpha-induced Monocytic Cell Adhesion to HUVECs by Suppression of Vascular Cell Adhesion Molecule-1 Expression, Reactive Oxygen Species Generation and NF-kappaB Activation. *Phytother. Res.,* 25**,** 965-74.

KONG, J. M., CHIA, L. S., GOH, N. K., CHIA, T. F. & BROUILLARD, R. 2003. Analysis and biological activities of anthocyanins. *Phytochemistry,* 64**,** 923-33.

KROPAT, C., MUELLER, D., BOETTLER, U., ZIMMERMANN, K., HEISS, E. H., DIRSCH, V. M., ROGOLL, D., MELCHER, R., RICHLING, E. & MARKO, D. 2013. Modulation of Nrf2-dependent gene transcription by bilberry anthocyanins in vivo. *Mol. Nutr. Food Res.,* 57**,** 545-550.

KUWANO, Y., KAWAHARA, T., YAMAMOTO, H., TESHIMA-KONDO, S., TOMINAGA, K., MASUDA, K., KISHI, K., MORITA, K. & ROKUTAN, K. 2006. Interferon-gamma activates transcription of NADPH oxidase 1 gene and upregulates production of superoxide anion by human large intestinal epithelial cells. *Am. J Physiol. Cell Physiol.,* 290**,** C433-43.

LANDBERG, R., NAIDOO, N. & VAN DAM, R. M. 2012. Diet and endothelial function: from individual components to dietary patterns. *Curr. Opin. Lipidol.,* 23**,** 147-55.

LANDMESSER, U., HORNIG, B. & DREXLER, H. 2004. Endothelial function: a critical determinant in atherosclerosis? *Circulation,* 109**,** II27-33.

LASSEGUE, B. & CLEMPUS, R. E. 2003. Vascular NAD(P)H oxidases: specific features, expression, and regulation. *Am. J Physiol. Regul. Integr. Comp. Physiol.,* 285**,** R277-97.

LASSEGUE, B. & GRIENDLING, K. K. 2010. NADPH oxidases: functions and pathologies in the vasculature. *Arterioscler. Thromb. Vasc. Biol.,* 30**,** 653-61.

LAZZE, M. C., PIZZALA, R., PERUCCA, P., CAZZALINI, O., SAVIO, M., FORTI, L., VANNINI, V. & BIANCHI, L. 2006. Anthocyanidins decrease endothelin-1 production and increase endothelial nitric oxide synthase in human endothelial cells. *Mol. Nutr. Food Res.,* 50**,** 44-51.

LEE, S. E., JEONG, S. I., YANG, H., PARK, C.-S., JIN, Y.-H. & PARK, Y. S. 2011. Fisetin induces Nrf2-mediated HO-1 expression through PKC-δ and p38 in human umbilical vein endothelial cells. *J Cell. Biochem.,* 112**,** 2352-2360.

LEOPOLD, J. A. & LOSCALZO, J. 2009. Oxidative risk for atherothrombotic cardiovascular disease. *Free Radic. Biol. Med.,* 47**,** 1673-706.

LEVERENCE, J. T., MEDHORA, M., KONDURI, G. G. & SAMPATH, V. 2011. Lipopolysaccharide-induced cytokine expression in alveolar epithelial cells: Role of PKCζ-mediated p47phox phosphorylation. *Chem. Biol. Interact.,* 189**,** 72-81.

LEVINE, M., RUMSEY, S. C., DARUWALA, R., PARK, J. B. & WANG, Y. 1999. Criteria and recommendations for vitamin C intake. *JAMA,* 281**,** 1415-23.

LI, J. M., FAN, L. M., CHRISTIE, M. R. & SHAH, A. M. 2005. Acute tumor necrosis factor alpha signaling via NADPH oxidase in microvascular endothelial cells: role of p47phox phosphorylation and binding to TRAF4. *Mol. Cell Biol.,* 25**,** 2320-30.

LI, J. M., MULLEN, A. M., YUN, S., WIENTJES, F., BROUNS, G. Y., THRASHER, A. J. & SHAH, A. M. 2002. Essential role of the NADPH oxidase subunit p47(phox) in endothelial cell superoxide production in response to phorbol ester and tumor necrosis factor-alpha. *Circ. Res.,* 90**,** 143-50.

LI, P., JIANG, H., YANG, L., QUAN, S., DINOCCA, S., RODRIGUEZ, F., ABRAHAM, N. G. & NASJLETTI, A. 2004. Angiotensin II induces carbon monoxide production in the perfused kidney: relationship to protein kinase C activation. *Am. J Physiol. Renal Physiol.,* 287**,** F914-F920.

LIANG, C., XUE, Z., CANG, J., WANG, H. & LI, P. 2011. Dimethyl sulfoxide induces heme oxygenase-1 expression via JNKs and Nrf2 pathways in human umbilical vein endothelial cells. *Mol. Cell Biochem.,* 355**,** 109-15.

LIBBY, P., RIDKER, P. M. & MASERI, A. 2002. Inflammation and atherosclerosis. *Circulation,* 105**,** 1135-43.

LIM, T.-G., JUNG, S. K., KIM, J.-E., KIM, Y., LEE, H. J., JANG, T. S. & LEE, K. W. 2013. NADPH oxidase is a novel target of delphinidin for the inhibition of UVB-induced MMP-1 expression in human dermal fibroblasts. *Exp. Dermatol.,* 22**,** 428-430.

LO, Y. Y., CONQUER, J. A., GRINSTEIN, S. & CRUZ, T. F. 1998. Interleukin-1 beta induction of c-fos and collagenase expression in articular chondrocytes: involvement of reactive oxygen species. *J Cell Biochem.,* 69**,** 19-29.

LOFFREDO, L., CARNEVALE, R., CANGEMI, R., ANGELICO, F., AUGELLETTI, T., DI SANTO, S., CALABRESE, C. M., DELLA VOLPE, L., PIGNATELLI, P., PERRI, L., BASILI, S. & VIOLI, F. 2013. NOX2 up-regulation is associated with artery dysfunction in patients with peripheral artery disease. *Int. J Cardiol.,* 165**,** 184-192.

LOFFREDO, L., CARNEVALE, R., PERRI, L., CATASCA, E., AUGELLETTI, T., CANGEMI, R., ALBANESE, F., PICCHERI, C., NOCELLA, C., PIGNATELLI, P. & VIOLI, F. 2011. NOX2-mediated artery dysfunction in smokers: acute effect of dark chocolate. *Heart,* 97**,** 1776-81.

MACARTHUR, P. H., SHIVA, S. & GLADWIN, M. T. 2007. Measurement of circulating nitrite and S-nitrosothiols by reductive chemiluminescence. *J Chromatogr. B Analyt. Technol. Biomed. Life Sci.,* 851**,** 93-105.

MAGHZAL, G., KRAUSE, K.-H., STOCKER, R. & JAQUET, V. 2012. Detection of reactive oxygen species derived from the family of NOX NADPH oxidases. *Free Radic. Biol. Med.,* 53**,** 1903-1918.

MAHADEV, K., MOTOSHIMA, H., WU, X., RUDDY, J. M., ARNOLD, R. S., CHENG, G., LAMBETH, J. D. & GOLDSTEIN, B. J. 2004. The NAD(P)H oxidase homolog Nox4 modulates insulin-stimulated generation of H2O2 and plays an integral role in insulin signal transduction. *Mol. Cell Biol.,* 24**,** 1844-54.

MAHER, J. & YAMAMOTO, M. 2010. The rise of antioxidant signaling--the evolution and hormetic actions of Nrf2. *Toxicol Appl Pharmacol,* 244**,** 4-15.

MANACH, C., WILLIAMSON, G., MORAND, C., SCALBERT, A. & REMESY, C. 2005. Bioavailability and bioefficacy of polyphenols in humans. I. Review of 97 bioavailability studies. *Am. J Clin. Nutr.,* 81**,** 230S-242S.

MANEA, A., TANASE, L. I., RAICU, M. & SIMIONESCU, M. 2010. Transcriptional regulation of NADPH oxidase isoforms, Nox1 and Nox4, by nuclear factor-κB in human aortic smooth muscle cells. *Biochem. Biophys. Res. Commun.,* 396**,** 901-907.

MASSARO, M., HABIB, A., LUBRANO, L., TURCO, S. D., LAZZERINI, G., BOURCIER, T., WEKSLER, B. B. & DE CATERINA, R. 2006. The omega-3 fatty acid docosahexaenoate attenuates endothelial cyclooxygenase-2 induction through both NADP(H) oxidase and PKCε inhibition. *Proc. Natl. Acad. Sci. U S A. ,* 103**,** 15184-15189.

MATSUMOTO, H., INABA, H., KISHI, M., TOMINAGA, S., HIRAYAMA, M. & TSUDA, T. 2001. Orally administered delphinidin 3-rutinoside and cyanidin 3-rutinoside are directly absorbed in rats and humans and appear in the blood as the intact forms. *J Agric. Food Chem.,* 49**,** 1546-51.

MAZZA, G., KAY, C. D., COTTRELL, T. & HOLUB, B. J. 2002. Absorption of anthocyanins from blueberries and serum antioxidant status in human subjects. *J Agric. Food Chem.,* 50**,** 7731-7.

MAZZA, G. J. 2007. Anthocyanins and heart health. *Ann Ist Super Sanita,* 43**,** 369-74.

MCCULLOUGH, M. L., PETERSON, J. J., PATEL, R., JACQUES, P. F., SHAH, R. & DWYER, J. T. 2012. Flavonoid intake and cardiovascular disease mortality in a prospective cohort of US adults. *Am. J Clin. Nutr.,* 95**,** 454-64.

MCGHIE, T. K. & WALTON, M. C. 2007. The bioavailability and absorption of anthocyanins: towards a better understanding. *Mol. Nutr. Food Res.,* 51**,** 702-13.

MCNALLY, J. S., DAVIS, M. E., GIDDENS, D. P., SAHA, A., HWANG, J., DIKALOV, S., JO, H. & HARRISON, D. G. 2003. Role of xanthine oxidoreductase and NAD(P)H oxidase in endothelial superoxide production in response to oscillatory shear stress. *Am. J Physiol. Heart Circ. Physiol.,* 285**,** H2290-7.

MEYER, M. C., KELL, P. J., CREER, M. H. & MCHOWAT, J. 2005. Calcium-independent phospholipase A2 is regulated by a novel protein kinase C in human coronary artery endothelial cells. *Am. J Physiol. Cell Physiol.,* 288**,** C475-C482.

MICHEL, T. & VANHOUTTE, P. M. 2010. Cellular signaling and NO production. *Pflugers Arch.,* 459**,** 807-16.

MILBURY, P. E., CAO, G., PRIOR, R. L. & BLUMBERG, J. 2002. Bioavailablility of elderberry anthocyanins. *Mech. Ageing Dev.,* 123**,** 997-1006.

MILBURY, P. E., VITA, J. A. & BLUMBERG, J. B. 2010. Anthocyanins are bioavailable in humans following an acute dose of cranberry juice. *J Nutr.,* 140**,** 1099-104.

MINK, P. J., SCRAFFORD, C. G., BARRAJ, L. M., HARNACK, L., HONG, C. P., NETTLETON, J. A. & JACOBS, D. R., JR. 2007. Flavonoid intake and cardiovascular disease mortality: a prospective study in postmenopausal women. *Am. J Clin. Nutr.,* 85**,** 895-909.

MONTEZANO, A. C., BURGER, D., CERAVOLO, G. S., YUSUF, H., MONTERO, M. & TOUYZ, R. M. 2011. Novel Nox homologues in the vasculature: focusing on Nox4 and Nox5. *Clin. Sci. (Lond),* 120**,** 131-41.

MUNDEL, T. M., YLINIEMI, A. M., MAESHIMA, Y., SUGIMOTO, H., KIERAN, M. & KALLURI, R. 2008. Type IV collagen alpha6 chain-derived noncollagenous domain 1 (alpha6(IV)NC1) inhibits angiogenesis and tumor growth. *Int. J Cancer,* 122**,** 1738-44.

MUNOZ, R., ARIAS, Y., FERRERAS, J. M., JIMENEZ, P., ROJO, M. A. & GIRBES, T. 2001. Sensitivity of cancer cell lines to the novel non-toxic type 2 ribosome-inactivating protein nigrin b. *Cancer Lett.,* 167**,** 163-9.

MUNOZ, R., ARIAS, Y., FERRERAS, J. M., ROJO, M. A., GAYOSO, M. J., NOCITO, M., BENITEZ, J., JIMENEZ, P., BERNABEU, C. & GIRBES, T. 2007. Targeting a marker of the tumour neovasculature using a novel anti-human CD105-immunotoxin containing the non-toxic type 2 ribosome-inactivating protein nigrin b. *Cancer Lett.,* 256**,** 73-80.

MUZAFFAR, S., SHUKLA, N., ANGELINI, G. & JEREMY, J. Y. 2004. Nitroaspirins and morpholinosydnonimine but not aspirin inhibit the formation of superoxide and the expression of gp91phox induced by endotoxin and cytokines in pig pulmonary artery vascular smooth muscle cells and endothelial cells. *Circulation,* 110**,** 1140-7.

NASEEM, K. M. 2005. The role of nitric oxide in cardiovascular diseases. *Mol. Aspects Med.,* 26**,** 33-65.

NAUSEEF, W. M. 2013. Detection of superoxide anion and hydrogen peroxide production by cellular NADPH oxidases. *Biochim. Biophys. Acta,* In press.

NEVEU, V., PEREZ-JIMÉNEZ, J., VOS, F., CRESPY, V., DU CHAFFAUT, L., MENNEN, L., KNOX, C., EISNER, R., CRUZ, J., WISHART, D. & SCALBERT, A. 2010. Phenol-Explorer: an online comprehensive database on polyphenol contents in foods. *Database*.

NGAMWONGSATIT, P., BANADA, P. P., PANBANGRED, W. & BHUNIA, A. K. 2008. WST-1-based cell cytotoxicity assay as a substitute for MTT-based assay for rapid detection of toxigenic Bacillus species using CHO cell line. *J Microbiol. Methods,* 73**,** 211-5.

NIJVELDT, R. J., VAN NOOD, E., VAN HOORN, D. E., BOELENS, P. G., VAN NORREN, K. & VAN LEEUWEN, P. A. 2001. Flavonoids: a review of probable mechanisms of action and potential applications. *Am. J Clin. Nutr.,* 74**,** 418-25.

NISHIKAWA, H., WAKANO, K. & KITANI, S. 2007. Inhibition of NADPH oxidase subunits translocation by tea catechin EGCG in mast cell. *Biochem. Biophys. Res. Commun.,* 362**,** 504-509.

NORDSKOG, B. K., BLIXT, A. D., MORGAN, W. T., FIELDS, W. R. & HELLMANN, G. M. 2003. Matrix-degrading and pro-inflammatory changes in human vascular endothelial cells exposed to cigarette smoke condensate. *Cardiovasc. Toxicol.,* 3**,** 101-17.

OTANI, M., NATSUME, T., WATANABE, J. I., KOBAYASHI, M., MURAKOSHI, M., MIKAMI, T. & NAKAYAMA, T. 2000. TZT-1027, an antimicrotubule agent, attacks tumor vasculature and induces tumor cell death. *Jpn J Cancer Res.,* 91**,** 837-44.

PAIXÃO, J., DINIS, T. C. P. & ALMEIDA, L. M. 2012. Malvidin-3-glucoside protects endothelial cells up-regulating endothelial NO synthase and inhibiting peroxynitrite-induced NF-kB activation. *Chem. Biol. Interact.,* 199**,** 192-200.

PASSAMONTI, S., VRHOVSEK, U. & MATTIVI, F. 2002. The interaction of anthocyanins with bilitranslocase. *Biochem. Biophys. Res. Commun.,* 296**,** 631-6.

PASSAMONTI, S., VRHOVSEK, U., VANZO, A. & MATTIVI, F. 2003. The stomach as a site for anthocyanins absorption from food. *FEBS Lett.,* 544**,** 210-3.

PENDYALA, S., MOITRA, J., KALARI, S., KLEEBERGER, S. R., ZHAO, Y., REDDY, S. P., GARCIA, J. G. & NATARAJAN, V. 2011. Nrf2 regulates hyperoxia-induced Nox4 expression in human lung endothelium: Identification of functional antioxidant response elements on the Nox4 promoter. *Free Radic. Biol. Med.,* 50**,** 1749-59.

PEREZ-JIMENEZ, J., HUBERT, J., HOOPER, L., CASSIDY, A., MANACH, C., WILLIAMSON, G. & SCALBERT, A. 2010. Urinary metabolites as biomarkers of polyphenol intake in humans: a systematic review. *Am. J Clin. Nutr.,* 92**,** 801-9.

PERSSON, I. A., JOSEFSSON, M., PERSSON, K. & ANDERSSON, R. G. 2006. Tea flavanols inhibit angiotensin-converting enzyme activity and increase nitric oxide production in human endothelial cells. *J Pharm. Pharmacol.,* 58**,** 1139-44.

PERSSON, I. A. L., PERSSON, K. & ANDERSSON, R. G. G. 2009. Effect of Vaccinium myrtillus and Its Polyphenols on Angiotensin-Converting Enzyme Activity in Human Endothelial Cells. *J Agric. Food Chem.,* 57**,** 4626-4629.

PETERSON, J. J., DWYER, J. T., JACQUES, P. F. & MCCULLOUGH, M. L. 2012. Associations between flavonoids and cardiovascular disease incidence or mortality in European and US populations. *Nutrition Reviews,* 70**,** 491-508.

PI, J., FREEMAN, M. L. & YAMAMOTO, M. 2010. Nrf2 in toxicology and pharmacology: the good, the bad and the ugly? *Toxicol. Appl. Pharmacol.,* 244**,** 1-3.

PIGNATELLI, P., CARNEVALE, R., CANGEMI, R., LOFFREDO, L., SANGUIGNI, V., STEFANUTTI, C., BASILI, S. & VIOLI, F. 2009. Atorvastatin Inhibits gp91phox Circulating Levels in Patients With Hypercholesterolemia. *Arterioscler. Thromb. Vasc. Biol.,* 30**,** 360-367.

POTAPOVA, I. A., COHEN, I. S. & DORONIN, S. V. 2009. Apoptotic endothelial cells demonstrate increased adhesiveness for human mesenchymal stem cells. *J Cell Physiol.,* 219**,** 23-30.

QIN, Y., XIA, M., MA, J., HAO, Y., LIU, J., MOU, H., CAO, L. & LING, W. 2009. Anthocyanin supplementation improves serum LDL- and HDL-cholesterol concentrations associated with the inhibition of cholesteryl ester transfer protein in dyslipidemic subjects. *Am. J Clin. Nutr.,* 90**,** 485-92.

QUINTIERI, A. M., BALDINO, N., FILICE, E., SETA, L., VITETTI, A., TOTA, B., DE CINDIO, B., CERRA, M. C. & ANGELONE, T. 2013. Malvidin, a red wine polyphenol, modulates mammalian myocardial and coronary performance and protects the heart against ischemia/reperfusion injury. *J. Nutr. Biochem.,* 24**,** 1221-31.

RAY, R., MURDOCH, C. E., WANG, M., SANTOS, C. X., ZHANG, M., ALOM-RUIZ, S., ANILKUMAR, N., OUATTARA, A., CAVE, A. C., WALKER, S. J., GRIEVE, D. J., CHARLES, R. L., EATON, P., BREWER, A. C. & SHAH, A. M. 2011. Endothelial Nox4 NADPH Oxidase Enhances Vasodilatation and Reduces Blood Pressure In Vivo. *Arterioscler. Thromb. Vasc. Biol.,* 31**,** 1368-76.

RECHNER, A. R. & KRONER, C. 2005. Anthocyanins and colonic metabolites of dietary polyphenols inhibit platelet function. *Thromb. Res.,* 116**,** 327-34.

RECHNER, A. R., KUHNLE, G., HU, H., ROEDIG-PENMAN, A., VAN DEN BRAAK, M. H., MOORE, K. P. & RICE-EVANS, C. A. 2002. The Metabolism of Dietary Polyphenols and the Relevance to Circulating Levels of Conjugated Metabolites. *Free Radic. Res.,* 36**,** 1229-1241.

RICE-EVANS, C. A., MILLER, N. J. & PAGANGA, G. 1996. Structure-antioxidant activity relationships of flavonoids and phenolic acids. *Free Radic. Biol. Med.,* 20**,** 933-56.

RICHARD, D., WOLF, C., BARBE, U., KEFI, K., BAUSERO, P. & VISIOLI, F. 2009. Docosahexaenoic acid down-regulates endothelial Nox 4 through a sPLA2 signalling pathway. *Biochem. Biophys. Res. Commun.,* 389**,** 516-522.

RIMM, E. B., GIOVANNUCCI, E. L., WILLETT, W. C., COLDITZ, G. A., ASCHERIO, A., ROSNER, B. & STAMPFER, M. J. 1991. Prospective study of alcohol consumption and risk of coronary disease in men. *Lancet,* 338**,** 464-8.

RISO, P., KLIMIS-ZACAS, D., BO', C., MARTINI, D., CAMPOLO, J., VENDRAME, S., MØLLER, P., LOFT, S., MARIA, R. & PORRINI, M. 2013. Effect of a wild blueberry (Vaccinium angustifolium) drink intervention on markers of oxidative stress, inflammation and endothelial function in humans with cardiovascular risk factors. *Eur. J Nutr.,* 52**,** 949-61.

ROBINSON, M. J. & COBB, M. H. 1997. Mitogen-activated protein kinase pathways. *Curr. Opin. Cell Biol.,* 9**,** 180-6.

RODRIGUEZ-MATEOS, A., RENDEIRO, C., BERGILLOS-MECA, T., TABATABAEE, S., GEORGE, T. W., HEISS, C. & SPENCER, J. P. 2013. Intake and time dependence of blueberry flavonoid–induced improvements in vascular function: a randomized, controlled, double-blind, crossover intervention study with mechanistic insights into biological activity. *Am. J Clin. Nutr.***,** In press.

ROMERO, M., JIMENEZ, R., SANCHEZ, M., LOPEZ-SEPULVEDA, R., ZARZUELO, M. J., O'VALLE, F., ZARZUELO, A., PEREZ-VIZCAINO, F. & DUARTE, J. 2009. Quercetin inhibits vascular superoxide production induced by endothelin-1: Role of NADPH oxidase, uncoupled eNOS and PKC. *Atherosclerosis,* 202**,** 58-67.

ROSS, R. 1999. Atherosclerosis--an inflammatory disease. *N. Engl. J Med.,* 340**,** 115-26.

ROWLANDS, D. J., CHAPPLE, S., SIOW, R. C. & MANN, G. E. 2011. Equol-Stimulated Mitochondrial Reactive Oxygen Species Activate Endothelial Nitric Oxide Synthase and Redox Signaling in Endothelial Cells: Roles for F-Actin and GPR30. *Hypertension,* 57**,** 833-40.

RUECKSCHLOSS, U., GALLE, J., HOLTZ, J., ZERKOWSKI, H. R. & MORAWIETZ, H. 2001. Induction of NAD(P)H oxidase by oxidized low-density lipoprotein in human endothelial cells: antioxidative potential of hydroxymethylglutaryl coenzyme A reductase inhibitor therapy. *Circulation,* 104**,** 1767-72.

RUECKSCHLOSS, U., QUINN, M. T., HOLTZ, J. & MORAWIETZ, H. 2002. Dose-dependent regulation of NAD(P)H oxidase expression by angiotensin II in human endothelial cells: protective effect of angiotensin II type 1 receptor blockade in patients with coronary artery disease. *Arterioscler. Thromb. Vasc. Biol.,* 22**,** 1845-51.

RYTER, S. W., ALAM, J. & CHOI, A. M. 2006. Heme oxygenase-1/carbon monoxide: from basic science to therapeutic applications. *Physiol. Rev.,* 86**,** 583-650.

RYTER, S. W., OTTERBEIN, L. E., MORSE, D. & CHOI, A. M. 2002. Heme oxygenase/carbon monoxide signaling pathways: regulation and functional significance. *Mol. Cell. Biochem.,* 234-235**,** 249-63.

SAKURAI, D., TSUCHIYA, N., YAMAGUCHI, A., OKAJI, Y., TSUNO, N. H., KOBATA, T., TAKAHASHI, K. & TOKUNAGA, K. 2004. Crucial role of inhibitor of DNA binding/differentiation in the vascular endothelial growth factor-induced activation and angiogenic processes of human endothelial cells. *J Immunol.,* 173**,** 5801-9.

SANCHEZ, M., GALISTEO, M., VERA, R., VILLAR, I. C., ZARZUELO, A., TAMARGO, J., PEREZ-VIZCAINO, F. & DUARTE, J. 2006. Quercetin downregulates NADPH oxidase, increases eNOS activity and prevents endothelial dysfunction in spontaneously hypertensive rats. *J Hypertens.,* 24**,** 75-84.

SANCHEZ, M., LODI, F., VERA, R., VILLAR, I. C., COGOLLUDO, A., JIMENEZ, R., MORENO, L., ROMERO, M., TAMARGO, J., PEREZ-VIZCAINO, F. & DUARTE, J. 2007. Quercetin and Isorhamnetin Prevent Endothelial Dysfunction, Superoxide Production, and Overexpression of p47phox Induced by Angiotensin II in Rat Aorta. *J Nutr.,* 137**,** 910-915.

SCHEWE, T., STEFFEN, Y. & SIES, H. 2008. How do dietary flavanols improve vascular function? A position paper. *Arch. Biochem. Biophys.,* 476**,** 102-106.

SCHMITTGEN, T. D. & LIVAK, K. J. 2008. Analyzing real-time PCR data by the comparative C(T) method. *Nat. Protoc.,* 3**,** 1101-8.

SCHRAMM, A., MATUSIK, P., OSMENDA, G. & GUZIK, T. J. 2012. Targeting NADPH oxidases in vascular pharmacology. *Vascul. Pharmacol.,* 56**,** 216-31.

SCHRODER, K. 2010. Isoform specific functions of Nox protein-derived reactive oxygen species in the vasculature. *Curr. Opin. Pharmacol.,* 10**,** 122-6.

SCHWARZ, R. E., AWASTHI, N., KONDURI, S., CAFASSO, D. & SCHWARZ, M. A. 2010. EMAP II-based antiangiogenic-antiendothelial in vivo combination therapy of pancreatic cancer. *Ann. Surg. Oncol.,* 17**,** 1442-52.

SCHWEPPE, C. H., BIELASZEWSKA, M., POHLENTZ, G., FRIEDRICH, A. W., BUNTEMEYER, H., SCHMIDT, M. A., KIM, K. S., PETER-KATALINIC, J., KARCH, H. & MUTHING, J. 2008. Glycosphingolipids in vascular endothelial cells: relationship of heterogeneity in Gb3Cer/CD77 receptor expression with differential Shiga toxin 1 cytotoxicity. *Glycoconj. J,* 25**,** 291-304.

SHAUL, P. W. 2002. Regulation of endothelial nitric oxide synthase: location, location, location. *Annu. Rev. Physiol.,* 64**,** 749-74.

SIES, H. 2007. Total antioxidant capacity: appraisal of a concept. *J Nutr.,* 137**,** 1493-5.

SIES, H. 2010. Polyphenols and health: update and perspectives. *Arch. Biochem. Biophys.,* 501**,** 2-5.

SIMONCINI, T., LENZI, E., ZOCHLING, A., GOPAL, S., GOGLIA, L., RUSSO, E., POLAK, K., CASAROSA, E., JUNGBAUER, A., GENAZZANI, A. D. & GENAZZANI, A. R. 2011. Estrogen-like effects of wine extracts on nitric oxide synthesis in human endothelial cells. *Maturitas,* 70**,** 169-75.

SIMONS, K. & TOOMRE, D. 2000. Lipid rafts and signal transduction. *Nat. Rev. Mol. Cell Biol.,* 1**,** 31-9.

SIOW, R. C., SATO, H. & MANN, G. E. 1999. Heme oxygenase-carbon monoxide signalling pathway in atherosclerosis: anti-atherogenic actions of bilirubin and carbon monoxide? *Cardiovasc. Res.,* 41**,** 385-94.

SKEMIENE, K., RAKAUSKAITE, G., TRUMBECKAITE, S., LIOBIKAS, J., BROWN, G. C. & BORUTAITE, V. 2012. Anthocyanins block ischaemia-induced apoptosis in the perfused heart and support mitochondrial respiration potentially by reducing cytosolic cytochrome c. *Int. J Biochem. Cell. Biol.,* 45**,** 23-29.

SOHN, H. Y., RAFF, U., HOFFMANN, A., GLOE, T., HEERMEIER, K., GALLE, J. & POHL, U. 2000. Differential role of angiotensin II receptor subtypes on endothelial superoxide formation. *Br. J Pharmacol.,* 131**,** 667-72.

SORRENTI, V., MAZZA, F., CAMPISI, A., DI GIACOMO, C., ACQUAVIVA, R., VANELLA, L. & GALVANO, F. 2007. Heme oxygenase induction by cyanidin-3-O-beta-glucoside in cultured human endothelial cells. *Mol. Nutr. Food Res.,* 51**,** 580-6.

SPECIALE, A., CANALI, R., CHIRAFISI, J., SAIJA, A., VIRGILI, F. & CIMINO, F. 2010. Cyanidin-3-O-glucoside protection against TNF-alpha-induced endothelial dysfunction: involvement of nuclear factor-kappaB signaling. *J Agric. Food Chem.,* 58**,** 12048-54.

SPENCER, J. P. E. 2010. The impact of fruit flavonoids on memory and cognition. *Br. J Nutr.,* 104**,** S40-S47.

STALMACH, A., EDWARDS, C. A., WIGHTMAN, J. D. & CROZIER, A. 2012. Gastrointestinal stability and bioavailability of (poly)phenolic compounds following ingestion of Concord grape juice by humans. *Mol. Nutr. Food Res.,* 56**,** 497-509.

STEFFEN, Y., GRUBER, C., SCHEWE, T. & SIES, H. 2008. Mono-O-methylated flavanols and other flavonoids as inhibitors of endothelial NADPH oxidase. *Arch. Biochem. Biophys.,* 469**,** 209-19.

STEFFEN, Y., JUNG, T., KLOTZ, L. O., SCHEWE, T., GRUNE, T. & SIES, H. 2007a. Protein modification elicited by oxidized low-density lipoprotein (LDL) in endothelial cells: protection by (-)-epicatechin. *Free Radic. Biol. Med.,* 42**,** 955-70.

STEFFEN, Y., SCHEWE, T. & SIES, H. 2005. Epicatechin protects endothelial cells against oxidized LDL and maintains NO synthase. *Biochem. Biophys. Res. Commun.,* 331**,** 1277-83.

STEFFEN, Y., SCHEWE, T. & SIES, H. 2007b. (-)-Epicatechin elevates nitric oxide in endothelial cells via inhibition of NADPH oxidase. *Biochem. Biophys. Res. Commun.,* 359**,** 828-33.

STEINERT, J. R., WYATT, A. W., POSTON, L., JACOB, R. & MANN, G. E. 2002. Preeclampsia is associated with altered Ca2+ regulation and NO production in human fetal venous endothelial cells. *FASEB J,* 16**,** 721-3.

STIELOW, C., CATAR, R. A., MULLER, G., WINGLER, K., SCHEURER, P., SCHMIDT, H. H. & MORAWIETZ, H. 2006. Novel Nox inhibitor of oxLDL-induced reactive oxygen species formation in human endothelial cells. *Biochem. Biophys. Res. Commun.,* 344**,** 200-5.

STOLK, J., HILTERMANN, T. J., DIJKMAN, J. H. & VERHOEVEN, A. J. 1994. Characteristics of the inhibition of NADPH oxidase activation in neutrophils by apocynin, a methoxy-substituted catechol. *Am. J Respir. Cell Mol. Biol.,* 11**,** 95-102.

STREETER, J., THIEL, W., BRIEGER, K. & MILLER JR, F. J. 2013. Opportunity Nox: The Future of NADPH Oxidases as Therapeutic Targets in Cardiovascular Disease. *Cardiovasc. Ther.,* 31**,** 125-37.

STURROCK, A., CAHILL, B., NORMAN, K., HUECKSTEADT, T. P., HILL, K., SANDERS, K., KARWANDE, S. V., STRINGHAM, J. C., BULL, D. A., GLEICH, M., KENNEDY, T. P. & HOIDAL, J. R. 2006. Transforming growth factor-beta1 induces Nox4 NAD(P)H oxidase and reactive oxygen species-dependent proliferation in human pulmonary artery smooth muscle cells. *Am. J Physiol. Lung Cell Mol. Physiol.,* 290**,** L661-L673.

SUMIMOTO, H., MIYANO, K. & TAKEYA, R. 2005. Molecular composition and regulation of the Nox family NAD(P)H oxidases. *Biochem. Biophys. Res. Commun.,* 338**,** 677-86.

TAKAC, I., SCHRODER, K. & BRANDES, R. P. 2011. The Nox Family of NADPH Oxidases: Friend or Foe of the Vascular System? *Curr. Hypertens. Rep.,* 14**,** 70-8.

TAUBERT, D., BREITENBACH, T., LAZAR, A., CENSAREK, P., HARLFINGER, S., BERKELS, R., KLAUS, W. & ROESEN, R. 2003. Reaction rate constants of superoxide scavenging by plant antioxidants. *Free Rad. Biol. Med.,* 35**,** 1599-1607.

TERRY, C. M., CLIKEMAN, J. A., HOIDAL, J. R. & CALLAHAN, K. S. 1998. Effect of tumor necrosis factor-α and interleukin-1α on heme oxygenase-1 expression in human endothelial cells. *Am. J Physiol. Heart Circ. Physiol.,* 274**,** H883-H891.

TERRY, C. M., CLIKEMAN, J. A., HOIDAL, J. R. & CALLAHAN, K. S. 1999. TNF-α and IL-1α induce heme oxygenase-1 via protein kinase C, Ca2+, and phospholipase A2 in endothelial cells. *Am. J Physiol. Heart Circ. Physiol.,* 276**,** H1493-H1501.

TESMER, J. J. 2010. The quest to understand heterotrimeric G protein signaling. *Nat. Struct. Mol. Biol.,* 17**,** 650-2.

TOUYZ, R. M. 2004. Reactive oxygen species, vascular oxidative stress, and redox signaling in hypertension: what is the clinical significance? *Hypertension,* 44**,** 248-52.

TOUYZ, R. M. & MONTEZANO, A. C. 2012. Vascular nox4: a multifarious NADPH oxidase. *Circ. Res.,* 110**,** 1159-61.

TSIKAS, D. 2007. Analysis of nitrite and nitrate in biological fluids by assays based on the Griess reaction: appraisal of the Griess reaction in the L-arginine/nitric oxide area of research. *J Chromatogr. B Analyt. Technol. Biomed. Life Sci.,* 851**,** 51-70.

TSUDA, T. 2011. Dietary anthocyanin-rich plants: Biochemical basis and recent progress in health benefits studies. *Mol. Nutr. Food Res.,* 56**,** 159-70.

UNGVARI, Z., BAGI, Z., FEHER, A., RECCHIA, F. A., SONNTAG, W. E., PEARSON, K., DE CABO, R. & CSISZAR, A. 2010. Resveratrol confers endothelial protection via activation of the antioxidant transcription factor Nrf2. *Am. J Physiol. Heart Circ. Physiol.,* 299**,** H18-H24.

USDA 2007. USDA Database for the Flavonoid Content of Selected Foods (Release 2.1, 2007). *Database.* U.S. Department of Agriculture, Agricultural Research Service.

USHIO-FUKAI, M., TANG, Y., FUKAI, T., DIKALOV, S. I., MA, Y., FUJIMOTO, M., QUINN, M. T., PAGANO, P. J., JOHNSON, C. & ALEXANDER, R. W. 2002. Novel Role of gp91phox-Containing NAD(P)H Oxidase in Vascular Endothelial Growth Factor–Induced Signaling and Angiogenesis. *Circ. Res.,* 91**,** 1160-1167.

VANDESOMPELE, J., DE PRETER, K., PATTYN, F., POPPE, B., VAN ROY, N., DE PAEPE, A. & SPELEMAN, F. 2002. Accurate normalization of real-time quantitative RT-PCR data by geometric averaging of multiple internal control genes. *Genome Biol.,* 3**,** RESEARCH0034.

VIDAVALUR, R., PENUMATHSA, S. V., ZHAN, L., THIRUNAVUKKARASU, M. & MAULIK, N. 2006. Sildenafil induces angiogenic response in human coronary arteriolar endothelial cells through the expression of thioredoxin, hemeoxygenase and vascular endothelial growth factor. *Vascul. Pharmacol.,* 45**,** 91-95.

VILLANUEVA, C. & GIULIVI, C. 2010. Subcellular and cellular locations of nitric oxide synthase isoforms as determinants of health and disease. *Free Radic. Biol. Med.,* 49**,** 307-16.

VIOLI, F., SANGUIGNI, V., CARNEVALE, R., PLEBANI, A., ROSSI, P., FINOCCHI, A., PIGNATA, C., DE MATTIA, D., MARTIRE, B., PIETROGRANDE, M. C., MARTINO, S., GAMBINERI, E., SORESINA, A. R., PIGNATELLI, P., MARTINO, F., BASILI, S. & LOFFREDO, L. 2009. Hereditary deficiency of gp91(phox) is associated with enhanced arterial dilatation: results of a multicenter study. *Circulation,* 120**,** 1616-22.

VITA, J. A. 2005. Polyphenols and cardiovascular disease: effects on endothelial and platelet function. *Am. J Clin. Nutr.,* 81**,** 292S-297S.

VITA, J. A. & KEANEY, J. F., JR. 2002. Endothelial function: a barometer for cardiovascular risk? *Circulation,* 106**,** 640-2.

VITAGLIONE, P., DONNARUMMA, G., NAPOLITANO, A., GALVANO, F., GALLO, A., SCALFI, L. & FOGLIANO, V. 2007. Protocatechuic acid is the major human metabolite of cyanidin-glucosides. *J Nutr.,* 137**,** 2043-8.

WALLACE, T. C. 2011. Anthocyanins in Cardiovascular Disease. *Adv. Nutr.,* 2**,** 1-7.

WALLE, T. 2004. Absorption and metabolism of flavonoids. *Free Radic. Biol. Med.,* 36**,** 829-37.

WALLERATH, T., DECKERT, G., TERNES, T., ANDERSON, H., LI, H., WITTE, K. & FÖRSTERMANN, U. 2002. Resveratrol, a Polyphenolic Phytoalexin Present in Red Wine, Enhances Expression and Activity of Endothelial Nitric Oxide Synthase. *Circulation,* 106**,** 1652-1658.

WANG, D., WEI, X., YAN, X., JIN, T. & LING, W. 2010a. Protocatechuic acid, a metabolite of anthocyanins, inhibits monocyte adhesion and reduces atherosclerosis in apolipoprotein E-deficient mice. *J Agric. Food Chem.,* 58**,** 12722-8.

WANG, L., ZHU, L.-H., JIANG, H., TANG, Q.-Z., YAN, L., WANG, D., LIU, C., BIAN, Z.-Y. & LI, H. 2010b. Grape seed proanthocyanidins attenuate vascular smooth muscle cell proliferation via blocking phosphatidylinositol 3-kinase-dependent signaling pathways. *J Cell Physiol.,* 223**,** 713-726.

WANG, Y. & HO, C. T. 2009. Metabolism of flavonoids. *Forum Nutr.,* 61**,** 64-74.

WEVER, R., STROES, E. & RABELINK, T. J. 1998. Nitric oxide and hypercholesterolemia: a matter of oxidation and reduction? *Atherosclerosis,* 137 Suppl**,** S51-60.

WHO 2013. Cardiovascular diseases (CVDs). Fact sheet N°317. Available at: http://www.who.int/mediacentre/factsheets/fs317/en/index.html. March 2013.

WICZKOWSKI, W., ROMASZKO, E. & PISKULA, M. K. 2010. Bioavailability of Cyanidin Glycosides from Natural Chokeberry (Aronia melanocarpa) Juice with Dietary-Relevant Dose of Anthocyanins in Humans. *J Agric. Food Chem.,* 58**,** 12130-12136.

WIDLANSKY, M. E., GOKCE, N., KEANEY, J. F., JR. & VITA, J. A. 2003. The clinical implications of endothelial dysfunction. *J Am. Coll. Cardiol.,* 42**,** 1149-60.

WILLIAMSON, G. & CLIFFORD, M. N. 2010. Colonic metabolites of berry polyphenols: the missing link to biological activity? *Br. J Nutr.,* 104**,** S48-S66.

WOLIN, M. S. & ABRAHAM, N. G. 2006. Heme Oxygenase-1 Inhibition of Nox Oxidase Activation Is a Microvascular Endothelial Antioxidant Effect of NO. *Hypertension,* 48**,** 826-827.

WOODWARD, G., KROON, P., CASSIDY, A. & KAY, C. 2009. Anthocyanin stability and recovery: implications for the analysis of clinical and experimental samples. *J Agric. Food Chem.,* 57**,** 5271-8.

WOODWARD, G. M. 2010. *Anthocyanin Stability, Metabolic Conjugation and in vitro Modulation of Endothelial Superoxide Production.* Thesis Doctor of Philosophy, University of East Anglia.

WU, B. J., CHEN, K., BARTER, P. J. & RYE, K.-A. 2012. Niacin Inhibits Vascular Inflammation via the Induction of Heme Oxygenase-1. *Circulation,* 125**,** 150-158.

WU, C. C., HSU, M. C., HSIEH, C. W., LIN, J. B., LAI, P. H. & WUNG, B. S. 2006a. Upregulation of heme oxygenase-1 by Epigallocatechin-3-gallate via the phosphatidylinositol 3-kinase/Akt and ERK pathways. *Life Sci.,* 78**,** 2889-2897.

WU, X., BEECHER, G. R., HOLDEN, J. M., HAYTOWITZ, D. B., GEBHARDT, S. E. & PRIOR, R. L. 2006b. Concentrations of anthocyanins in common foods in the United States and estimation of normal consumption. *J Agric. Food Chem.,* 54**,** 4069-75.

XU, H., GOETTSCH, C., XIA, N., HORKE, S., MORAWIETZ, H., FÖRSTERMANN, U. & LI, H. 2008. Differential roles of PKCα and PKCε in controlling the gene expression of Nox4 in human endothelial cells. *Free Radic. Biol. Med.,* 44**,** 1656-1667.

XU, J. W., IKEDA, K. & YAMORI, Y. 2004a. Cyanidin-3-glucoside regulates phosphorylation of endothelial nitric oxide synthase. *FEBS Lett.,* 574**,** 176-80.

XU, J. W., IKEDA, K. & YAMORI, Y. 2004b. Upregulation of endothelial nitric oxide synthase by cyanidin-3-glucoside, a typical anthocyanin pigment. *Hypertension,* 44**,** 217-22.

YAMAGISHI, S., NAKAMURA, K., UEDA, S., KATO, S. & IMAIZUMI, T. 2005. Pigment epithelium-derived factor (PEDF) blocks angiotensin II signaling in endothelial cells via suppression of NADPH oxidase: a novel anti-oxidative mechanism of PEDF. *Cell Tissue Res.,* 320**,** 437-45.

YANG, D., ELNER, S. G., BIAN, Z. M., TILL, G. O., PETTY, H. R. & ELNER, V. M. 2007. Pro-inflammatory cytokines increase reactive oxygen species through mitochondria and NADPH oxidase in cultured RPE cells. *Exp. Eye Res.,* 85**,** 462-72.

YANG, Y., ANDREWS, M. C., HU, Y., WANG, D., QIN, Y., ZHU, Y., NI, H. & LING, W. 2011. Anthocyanin extract from black rice significantly ameliorates platelet hyperactivity and hypertriglyceridemia in dyslipidemic rats induced by high fat diets. *J Agric. Food Chem.,* 59**,** 6759-64.

YANG, Y., SHI, Z., REHEMAN, A., JIN, J. W., LI, C., WANG, Y., ANDREWS, M. C., CHEN, P., ZHU, G., LING, W. & NI, H. 2012. Plant Food Delphinidin-3-Glucoside Significantly Inhibits Platelet Activation and Thrombosis: Novel Protective Roles against Cardiovascular Diseases. *PLoS One,* 7**,** e37323.

YET, S.-F., LAYNE, M. D., LIU, X., CHEN, Y.-H., ITH, B., SIBINGA, N. E. S. & PERRELLA, M. A. 2003. Absence of heme oxygenase-1 exacerbates atherosclerotic lesion formation and vascular remodeling. *FASEB J*.

YOSHIDA, L. S. & TSUNAWAKI, S. 2008. Expression of NADPH oxidases and enhanced H(2)O(2)-generating activity in human coronary artery endothelial cells upon induction with tumor necrosis factor-alpha. *Int. Immunopharmacol.,* 8**,** 1377-85.

YOUDIM, K. A., MCDONALD, J., KALT, W. & JOSEPH, J. A. 2002. Potential role of dietary flavonoids in reducing microvascular endothelium vulnerability to oxidative and inflammatory insults. *J Nutr. Biochem.,* 13**,** 282-288.

YUN, M. R., IM, D. S., LEE, J.-S., SON, S. M., SUNG, S.-M., BAE, S. S. & KIM, C. D. 2006. NAD(P)H oxidase-stimulating activity of serum from type 2 diabetic patients with retinopathy mediates enhanced endothelial expression of E-selectin. *Life Sci.,* 78**,** 2608-2614.

ZALBA, G., BEAUMONT, F. J., SAN JOSE, G., FORTUNO, A., FORTUNO, M. A., ETAYO, J. C. & DIEZ, J. 2000. Vascular NADH/NADPH oxidase is involved in enhanced superoxide production in spontaneously hypertensive rats. *Hypertension,* 35**,** 1055-61.

ZAMORA-ROS, R., ANDRES-LACUEVA, C., LAMUELA-RAVENTOS, R. M., BERENGUER, T., JAKSZYN, P., BARRICARTE, A., ARDANAZ, E., AMIANO, P., DORRONSORO, M., LARRANAGA, N., MARTINEZ, C., SANCHEZ, M. J., NAVARRO, C., CHIRLAQUE, M. D., TORMO, M. J., QUIROS, J. R. & GONZALEZ, C. A. 2010. Estimation of dietary sources and flavonoid intake in a Spanish adult population (EPIC-Spain). *J Am. Diet Assoc.,* 110**,** 390-8.

ZAMORA-ROS, R., KNAZE, V., LUJAN-BARROSO, L., SLIMANI, N., ROMIEU, I., TOUILLAUD, M., KAAKS, R., TEUCHER, B., MATTIELLO, A., GRIONI, S., CROWE, F., BOEING, H., FORSTER, J., QUIROS, J. R., MOLINA, E., HUERTA, J. M., ENGESET, D., SKEIE, G., TRICHOPOULOU, A., DILIS, V., TSIOTAS, K., PEETERS, P. H., KHAW, K. T., WAREHAM, N., BUENO-DE-MESQUITA, B., OCKE, M. C., OLSEN, A., TJONNELAND, A., TUMINO, R., JOHANSSON, G., JOHANSSON, I., ARDANAZ, E., SACERDOTE, C., SONESTEDT, E., ERICSON, U., CLAVEL-CHAPELON, F., BOUTRON-RUAULT, M. C., FAGHERAZZI, G., SALVINI, S., AMIANO, P., RIBOLI, E. & GONZALEZ, C. A. 2011. Estimation of the intake of anthocyanidins and their food sources in the European Prospective Investigation into Cancer and Nutrition (EPIC) study. *Br. J Nutr.,* 106**,** 1090-9.

ZHAO, B., HUANG, W., ZHANG, W.-Y., ISHII, I. & KRUTH, H. S. 2004. Retention of aggregated LDL by cultured human coronary artery endothelial cells. *Biochem. Biophys. Res. Commun.,* 321**,** 728-735.

ZHENG, Y., MORRIS, A., SUNKARA, M., LAYNE, J., TOBOREK, M. & HENNIG, B. 2012. Epigallocatechin-gallate stimulates NF-E2-related factor and heme oxygenase-1 via caveolin-1 displacement. *J Nutr. Biochem.,* 23**,** 163-168.

ZHENG, Y., TOBOREK, M. & HENNIG, B. 2010. Epigallocatechin gallate–mediated protection against tumor necrosis factor-α–induced monocyte chemoattractant protein–1 expression is heme oxygenase–1 dependent. *Metabolism,* 59**,** 1528-1535.

ZHU, Y., LING, W., GUO, H., SONG, F., YE, Q., ZOU, T., LI, D., ZHANG, Y., LI, G., XIAO, Y., LIU, F., LI, Z., SHI, Z. & YANG, Y. 2012. Anti-inflammatory effect of purified dietary anthocyanin in adults with hypercholesterolemia: A randomized controlled trial. *Nutr. Metab. Cardiovasc. Dis.,* In press.

ZHU, Y., XIA, M., YANG, Y., LIU, F., LI, Z., HAO, Y., MI, M., JIN, T. & LING, W. 2011. Purified Anthocyanin Supplementation Improves Endothelial Function via NO-cGMP Activation in Hypercholesterolemic Individuals. *Clin. Chem.,* 57**,** 1524-33.

ZIBERNA, L., LUNDER, M., TRAMER, F., DREVENSEK, G. & PASSAMONTI, S. 2013. The endothelial plasma membrane transporter bilitranslocase mediates rat aortic vasodilation induced by anthocyanins. *Nutr. Metab. Cardiovasc. Dis.,* 23**,** 68-74.

ZIEGER, M. A. J. & GUPTA, M. P. 2009. Hypothermic preconditioning of endothelial cells attenuates cold-induced injury by a ferritin-dependent process. *Free Radic. Biol. Med.,* 46**,** 680-691.

9 Appendices

9.1 Cytotoxicity assay (WST-1 reagent): method optimisation

Method development. Initial cytotoxicity assays were conducted using HUVECs seeded at densities of 1,600–2,560 cells/well, and grown to confluence, in 96-well microplates. However, these experiments generated inconsistent results across the concentration range utilised, and between repeat experiments. Reduced cell viability was observed with the vehicle control treatment (0.05% DMSO in Medium 199 with 2% FBS) relative to the control, yet this effect was not uniform across all concentrations of treatment compounds (at 0.05% DMSO in the same medium).

In order to address these discrepancies, published scientific literature was reviewed for previous reports of cytotoxicity assessment in HUVECs using WST-1 reagent, to optimise the method for key parameters. Several manufacturers' protocols for this reagent were also examined, to compare recommended assay procedures. Overall, eleven research papers and three protocols were selected and analysed, and data extracted for nine method parameters; including cell seeding density, incubation time with treatment compound(s), incubation time with WST-1 reagent, and volume of WST-1 reagent (Appendix Table 9.2.1).

Cytotoxicity assay method development was conducted using cell seeding densities of 2,000, 3,500, 5,000, 10,000 and 12,000 cells/well; to determine the optimum seeding density. In addition, absorbance measurements were recorded after 2.0, 2.5, 3.0, 3.5 and 4.0 hours incubation with WST-1 reagent, such that incubation time could be optimised. Finally, assays were performed using control, vehicle control, 0.1 and 100µM protocatechuic acid treatments, to confirm the suitability of the selected maximum dose of treatment compound. Figure 9.1.1 summarises this method development process, and optimised parameters identified at each stage.

Figure 9.1.1 Cytotoxicity assay method development flow chart.

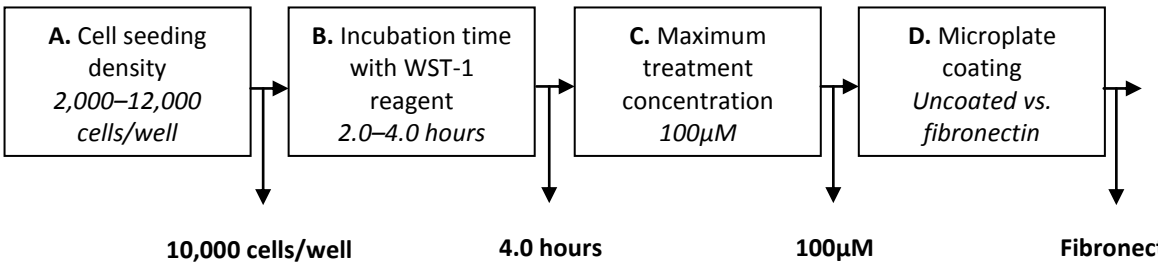

Cell seeding density (Figure 9.1.1 A). The effect of HUVEC seeding density (Figure 9.1.1 A) upon absorbance at 440nm was measured for the control (Medium 199 with 2% FBS) and vehicle control (Medium 199 with 2% FBS and 0.05% DMSO) following a four hour incubation with WST-1 reagent (Figure 9.1.2). No absorbance was detected for cells seeded at 2,000 cells/well, irrespective of

treatment or time point. The mean absorbance at all other seeding densities demonstrated a clear trend for increased absorbance at elevated cell densities. Moreover, the difference between mean absorbance measured at the higher (10,000 and 12,000 cells/well) and the lower (≤ 5,000 cells/well) densities was statistically significant for the control (at 5,000 cells/well or fewer) and vehicle control (at 3,500 cells/well or fewer). Differences between mean absorbance for the control and vehicle control were not significant at any seeding density; nor was there a significant difference between mean absorbance at the two highest seeding densities. Therefore, elevated cell seeding densities (≥ 10,000 cells/well) resulted in improved assay sensitivity (as evidenced by increased mean absorbance) and were utilised in subsequent stages of method development.

Figure 9.1.2 Effect of HUVEC seeding density on mean absorbance at 440nm with control (A) or vehicle control (B) treatment.

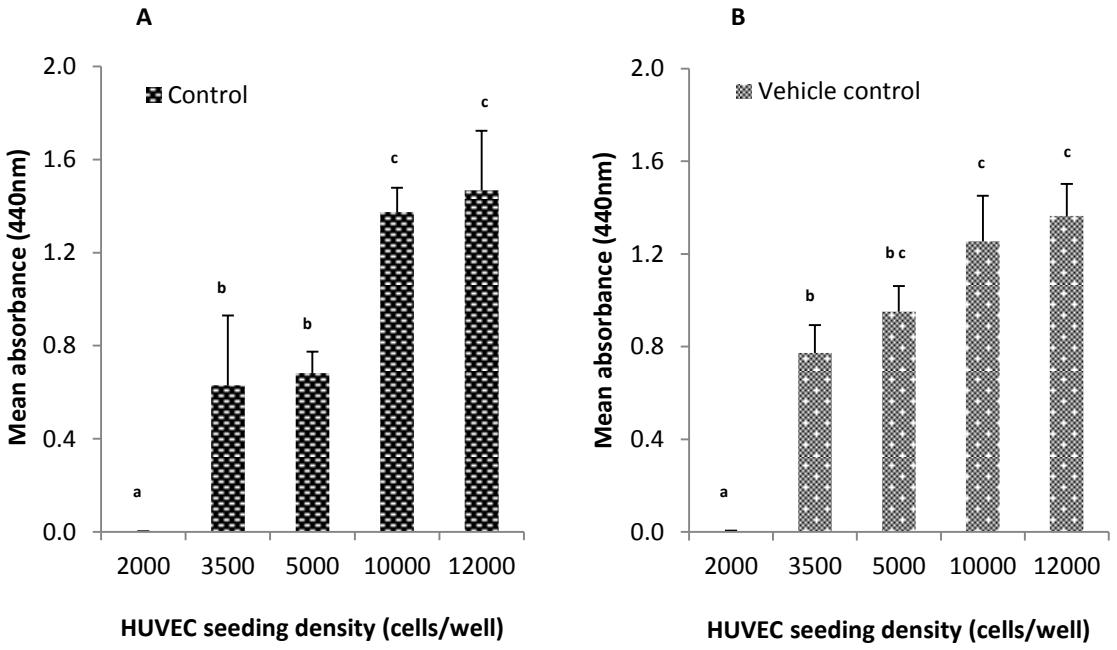

Mean absorbance for HUVECs seeded at varying densities in 96-well plate, following 24h incubation with either control (A; Medium 199 with 2% FBS) or vehicle control (B; control with 0.05% DMSO) and after 4h incubation with WST-1 reagent. Data are shown as mean ± SD (n=3); columns with different superscript letters are significantly different ($p < 0.05$).

Incubation time with WST-1 reagent (Figure 9.1.1 B). In order to establish whether increased incubation time with WST-1 reagent resulted in increased assay sensitivity, absorbance at 440nm was measured at multiple time points (Figure 9.1.1 B). No statistically significant differences in mean absorbance between the control and vehicle control were observed at any time point with a seeding density of 10,000 cells/well (Figure 9.1.3). However, the control mean absorbance at four hours was significantly different from that for the two hour time point. A significant difference was also observed between mean absorbance for the vehicle control after four hours incubation with WST-1

reagent, as compared with the two hour time point, at a seeding density of 12,000 cells/well. Therefore, an extended incubation with WST-1 reagent increased mean absorbance at 440nm, thereby improving the assay sensitivity; and was used during subsequent stages of method development.

Figure 9.1.3 Effect of incubation time with WST-1 reagent on mean absorbance at 440nm for HUVECs seeded at 10,000 cells/well.

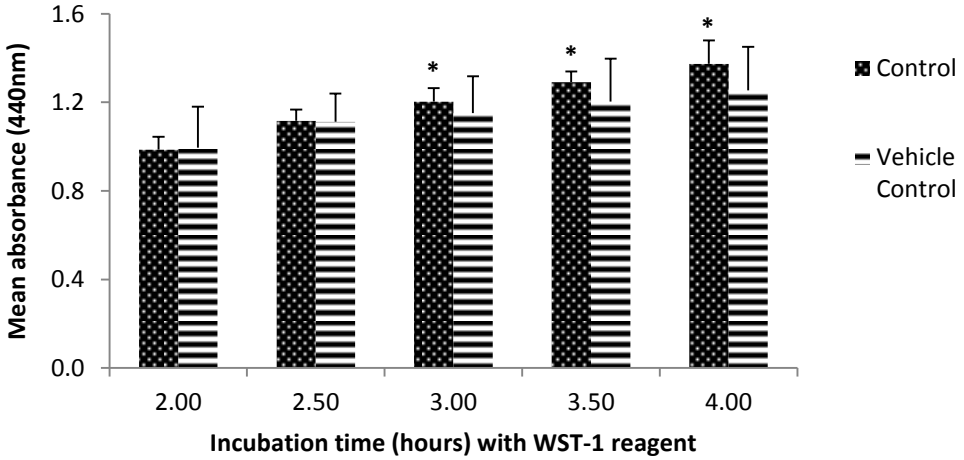

Mean absorbance following 24h incubation with either control (Medium 199 with 2% FBS) or vehicle control (control with 0.05% DMSO) treatments and after 2, 2.5, 3, 3.5 and 4h incubation with WST-1 reagent. Data are shown as mean ± SD (n=3). *Significant difference relative to 2h time point with either control or vehicle control treatment ($p < 0.05$).

Maximum treatment concentration (Figure 9.1.1 C). The cytotoxicity of 0.1µM and 100µM protocatechuic acid (PCA) (Figure 9.1.1 C) was assessed during a 24 hour incubation at each HUVEC seeding density. HUVEC viability was reduced following exposure to 100µM PCA at cell densities of 10,000 cells/well (Table 9.1.1) or less, with a statistically significant difference from the control observed at 5,000 and 10,000 cells/well. By contrast, 0.1µM PCA appeared to increase cell viability or respiration relative to control at all seeding densities, though this difference was not significant for 3,500 cells/well. Thus a maximum concentration of 100µM of treatment compound(s) was suitable for demonstrating cytotoxicity using the WST-1 reagent, and was utilised during subsequent stages of method development.

Table 9.1.1 Assessment of cytotoxicity of 0.1µM and 100µM protocatechuic acid/PCA following 24 hour incubation with HUVECs seeded at 10,000 cells/well.

HUVEC seeding density (cells/well)	Cell viability (percentage of control)	
	0.1µM PCA	***100µM PCA***
10,000	136.37 ± 16.10 *	62.24 ± 15.73 *

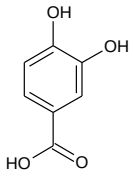

Mean absorbance as percentage of mean control absorbance following 24h incubation with either 0.1µM or 100µM PCA (structure inset) after 4h incubation with WST-1 reagent. Data are shown as mean ± SD (n=3). *Significant difference relative to control ($p < 0.05$).

Microplate coating (Figure 9.1.1 D). Cytotoxicity screening conducted utilising the parameters identified above indicated all treatment compounds tested were cytotoxic, but no consistent dose-response relationship was evident. Therefore, fibronectin coating of microplates (Baudin et al., 2007) was investigated in order to improve assay reliability and reproducibility (Figure 9.1.1 D).

Microplates were washed with warm phosphate-buffered saline (PBS), and incubated with 25µl/well of 5µg/ml fibronectin (in PBS) for 60 minutes at room temperature. Plates were then rinsed with PBS, dried, and stored at 4°C until use. Treatment compounds were subsequently screened for endothelial cytotoxicity using HUVECs cultured on fibronectin-coated microplates, which yielded reproducible data. Thus, the use of fibronectin-coated microplates enhanced cytotoxicity assay reliability, and was utilised in the optimised method.

Optimised parameters. The optimised cytotoxicity assay was conducted using 96-well microplates (BD Falcon®) coated with fibronectin (0.42µg/cm^2), which were seeded with HUVECs at a density of ~10,000 cells/well. Cells were subsequently grown to confluence (~24 - 48 hours at 37°C and 5% CO_2). Culture medium was then aspirated, and solutions of the treatment compounds (0.5, 1, 10, 50 or 100µM; maximum 0.25% DMSO) prepared in supplemented large vessel endothelial cell growth medium were added to relevant wells at a volume of 100µl/well. The assay controls consisted of wells with media only (control), wells with DMSO in media (vehicle control), and blank wells (vehicle control only, no cells). Four replicate wells were used for each control and treatment solution. The microplates were incubated for 24 hours at 37°C and 5% CO_2; after which 10µl WST-1 reagent was added to each well, and plates were incubated for a further four hours prior to brief agitation. Absorbance was then measured at 440-450nm using a microplate reader [Fluostar Omega or Polarstar Optima, BMG Labtech (Aylesbury, UK)].

9.2 Method optimisation tables

Table 9.2.1 Method optimisation table for cytotoxicity assay (WST-1 reagent).

Source	Cell type & passage number	Cell seeding density (cells/well)	Culture after seeding & prior to assay	Volume of WST-1 reagent	Incubation time with treatment compound(s) (hours)	Incubation time with reagent (hours)	Incubation conditions with reagent	Detection λ (nm)	Presentation of data
Current internal protocol	HUVEC, P2-4	1,600 – 2,560	Until cells confluent (2 – 4 days)	10µl per 100µl	24	2	37°C / 5% CO_2	440	Plot of mean absorbance for treatments normalised to control
Roche WST-1 protocol (October 2007)[2]	N/A	1,000 – 50,000	Cells seeded with treatment compound in media in examples cited	10µl per 100µl	24 – 96	0.5 – 4	37°C / 5% CO_2	420-480	Plot of absorbance versus treatment concentration or cell number
Clontech WST-1 user manual (January 2007)[3]	N/A	1,000 - 50,000	Cells seeded with treatment compound in media in examples cited	10µl per 100µl	24 – 96	0.5 – 4	37°C / 5% CO_2	420-480	Plot of absorbance versus treatment concentration
Millipore Cell Proliferation Assay Kit datasheet (October 2005)[4]	N/A	1,000 - 50,000	Cells seeded with treatment compound(s) in media	10µl	24 – 96	0.5 – 4	Not specified	420-480	N/A
(Kim et al., 2011)	HUVEC, P2-10	3,000	24 hours + 16 hours serum-starved	10µl	24	2	37°C / 5% CO_2	450	Plot of mean absorbance versus treatment
(Schwarz et al., 2010)	HUVEC	4,000	16 hours + 5 hours in basal medium	10µl	72	2	37°C / 5% CO_2	450	Plot of mean absorbance for treatments normalised to control

[2] https://www.roche-applied-science.com/pack-insert/1644807a.pdf
[3] http://www.clontech.com/images/pt/PT3946-1.pdf
[4] http://www.millipore.com/publications.nsf/a73664f9f981af8c852569b9005b4eee/bbb066008837e3f98525730600754a40/$FILE/2210.pdf

Source	Cell type & passage number	Cell seeding density (cells/well)	Culture after seeding & prior to assay	Volume of WST-1 reagent	Incubation time with treatment compound(s) (hours)	Incubation time with reagent (hours)	Incubation conditions with reagent	Detection λ (nm)	Presentation of data
(Felice et al., 2010)	HUVEC, P4-5	Not specified	Until sub-confluent	10µl	48 – 96	4	37°C / 5% CO_2	450	Plot of mean absorbance versus treatment
(Jeon et al., 2010)	HUVEC, P3-6	5,000	12 hours serum starved before treatment	10µl	72	Not specified	Not specified	450	Plot of mean proliferation (% of control) versus treatment
(Potapova et al., 2009)	HUVEC, P2-5	Not specified (confluent cells)	Not specified	10µl per 100µl	4	4	37°C / 5% CO_2	450	Plot of mean absorbance versus treatment
(Schweppe et al., 2008)	EA.hy 926 (HUVEC-derived)	30,000	24 hours	10µl	54	3	37°C / 5% CO_2	450	Plot of viable cells (% of control) versus treatment concentration
(Mundel et al., 2008)	HUVEC, P2-6	4,000	Cells seeded with treatment compound in media	10µl	48	4	37°C / 5% CO_2	450	Plot of mean absorbance versus treatment
(Munoz et al., 2007) Some method details from (Munoz et al., 2001)	HUVEC	3,000	24 hours	Not specified	48	2	37°C / 5% CO_2	450	Plot of cell viability (%) versus treatment concentration
(Sakurai et al., 2004)	HUVEC, up to P7	20,000	N/A	10µl	24	4	37°C / 5% CO_2	480[5]	Plot of cell proliferation versus treatment[6]
(Otani et al., 2000)	HUVEC	~5,000 cells/cm^2 (1,600 cells/well assuming surface area of 0.32cm^2)	Until confluent	Not specified	24	Not specified	37°C / 5% CO_2	Not specified	Plot of mean cell viability (%) versus treatment concentration[7]

[5] Supernatant solutions transferred to new 96-well plate
[6] Proliferative activity calculated as mean ± SD of triplicate wells for each experiment divided by that of the controls
[7] Cell viability expressed as a percentage of vehicle-treated control.

Table 9.2.2 Method optimisation table for stimulated superoxide production assay.

Source	Cell type & passage number	Cell seeding density & type of culture dish (cells/well)	Culture after seeding & before assay	Assay medium used	Percentage of serum in assay medium	Pre-treatment	Stress agent used	Glucose present Y/N	Incubation time with stress agent, +/- treatment (where relevant)
Current internal protocol(s)	HUVEC, P2-4	6-well plate: 47,500 – 57,000 24-well plate: 10,000 – 16,000	Until confluent	Medium 199 (phenol-red free)	2%	24 hour equilibration in assay medium	Angiotensin II (0.1µM)	Y, in Medium 199 (5.56mM)	6 hours
(Rowlands et al., 2011)[8]	HUVEC	Not specified	Confluent monolayer	Krebs buffer	None specified	4 hour incubation in Medium 199 with 1% FCS, then 30 minute incubation in Krebs buffer +/- treatment compounds[9]	Equol (0.1µM)	Y, 10mM D-glucose in Krebs buffer	2 minutes (enhanced chemiluminescence measured over 40 minutes)
(He et al., 2010)[10]	Bovine aortic endothelial cells/BAEC	Not specified	Confluent cells	DMEM (incubation) then Krebs buffer (measurement of ROS)	1%	24 hour equilibration in DMEM (1% FCS)	AGE (advanced glycation end products)-modified BSA (100µg/ml)[11]	Present in DMEM (5.5mM)	0-24 hours; then ROS generation measured immediately over 0-40 minutes in Krebs buffer[12]
(Steffen et al., 2008)	HUVEC, P2-4	~10^6 cells/dish	Confluent	Hepes-buffered isotonic salt medium	None	Pre-incubation with treatment compounds (in serum-free medium) for 6 or 24 hours	Angiotensin II (1µM)	Y, in medium (5.5mM)	6 hours
(Steffen et al., 2007b)	HUVEC, P2-4	~10^7 cells; vessel not specified	Confluent cells	Hepes-buffered isotonic salt medium	None	Not specified	Angiotensin II (1µM)	Y, in medium (5.5mM)	6 hours
(Steffen et al., 2007a)	HUVEC, P2-4	~10^7 cells; culture dish	Not specified	Not specified – cells cultured in supplemented Medium 199	Not specified – 20% FCS in culture medium	2-deoxyglucose (10mM) or (–)-epicatechin (10µM) or apocynin (10 or 100µM) for 30 minutes	MPO/H_2O_2/nitrite-oxLDL (100µg/ml), or angiotensin II (0.1µM)	Present in Medium 199	24 hours (MPO/H_2O_2/nitrite-oxLDL) or 4 hours (angiotensin II)

[8] Chemiluminescent detection of ROS using lucigenin.
[9] In absence or presence of SOD or other inhibitors.
[10] Chemiluminescent detection of ROS using luminol analogue L-012.
[11] In absence or presence of superoxide chelator or other inhibitors.
[12] Cells incubated in Krebs buffer containing L-012 with/without stress agent and inhibitors.

Source	Cell type & passage number	Cell seeding density & type of culture dish (cells/well)	Culture after seeding & before assay	Assay medium used	Percentage of serum in assay medium	Pre-treatment	Stress agent used	Glucose present Y/N	Incubation time with stress agent, +/- treatment (where relevant)
(Afzal-Ahmed et al., 2007)	HUVEC (primary culture)	Density not specified[13]; 96-well plate	Not specified	Not specified – cells cultured in supplemented Medium 199	Not specified – 10% FCS & 10% newborn calf serum in culture medium	Not specified	Angiotensin II (0.1µM) or phorbol myristate acetate (PMA, 0.1µM)	Experiments conducted in presence & absence of 5mM D-glucose	0-3 hours
(Rueckschloss et al., 2002)[14]	HUVEC (primary culture)	Not specified	Confluent culture	Medium 199 (phenol-red free)	None	24 hour incubation in medium with 0.5% calf serum; then 6 hour pre-incubation with/without angiotensin II +/- AT receptor inhibitors in same medium	Angiotensin II (1nM – 1µM)	Present in Medium 199	1-24 hours
(Rueckschloss et al., 2001)[14]	HUVEC (primary culture)	Not specified	Not specified	Medium 199	Not specified	Not specified	PMA (1µM) or oxLDL (100µg/ml)	Present in Medium 199	~1-6 hours (PMA) or 2-4 hours (oxLDL)
(Sohn et al., 2000)	HUVEC	Not specified	Confluent culture	Medium 199 (incubation) then Hepes (20mM) – Tyrode buffer (measurement of superoxide)	None specified	Serum starved for 24 hours, then 6 hour incubation with angiotensin II +/- AT receptor inhibitors	Angiotensin II (0.1-1µM)	Present in Medium 199	6 hours (see pre-treatment); then 30 minutes in Hepes buffer (supernatant sampled for analysis)
(Heinloth et al., 2000)	HUVEC, P5	~1 x 10^5 cells; culture dish	Not specified	Supplemented endothelial basal medium	2%	18 hour pre-incubation with stress agent, followed by transfection with sense or antisense oligo-nucleotide for $p22^{phox}$ (4 hours)	oxLDL (100µg/ml) or lysophosphatidyl-choline/LPC (10µM)	Not specified	4 hours (22 hours in total – see pre-treatment)

[13] Superoxide production expressed as nmoles/min/10^6 cells

[14] NADPH oxidase-derived superoxide production estimated using flavin-containing enzyme inhibitor diphenylene iodonium.

Table 9.2.3 Method optimisation table for immunoblot analysis of endothelial NOX (and eNOS) expression.

Source	Cell type	Protein loaded for SDS-PAGE	Gel percentages for SDS-PAGE	Primary NOS/NOX antibody (supplier)	Primary immunogen	Primary band size (kDa)	Primary antibody concentration	Loading control antibody	Loading band size (kDa)	Loading control concentration
Current internal protocol(s)	HUVEC P2-4	Current maximum ~10µg[15] per lane	10% resolving, 4% stacking	Polyclonal rabbit anti-NOX4 (Abcam)[16]	C terminal residues 500-578 of human NOX4	67 (predicted)	1 in 500	Polyclonal chicken anti-GAPDH (Millipore)[17]	~ 36	1 in 2000 (best result to date)
(Rowlands et al., 2011)	HUVEC P3	-	-	Monoclonal anti-eNOS (Santa Cruz)[18] Monoclonal anti-p-eNOS (Cell Signalling)[19]	Human NOS3, amino acids 2-160 Synthetic phosphor-peptide; corresponds to residues surrounding Ser1177 of human eNOS	140 140	-	Mono-clonal anti-α-tubulin (Chemicon/ Millipore)[20]	~ 50-60	-
(Steffen et al., 2007a)	HUVEC P2-4	25µg per lane	10% resolving	Polyclonal rabbit anti-iNOS (Cayman Chemical Co.)[21] Monoclonal mouse anti-eNOS (Transduction Laboratories)[22]	Purified murine enzyme Human eNOS, amino acids. 1025-1203	133 144	-	Anti-GAPDH	39	-

[15] From maximum seeding density of 57,000 cells/well
[16] http://www.abcam.com/NOX4-antibody-HRP-ab81967.html
[17] http://www.millipore.com/catalogue/item/ab2302
[18] http://www.scbt.com/datasheet-136977-nos3-b-5-antibody.html
[19] http://www.cellsignal.com/products/9570.html
[20] http://www.millipore.com/search.do?q=Anti-%ce%b1-Tubulin&tabValue=PC&filterProductTypes=taxonomy%3a%5e73UUAR%2f73UUB8&show=10#0:0
[21] http://www.caymanchem.com/app/template/Product.vm/catalog/160862
[22] http://www.bdbiosciences.com/ptProduct.jsp?prodId=32086&key=eNOS&param=search&mterms=true

Source	Cell type	Protein loaded for SDS-PAGE	Gel percentages for SDS-PAGE	Primary NOS/NOX antibody (supplier)	Primary immunogen	Primary band size (kDa)	Primary antibody concentration	Loading control antibody	Loading band size (kDa)	Loading control concentration
(Jiang et al., 2006)	Human micro-vascular endothelial cells (HMEC) P<25	-	10% resolving	Anti-NOX4[23] (Santa Cruz) Anti-NOX1[24] (Santa Cruz) Anti-gp91phox (NOX2) (Upstate/ Millipore)[25]	Peptide mapping at N-terminus of human NOX4 Amino acids 121-195 of human NOX1 Synthetic peptide; corresponds to amino acids 548-560 of human gp91-phox	70 ~33 ~75 (band) 75-91 (smear)	-	Anti-β-actin	~ 43[26]	-
(Hu et al., 2005)	HUVEC P2-6	40µg	10% resolving	Polyclonal rabbit anti-NOX4 (in-house)	C-terminal amino acids 320 - 428 of human NOX4 (Mahadev et al., 2004)	~65	1:1,500	-	-	-
(Feng et al., 2005)	HUVEC	50µg per lane	15% (NOX) or 7% (eNOS) resolving	Monoclonal anti-$p47^{phox}$ (from collaborator) Anti-eNOS (Cell Signalling Technology)[27]	- Human eNOS (synthetic peptide/recombinant protein	44 140	1:1000 1:1000	Anti-β-actin	42	1:5000
(Steinert et al., 2002)	HUVEC	20µg per lane	8% resolving, 3% stacking	Monoclonal anti-eNOS (Affiniti/Enzo)	-	~133	1:2500	Mono-clonal anti-α-tubulin (Chemicon/ Millipore)[28]	~53	1:2000
(Rueckschloss et al., 2002)	HUVEC (primary culture)	-	-	Monoclonal $gp91^{phox}$-specific (NOX2)	-	~75 (predicted)	-	-	-	-

[23] http://www.scbt.com/datasheet-21860-nox4-n-15-antibody.html
[24] http://www.scbt.com/datasheet-25545-mox1-h-75-antibody.html
[25] http://www.millipore.com/catalogue/item/07-024
[26] From http://www.millipore.com/catalogue/item/04-1116
[27] http://www.cellsignal.com/products/9586.html or http://www.cellsignal.com/products/5880.html
[28] http://www.millipore.com/search.do?q=Anti-%ce%b1-Tubulin&tabValue=PC&filterProductTypes=taxonomy%3a%5e73UUAR%2f73UUB8&show=10#0:0

Table 9.2.4 Method optimisation table for stimulated expression of NOX isoforms/subunits (for RT-qPCR and/or immunoblotting).

Source	Cell type & passage number	Cell seeding density & type of culture dish	Culture after seeding	Assay medium used	Pre-treatment	Stimulant	Treatments/ controls	Incubation time (hours)	RT-qPCR and/or immunoblot (& reference gene/protein)	Isoforms and/or subunits examined
(Deng et al., 2012)	HUVEC (P2-4)	2 x 10^5 cells; flask	Until 80% confluent	Serum free media with 1% foetal bovine serum	24h pre-incubation in assay medium	40ng/ml TNF-α	Untreated, TNF-α, or TNF-α with inhibitors[29]	24	RT-qPCR & immunoblot (β-actin control for both)	NOX2, NOX4, $p22^{phox}$, $p47^{phox}$ [30], $p67^{phox}$
(Alvarez et al., 2010)	HUVEC (P4-10)	10,000 cells/well in 96-well plate	-	Supplemented endothelial cell growth medium	12h serum/ supplement starvation	Angiotensin II (100nM)	Ang II, Ang II with pravastatin (NOX4, $p22^{phox}$)	6	RT-qPCR (β-actin control)	NOX1-5[31], $p22^{phox}$
(Kamiyama et al., 2009)	HUVEC (≤ P6)	-	Confluent	Endothelial cell growth medium	-	50µg/ml oxLDL	Equol	Unclear - possibly 48	RT-qPCR (36B4 control) & immunoblot	$p22^{phox}$, $p47^{phox}$, $p67^{phox}$ (RT-qPCR); Rac1 (immunoblot)
(Jiang et al., 2006)	Human micro-vascular endothelial cells (HMEC) P<25	6-well plate for RT-qPCR	Confluent culture	Supplemented MCDB-131 medium	24h incubation in low serum (0.1%) medium	-	NONOate[32] (1mM)	6	RT-qPCR & immunoblot (β-actin control for immunoblot)	NOX1, NOX2 NOX4, $p22^{phox}$, $p47^{phox}$ (RT-qPCR)[33]; NOX1, NOX2, NOX4 (immunoblot)
(Feng et al., 2005)	HUVEC	10^5 cells ml^{-1}	Confluent culture	Supplemented F12K medium	-	Endothelin-1 (1nM)	-	24	Immunoblot (β-actin control)	$p47^{phox}$
(Rueckschloss et al., 2002)	HUVEC (primary culture)	Not specified	Confluent culture	Supplemented Medium 199	24 hour incubation in medium with 0.5% calf serum	Angiotensin II (10nM, 100nM, 1µM)	AT1 receptor antagonist candesartan (NOX2 RT-PCR only)	7-8	RT-PCR[34] & immunoblot	NOX2, $p22^{phox}$, $p47^{phox}$, $p67^{phox}$ (RT-PCR); NOX2 (immunoblot)

[29] Inhibitors: rottlerin (PKC δ), CGP53353 (PKC β_2), gp91ds-tat (NADPH oxidase), apocynin (NADPH oxidase)

[30] Also translocation of $p47^{phox}$ and $p67^{phox}$ between membrane & cytosol

[31] No PCR product detected for NOX1-3 in unstimulated cells

[32] NO donor

[33] No mRNA detected for NOX1 or NOX2 (but NOX2 detected by immunoblot)

[34] Quantification of mRNA by multi-standard assisted competitive RT-PCR

Table 9.2.5 Method optimisation table for positive controls for stimulated expression of NOX isoforms/subunits.

Source	Cell type	Mediator	Concentration	Incubation time	Scope (NOX bioactivity and/or expression)
(Deng et al., 2012)	HUVEC	TNF-α	40ng/ml	24 hours	Bioactivity and mRNA/protein expression
(Kamizato et al., 2009)	Human colonic epithelial cells	TNF-α	20ng/ml	0-24 hours	Used to upregulate ROS production and NOX1/NOXO1 mRNA & protein
(Yoshida and Tsunawaki, 2008)	Human coronary artery EC	TNF-α	10ng/ml	6 & 21 hours (mRNA)	Bioactivity and mRNA/protein expression **Note:** no effect on NOX4/$p22^{phox}$ mRNA in this system
(Yang et al., 2007)	Human retinal pigment epithelial cells	TNF-α	0-50ng/ml	0-60 minutes	Bioactivity
(Li et al., 2005)	Human dermal microvascular EC	TNF-α	100U/ml	0-60 minutes	Bioactivity ($p47^{phox}$ phosphorylation/translocation/association)
(Muzaffar et al., 2004)	Porcine pulmonary artery VSMC and EC	TNF-α	10ng/ml	16 hours	Bioactivity and protein expression
(Frey et al., 2002)	Human pulmonary artery EC	TNF-α	500U/ml	0-15 minutes	Bioactivity ($p47^{phox}$ phosphorylation/translocation)
(Kamizato et al., 2009)	Human colonic epithelial cells	IFN-γ	1000U/ml	0-12 hours	Used to upregulate ROS production and NOX1/NOXO1 mRNA & protein
(Yang et al., 2007)	Human retinal pigment epithelial cells	IFN-γ	0-20U/ml	0-60 minutes	Bioactivity
(Kuwano et al., 2006)	Human colonic epithelial cells	IFN-γ	0-10,000U/ml	0-24 hours	ROS production & expression of NOX1/NOXO1/NOXA1 **Note:** no effect on NOX2/4 mRNA in this system
(Yang et al., 2007)	Human retinal pigment epithelial cells	IL-1β	0-40ng/ml	0-60 minutes	Bioactivity
(Kaur et al., 2004)	Human coronary artery SMC	IL-1β	25U/ml & 50U/ml	24 hours	Bioactivity
(Lo et al., 1998)	Bovine chondrocytes	IL-1β	20ng/ml	20 minutes (ROS)	Stimulation of ROS production
(Muzaffar et al., 2004)	Porcine pulmonary artery VSMC and EC	IL-1α	10ng/ml	16 hours	Bioactivity and protein expression
(Sturrock et al., 2006)	Human pulmonary artery SMC	TGF-β1	1ng/ml	24 hours (mRNA)	Bioactivity and mRNA/protein expression **Note:** no effect of IFN-γ at 2000U/ml on NOX4 mRNA in this system
(Cucoranu et al., 2005)	Human cardiac fibroblast cells	TGF-β1	10ng/ml	0-24 hours (mRNA)	Bioactivity and mRNA/protein expression **Note:** Effect on NOX4/5 mRNA only, but upregulation of NOX4 mRNA noted from 2h onwards

Table 9.2.6 Method optimisation table for stimulated p47^{phox} translocation: preparation of cytosolic & membrane fractions

Source	Cell type & passage number	Cell seeding density & type of culture dish	Stimulant	Incubation time (minutes)	Lysis/extraction buffer	Homogenisation	P1[35]/S1	P2[36] (from S1)	S3 (from P2)	p47^{phox} antibody
(Deng et al., 2012)	HUVEC (P2-4)	2 x 10^5 cells; size of vessel not specified	40ng/ml TNF-α	24 hours	10mM Tris HCl (pH 7.5), 5mM EDTA, 50µg/ml PMSF[37]	-	-	100,000*g* at 4°C for 60 minutes – supernatant designated as cytosolic fraction	Pellet re-suspended in lysis buffer (with 1% Triton X-100), sonicated, & incubated at 4°C for 45 minutes. Lysate centrifuged at 4°C & supernatant designated membrane fraction	Millipore - polyclonal
(Wang et al., 2010b)	Rat VSMC (P5-12)	-	High glucose (25mM) or normal glucose (5mM)	0-120	RIPA buffer[38] with protease inhibitor mixture (Santa Cruz)	-	3000*g* for 10 minutes	100,000*g* at 4°C for 90 minutes – supernatant defined as cytosolic fraction and pellet as membrane fraction[39]	-	Santa Cruz Biotechnology[40]

[35] Unbroken cells/debris, also pelleted nuclei
[36] Crude membrane pellet
[37] Phenylmethylsulfonylfluoride – serine protease inhibitor
[38] Radio-immunoprecipitation assay buffer
[39] Integrin-β1 used as marker of membrane fraction
[40] Immunoprecipitation to detect phosphorylated p47^{phox} (using anti-phosphoserine)

Source	Cell type & passage number	Cell seeding density & type of culture dish	Stimulant	Incubation time (minutes)	Lysis/extraction buffer	Homogenisation	P1[35]/S1	P2[36] (from S1)	S3 (from P2)	p47^{phox} antibody
(Fortuño et al., 2009)	PBMCs (peripheral blood mononuclear cells)	5 x 10^6 cells	3.2µM PMA	15	10mM Tris (pH 8), 150mM NaCl with protease inhibitor cocktail (Roche Complete)	-	2000*g* for 10 minutes	100,000*g* at 4°C for 60 minutes – supernatant used as cytosolic fraction	P2 used as membrane fraction	Santa Cruz Biotechnology
(Carluccio et al., 2007)	HUVEC (P1-3)	-	100µM homocysteine	0-30	7.5mM Tris HCl (pH 7.5), 2mM EGTA,2mM EDTA, 0.25M sucrose, 1mM DTT, 1mM PMSF, 1mg/ml aprotinin, 1mg/ml leupeptin	Sonication on ice, 3 x 15s	500*g* for 10 minutes	100,000*g* at 4°C for 60 minutes – supernatant saved as cytosolic fraction	P2 re-suspended in extraction buffer with 1% Triton X-100; centrifuged at 100,000*g* for 60 minutes - supernatant saved as membrane-enriched fraction	Santa Cruz Biotechnology
(Nishikawa et al., 2007)	CM-MC (cutaneous mastocytoma cells)	10^8 cells	30µg/ml compound 48/80	0-10	10mM Tris HCl, 5mM EGTA, 2mM PMSF, 10µg/ml aprotinin, 10µg/ml leupeptin	Sonication on ice	10,000*g* at 4°C for 10 minutes	100,000*g* at 4°C for 60 minutes – separation into membrane and cytosolic fractions	P2 dissolved in lysis buffer (plus 1% sodium deoxycholate & 1% NP-40) with sonication	Santa Cruz Biotechnology
(Massaro et al., 2006)	HSVEC (human saphenous vein EC; ≤ P5)	-	10ng/ml IL-1α	20	7.5mM Tris HCl (pH 7.5), 2mM EGTA, 2mM EDTA, 0.25M sucrose, 1mM DTT, 1mM PMSF, 1mg/ml aprotinin, 1mg/ml leupeptin	Sonication on ice, 3 x 15s	500*g* for 10 minutes	100,000*g* at 4°C for 60 minutes – supernatant saved as cytosolic fraction	P2 re-suspended in extraction buffer with 1% Triton X-100; centrifuged at 100,000*g* for 60 minutes – supernatant saved as membrane-enriched fraction	Santa Cruz Biotechnology - monoclonal

Source	Cell type & passage number	Cell seeding density & type of culture dish	Stimulant	Incubation time (minutes)	Lysis/extraction buffer	Homogenisation	P1[35]/S1	P2[36] (from S1)	S3 (from P2)	p47^{phox} antibody
(Ushio-Fukai et al., 2002)	HUVEC (P2-5)	Gelatin-coated plates	20ng/ml human recombinant $VEGF_{165}$	0-60	Ice-cold 10mM Tris (pH 7.4), 1.5mM $MgCl_2$, 5mM KCl, 1mM DTT, 0.2mM sodium vanadate, 1mM PMSF, 1µg/ml aprotinin, 1µg/ml leupeptin (5 minute treatment)	Lysate drawn through 1ml syringe (rapid stokes)	2000*g* at 4°C for 5 minutes	100,000*g* at 4°C for 90 minutes – supernatant saved as cytosolic fraction	14,000rpm at 4°C for 20 minutes – supernatant saved as membrane fraction	N/A – examining Rac1 translocation
(Heyworth et al., 1991)	Human neutrophils	3×10^7 cells	100ng/ml PMA	5	100mM KCl, 3mM NaCl, 3.5mM $MgCl_2$, 1.25mM EGTA, 10mM piperazine diethane sulfonic acid (pH 7.3)	Sonication, 5s burst, at 4°C	250*g* at 4°C for 5 minutes	115,000*g* at 4°C for 20 minutes – supernatant saved as cytosolic fraction	P2 washed with 0.6ml buffer; centrifuged at 115,000*g* at 4°C for 20 minutes – pellet (membrane fraction) resuspended in buffer & subject to sonication (2-3s burst)	Polyclonal antiserum binding p47^{phox} and p67^{phox}

Table 9.2.7 Method optimisation table for p47^{phox} immunoblotting: potential cell stimulants

Source	Cell type	Mediator	Concentration	Incubation time	Scope (NOX bioactivity and/or expression)
(Deng et al., 2012)	HUVEC	TNF-α	40ng/ml	24 hours	Bioactivity, including p47^{phox} translocation, and mRNA/protein expression
(Li et al., 2005)	Human dermal microvascular EC	TNF-α	100U/ml	0-60 minutes	Bioactivity (p47^{phox} phosphorylation/translocation/ association)
(Muzaffar et al., 2004)	Porcine pulmonary artery EC and VSMC	TNF-α	10ng/ml	16 hours	Bioactivity and protein expression
(Frey et al., 2002)	Human pulmonary artery EC	TNF-α	500U/ml	0-15 minutes	Bioactivity (p47^{phox} phosphorylation/translocation)
(Li et al., 2002)	Murine coronary microvascular endothelial cells	TNF-α	100U/ml	10 minutes (pre-incubation)	Role of p47^{phox} in NOX activity/ROS production
(Li et al., 2002)	Murine coronary microvascular endothelial cells	PMA	100ng/ml	10 minutes (pre-incubation)	Role of p47^{phox} in NOX activity/ROS production
(Görlach et al., 2000)	HUVEC (also SMC)	PMA	0.01 -1μM	~20-40 minutes	ROS production, NOX2 isoform & subunit expression
(Ushio-Fukai et al., 2002)	HUVEC	Human recombinant $VEGF_{165}$	20ng/ml	0-60 minutes	Bioactivity
(Massaro et al., 2006)	Human saphenous vein EC	IL-1α	10ng/ml	20 & 60 minutes (NOX)	p47^{phox} translocation, NOX activity (as part of wider study)
(Muzaffar et al., 2004)	Porcine pulmonary artery EC and VSMC	IL-1α	10ng/ml	16 hours	Bioactivity and protein expression
(Carluccio et al., 2007)	HUVEC	Homo-cysteine	100μM	0-30 minutes (p47^{phox} translocation)	p47^{phox} translocation, NOX activity (as part of wider study)
(Chen et al., 2009)	HUVEC	oxLDL	150μg/ml	60 minutes (ROS production)	ROS production, mRNA levels
(Rueckschloss et al., 2001)	HUVEC	oxLDL	100μg/ml	1 – 7 hours	ROS production, NOX2 expression

Table 9.2.8 Method optimisation table for endothelial expression of HO-1 (for mRNA/protein quantification)

Source	Cell type & passage number	Cell seeding density & type of culture dish	Culture after seeding	Assay medium used	Pre-treatment	Stimulant	Treatments/ controls	Incubation time (hours)	Quantification of HO-1 mRNA/protein	Concentration and/or time for maximal effect
(Zheng et al., 2012)	Porcine aortic endothelial cells	Not specified	Not specified	Supplemented Medium 199 (5% foetal bovine serum)	Transfection with control or caveolin-1 siRNA	-	Epigallocatechin-3-gallate (EGCG) at 30µM	6	Immunoblotting	-
(Wu et al., 2012)	HCAEC	6-well plate: 2 x 10^5 cells	Until confluent	Serum-free DMEM[41]	12h incubation in assay medium	-	0.25-1mM niacin	0-24	RT-qPCR & immunoblotting	mRNA: ~3-fold (1mM niacin, 6 hours) Protein: ~5-6-fold (1mM niacin, 6 hours; detectable basal signal)
(Donovan et al., 2012)	HCAEC, P3-12	65mm dish	Until ≥80% confluent	-	-	None for immunoblot analysis	1-50µg/ml Protandim[42]	12	Immunoblotting	Protein: ~8-fold (20µg/ml Protandim; weak basal HO-1 band)
(Lee et al., 2011)	HUVEC (P4-9)	Not specified	~80% confluent	Supplemented Medium 199	+/- siRNA or inhibitors	H_2O_2 for cell death assays only	Fisetin (5-25µM)	1-24	RT-PCR; immunoblotting	mRNA: 25µM (1h) & 1h (10µM)[43] Protein: 25µM (16h) & 16h (10µM)
(Zheng et al., 2010)	Porcine aortic endothelial cells	Not specified	Confluent culture	Supplemented Medium 199 (5% foetal bovine serum)	24h incubation in low serum (1%) conditions; +/- siRNA	2ng/ml TNF-α	EGCG at 30µM	4 or 8[44]	RT-qPCR[45]; immunoblotting	-

[41] Dulbecco's modified Eagle's medium
[42] Marketed dietary supplement comprised of phytochemicals from five well-characterised medicinal plants
[43] HO-1 mRNA/protein detected at time points up to & including 24h
[44] 4h co-incubation with stimulant; or 2h pre-incubation with EGCG followed by 6h exposure to TNF-α
[45] Primers for HO-1 listed, but no data shown

Source	Cell type & passage number	Cell seeding density & type of culture dish	Culture after seeding	Assay medium used	Pre-treatment	Stimulant	Treatments/ controls	Incubation time (hours)	Quantification of HO-1 mRNA/protein	Concentration and/or time for maximal effect
(Ungvari et al., 2010)	HCAEC	-	-	-	-	None for RT-qPCR analysis	0.1-100μM resveratrol	Not stated – possibly 24	RT-qPCR	mRNA: ~3-fold at 50μM resveratrol
(Khoo et al., 2010)	HCAEC, P3-7	-	Until confluent	Complete medium with 10% serum	Serum-deprived for 16h	-	2.5 & 5μM nitro-oleic acid; also oleic acid (concentration not specified)	16 (mRNA) 24 (protein)	RT-qPCR & immunoblotting	mRNA: ~12-fold (5μM nitro-oleic acid) Protein: blot only (weak basal HO-1 band)
(Zieger and Gupta, 2009)	HCAEC, P5-10	T25 flasks: 13,000 cells/cm^2	Until confluent	EGM2-MV	-	-	10μM haemin chloride	1 (with treatment) + 2 (EGM only)	ELISA	Protein: ~2-fold
(Sorrenti et al., 2007)	Human iliac artery endothelial cells	Not specified	Until sub-confluent	Supplemented F12K medium (10% foetal bovine serum)	24h incubation in low serum (0.5%) medium	10% foetal bovine serum (ie assay medium)	Cyanidin-3-glucoside (6.25nM to 250μM)	24	Immunoblotting	-
(Vidavalur et al., 2006)	HCAEC	100mm dishes	Until confluent	Supplemented EGM-2	-	-	10 & 20μM sildenafil	24	Immunoblotting	Protein: ~3-fold (20μM sildenafil; weak basal HO-1 band)
(Lazze et al., 2006)	HUVEC	Not specified	Confluent culture	Supplemented Medium 199	-	-	Cyanidin, delphinidin (both at 50 or 100μM)	24	ELISA	-
(Wu et al., 2006a)	Bovine aortic endothelial cells	Petri dish	Confluent culture	Not clear – serum-free DMEM	12 hour incubation in serum-free DMEM	-	EGCG at 25-100μM (+/- inhibitors or antioxidants); also epicatechin-3-gallate, epigallocatechin, or epicatechin (at 50 or 100μM)	3-24	Northern blot analysis; immunoblotting	Protein: 100μM (6h) and 6-12h (100μM)

Source	Cell type & passage number	Cell seeding density & type of culture dish	Culture after seeding	Assay medium used	Pre-treatment	Stimulant	Treatments/ controls	Incubation time (hours)	Quantification of HO-1 mRNA/protein	Concentration and/or time for maximal effect
(Kaga et al., 2005)	HCAEC, P3-5	-	-	-	-	-	1-50μM resveratrol, 1–1000nM thioredoxin-1 (with or without 10μM SnPP[46])	12	Immunoblotting	Protein: blot only, basal HO-1 band visible
(Nordskog et al., 2003)	HCAEC, P4-5	Flasks	-	EGM-2-MV	-	-	Cigarette smoke condensate (30μg/ml total particulate matter)	24	cDNA array analysis	mRNA: ~3-fold Note: no HO-1 band detected for aortic endothelial cell lysates following exposure to 0.7% DMSO
(Terry et al., 1999)	HUVEC (P1)	Cells in 60mm dishes (1% gelatin coating)	Until confluent	Neuman Tytell media[47]	3-4h incubation in Neuman Tytell medium	500U/ml TNF-α[48] (or 50U/ml IL-1α)	Agonists/ inhibitors including PMA[49]	4	Northern blot analysis; immunoblotting	-
(Terry et al., 1998)	HUVEC (P1)	Cells in 60mm dishes (1% gelatin coating)	Until confluent	Endothelial cell growth media (≥ 12h treatment) or Neuman Tytell media (< 12h treatment)	3-4h incubation in Neuman Tytell medium	10-1,000U/ml TNF-α (also 1-500U/ml IL-1α)	Actinomycin D/cycloheximide/ curcumin[50]	2-8	Northern blot analysis; immunoblotting	mRNA: 4h incubation with 500U/ml TNF-α or 50U/ml IL-1α Protein: 6h incubation with 500U/ml TNF-α or 50U/ml IL-1α

[46] Tin-protoporphyrin IX
[47] Serumless media
[48] TNF-α used at 20ng/ml in current study (approximately 400-1000U/ml, based on manufacturer's datasheet)
[49] PMA: phorbol 12-myristate 13-acetate
[50] Transcription inhibitor/protein synthesis inhibitor/inhibitor of AP-1, NF-κB activation respectively

9.3 Stimulated superoxide production assay: reduction of cytochrome c (mM) measured at 550nm

Figure 9.3.1 **Elevation of superoxide levels by angiotensin II (0.1µM) following 6h incubation in HUVEC model (reduction of cytochrome c at 550nm).**

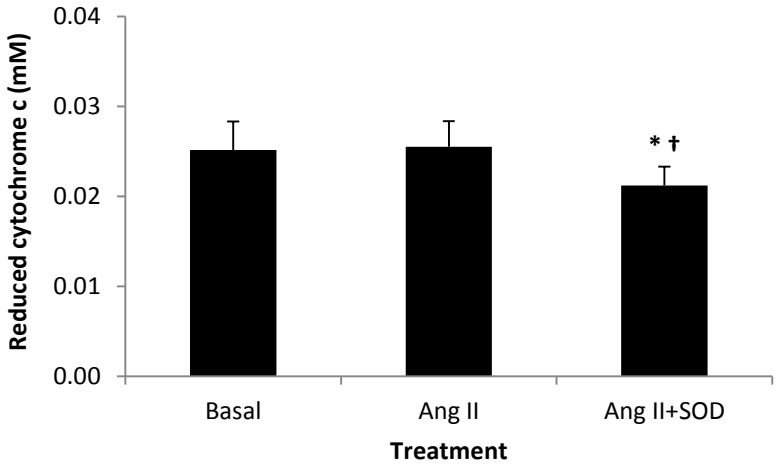

Reduction of cytochrome c (mM) measured at 550nm (molar extinction coefficient/ε = 21.1mM^{-1} cm^{-1}) for basal (unstimulated) cells, angiotensin II control (Ang II, 0.1µM) and Ang II with superoxide dismutase (SOD) in stimulated superoxide production assay (24-well plate format) at 0.1, 1 and 10µM. Data are graphed as mean ± SD (n=8). *Significant difference versus basal ($p < 0.05$); †significant difference versus Ang II ($p < 0.05$).

Figure 9.3.2 **Modulation of angiotensin II-stimulated endothelial superoxide production by NOX inhibitor VAS2870 (reduction of cytochrome c at 550nm).**

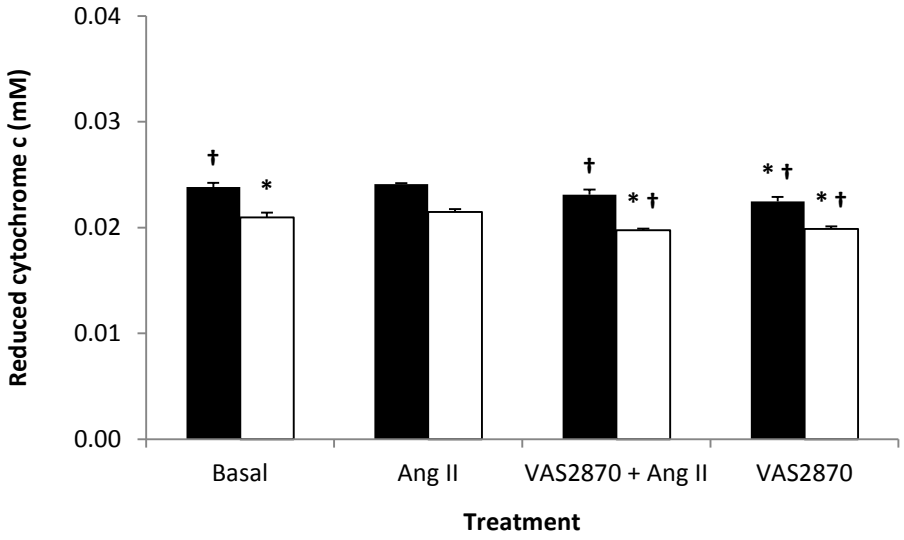

Reduction of cytochrome c (mM) measured at 550nm (molar extinction coefficient/ε = 21.1mM^{-1} cm^{-1}) with and without superoxide dismutase (SOD) correction (white & black bars respectively) for basal (unstimulated) cells, angiotensin II control (Ang II, 0.1µM), 5µM VAS2870 (NOX inhibitor) with 0.1µM Ang II (VAS2870 + Ang II), and 5µM VAS2870 in stimulated superoxide production assay (24-well plate format). Data are graphed as mean ± SD (n=3). *Significant difference versus Ang II ($p < 0.05$); †significant difference versus Ang II + SOD ($p < 0.05$).

Figure 9.3.3 **Modulation of superoxide levels by cyanidin-3-glucoside (A), peonidin-3-glucoside (B), malvidin-3-glucoside (C), petunidin-3-glucoside (D), protocatechuic acid (E), vanillic acid (F), and syringic acid (G) following 6h incubation in angiotensin II-stimulated HUVEC model (reduction of cytochrome c at 550nm).**

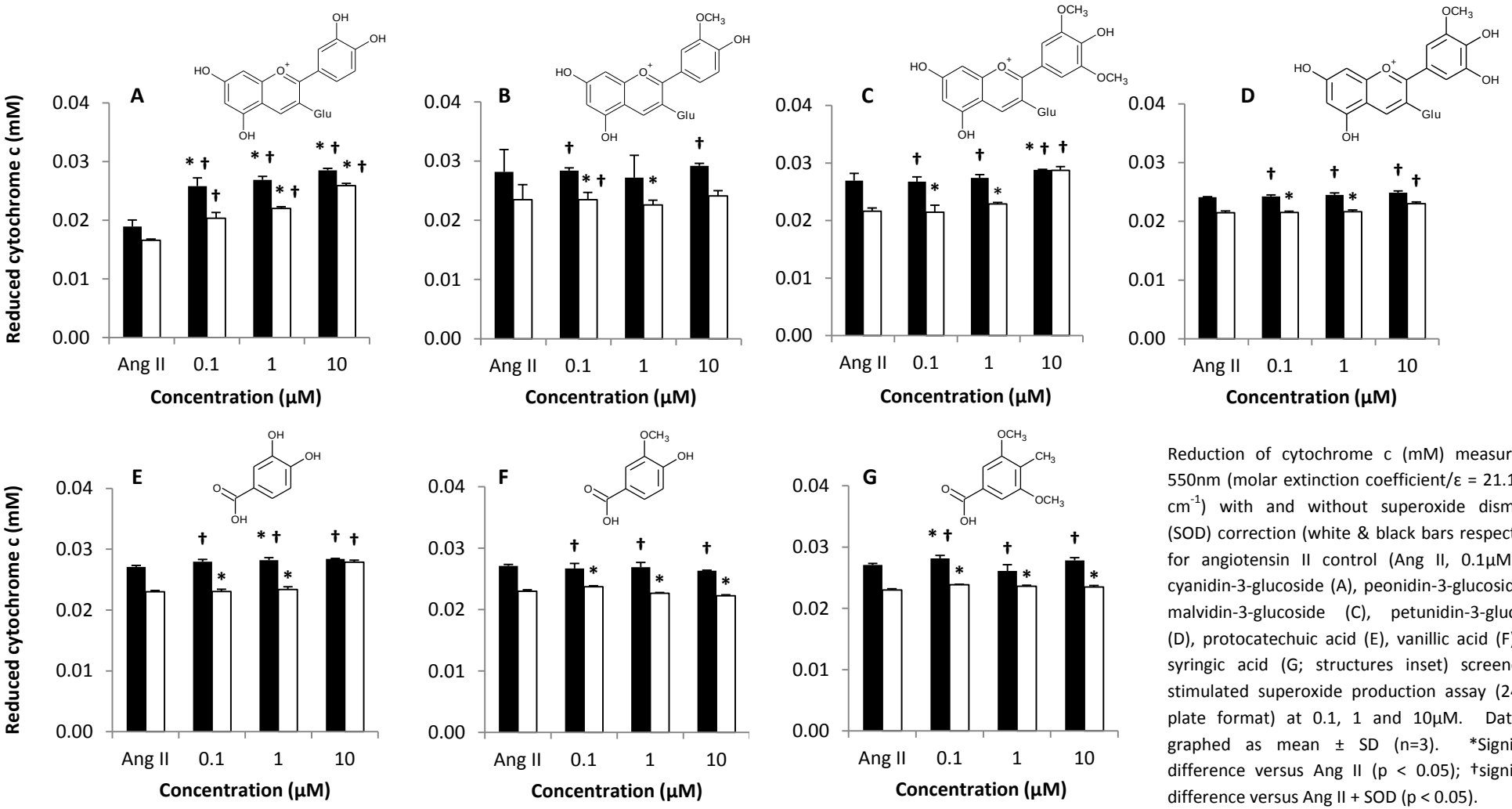

Reduction of cytochrome c (mM) measured at 550nm (molar extinction coefficient/ε = 21.1mM^{-1} cm^{-1}) with and without superoxide dismutase (SOD) correction (white & black bars respectively) for angiotensin II control (Ang II, 0.1µM) and cyanidin-3-glucoside (A), peonidin-3-glucoside (B), malvidin-3-glucoside (C), petunidin-3-glucoside (D), protocatechuic acid (E), vanillic acid (F), and syringic acid (G; structures inset) screened in stimulated superoxide production assay (24-well plate format) at 0.1, 1 and 10µM. Data are graphed as mean ± SD (n=3). *Significant difference versus Ang II ($p < 0.05$); †significant difference versus Ang II + SOD ($p < 0.05$).

Figure 9.3.4 **Modulation of superoxide levels by cyanidin-3-glucoside (A) or protocatechuic acid (B) in combination with epicatechin, quercetin and ascorbic acid following 6h incubation in angiotensin II-stimulated HUVEC model (reduction of cytochrome c at 550nm).**

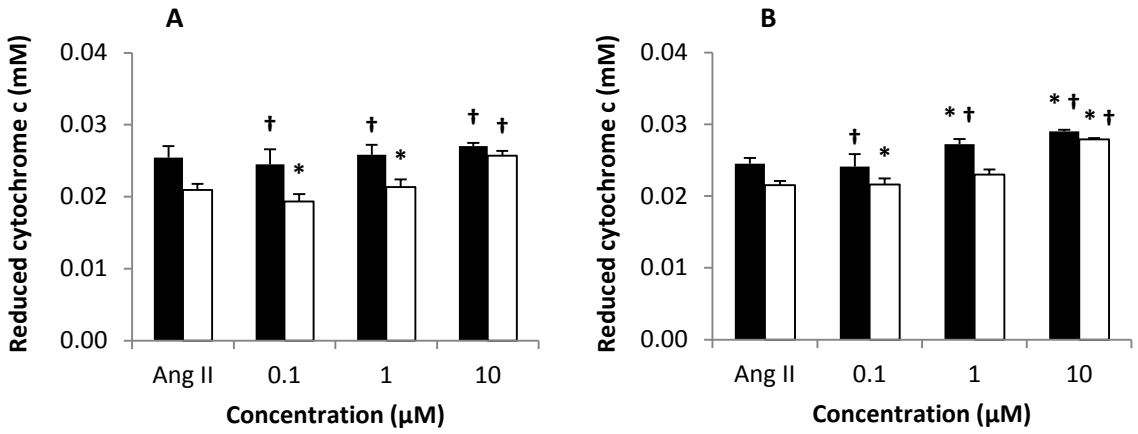

Reduction of cytochrome c (mM) measured at 550nm (molar extinction coefficient/ε = 21.1mM^{-1} cm^{-1}) with and without superoxide dismutase (SOD) correction (white & black bars respectively) for angiotensin II control (Ang II, 0.1µM) and equimolar ratio of cyanidin-3-glucoside (A) or protocatechuic acid (B) with epicatechin, quercetin and ascorbic acid, screened in stimulated superoxide production assay (24-well plate format) at 0.1, 1 and 10µM. Data are graphed as mean ± SD (n=3). *Significant difference versus Ang II ($p < 0.05$); †significant difference versus Ang II + SOD ($p < 0.05$).

9.4 Reverse transcription – quantitative polymerase chain reaction: melt curve data for NOX custom primer sets

Figure 9.4.1 Specificity of real time PCR amplification for NOX2 (A), p47^{phox} (B), and p67^{phox} (C) primer sets (melt curve analysis).

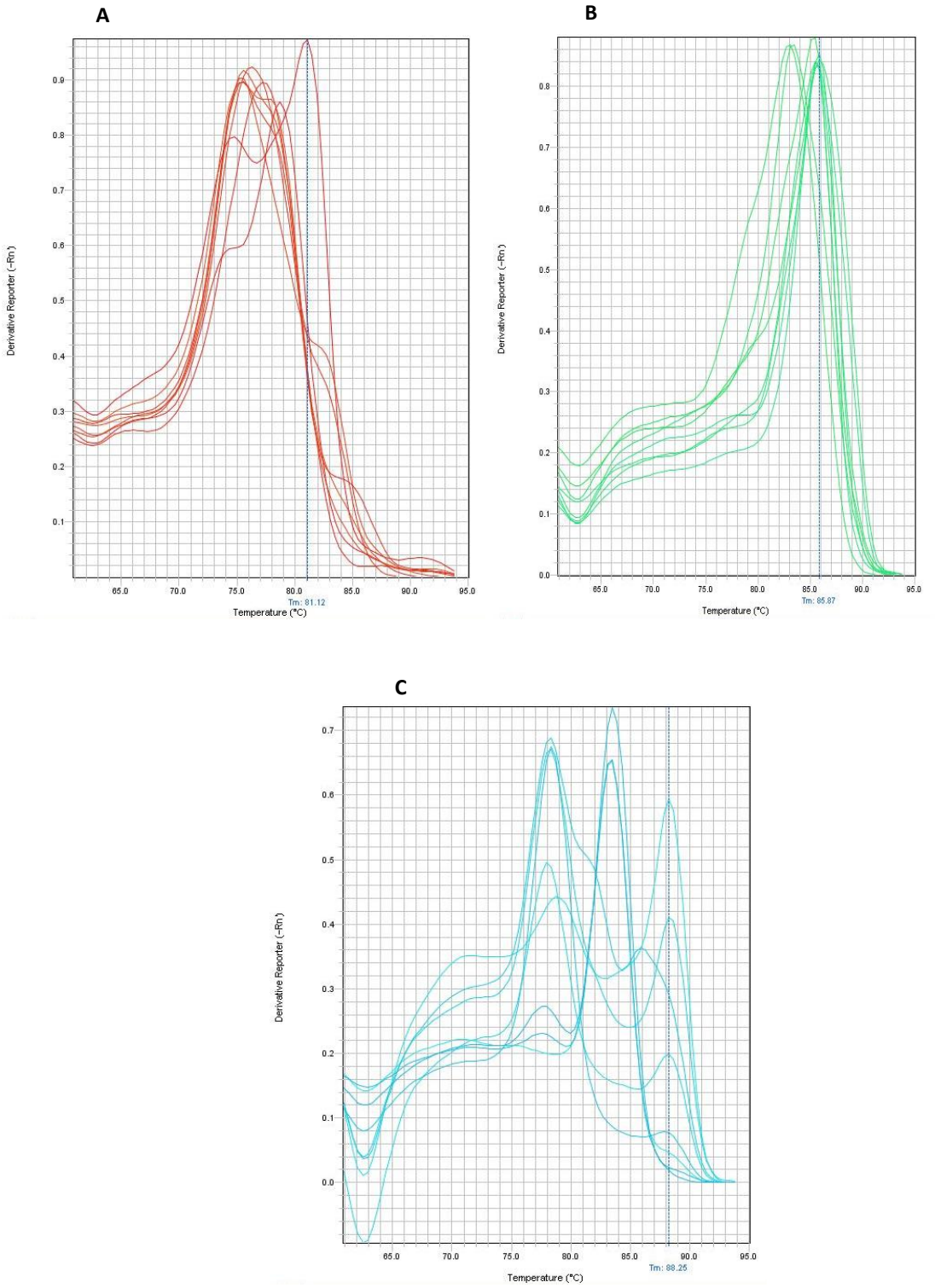

Melt curve analysis of real time PCR product following 50 cycles denaturation/data collection using primer sets for NOX2 (A), p47^{phox} (B), and p67^{phox} (C). Real time PCR was conducted using 25ng cDNA generated from basal (unstimulated) HUVEC, and cells incubated with 0.1µM angiotensin II for 4 hours (n=4 per treatment group, n=8 overall).

Figure 9.4.2 Specificity of real time PCR amplification for NOX4 (A) and p22^{phox} (B) primer sets (melt curve analysis).

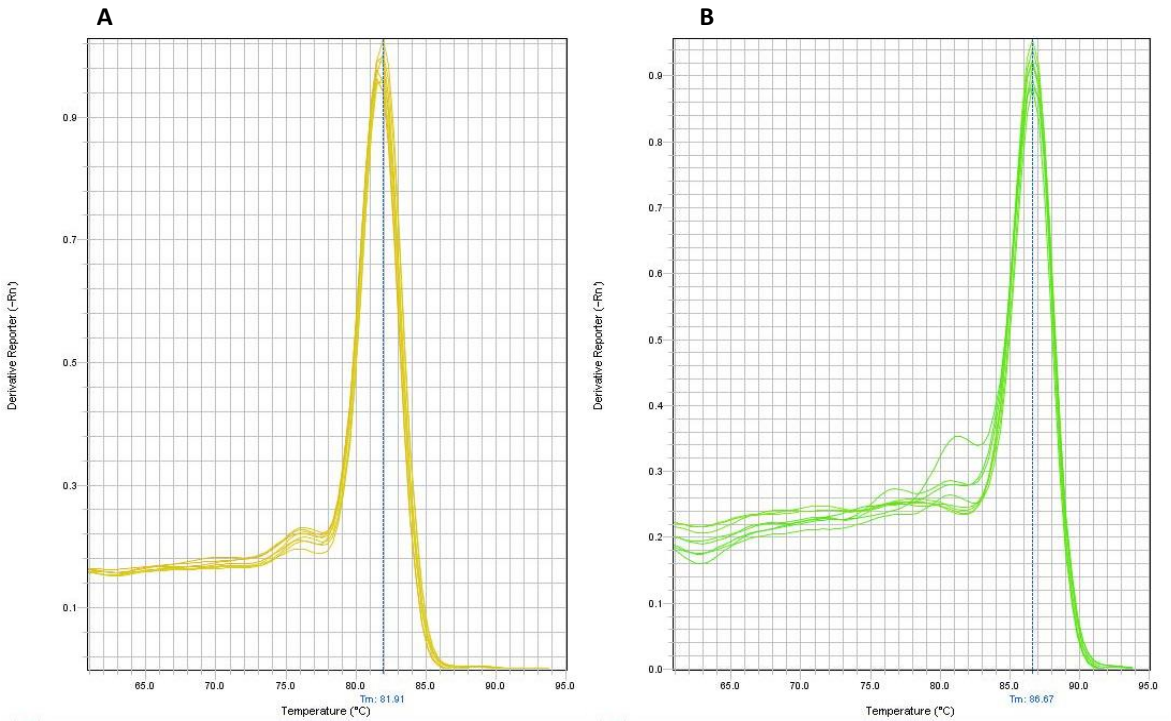

Melt curve analysis of real time PCR product following 50 cycles denaturation/data collection using primer sets for NOX4 (A) and p22^{phox} (B). Real time PCR was conducted using 25ng cDNA generated from basal (unstimulated) HUVEC, and cells incubated with 0.1µM angiotensin II for 4 hours (n=4 per treatment group, n=8 overall).